Biogeochemical processes and trace element mobility in alkaline waste affected soils

Cindy Louise Lockwood

Submitted in accordance with the requirements for the degree of Doctor of Philosophy

The University of Leeds

School of Earth and Environment

May 2014

The candidate confirms that the work submitted is her own, except where work which has formed part of jointly authored publications has been included. The contribution of the candidate and the other authors to the work has been explicitly indicated below. The candidate confirms that appropriate credit has been given within the thesis where reference has been made to the work of others.

The work in Chapter 5 of the thesis has appeared in publication as follows:

Lehoux A. P., **Lockwood C. L.**, Mayes W. M., Stewart D. I., Mortimer R. J. G., Gruiz K., and Burke I. T. (2013) Gypsum addition to soils contaminated by red mud: Implications for aluminium, arsenic, molybdenum and vanadium solubility. *Environmental Geochemistry and Health, 35(5), 643-656.*

I was responsible for the sampling of the soil and red mud at Ajka, the interpretation of the soil characterisation of the soil and red mud sampled above, arranging for analysis and preparing samples for XRD, XRF and TOC analysis, carrying out the experimental work (Soil pH, BET), providing laboratory assistance to the main author and assistance with the collection of data especially with regards to ICP-MS and writing of the manuscript with regards to the soil characterisation. Alizée Lehoux carried out the majority of laboratory work (except for soil characterisation, see above) and contributed to the interpretation of the data and writing of the manuscript. William Mayes acted as fieldwork support and carried out extensive manuscript review, together with the contribution of Principle Component Analysis. Douglas Stewart and Robert Mortimer acted as field work support and carried out manuscript review. Katalin Gruiz granted site access and offered advice and comments on the manuscript. Ian Burke acted as fieldwork support, MSc supervisor to Miss Lehoux and contributed

considerably to the interpretation of the results together with writing the majority of the manuscript.

The work in Chapter 6 of the thesis has been prepared for publication for submission as follows:

Lockwood C. L., Mortimer R. J. G., Stewart D. I., Mayes, W. M., Peacock C. L., Polya D. A., Lythgoe P. R., Lehoux A. P., Gruiz K., Burke I. T. (*Submitted to Applied Geochemistry, June 2014)*

I was responsible for the sampling the soil and red mud at Ajka, arranging for analysis and preparing samples for XRD, XRF and TOC analysis, sampling, experimental design, processing and analysis of all microcosms, data collection, interpretation of data and statistical analysis, writing the paper and preparation of all tables and figures, except where listed below. Robert Mortimer acted as field work support and manuscript review. Douglas Stewart acted as fieldwork support, carried out manuscript review and assisted with the collection of XAS data. William Mayes acted as fieldwork support, carried out manuscript review, together with the contribution of Principle Component Analysis. Caroline Peacock assisted with the collection of XAS data and offered advice and comments on the manuscript. David Polya was responsible for organising the HPLC-ICP-MS analysis and offered advice and comments on the manuscript. Paul Lythgoe carried out HPLC-ICP-MS analysis for As speciation. Alizée Lehoux provided the data for the red mud leaching batch tests. Katalin Gruiz granted site access and assisted with site orientation. Ian Burke acted as fieldwork support, assisted with collection of XAS data and interpretation of As EXAFS data and provided extensive manuscript review.

The work in Chapter 7 of the thesis has been prepared for publication for submission as follows:

Lockwood C. L., Stewart D. I., Mortimer R. J. G., Mayes, W. M., Gruiz K., Burke I. T., Leaching of copper and nickel in soil-water systems contaminated by red mud from Ajka, Hungary: The importance of soil organic matter. *(in preparation for The Journal of Hazardous Materials, 2014)*

I was responsible for the sampling the soil and red mud at Ajka, arranging for analysis and preparing samples for XRD, XRF and TOC analysis, sampling, experimental design, processing and analysis of anaerobic and aerobic microcosms, data collection, interpretation and statistical analysis, writing the paper and preparation of tables and figures. Douglas Stewart acted as fieldwork support, carried out extensive manuscript review. Robert Mortimer acted as field work support and manuscript review. William Mayes acted as fieldwork support together with the contribution of Principle Component Analysis. Katalin Gruiz granted site access and assisted with site orientation. Ian Burke acted as fieldwork support and provided manuscript review.

Acknowledgements

I would like to express my sincere thanks to Doug Stewart, Will Mayes, Rob Mortimer and Ian Burke and for their invaluable help, support and enthusiasm throughout my PhD. I would also like to thank them for all their personal advice, encouragement and for putting up with my excessive bouts of worrying. Field trips were always a great source of amusement; I'm sure that there is a joke that starts "There were four academics and a PhD student in car travelling to Budapest". I would to thank Katalin Gruiz and her team at BME in Budapest for field support and site orientation in Hungary. I would also like to thank others who have helped me out with technical guidance and data collection including but not limited to; David Ashley, Rachel Gasior, Lesley Neve, Clare Gordon, David Elliot, Sheena Bennett, Ann Mennim, Nick Marsh, Fred Mosselmans, Tina Geraki, Alizée Lehoux and Stephen Reid. A massive massive 'thank you' goes to Bob Knight and Sam Allshorn, my all time PhD heros. A big thanks to members past and present of Cohen Geochemistry a.k.a. 'Cohenites' especially; Liane Benning, for always being interested and giving out good advice, Caroline Peacock, for beamtime help and advice, Rob Whittleston and Sarah Wallace for having done it all before me and sharing their experiences, Romain Guilbaud for helping me with a very important presentation and Jörgen Rosenqvist, my PhD therapist. Thank you to all the occupants of office 8.154 over the past 3 1/2 years especially Andy Bray, Steffi Lutz, Pieter Bots, Santiago Clerici and Daniela Meier for their willingness to help and, listen to me whinge but mainly for their tolerance of my grumpiness. A special thank you to Lizzy Moyce, Janice Littlewood and Amy Atkins – it has been an absolute pleasure, I really don't think I could have come this far without your friendship.

Outside of University Life, to my friends; Jax Spud, LB, Rads, Heather, Andy W, Guy ‘Oatcake’ Hassall, Mr. Wasif, Peaches, Tori and even Mr. Strange; my fellow Captains of the Ruptured Core Confederation, Timothy Taylor for his Championship Beers, Mr. Scratchings for his tasty pork rinds and all the whippets and rabbits on the internet - thank you all, for keeping me sane.

A huge thank you to my family and extended family of Jones’, Phil, Kath and Tobes, my sister Sally, my beautiful niece Jess, my epic nephew Lucas and most of all my Mum and Dad, you have all been so supportive and I am eternally grateful. Finally, lots of love and thanks to Andy ‘The Jones’ Jones for putting up with and helping me get through this with my sense of humour intact, ‘Loving you is easy cos you make good food’. Now let’s go for a pint.

This project has been funded by the UK Engineering and Physical Science Research Council (Doctoral training award EP/P505593/1) and I thank Diamond Light Source for access to beamline I18 (Grant SP7525) that contributed to the results presented in this thesis.

Abstract

High pH leachates can mobilise oxyanion forming elements from alkaline waste, such as iron and steel slags and bauxite ore processing residue, into the wider environment. Red mud is a highly alkaline waste product from bauxite ore processing. It contains elevated concentrations of oxyanion forming elements such as Al, As, V and Mo that are mobilised at high pH together with other trace metals including Cu and Ni. The red mud spill at Ajka, Hungary released 1 million m^3 of caustic red mud into the surrounding area. As part of the initial clean-up, some thinner red mud deposits (< 5 cm) were ploughed into fields to prevent dust formation whereas wetland areas were left untreated. This study used aerobic and anaerobic batch microcosms together with XAS spectroscopy, (HPLC)-ICP-MS and solid phase extraction techniques to investigate the effects of red mud addition to unaffected soils with respect to biogeochemical processes and trace element release. Experiments were designed to be analogous to soil conditions following the remediation efforts. The results showed that the effect of red mud addition to soils was highly dependent upon soil properties, experimental pH, and total organic carbon (TOC) content. As and V were found to be persistently mobile under both aerobic and anaerobic conditions. Red mud addition to soils with a high TOC content mobilised high aqueous concentrations of organic matter complexing metals such as Cu, Ni and V under anaerobic conditions. Gypsum addition to red mud affected soils showed a reduction in aqueous oxyanion concentrations compared to soils with red mud addition alone indicating that it is potential ameliorant for red mud contaminated soils. The results showed that the extensive remediation efforts by the Hungarian authorities were justified but that red mud should be used with caution as a soil amendment.

Table of Contents

ABBREVIATIONS **1**

CHAPTER 1 INTRODUCTION **2**

1.1 PROJECT BACKGROUND AND SIGNIFICANCE 2
1.2 RESEARCH OBJECTIVES 4
1.2.1 Hownsgill Valley, nr Consett, U.K. *4*
1.2.2 Ajka, western Hungary *4*
1.3 EXPERIMENTAL APPROACHES 6
1.4 THESIS STRUCTURE 8
1.5 REFERENCES 9

CHAPTER 2 BACKGROUND INFORMATION AND SITE PROCESSES **11**

2.1 ALKALINE ENVIRONMENTS 11
2.2 ALKALINE INDUSTRIAL WASTES 12
2.2.1 Problems associated with high alkaline industrial wastes *12*
2.2.2 Iron and steel slags *14*
2.2.3 Bauxite ore processing waste (red mud) *16*
2.3 FATE AND TRANSPORT OF METAL/LOIDS IN THE ENVIRONMENT 19
2.3.1 Brief introduction to the contaminants of interest *20*
2.3.2 Sorption *22*
2.3.3 Complexation with natural organic matter (NOM) *25*
2.3.4 Biogeochemical Redox processes *26*
2.4 SOIL MICROORGANISMS 30
2.4.1 Alkaliphiles *30*
2.4.2 Microbial metal/loid reduction *31*
2.5 STUDY SITES 33
2.5.1 Hownsgill Valley, near Consett *33*
2.7.2 Ajka, Vesprém County, western Hungary *39*
2.8 REFERENCES 44

CHAPTER 3 MATERIALS AND METHODS **55**

3.1 SAMPLE COLLECTION 55
3.1.1 Hownsgill Valley Site *55*
3.1.2 Veszprém County, western Hungary *56*
3.1.2.1 Sandy Soil (SS) 56
3.1.2.2 Organic-rich Soil (OR) 57
3.1.2.3 Wetland Soil (WL) 57
3.1.2.4 Tailings Pond (X), MAL Zrt 58
3.1.3 Principle Component Analysis *59*
3.2 SAMPLE CHARACTERISATION 59
3.2.1 Sample pH *59*
3.2.2 % 0.5 M Acid extractable Iron as Fe(II) *60*
3.2.3 X-ray powder diffraction (XRD) *62*
3.2.4 X-ray fluorescence *63*
3.2.5 BET specific surface area *63*
3.2.6 Total carbon, organic and inorganic carbon *64*
3.2.7 Inorganic phosphate in samples *64*
3.3 BATCH MICROCOSM EXPERIMENTS 65

3.3.1 Microcosm Sterilisation *65*
3.3.1.1 Gamma (γ-) irradition 66
3.3.1.2 Chemical Sterilisation 66
3.3.1.3 Heat Sterilisation 67
3.3.2 Microcosm sampling technique *68*
3.4 Geochemical Analysis 69
3.4.1 Determination of Vanadium (V) *69*
3.4.2 Anion analysis by Ion Chromatography *69*
3.4.3 Aqueous trace metal/loid analysis by Inductively Coupled Plasma Mass Spectrometry (ICP-MS) *70*
3.4.4 Aqueous trace metal/loid analysis by Inductively Coupled Plasma Optical Emission Spectroscopy *72*
3.4.5 Aqueous arsenic speciation analysis by High Performance Liquid Chromatography, Inductively Coupled Plasma Mass Spectrometry *73*
3.5 Organic Geochemistry 74
3.5.1 Dissolved Organic Carbon Analysis *74*
3.5.2 Solid Phase Extraction by C18 Resin Filters *75*
3.6 X-Ray Absorption Spectroscopy 76
3.6.1 EXAFS modelling *79*
3.7 Microbial Community Analysis 80
3.7.1 DNA Extraction, Sequencing and Analysis *80*
3.7.2 16S rRNA gene sequencing *80*
3.7.3 Phylogenetic assignment *81*
3.7.4 Phylogenetic tree building *82*
3.8 Statistical Analysis 82
3.8.1 Standard deviation, relative standard deviation and relative error. *82*
3.8.2 Pearson's correlation measures (r and p-values) *83*
3.9 References 84

CHAPTER 4 BIOGEOCHEMICAL PROCESSES CONTROLLING THE FATE OF VANADIUM AT A LEGACY STEEL SLAG DISPOSAL SITE. 88

Abstract 88
4.1 Introduction 89
4.2 Material and Methods 93
4.2.1 Site Description *93*
4.2.2 Site Sampling *94*
4.2.3 Sample Characterisation *95*
4.2.4 Reduction Microcosm Experiments *96*
4.2.5 Geochemical Analysis *97*
4.2.6 X-ray Absorption Near Edge Structure Spectroscopy (XANES) *98*
4.2.7 DNA Extraction, Sequencing and Analysis *98*
4.2.8 16S rRNA gene sequencing *99*
4.2.9 Phylogenetic tree building *100*
4.3 Results 101
4.3.1 Soil Characterisation and Groundwater Analysis *101*
4.3.2 Reduction microcosm experiments *104*
4.3.3 XANES spectroscopy *107*
4.3.4 DNA extraction, amplification and sequencing *109*
4.4 Discussion 112
4.4.1 Extent of Soil Alteration by highly alkaline steel slag leachates *112*

4.4.2 Microcosm experiments *112*
4.4.3 Microbial Community Analysis *116*
4.5 Conclusions 117
4.6 References 119

CHAPTER 5 GYPSUM ADDITION TO SOILS CONTAMINATED BY RED MUD: IMPLICATIONS FOR ALUMINIUM, ARSENIC, MOLYBDENUM AND VANADIUM SOLUBILITY. 125

Abstract 125
5.1 Introduction 127
5.2 Materials and Methods 130
5.2.1 Sample Collection *130*
5.2.2 Sample Characterisation *130*
5.2.3 Batch Experiments *131*
5.2.4 Column Experiments *132*
5.2.5 Geochemical Analysis *133*
5.3 Results 133
5.3.1 Sample Characterization *133*
5.3.2 Red Mud Addition to Soils *137*
5.3.3 Gypsum Addition to Red Mud / Soil Mixtures *139*
5.3.4 Column Experiments *140*
5.4 Discussion 141
5.4.1 Effect of red mud contamination on Hungarian soils *141*
5.4.2 Effectiveness of Gypsum for the Treatment of Red Mud contaminated soils *143*
5.5 Conclusions and implications for remediation 146
5.6 References 149

CHAPTER 6 MOBILISATION OF ARSENIC FROM BAUXITE RESIDUE (RED MUD) AFFECTED SOILS: EFFECT OF PH AND REDOX CONDITIONS. 153

Abstract 153
6.1 Introduction 155
6.2 Materials and Methods 158
6.2.1 Field Sampling and Sample Handling *158*
6.2.2 Sample Characterization *158*
6.2.3 Red mud batch leaching tests *159*
6.2.4 Aerobic batch experiments *159*
6.2.5 Anaerobic batch experiments *160*
6.2.6 Geochemical Methods *161*
6.2.7 X-ray Absorption Spectroscopy (XAS) *161*
6.3 Results 162
6.3.1 Sample Characterization *162*
6.3.2 Arsenic in red mud *162*
6.3.3 Effect of red mud addition on experimental pH and ORP *166*
6.3.4 Biogeochemical Redox Indicators *170*
6.3.5 Arsenic in microcosm experiments *176*
6.4 Discussion 180
6.4.1 The occurrence of As in red mud and the effect of pH / completing ions on As solubility . *180*
6.4.2 Controls on As release during aerobic incubation *180*
6.4.3 Effects of red mud addition on biogeochemical redox processes *181*
6.4.4 As release in anaerobic experiments with no red mud addition *184*
6.4.5 As release in anaerobic experiments with red mud addition *185*

6.5 Conclusions 186
6.6 References 189

CHAPTER 7 LEACHING OF COPPER AND NICKEL IN SOIL-WATER SYSTEMS CONTAMINATED BY RED MUD FROM AJKA, HUNGARY: THE IMPORTANCE OF SOIL ORGANIC MATTER 194

Abstract 194
7.1 Introduction 195
7.2 Materials and Methods 199
7.2.1 Field Sampling and Sample Handling 199
7.2.2 Long-Term Batch Experiments 199
7.2.3 Geochemical Methods. 200
7.2.4 Solid Phase Extraction (SPE) 201
7.3 Results 201
7.3.1 Sample Characterization 201
7.3.2 Effect of RM addition on microcosm pH and DOC 202
7.3.3 Mobilisation of Cu and Ni from RM affected soil-water systems 204
7.3.5 Organically bound metals 209
7.4 Discussion 210
7.4.1 Effect of red mud addition on soil pH and DOC 210
7.4.2 Controls on Cu release 212
7.4.3 Controls on Ni release 214
7.5 Conclusions 218
7.6 References 220

CHAPTER 8 LEACHING OF VANADIUM IN SOIL-WATER SYSTEMS CONTAMINATED BY RED MUD FROM AJKA, HUNGARY 224

Abstract 224
8.1 Introduction 225
8.2 Materials and Methods 227
8.2.1 Field Sampling and Sample Handling. 227
8.2.2 Reduction Microcosm Experiments 228
8.2.3 Geochemical Methods. 228
8.2.4 Solid Phase Extraction (SPE) 229
8.2.5 X-ray Absorption Near Edge Structure Spectroscopy (XANES) 229
8.3 Results 231
8.3.1 Sample Characterization 231
8.3.2 Evolution of V from red mud affected soil-waters systems 231
8.3.5 % Organically bound vanadium 234
8.3.6 XAS Spectroscopy 235
..... 236
8.4 Discussion 237
8.5 Conclusions 242
8.6 References 243

CHAPTER 9 SUMMARY AND FUTURE CONSIDERATIONS 246

9.1 Summary 246
9.2 Preliminary hypotheses revisited and major findings 246
9.2.1 V from iron and steel slag - Hownsgill Valley, nr Consett, U. K 246
9.2.2 Addition of red mud to soils (Chapters 5 -8) 247
9.2.3 Red mud addition to aerobic soil-water systems (Chapters 6 -8) 250

9.2.4 Red mud addition to anaerobic soil-water systems (Chapters 6 - 8) 250
9.3 IMPLICATIONS 252
9.4 FUTURE CONSIDERATIONS 254
9.6 REFERENCES 256

APPENDIX A ADDITIONAL RESULTS 258

A1 Clone Library 258
A2 XRD Patterns 259

APPENDIX B ASSOCIATED PUBLICATIONS 263

B1 RELEVANT PUBLICATIONS 263
B2 OTHER PUBLICATIONS 263
B3 CONFERENCE PROCEEDINGS 263

List of Figures

Figure 2.1	Molecular Environmental Processes affecting contaminants	19
Figure 2.2	Adsorption of metals cations on ferrihydrite	24
Figure 2.3	Adsorption of metal/loid oxyanions on ferrihydrite	24
Figure 2.4	Historic map of The Grove Heaps, nr Consett	35
Figure 2.5	Satellite image of Hownsgill Valley, nr Consett	36
Figure 2.6	Digital photograph of alkaline leachate pond	37
Figure 2.7	Digital photograph of calcite precipitates around leachate pond	37
Figure 2.8	Satellite image showing extent of red mud release	41
Figure 2.9	Digital photograph of red mud house, awaiting destruction	41
Figure 3.1	Digital photograph of Consett Soil	56
Figure 3.2	Map of affected area at Ajka, with sampling locations	57
Figure 4.1	Schematic diagram of Hownsgill Valley site, nr Consett	95
Figure 4.2	Geochemical responses for Consett batch experiments	106
Figure 4.3	V K-Edge XANES spectra for Consett samples	108
Figure 4.4	V K-Edge XANES plot	109
Figure 4.5	Rarefaction curve for Consett soil sample	110
Figure 4.6	Pie chart showing microbial community of Consett soil sample	110
Figure 4.7	Phylogenetic tree – sequence CL-R0-38	111
Figure 4.8	Eh/pH diagram of V species for Consett experiments	115
Figure 5.1	PCA analysis of Ajka red mud and soils	134
Figure 5.2	Red mud additions to Hungarian soils, pH, TDS and DOC	138
Figure 5.3	Red mud additions to Hungarian soils, oxyanions (no gypsum)	138
Figure 5.4	Red mud additions to Hungarian soils, oxyanions (with gypsum)	140
Figure 5.5	Column experiments, evolution of pH, TDS and DOC	141
Figure 5.6	Oxyanion concentration vs pH (with and without gypsum)	145
Figure 6.1	As K-Edge XANES for red mud sample	164
Figure 6.2	As EXAFS for red mud sample	165
Figure 6.3	Red mud batch leaching tests	166
Figure 6.4	Geochemical time series; pH and ORP (aerobic)	168

Figure 6.5	Geochemical time series; pH and ORP (anaerobic)	169
Figure 6.6	Geochemical time series; nitrate and nitrite (anaerobic)	172
Figure 6.7	Geochemical time series; Fe(II), As (aerobic)	173
Figure 6.8	Geochemical time series; Fe(II), SO_4^{2-}, As (anaerobic)	174
Figure 6.9	Geochemical time series; pH, Fe(II), SO_4^{2-} (heat treated controls)	175
Figure 6.10	As K-Edge XANES for anaerobic experiments	179
Figure 6.11	[As] vs pH for aerobic and anaerobic experiments	188
Figure 7.1	Geochemical time series; Cu and Ni (unamended controls)	206
Figure 7.2	Geochemical time series; Cu and Ni (aerobic and anaerobic)	207
Figure 7.3	Eh/pH diagram of Cu species	216
Figure 7.4	Eh/pH diagram of Ni species	217
Figure 8.1	Geochemical time series; V (aerobic and anaerobic)	233
Figure 8.2	V K-Edge XANES for anaerobic experiments	236
Figure 8.3	V K-Edge XANES plot	237
Figure 8.4	Eh/pH diagram of V species	241
Figure A1	XRD pattern – Consett surface soil	259
Figure A2	XRD pattern – Consett deep soil	260
Figure A3	XRD patterns – Ajka soils	261
Figure A4	XRD pattern – Ajka red mud	262

List of Tables

Table 2.1	Chemical composition of iron and steel slags	16
Table 2.2	Elemental and mineral composition of various red muds	18
Table 2.3	Environmentally significant microbial half reaction reduction potentials	29
Table 2.4	Typical slag analyses from former Consett Steelworks	34
Table 2.5	Mean hydrochemical composition of Consett leachate	38
Table 2.6	Composition of digested sediments from Hownsgill Valley	38
Table 4.1	Consett soil elemental composition	102
Table 4.2	Consett soil characterisation	103
Table 4.3	Consett groundwater analysis	103
Table 4.4	V K-Edge XANES summary	107
Table 5.1	Red mud and Hungarian soil characterisation	135
Table 5.2	Red mud and Hungarian soil elemental analysis	136
Table 6.1	As K-Edge EXAFS fitting	163
Table 6.2	% As(V) and As(III) in aqueous phase	177
Table 7.1	DOC concentrations	203
Table 7.2	Range of other metal concentrations from end point solutions	208
Table 7.3a	% Organically bound Cu and Ni from anaerobic experiments	209
Table 7.3b	% Organically bound Cu and Ni from aerobic experiments	209
Table 7.4	Pearson's regression analysis; DOC, pH for Cu and Ni	215
Table 8.1	% Organically bound V from aerobic and anaerobic experiments	234
Table 8.2	V K-Edge XANES summary	235
Table 8.3	Pearson's regression analysis; DOC and pH for V	239
Table A1	Clone library – Consett soil microbial sequences	258
Table A2	Data from duplicate batch experiment data	262

Abbreviations

AMD	Acid Mine Drainage
BDRA	Bauxite Disposal Residue Area
COPR	Chromate Ore Processing Residue
BF	Blast Furnace
BOF	Basic Oxygen Furnace
CRM	Certified Reference Material
DCTA	1,2-diaminocyclohexanetetra acetic acid
DIW	Deionised Water
DOC/M	Dissolved Organic Carbon / Matter
EAF	Electric Arc Furnace
EXAFS	Extended X-Ray Absorption Fine Structure
FT	Fourier Transform
IC	Ion Chromatography
ICP-MS / OES	Inductively Coupled Plasma-Mass Spectrometry / Optical Emission Spectrometry
LOI	Loss on Ignition
$[M^+]$	Concentration of metal ions
NOM / OM	Natural Organic Matter / Organic Matter
OFN	Oxygen Free Nitrogen
ORP	Oxidation/Reduction Potential
OTU	Operational Taxonomic Unit
PCA	Principle Component Analysis
PCR	Polymerase Chain Reaction
RDP	Ribosomal Database Project
SD / RSD	Standard Deviation / Relative Standard Deviation
SOM	Soil Organic Matter
SPE	Solid Phase Extraction
TEA / P	Terminal Electron Acceptors / Accepting Process
TCLP	Toxic Characteristic Leaching Procedure
TDS	Total Dissolved Solids
WHO	World Health Organisation
XANES	X-ray Absorption Near Edge Structure
XAS	X-Ray Absorption Spectroscopy
XRD / F	X-Ray Diffraction / Fluorescence

Chapter 1 Introduction

1.1 Project background and significance

The main focus of this thesis was to investigate the fate and environmental behaviour of potentially toxic trace elements derived from alkaline waste into the wider environment.

Past research and legislation relating to waste management has focussed on heavy metal contamination from mining activities. The environmental problems associated with acid mine/rock drainage from sulfide minerals are well documented (Johnson and Hallberg, 2005). These acidic waters often contain elevated concentrations of Cu, Cd Fe, Mn, Pb, Ni and Zn which are mobilised due to their increased solubility at low pH and can have a considerable impact on the surrounding environment (Younger et al., 2005)

In the past, alkaline wastes, usually derived from industrial activities such as; bauxite ore processing, steel production, chromite ore processing, have received less attention due to relatively low volumes of waste. However, recent increases in production of steel (worldwide steel production increased from 851 Mt in 2001 to 1,607 Mt in 2013 (World Steel Association, 2014)) and a lack of economically viable recycling options for bauxite processing waste (Power et al., 2011) means that the problems associated with alkaline wastes are gaining more attention. Alkaline wastes give cause for concern not only due to the high concentrations of heavy metals found in the wastes but high pH leachates can mobilise toxic oxyanion forming elements such as As, Cr, Mo, Se and V (Cornelis et al., 2008).

The original aim of this thesis was to investigate the processes controlling the fate and transport of vanadium (and then possibly other metals such as Cr) from a legacy steel slag site; the Hownsgill Valley, nr Consett, County Durham, U.K. The Hownsgill Valley was used to dump iron and steel slags for over a century until the closure of the Consett Steelworks in 1980. The valley contains a wetland that has been affected by high pH leachates percolating through the slag wastes forming a large alkaline leachate pond. The surrounding soil is characterised by high rates of calcite precipitation and relatively high aqueous vanadium concentrations occur across the site (Mayes et al., 2006; Mayes et al., 2008).

However, on the 4th October 2010, towards the start of the doctoral research, a spill occurred at a bauxite residue disposal area (BDRA) in Ajka, western Hungary where 1 million m^3 of caustic red mud suspension was released from a failed tailings dam. The spill caused 10 deaths, injured over 100 people, ruined homes, property and land. A red mud spill of this magnitude was unprecedented and relief efforts were hampered due to a lack of knowledge of the contaminant material (Adam et al., 2011a). It is now known that the Ajka red mud has a very high pH (pH >13) and contains high concentrations of oxyanion forming elements as well as other potentially toxic metals (Ruyters et al., 2011; Mayes et al., 2011). The opportunity to go to the area affected by the red mud spill arose and the aim of the thesis shifted to an investigation of the mobilisation of trace metals from Ajka red mud with a particular focus on soils and wetland areas inundated by red mud as a result of the spill.

1.2 Research objectives

This thesis reports the findings of an investigation into the mobilisation of trace elements from red mud into soil-water systems and a pilot study into the mobilisation of V from steel slag. The research hypotheses for these two sites have therefore been shown separately.

1.2.1 Hownsgill Valley, nr Consett, U.K.

The pilot study beginning the investigation into the processes controlling V mobilisation from steel slag started with the following hypotheses:

- Soils affected by steel slag leachates will contain an indigenous population of microorganisms that are adapted to survive and grow at high pH; microbial bioreduction processes will, therefore be supported in this environment.
- The observed decrease in aqueous vanadium concentrations in the alkaline leachate with distance away from the source is (at least in part) due to in situ microbially mediated reduction of V(V) to produce less soluble V(IV) species.

1.2.2 Ajka, western Hungary

The following research hypotheses were used as a guide to the main body of the research:

- Addition of caustic red mud to soils will cause an increase in soil pH and as a consequence concentrations of several toxic oxyanion forming elements (e.g.

As, Al, V, Mo) will increase in associated waters due to their lower sorption to minerals at high pH.

- Soils containing higher concentrations of organic matter (or larger quantities of clay minerals) content will have a higher intrinsic buffering capacity with respect to addition of alkalinity (from red mud), producing lower soil pH, and lower aqueous concentrations of oxyanion forming elements.

- Addition of red mud in soils will cause the solubilisation of soil organic matter (due to higher pH), resulting in increased dissolved organic carbon (DOC) concentrations, and, higher concentrations of elements known to complex strongly with DOC (e.g. Cu and Ni).

- Increasing the concentration of anionic species in solution (e.g. phosphate, carbonate) that are known to compete for available sorption sites on minerals, will result in enhanced solubility of toxic oxyanion forming species (such as As) regardless of soil pH.

- Addition of gypsum (as a source of Ca^{2+}) to red mud affected soils will promote OH^- consuming carbonate precipitation reactions, reducing soil pH, and producing lower oxyanion concentrations due to enhanced sorption at circumneutral pH.

- In aerobic soil-water systems containing red mud, equilibration with atmospheric CO_2 will also result in lower soil pH and lower oxyanion concentrations.

- In anaerobic soil-water systems containing red mud, microbial bioreduction processes will produce reducing conditions with time, promoting the reduction

of As(V) to generally more soluble As(III) species, thus increasing the risk of enhanced As mobility.

- Conversely, bioreduction processes will also promote the transformation of V(V) to V(IV) species, which strongly adsorbs to minerals at alkaline pH, resulting in lower solution concentrations.

- Soil affected by red mud additions will not contain microbial communities that are adjusted to alkaline conditions, therefore bioreduction processes will be inhibited at high pH.

1.3 Experimental approaches

To test these hypotheses, a multidisciplinary approach was taken. To this end, research methods and analytical techniques from a variety of scientific disciplines including; geochemistry, biogeochemistry and molecular biology were employed. Extensive soil and sample characterisation was completed on the soils from both sites and the red mud using various techniques such as XRD, XRF and BET specific surface area.

At the Ajka site, three main comparisons were made, being the differences between 1) unremediated wetland areas and soils where red mud had been ploughed into the soil, 2) aerobic and anaerobic conditions and, 3) oxyanion forming elements (As and V) and cationic elements (Cu and Ni). In order to fully elucidate these differences batch microcosm experiments were prepared using unaffected Hungarian soils mixed with red mud. Heat treated controls were prepared to distinguish between biotic and abiotic processes and soil-only microcosms were prepared to determine

background concentrations. The aqueous phase and sediment sampled from the microcosms at various time points were then tested for aqueous metal/loid ion evolution, biogeochemical indicators (Fe(II), nitrate, sulfate), pH and redox potential over time. This enabled the production of time series data and a comparison between the changes during the development of microbial anoxia and without. Only a small volume of sample was extracted during the time series making it difficult for lots of different analyses but further testing at the end of the incubation periods on both the aqueous phase and sediment allowed for the use of additional techniques including: XAS analysis, As speciation via HPLC-ICP-MS, dissolved organic carbon, and % organically bound metals using a solid phase extraction technique.

Anaerobic batch microcosms were also used for the pilot study at the Hownsgill Valley site but the amount of additional analysis was less extensive. An important aspect at this site however, was to establish the presence of an alkaliphilic microbial community. 16s rRNA gene fragments were recovered in order to determine the microorganisms present. The quality of each sequence was assessed and non-chimeric sequences were uploaded to the EMBL Genbank database. A combination of the Ribosomal Database Project (RDP) Naïve Bayesian classifier (Wang et al., 2007), the construction of a phylogenetic tree and MOTHUR analysis (Schloss et al., 2009) allowed for these sequences to be assigned to taxonomy and the community structure to be investigated. This allowed for the comparison of the dominant species to be compared to those found at other important alkaline waste sites (Whittleston et al., 2013).

1.4 Thesis structure

This thesis consists of nine chapters. The thesis begins with an introduction to the problems associated with alkaline wastes and specifically steel slags and red mud. This is followed with an overview of the chemistry and processes that govern the fate of As, Cu, Ni and V in the environment. There is also a brief introduction to the two study sites that are the focus of this research. A detailed chapter of the methods and analytical techniques then follows. Results are in the form of five working chapters, three of which have been prepared or are in the processes of preparation for publication and two pilot studies into the behaviour of vanadium at the different sites. Finally, the results from chapters 4 to 8 are summarised and discussed in chapter 9. In addition, comprehensive appendices of additional data are included together with a list of associated publications.

1.5 References

ADAM, J., BANVOLGYI, G., DURA, G., GRENERCZY, G., GUBECK, N., GUPTER, I., SIMON, G., SZEGFALVI, Z., SZEKACS, A., SZEPVOLGYI, J. & UJLAKY, E. 2011. The Kolontar report: Causes and Lessons from the Red Mud Disaster. In: B, J. (ed.). Budapest: Sustainable Development Committee of the Hungarian Parliament.

CORNELIS, G., JOHNSON, C. A., VAN GERVEN, T. & VANDECASTEELE, C. 2008. Leaching mechanisms of oxyanionic metalloid and metal species in alkaline solid wastes: A review. Applied Geochemistry, 23, 955-976.

JOHNSON, D. B. & HALLBERG, K. B. 2005. Acid mine drainage remediation options: a review. Science of the Total Environment, 338, 3-14.

MAYES, W. M., JARVIS, A. P., BURKE, I. T., WALTON, M., FEIGL, V., KLEBERCZ, O. & GRUIZ, K. 2011. Dispersal and Attenuation of Trace Contaminants Downstream of the Ajka Bauxite Residue (Red Mud) Depository Failure, Hungary. Environmental Science & Technology, 45, 5147-5155.

MAYES, W. M., YOUNGER, P. L. & AUMONIER, J. 2006. Buffering of alkaline steel slag leachate across a natural wetland. Environmental Science & Technology, 40, 1237-1243.

MAYES, W. M., YOUNGER, P. L. & AUMONIER, J. 2008. Hydrogeochemistry of alkaline steel slag leachates in the UK. Water Air and Soil Pollution, 195, 35-50.

POWER, G., GRAFE, M. & KLAUBER, C. 2011. Bauxite residue issues: I. Current management, disposal and storage practices. Hydrometallurgy, 108, 33-45.

RUYTERS, S., MERTENS, J., VASSILIEVA, E., DEHANDSCHUTTER, B., POFFIJN, A. & SMOLDERS, E. 2011. The Red Mud Accident in Ajka (Hungary): Plant Toxicity and Trace Metal Bioavailability in Red Mud Contaminated Soil. Environmental Science & Technology, 45, 1616-1622.

SCHLOSS, P. D., WESTCOTT, S. L., RYABIN, T., HALL, J. R., HARTMANN, M., HOLLISTER, E. B., LESNIEWSKI, R. A., OAKLEY, B. B., PARKS, D. H., ROBINSON, C. J., SAHL, J. W., STRES, B., THALINGER, G. G., VAN HORN, D. J., WEBER, C. F. 2009. Introducing mothur: Open-Source, Platform-Independent, Community-Supported Software for Describing and Comparing Microbial Communities. Applied and Environmental Microbiology, 75, 7537-7541.

WANG, Q., GARRITY, G. M., TIEDJE, J. M. & COLE, J. R. 2007. Naive Bayesian classifier for rapid assignment of rRNA sequences into the new bacterial taxonomy. Applied and Environmental Microbiology, 73, 5261-5267.

WHITTLESTON, R. A., STEWART, D. I., MORTIMER, R. J. G. & BURKE, I. T. 2013. Enhancing microbial iron reduction in hyperalkaline, chromium contaminated sediments by pH amendment. Applied Geochemistry, 28, 135-144.

WORLD STEEL ASSOCIATION. 2014. Key Facts about the world of steel [Online]. Available: http://www.worldsteel.org/media-centre/key-facts.html [Accessed 18th April 2014]

YOUNGER, P. L., COULTON, R. H. & FROGGATT, E. C. 2005. The contribution of science to risk-based decision-making: lessons from the development of full-scale treatment measures for acidic mine waters at Wheal Jane, UK. Science of the Total Environment, 338, 137-154.

Chapter 2 Background Information and Site Processes

This chapter provides an overview of industrial processes responsible for the production of alkaline waste whilst looking specifically at the contaminants: arsenic, copper, nickel and vanadium and the main processes controlling the transport of these contaminants from alkaline waste into affected soils. This chapter will also provide an introduction to the study sites investigated in this thesis.

2.1 Alkaline Environments

Alkaline environments occur both naturally and as a direct result of anthropogenic activities. Naturally occurring alkaline environments are relatively uncommon. Typical examples are; soda lakes (Jones et al., 1998), some thermal springs (e.g. Mushroom Springs at Yellowstone National Park (Ward et al., 2006)), oceanographic cold seeps (Takai et al., 2005) and ground-waters affected by the weathering of ultramafic rocks (Tiago et al., 2004). Soda lakes, such as those found in the East African Rift Valley and in the western United States typically have a pH of between 9 -12 and high salinity (ranging from brackish to hyper-saline) (Jones et al., 1998; Lanzen et al., 2013). Despite high salinity and high pH, soda lakes have been found to be areas of high microbial productivity (Jones et al., 1998; Pollock et al., 2007; Zhilina et al., 2009).

Much more common are anthropogenic sites, which occur as a result of high pH industrial waste. Industries such as chromium ore processing (Deakin et al., 2001), lime burning (Burke et al., 2012b), borax production (Ye et al., 2004), bauxite mining (Grafe et al., 2011) and steel manufacturing (Mayes et al., 2008) generate alkaline wastes.

Although each of these wastes are essentially different due to the origin of ores and differing production processes, there are some similarities (Cornelis et al., 2008). When alkaline wastes are left to degrade in the open, equilibration takes place with the external environment which results in a leaching process. Typically the leachate generated has a very high pH (pH 10-13) due to the presence of Ca, Na and K oxides that hydrolyse in water to produce soluble metal hydroxides (Hind, et al., 1999). The mobilisation of these soluble metal hydroxides into adjacent soil and water systems are therefore a cause for environmental concern.

2.2 Alkaline industrial wastes

2.2.1 Problems associated with high alkaline industrial wastes

The legacy of the inefficient disposal of alkaline waste can lead to several environmental issues. Disposal sites rarely have impermeable barriers underneath the waste, therefore allowing the leachate to migrate and mobilise any soluble contaminants into the wider environment (Burke et al., 2012b). In some cases, the weathering of alkaline waste has resulted in the alkalisation of groundwater or the formation of large alkaline leachate ponds (Roadcap et al., 2005; Mayes et al., 2006; Czop et al., 2011). Large-scale infilling of wetlands with steel slag in the Lake Calumet region, Illinois, United States has resulted in an alkaline groundwater system where pH is as high as 12.8 (Roadcap et al., 2005). Bauxite processing residue dumped in a former limestone quarry has resulted in the formation of an alkaline pit lake (pH 11.5 - 13.3) in the Chrzanow region, southern Poland (Czop et al., 2011). The high pH water, can itself be toxic to some fish populations (Wilkie and Wood, 1996) but there are other environmental and ecological problems that are associated with alkaline leachates.

In many of the industries that produce alkaline wastes, lime is used in the production process and unless recycled is present in large quantities in the discarded waste. When lime (CaO) in the waste comes in contact with water it produces aqueous $Ca(OH)_2$ (Equation 2.1), which dissociates into its component ions and the alkalinity of the resulting solution, is increased by the presence of hydroxide ions (Equation 2.2).

$$CaO_{(s)} + H_2O_{(l)} \leftrightarrow Ca(OH)_{2\ (aq)} \quad (2.1)$$

$$Ca(OH)_{2(aq)} \leftrightarrow Ca^{2+}_{(aq)} + 2OH^-_{(aq)} \quad (2.2)$$

High concentrations of Ca^{2+} ions in the leachate can then cause further ecological impact by the precipitation of calcite. The formation of calcite hardpans can smother benthic habitats and reduce light penetration to benthic primary producers (Bayless and Schulz, 2003; Mayes et al., 2006). When the alkaline leachate comes into contact with atmospheric CO_2, as it does at the surface or a groundwater spring, carbonate precipitates, as shown in the following the reaction sequence (Equations 2.3 – 2.7). (Schwab et al., 2006; Mayes et al., 2008)

$$CO_{2(g)} \leftrightarrow CO_{2(aq)} \quad (2.3)$$

$$CO_{2(aq)} + H_2O \leftrightarrow H_2CO_{3(aq)} \quad (2.4)$$

$$H_2CO_{3(aq)} \leftrightarrow H^+ + HCO_3^-{}_{(aq)} \quad (2.5)$$

$$HCO_3^-{}_{(aq)} + OH^-_{(aq)} \leftrightarrow H_2O_{(l)} + CO_3^{2-}{}_{(aq)} \quad (2.6)$$

$$Ca^{2+}_{(aq)} + CO_3^{2-}{}_{(aq)} \leftrightarrow CaCO_{3(s)} \quad (2.7)$$

Another environmental problem associated with alkaline leachates is the elevated concentrations of aqueous metal and metalloids. In the past, research as been

mainly focused on metals that have been found at high solid concentrations in alkaline wastes such as; Cu, Cd, Hg, Pb and Zn (Cornelis et al., 2008). However, oxyanion forming elements, such as As, Cr, Mo and V, are often found in relatively high concentrations in alkaline leachates, despite being present at a low weight % in solid waste, due to their increased solubility at high pH (Langmuir, 1997; Cornelis et al., 2008). The mobilisation of oxyanion forming elements by leachates is dependent upon a number of factors including; redox state, precipitation and sorption with metal oxides and microbial processes, all of which will be explored further in this chapter.

2.2.2 Iron and steel slags

It is estimated that between 270 and 320 million tonnes of iron slag and 150 - 230 million tonnes of steel slag are produced annually worldwide (U.S. Geological Survey, 2013). The process of slag recycling is relatively modern and in the past slags have been dumped in slag heaps and left to degrade in the open allowing for contamination of the surrounding area (Roadcap et al., 2005; Mayes et al., 2008). However, slag recycling is becoming increasingly popular and it is currently used in the construction industry (Chaurand et al., 2007a; U.S. Geological Survey, 2013), as fertilizers or soil conditioners (Haynes et al., 2013) and some research suggests that it may be useful for CO_2 sequestration (Bonenfant et al., 2008). The recycling of slags is not without issues and several problems have been reported. Schwab et al. (2006) reported a high pH leachate with a strong sulfur odour emerging from weathered slag used in road construction only two years after construction. The use of basic slag containing ~3% vanadium when used as a soil fertilizer resulted in the death of 23 heifers from acute vanadium poisoning (Frank et al., 1996).

There are three main types of slag produced in the UK 1) blast furnace (BF) which is formed from the production of iron 2) basic oxygen furnace (BOF) which uses hot iron from BF or steel scraps to produce steel and 3) electric arc furnace (EAF) which uses cold scrap steel only for steel production (The European Slag Association, 2014). In each method of production, fluxing agents (limestone [$CaCO_3$] or dolomite [$CaMg(CO_3)_2$]) are added to increase heat transfer and remove impurities. The fluxing agents combine with impurities in the molten iron or steel to create slag. Once removed from the molten metal, the slag is either cooled by water or left to air cool and broken up for transport (The European Slag Association, 2014).

Due to the presence of the limestone and dolomite fluxing agents the composition of slag produced from each method is generally very similar, although there tend to be more impurity in BF originating from the iron ore (Proctor et al., 2000). The main components of slags, in varying concentrations, (see Table 2.1) are oxides of calcium, silicon, aluminium, magnesium, manganese and iron, with trace concentrations of various sulfates and phosphates (Proctor et al., 2000; Navarro et al., 2010). Slags can also contain, in varying concentrations, toxic elements such as As, Cr, Cd, Hg, Mo, Pb and V (Roadcap et al., 2005; Chaurand et al., 2007a; Navarro et al., 2010).

Although, slag is generally considered to be a non-hazardous material there is some environmental concern about the highly alkaline leachates produced from slag weathering and the mobilisation of trace metal/loids (Schwab et al., 2006; Chaurand et al., 2007a; Navarro et al., 2010). Toxicity characteristic leaching procedure (TCLP) tests have shown that many of the trace metals are not readily leachable (Proctor et al., 2000). However, the pH of the TCLP test is ~4.9 (United States Environmental Protection Agency, 1992) and the leachate produced from weathered slag is generally between pH 10 and 13 (Schwab et al., 2006; Cornelis et al., 2008). This large difference

between the pH of TCLP tests and high pH leachates has been shown to underestimate the release of trace metals from other alkaline wastes, such as red mud (see section 2.2.3) (Rubinos and Barral, 2013).

Table 2.1 Chemical composition of iron and steel slags (taken from Schwab et al. (2006)* and Geiseler (1996)**)

Type of Slag	CaO (%)	SiO_2 (%)	Al_2O_3 (%)	MgO (%)	MnO (%)	$Fe_{(total)}$ (%)
BF**	32-45	32-42	7-16	5-15	0.2-1.0	<4
BOF*	42-55	12-18	<3	<8	<5	14-20
EAF*	25-40	10-17	<7	4-15	<6	18-29

2.2.3 Bauxite ore processing waste (red mud)

Red mud is the name given to the fine fraction waste resulting from bauxite ore processing for the extraction of alumina via the Bayer process. The Bayer process is a high temperature, high pressure process. The main aluminium bearing minerals are gibbsite ($Al(OH)_3$) and/or boehmite (γ-AlOOH) (Grafe et al., 2011). The temperature and pressure of the process is dependent upon the mineralogy of the bauxite ore used, e.g. ore containing boehmite requires higher temperatures and pressures compared to gibbsite (Power et al., 2011). Sodium hydroxide (NaOH) is used to dissolve the Al^{3+} (as aluminate, $Al(OH)_4^-$) in the ore. Once dissolved, the sodium aluminate solution is retained for further refining to alumina and the remaining insolubles are disposed of as red mud waste. Any excess NaOH is then recycled back into the Bayer process. The use of NaOH during the Bayer process means that red mud has a very high pH (pH >13), even after repeated washing. Neutralization treatments; such sea water pumping or CO_2 sparging is sometimes carried out or red mud is dried and stored as dry filter cakes but

in other cases red mud is left untreated in wet lagoons (~20-30 wt.% solids) (Power et al., 2011).

The high temperatures and pressures of the Bayer process have a profound effect on the mineralogical composition of bauxite ore, therefore the mineralogical composition of red mud is highly altered. The specific composition of red mud is dependent upon the bauxite ore and some of the original ore minerals remain after processing such as; rutile (TiO_2) and gibbsite. Silicate minerals present in the ore (e.g. clays) are typically converted to characteristic neo-formed process solids such as; sodalite, cancrinite and calcite. Any iron oxides in the ore are recrystallized as goethite (FeOOH), hematite (Fe_2O_3) and magnetite (Fe_3O_4), and it is the ferric oxides that give the waste its distinctive colour (Table 2.2) (Hind et al., 1999; Grafe et al., 2011).

It takes between 2 and 3.6 tonnes of bauxite ore to produce just 1 tonne of alumina (Hind et al., 1999) resulting in large quantities of red mud waste. In excess of 2.7 billion tonnes of red mud are currently held in storage worldwide with an annual growth rate of 120 million tonnes (Klauber et al., 2011). A great deal of research has taken place attempting to find possible applications for red mud, however; an economically viable use has so far proved elusive. There are three main areas of red mud utilization currently under investigation: 1) for use in construction as a ceramic building product (Klauber et al., 2011) 2) environmental and agronomic applications either as a soil or waste water ameliorant (Gupta et al., 2001; Feigl et al., 2012) or 3) recovery of metals such as aluminium, iron, trace and rare earth metals (Piga et al., 1993).

Table 2.2 – Elemental and mineralogical composition of various worldwide red mud (taken from Grafe and Klauber (2011))

Element	Content % (avg ±std)	Minerals
Fe_2O_3	40.9 ±15.6	Hematite, Goethite, Magnetite
Al_2O_3	16.3 ± 6.4	Boehmite, Gibbsite, Diaspore,
SiO_2	9.6 ± 6.7	Quartz, sodalite, Cancrinite
TiO_2	8.8 ± 4.4	Rutile, Anatase, Perovskite, Ilmenite
CaO	8.6 ± 9.4	Calcite, Perovskite Whewellite, hydro-calumite
Na_2O	4.5 ± 3.3	Sodalite, Cancrinite, Dawsonite
LOI	10.0 ± 2.8	Water, oxalate, other organics

One of the main problems associated with red mud reuse is regarding the nature of red mud itself, not only does red mud have a very high pH but it also has a high salt content and is known to contain elevated concentrations of toxic and potentially toxic metal/loids (Czop et al., 2011; Grafe et al., 2011; Rubinos and Barral, 2013). In some cases, red mud can contain high concentrations of radiogenic elements such as Th and U (Gamaletsos et al., 2011). There has been much research on the use of red mud as a soil ameliorant, identifying it as a possible amendment for heavy metal or arsenic contaminated soils (Lombi et al., 2002; Castaldi et al., 2010; Garau et al., 2011). However, other researchers have shown that there can be a trade off effect to this type of soil remediation: when added in increasing quantities the use of red mud becomes unattractive due to the release of toxic oxyanion forming elements such as As, Cr and V (Summers et al., 1993; Friesl et al., 2004). Other researchers have shown that there are some eco-toxicological effects from the addition of red mud to soils due to increased soil pH and stress due to increased soil salinity (Ruyters et al., 2011; Klebercz et al., 2012).

2.3 Fate and transport of metal/loids in the environment

The chemistry and reactivity of each element is different (for example, solubility in water) and can change depending upon many factors; pH, Eh, elemental concentration, microbial transformation and complexation to inorganic and organic substrates. These factors control the chemical speciation, bioavailability (and thereby the toxicity) and transport mechanisms of contaminants in the environment. Figure 2.1 shows some of the important processes affecting trace metal/loids in the environment.

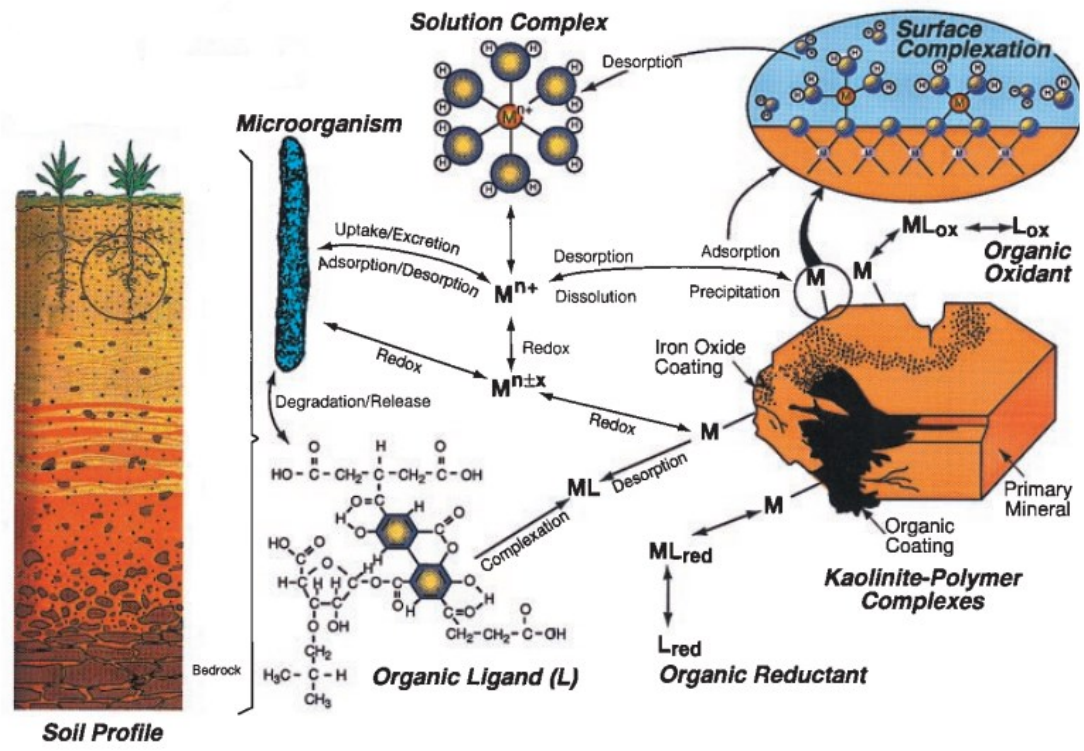

Figure 2.1 - Schematic illustration of a variety of molecular environmental processes affecting contaminant elements in soils and groundwater (adapted from Brown et al. (1999)).

2.3.1 Brief introduction to the contaminants of interest

High concentrations of some metal/loids in the environment are of concern due to their toxicity to humans and other biota. Certain metals are essential to life and a deficiency in these metals can be harmful but excessive concentrations can also result in serious illness or even death. The toxicity of a specific metal/loid depends upon its chemistry, speciation, concentration and the route of contact to the organism affected. In the case of contaminated land or water; a contaminant can be deemed to be a substance that is at a concentration above that of natural background levels. Common exposure pathways in which an organism can be affected by a contaminant in the environment are inhalation, ingestion or direct contact from contaminated ground or surface water, soil, air or food. Four potentially problematic and toxic metal/loids are investigated in this thesis with regards to their mobilisation from alkaline waste into the environment; As, Cu, Ni and V.

Arsenic is an extremely toxic metalloid that can exist in the environment in many different oxidation states (-3, 0, +3 and +5) but in most natural waters it forms oxyanions of As(III), arsenite and As(V), arsenate (Smedley and Kinniburgh, 2002). Arsenic is most toxic in a reduced form: As(III) is 60 times more toxic than As(V) (Ratnaike, 2003). Arsenic is an essential micronutrient for some animals but is not thought to be an essential trace metal for humans (Nielsen, 1991). Chronic arsenic poisoning is a large scale problem affecting over 120 million people in southern Asia who are exposed to drinking water extracted from groundwater which contains high concentrations of naturally occurring arsenic (Charlet and Polya, 2006).

Compared to arsenic there is a paucity of information on vanadium toxicity and there is much debate upon whether or not V is an essential trace element for humans

(Nielsen, 1991; Barceloux, 1999d). Vanadium is a transition element that occurs in many different oxidation states (-1 to +5) although the most common valences are +3, +4 and +5 (Wanty and Goldhaber, 1992). Unlike As, the most toxic form of V is the most oxidised; V(V) as the vanadate oxyanion and the most documented cases of vanadium poisoning are from the inhalation of vanadate dusts (Barceloux, 1999d).

Nickel is a transition metal which occurs mostly in the +2 oxidation state but can occur as +1 and +3. Like As, a deficiency of Ni in humans has yet to be observed so it is not deemed an essential micronutrient (Barceloux, 1999c). Nickel is a very common sensitising agent, causing contact dermatitis. Chronic nickel exposure is known to affect the respiratory system (Barceloux, 1999c; Cempel and Nikel, 2006). There is some evidence to suggest that in certain forms (i.e. metallic) that nickel may be a potent carcinogen (World Health Organisation, 2008).

Copper is also a transition metal and occurs in the environment mostly as Cu(0), Cu(I) and Cu(II) but unlike Ni and As, Cu is an essential micronutrient for plants, animals and humans (Barceloux, 1999b). However, it is very toxic to some forms of aquatic life and humans in high doses and, is used as a suicidal agent in some parts of the world (Bremner, 1998; Barceloux, 1999b). Some domestic animals, such as pigs, rabbits and horses can tolerate high levels of Cu in their diets (Flemming and Trevors, 1989; Barceloux, 1999b), however, sheep are very sensitive to Cu and can develop signs of copper toxicosis after a relatively low dietary intake of ~25 mg kg^{-1} (Bremner, 1998). In order for Cu to be biologically available and therefore toxic, it must be present in soluble form making the speciation of Cu very important when assessing Cu toxicity (Flemming and Trevors, 1989).

2.3.2 Sorption

Sorption can be defined as the accumulation of ions or molecular complexes to a mineral surface or structure. There are three main sorption mechanisms at the mineral-water interface: 1) simple electrostatic attraction of aqueous species often referred as physi-sorption or outer-sphere complexation 2) formation of chemical bonds between a mineral surface (sorbant) and an aqueous species (sorbate) often referred to as adsorption or inner-sphere complexation and 3) structural incorporation of aqueous species by replacement of structural ions often referred to as absorption or isomorphic substitution.

The effects from competitive sorption are important in environmental systems as the effects can lead to increased aqueous contaminant concentrations. When metals are bound by outer-sphere complexes it allows for similar sorbates to compete for sorption sites whereas inner-sphere complexes are able to resist desorption even at a high ionic strength of the competing sorbate (Brown and Parks, 2001). This is particularly important for environmental systems containing arsenate and phosphate, which can lead to increased aqueous As concentrations, especially with increasing pH (Gao and Mucci, 2001; Dixit and Hering, 2003). Vanadate can also act as a phosphate analogue (Rehder, 1991) so both anions will compete for sorption sites, however V(V) has been shown to only have a small competitive effect on As(V) uptake by Fe and Al oxides (Jeong et al., 2007). Other well known sorbates competing with As(V) for sorption sites are (bi)carbonates and silicates (Appelo et al., 2002; Jeong et al., 2007). Competitive sorbates for Cu and Ni are likely to be other divalent cations (such as Pb^{2+} for Cu^{2+} and Co^{2+} for Ni^{2+}) due to preferences for similar sorption sites (Brown and Parks, 2001).

Changes in environmental pH can enhance or inhibit the sorption of ions to a mineral surface. Figures 2.2 and 2.3 show the sorption edge for some metal cations and oxyanions onto ferrihydrite. For comparison purposes, the point of reference on a sorption edge plot is where 50% of the sorbate is bound to the mineral surface (Langmuir, 1997). For example; in neutral to acidic systems metal cations, such as Cu^{2+} and Ni^{2+} are less strongly sorbed to mineral surfaces thus increasing their concentration in aqueous phases (Figure 2.2) At low concentration and with pH >7, Ni^{2+} and Cu^{2+} generally form inner-sphere complexes with metal oxides whereas at pH <7 outer-sphere complexes are formed. Oxyanion forming elements are generally more strongly sorbed at low pH and their solubility increases in high pH systems (Figure 2.3). However, As and V can form both anions and cations due to the multiple oxidation states. Both As(V) and As(III) strongly sorb to mineral surfaces (Dixit and Hering, 2003). Oxyanion forming As(V) sorbs more strongly to mineral surfaces below pH 5-6 whereas above this pH, As(III) has a higher affinity for solids (Dixit and Hering, 2003). This is also true for vanadium, where the oxidised state, V(V) is more strongly sorbed at low pH but the reduced form, V(IV) is strongly sorbed and forms insoluble hydroxides in the pH range of natural waters (Wehrli and Stumm, 1989; Breit and Wanty, 1991).

The most important sorbants for the retention of metal/loids in soils and sediments are metal (oxyhydr)oxides (especially those of Al, Fe and Mn) and clay minerals (e.g. aluminosilicates) (Brown and Parks, 2001). These sorbents have a very large surface area and surface charge which are both very important for metal sorption (Sparks, 2005). The sorbative capacities of minerals and mineral based soil amendments (such as gypsum) can be used to immobilise metal/loids in contaminated soils and sediments. Precipitation of new minerals can incorporate metal/loids into the mineral structure or provide additional sites for sorption. Newly formed precipitates can be very

important for sequestering contaminants as they have the potential to permanently immobilise contaminants (O'Day and Vlassopoulos, 2010).

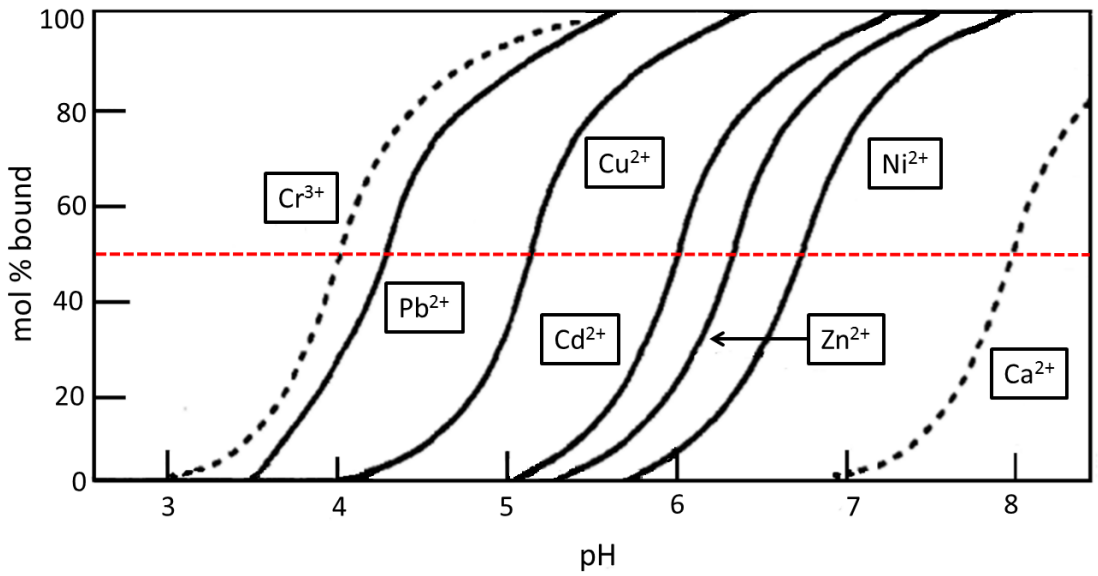

Figure 2.2 – Adsorption of metal cations (at 5 x 10^{-7}M) by ferrihydrite (∑Fe(III) = 10^{-3}M) as a function of pH at an ionic strength of 0.1 mol kg^{-1}. There 2 x 10^{-4} of reactive sites on the oxyhydroxide. The dashed curves have been calculated. The red dashed line indicates the sorption edge (plots after W. Stumm, Chemistry of the solid-water interface, Copyright © 1992 by John Wiley & Son Inc. via Langmuir (1997).

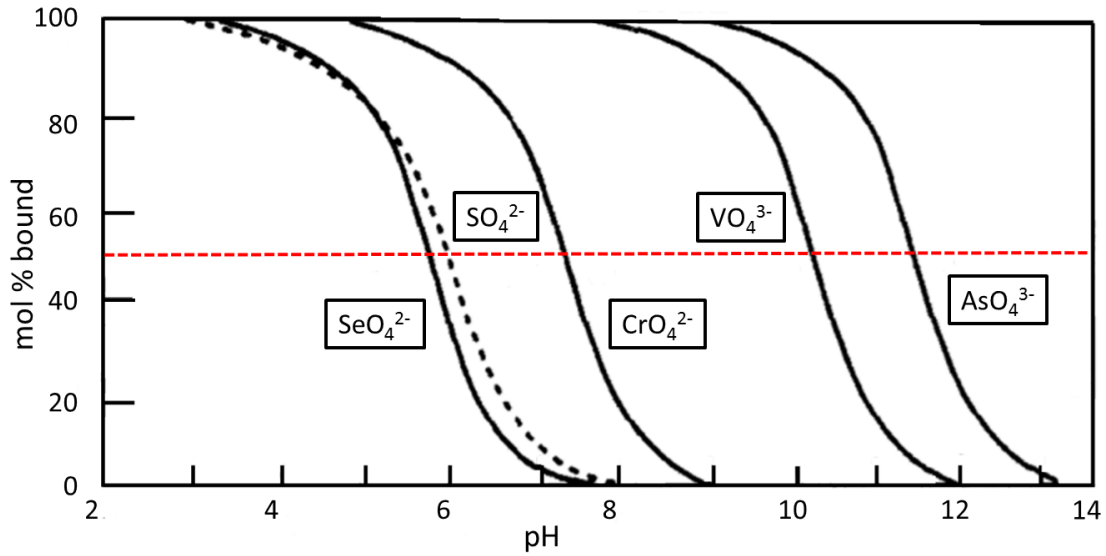

Figure 2.3 – Adsorption of metal/loid oxyanions (at 5 x 10^{-7}M) by ferrihydrite (∑Fe(III) = 10^{-3}M) as a function of pH at an ionic strength of 0.1 mol kg^{-1}. There 2 x 10^{-4} of reactive sites on the oxyhydroxide. The black dashed curve has been calculated. The red dashed line indicates the sorption edge. (plots after W. Stumm, Chemistry of the solid-water interface, Copyright © 1992 by John Wiley & Son Inc. via Langmuir (1997)

2.3.3 Complexation with natural organic matter (NOM)

Metals can form stable complexes with both solid phase and soluble organic matter therefore either enhancing or retarding the mobility of complexed metals. In soils and sediments, NOM is found as humic substances where it can sorb to soil and mineral surfaces together with complexed metals. Humic substances are formed by the microbial degradation of plant and animal detritus. They have a number of functional groups, including carboxylic, phenolic and alcoholic and behave as dibasic (and occasionally tribasic) acids (Stevenson, 1994). Humins, fulvic and humic acids are fractions of NOM, they differ due their solubility with pH. Fulvic acids are soluble above pH 2, humic acids are soluble at high pH and humins are the insoluble fraction (Stevenson, 1994). Therefore the stability of solid phase NOM decreases with increasing pH (Cheshire et al., 1977; Yin et al., 2002). This leads to increased aqueous concentrations of dissolved organic matter (DOM) and therefore any complexed metals. High concentrations of DOM in circumneutral and alkaline pore-waters can have a major impact on the aqueous concentration of trace metals (Davis, 1984; Lehman and Mills, 1994; Ashworth and Alloway, 2004). For example, Wu et al. (2001) found that Cu is mobile in alkaline soils when NOM is present but immobile when absent.

Some divalent metals can form very stable chelate complexes with NOM. Other metals can form less stable outer-sphere complexes with NOM, such as Na^{+} and Ca^{2+} (Stevenson, 1994). The stability sequence for a selection of divalent metals complexed with OM is $Cu^{2+}>Ni^{2+}>Co^{2+}>Zn^{2+}>Fe^{2+}>Mn^{2+}$ (Stevenson, 1994). The relationships of Cu and Ni and NOM is well known (Yin et al., 2002; Grybos et al., 2007; Fulda et al., 2013b) and it has been shown that Cu will preferentially complex with NOM rather than mineral surfaces in non-sulfate reducing conditions (Davis, 1984; Fulda et al., 2013a).

Sauve et al. (1997) found that nearly all Cu in contaminated soils was complexed with NOM. Problematic aqueous concentrations of Ni associated with DOM were reported as being released from soils treated with sewage sludge (Ashworth and Alloway, 2004).

Vanadium and to a lesser extent arsenic are also able to form complexes with OM. Vanadate can form complexes with OM between pH 7 - 9 (Lu et al., 1998) and can be reduced by OM to vanadyl as [VO^{2+}] (Szalay and Szilagyi, 1967). Vanadyl is not thermodynamically stable above pH 7 (Wehrli and Stumm, 1989) but it forms stable complexes with OM increasing its stability under a wide range of Eh and pH conditions (Goncalves and Mota, 1987). It has been estimated that between 20 – 80% of V in natural waters is complexed with DOM depending upon DOM concentrations (Breit and Wanty, 1991). It has been suggested that As binds to NOM via a cation bridge (such as Fe) to form a ternary As-M-NOM complex (Bauer and Blodau, 2006; Ritter et al., 2006; Sharma et al., 2010). These ternary complexes have shown to be important in mobilising As in iron-rich waters (Bauer and Blodau, 2009).

2.3.4 Biogeochemical Redox processes

An understanding of biological and geochemical redox processes in contaminated and uncontaminated systems is crucial for predicting the behaviour of contaminants with respect to their transport and fate into unaffected areas. The direct biotic and indirect abiotic redox mechanisms of elements such as; C, Fe, Mn, N and S control the speciation, bioavailability and toxicity of many other trace metal/loids in the environment (Borch et al., 2010).

It is generally accepted that bacterially mediated oxidation of organic matter (the electron donor) in soils, sediments and natural waters, follows a sequence of terminal-electron accepting processes (TEAPs). The sequence changes upon increasingly anoxic conditions which are usually related to depth. Once any O_2 in a system has been exhausted the sequence is followed by the availability of the next terminal electron acceptor (TEA) which gives the greatest free energy yield to the bacteria. Table 2.3 shows some of the most common redox processes in natural systems. In reality, the ideal system with well defined biogeochemical zones is an over-simplified one, research has shown there is a great deal of cross over in the vertical stratification (Postma and Jakobsen, 1996; Mortimer et al., 2004).

Iron is ubiquitous on the Earth's surface and is present in the environment as minerals or in clays for ions to sorb and associate with, complexed with NOM in an aqueous form or covered with NOM in a solid phase (Kappler, 2005). Fe(III)-(hydr)oxides form at circumneutral pH and act as highly effective sorbents for many metal/loids (see section 2.3.2). Fe(III)-(hydr)oxides can be reduced, either biotically (by dissimilatory iron reducing bacteria (Lovley, 1997) (Table 2.3) or abiotically (via sulfides (Afonso and Stumm, 1992). The reductive dissolution of Fe(III) minerals can release sorbates into surrounding pore-waters thus increasing contaminant concentrations (Zachara et al., 2001; Grybos et al., 2007). Fe(II) formed by the reduction process can then act as a reductant for other redox sensitive metals, such as Cu (Matocha et al., 2005) or can be oxidised back to Fe(III) by Fe(II) oxidising bacteria (Kappler, 2005).

It is thought that the release of As following the reductive dissolution of Fe-(hydr)oxides might be important in controlling As concentrations in contaminated aquifers in south-east Asia (Charlet et al., 2011). It is generally agreed that the

contamination occurs due to the release of As from host-phases although the actual controlling mechanisms are still the subject of much debate and research (Charlet and Polya, 2006; Borch et al., 2010; Charlet et al., 2011). Islam et al. (2004) found that in sediments from a contaminated aquifer in west Bengal, metal reducing bacteria, capable of Fe and As reduction (see section 2.4.2) were able to mobilise high concentrations of As(III) into solution but that the increase in aqueous As did not occur simultaneously with Fe(III) reduction. More recently, Burnol et al. (2007) found using ferrihydrite, that the two processes are indeed linked; after initial Fe(III)-reduction, As(V) resorbs to the remaining ferrihydrite and remains adsorbed until conditions are such that As(V)-reduction is more energetically favourable than Fe(III)-reduction, only then is As(III) is released into solution (Burnol et al., 2007).

Hydrogen sulfide [H_2S] is formed by the microbial reduction of sulfate and is a potent reductant of redox sensitive elements. Arsenic, copper, nickel and vanadium can all be reduced by sulfides. The metal/loid ions react with H_2S during sulfate reduction (see Table 2.3) to precipitate new sulfide minerals which can retard the metals under reducing conditions. Bacterial sulfate reduction has been shown to reduce aqueous concentration of As in groundwater (Kirk et al., 2004). Cu can be reduced by dissolved sulfides and form insoluble Cu sulfides which are important for controlling Cu mobility in reducing systems (Fulda et al., 2013a). Cu sulfides, in particular, are very stable in comparison with other metal sulfides and can form under relatively low sulfide concentrations. Ni sulfides are sparingly soluble are also important for controlling Ni concentrations (Richter and Theis, 1980). H_2S is known to reduce V(V) to V(IV) (Breit and Wanty, 1991) and has been shown to reduce V(IV) to V(III) in laboratory conditions (Wanty and Goldhaber, 1992).

Table 2.3 - Environmentally significant microbial half reaction reduction potentials: Standard Reduction Potential, E_0, and redox potential, Eh, at ph 7, 10.5 and 12 (at standard temperature and pressure)

Transformation	**Reaction**	**E_0 (V)**	**Eh @ pH 7**	**Eh @ pH 10.5**	**Eh @ pH 12**	**Assumptions**
O2 depletion[+]	$O_2 + 4H^+ + 4e^- = 2H_2O$	1.23	0.805	0.598	0.510[$]	P_{O2} = 0.2 bar
Denitrification[+]	$NO_3^- + 6H^+ + 5e^- = ½N_2 + 3H_2O$	1.24	0.713	0.464	0.884[$]	$[NO_3^-]$ = 1 mmol L^{-1}
						P_{N2} = 0.8 bar
Mn reduction[+]	$Mn_3O_4 + 2H^+ + 2H_2O + 2e^- = 3Mn(OH)_2$	0.480	0.066	-0.140	-0.230[$]	-
Mn(III) to Mn(II)						
Fe reduction[+]	$Fe(OH)_3 + HCO_3^- + 2H^+ + e^- = FeCO_3 + 3H_2O$	1.078	-	-0.266	- 0.453[$]	$[HCO_3^-]$ = 20 mmol L^{-1}
Fe(III) to Fe(II)+				0.321		$[HCO_3^-]$ = 1 mmol L^{-1}
Fe reduction[+]	$Fe(OH)^3 + H^+ + e^- = Fe(OH)_2 + H_2O$	0.257	-0.157	-0.364	-0.402[$]	-
Fe(III) to Fe(II) *						
Sulfate reduction[+]	$SO_4^{2-} + 10H^+ + 8e^- = H_2S + 4H_2O$	0.301	-0.217	-0.476	-0.587[$]	$[SO_4^{2-}] = [H_2S]$
S(VI) to S(-II)						
Bicarbonate reduction to acetate [x]	$2HCO_3^- + 9H^+ + 8e^- = CH_3COO^- + 4H_2O$	0.187	-0.292	-0.525	-0.648[$]	$[HCO_3^-] = [CH_3COO^-]$
C(IV) to C(0)						= 20 mmol L^{-1}

[+] after (Langmuir, 1997) [$] after (Burke et al., 2012b)
[x] calculated using thermodynamic data from Thauer (1977) via Whittleston et al. (2011)
[*]calculated using thermodynamic data from Stumm and Morgan (1996) via Whittleston et al. (2011)

2.4 Soil microorganisms

Soil microorganisms represent a huge fraction of the biomass in soils and sediments, for example; surface soils contain between 10^3 to 10^4 kg of microbial biomass per hectare (Fierer et al., 2007). Microorganisms have adapted to survive in nearly every extreme seen on earth; from high temperature in thermal vents (Tunnaclife, 1991) to high pressures of the deep sub-surface (Schippers et al., 2005). More recently, microorganisms have also adapted to living in areas of anthropogenic pollution such as; radiation (Fredickson et al., 2004), areas of heavy metal contamination (Whittleston et al., 2013), and in environments of both very low and very high pH (Baker and Banfield, 2006; Burke et al., 2012).

2.4.1 Alkaliphiles

Alkaliphiles are a variety of extremophile that grow "optimally or very well at pH values above 9 and often above 10 and 12 but cannot grow or grow very slowly at near neutral pH" (Horikoshi, 1999). The above definition means that the optimal growth pH of alkaliphilic bacteria is ~pH 9 whereas neutrophilic bacteria growth rates peak at pH 7. The main challenge for alkaliphiles is how to maintain a neutral intracellular pH, when the extracellular pH can be up to 2 pH units higher (Krulwich and Guffanti, 1989; Horikoshi, 1999). Sturr et al. (1994) report that alkaliphilic *Bacillis firmus* shows decreasing growth rates above an external pH of 11 which relates directly to an apparent decrease in the microbes ability to regulate internal pH. One mechanism for maintaining internal pH homeostasis by alkaliphiles is by the selective exchange of sodium and hydronium ions across plasma membranes via a Na^+/H^+ and K^+/H^+ antiporter system.

Here, Na^+ or K+ ions from within the cell are exchanged with external H^+ ions, thus decreasing internal pH (Ito et al., 1997; Horikoshi, 1999).

Alkaliphilic bacteria have been isolated from different types of alkaline environments; the guts of higher termites, animal manure, indigo fermentation waste, Mariana trench mud and soda lakes (Shiba et al., 1989; Hind et al., 1999; Horikoshi, 1999; Pollock et al., 2007; Zhilina et al., 2009). Alkaliphilic bacteria isolated from soda lakes have been capable of using alternative electron acceptors; O_2, Fe(III), As(V) nitrate and fumarate (Oremland et al., 2004; Pollock et al., 2007; Zhilina et al., 2009).

Alkaliphilic bacteria have also been isolated from sites where a hyper alkaline environment has been created due to industry. Ye et al. (2004) describes a metal reducing bacteria isolated from a leachate pond formed at the U. S. Borax Company site in Boron, California, United States. The bacteria show evidence of Fe(III)- reduction and had an optimum growth pH of 9.5 (Ye et al., 2004). Takai et al. (2001) report on the isolation of an extremely alkaliphilic bacterium from a deep South African gold mine. *Alkaliphilus transvaalensis* has an optimum growth pH of 10 and was capable of growth at a pH of 12.5 (Takai et al., 2001). Roadcap et al. (2006) report on a variety of alkaliphilic bacteria found in ground water located in the Lake Calumet area of Illinois, United States. The area has been used in the past for dumping steel slag where ground water had become hyper-alkaline due to high pH slag leachates (Roadcap et al., 2006).

2.4.2 Microbial metal/loid reduction

Microbial metal/loid reduction can occur in a range of environments. Some microorganisms have evolved to survive by incorporating changes in oxidation state of

toxic metals (Lloyd, 2003). Under certain conditions, microorganisms can mobilise toxic metals into the wider environment (Islam et al., 2004) or retard mobility by reducing metals to a less mobile and less toxic form (Whittleston et al., 2011).

Microbial As reduction has been much studied due to the problems it presents in contaminated aquifers (as discussed previously). Some microorganisms have adapted to tolerate high concentrations of As and are able to reduce As(V) to As(III) directly, a process known as dissimilatory arsenic reduction or to oxidise As(III) to As(V) (Oremland and Stolz, 2003). As(V) has been shown to be one of the main electron acceptors at Mono Lake and Searles Lake in California, United States (Zobrist et al., 2000; Oremland et al., 2000; Oremland et al., 2005). These lakes are extreme environments with respect to an alkaline pH (pH 9.8) (Lloyd and Oremland, 2006) and hypersalinity (Mono Lake salinity = 75-90g L^{-1} whereas Searles Lake is at or near saturation ~350 gL^{-1}) (Oremland et al., 2000; Hollibaugh et al., 2005; Oremland et al., 2005).

Microbial reduction of vanadium has not been studied to any great extent but several V(V) reducing organisms have been identified (Carpentier et al., 2003; Ortiz-Bernad et al., 2004; van Marwijk et al., 2009). It is thought that the process of V(V) reduction is not very important in the wider environment due to the relatively low concentrations of V, with respect to Fe(III) and other electron acceptors (Ortiz-Bernad et al., 2004). However, V(V) reduction may be an effective way of immobilising mobile V(V) where V contamination is problematic (Ortiz-Bernad et al., 2004).

2.5 Study Sites

2.5.1 Hownsgill Valley, near Consett

The Grove Heaps in the Hownsgill Valley, near Consett were used for slag tipping for nearly a century until the closure of Consett Steelworks in 1980. At the height of the steel industry the Consett Steelworks employed over 6000 people and resulted in the loss of jobs for over 3000 people when it was closed. Since the closure, the site of the steelworks and tip area (around 290 hectares) have been extensively landscaped and very little remains today of the former steelworks.

The Hownsgill Valley is a glacial melt water channel, overlying superficial alluvium above Lower Coal Measures strata (Mayes et al., 2006). To the North of the site runs the A692, Consett Road and to the South is the Hownsgill Viaduct (see Figure. 2.4). A large leachate pond, approximately 1500 m^2 (see Figure 2.5) has formed in the valley bottom where hyper-alkaline (pH 11-12) leachates have filtered through the slag heaps via subterranean tip drains. There is no vegetation around the leachate pond due to the high pH and an area of calcite has formed around the pond. Calcite precipitation rates at the site, have been estimated at between 0.4 and 15 g m^{-2} day^{-1} (Mayes et al., 2006). Downstream of the leachate pond the vegetation gradually becomes more dense, with reeds, rushes and grasses. The heaps are approximately 45 m in depth and consist of both blast bottom furnace and steel slag (see Table 2.4 for typical composition).

Buffering of the slag leachate across the natural wetland area is described by Mayes et al. (2006). The pH of the water upstream of the leachate flow was between pH 6.6 and 8.7 and changed dramatically at the confluence with the slag leachate when pH increased to between 11.5 and 12.5. High pH determinations were also concomitant with high electrical conductivity (EC) readings (between 1164 and 3747 µS cm^{-1}).

Progressive lowering of pH and EC occurred downstream of the leachate source across the wetland area. Calcite precipitation occurs across the wetland area, with peak precipitation rates around the leachate source and pond (Mayes et al., 2006). Hydrochemistry of the slag leachate and sediment composition was also described by Mayes et al. (2008). Major ions and trace elements from the Grove Heap leachate are shown in Table 2.5 and sediment composition in Table 2.6.

Table 2.4 – Typical slag analyses from the former Consett Steelworks (adapted from Sheffield (1996) via Mayes et al. (2008)). All values as % content by mass.

	CaO	SiO_2	Al_2O_3	MgO	FeO	MnO	P_2O_5	S
Consett blast furnace slag	41.7	33.6	15.2	5.8	0.4	0.4	-	1.63
Consett steel slag	38.0	8.8	0.8	8.4	40.5	6.0	1.4	-

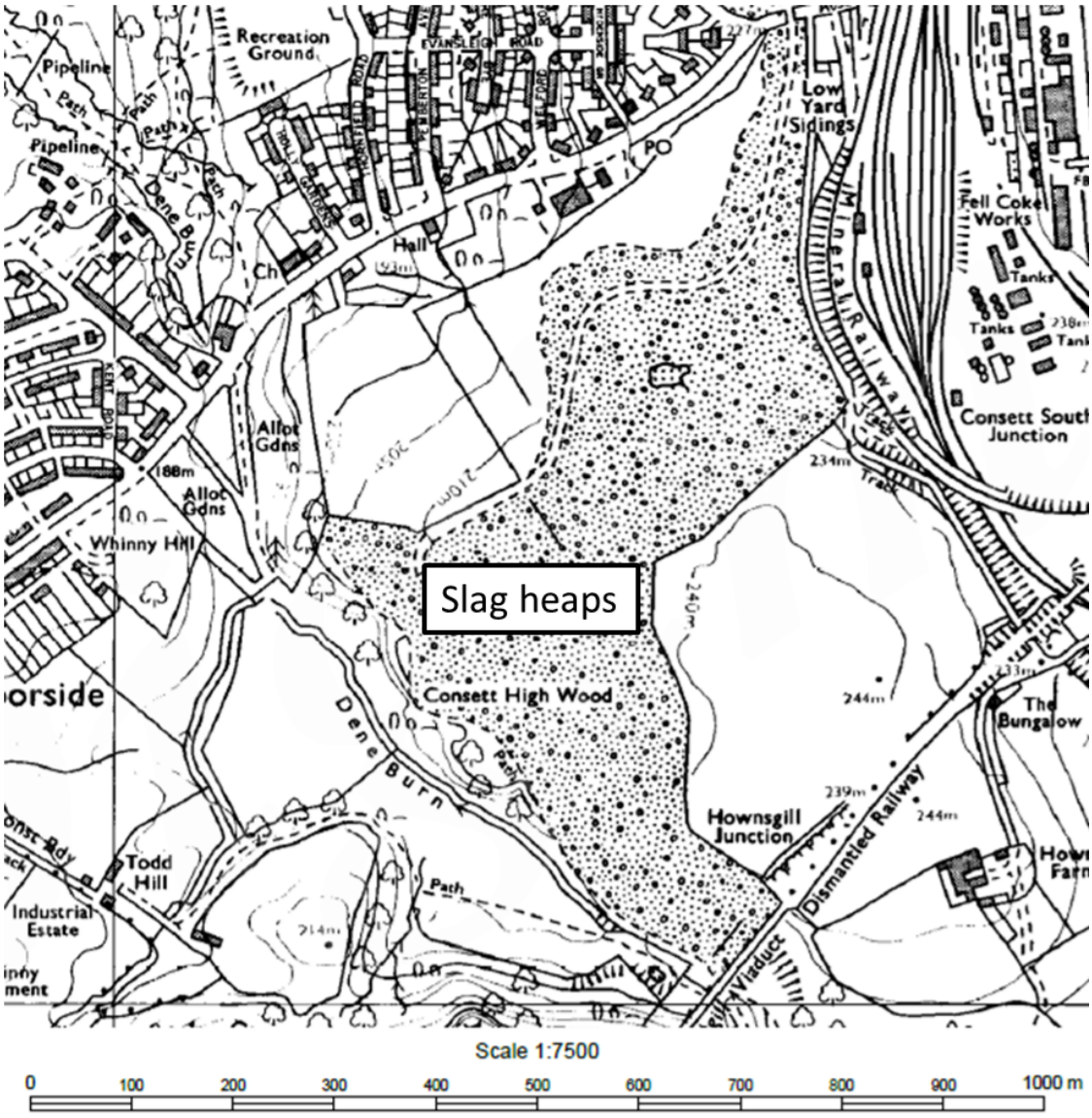

Figure 2.4 – Extent of the Grove Heaps, 1981 (reproduced from EDINA Digimap Historic [Accessed February 19, 2014] ©Landmark Information Group, Crown Copyright 2014)

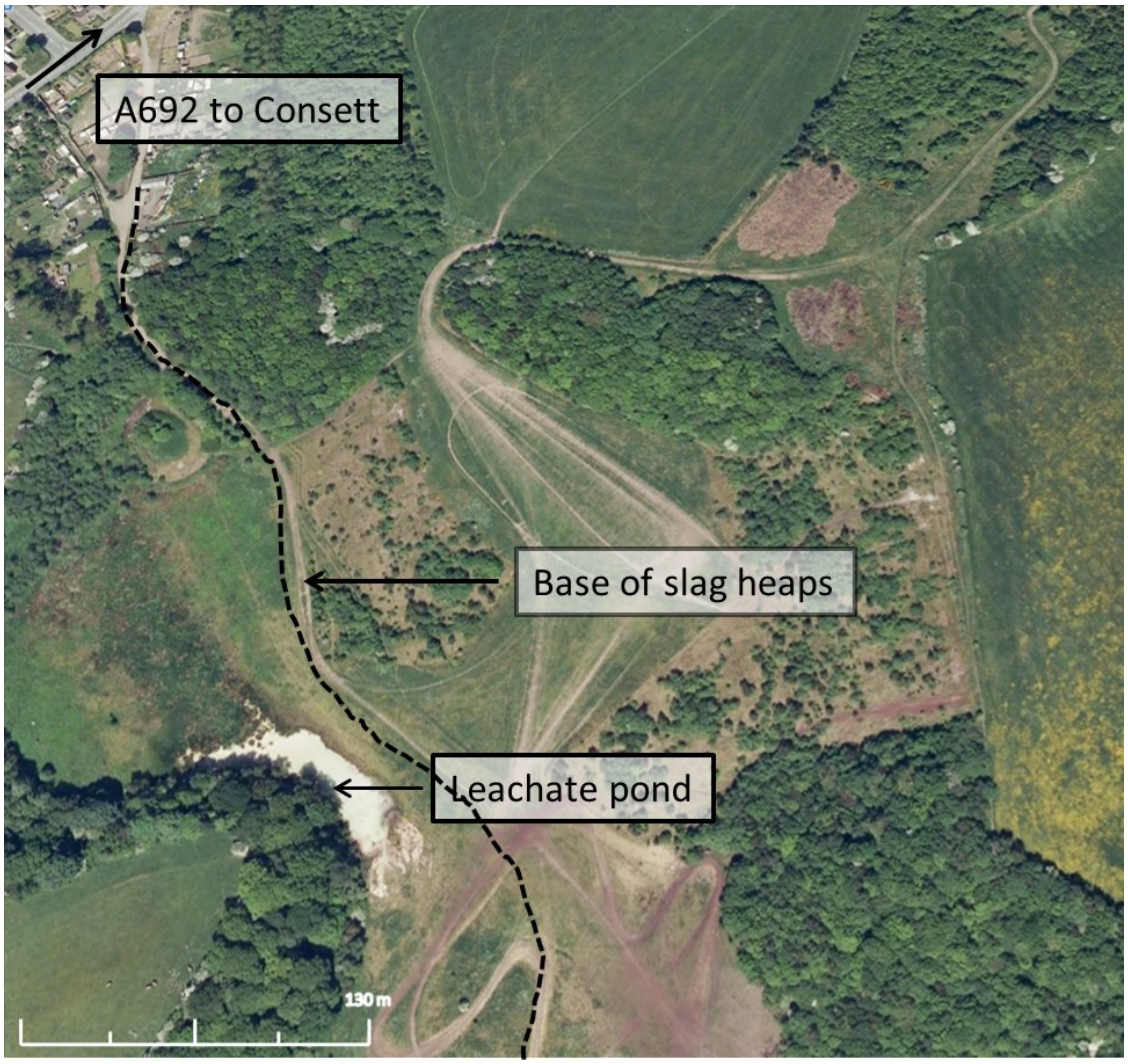

Figure 2.5 – The Hownsgill Valley site, near Consett, County Durham (Edited Satellite imaged downloaded from Google earth V 7.1.2.2041 (complied 10th July 2013) Image © 2014 Infoterra Ltd & BlueSky, Getmapping Plc and Google (accessed 1st April 2014).

Figure 2.6 - Digital photograph of the leachate pond (July 2010, courtesy of Doug Stewart)

Figure 2.7 – Digital photograph showing the extent of calcite precipitation around the leachate pond (July 2010).

Table 2.5 – Mean hydrochemical composition of Grove Heap leachate (taken from Mayes et al. (2008) (data in parentheses is the standard error of the mean, where n=8)

	Major ions (mg L^{-1})						Trace elements (µg L^{-1})											
	Ca	Mg	K	Na	Cl	SO_4^{2-}	Al	B	Ba	Cr	Cu	Fe	Mn	Mo	Ni	Si	Sr	V
Grove Heaps Leachate	194 (21)	1.6 (1)	11 (1)	13 (1)	34 (11)	45 (7)	330 (20)	40 (10)	80 (1)	<5	<5	370 (10)	<5	<5	<1 0	820 (430)	360 (10)	21 (3)

Table 2.6 - Composition of digested sediments from Grove Heap leachate source (taken from Mayes et al. (2008)

	Major elements (mg kg^{-1})							Minor elements (mg kg^{-1})										
	Ca	Mg	K	Na	Fe	Al	Si	As	B	Ba	Cr	Cu	Mn	Mo	Ni	Sr	Ti	V
Grove Heaps Sediment	360,400	7373	262	235	1865	4253	633	<0.2	7.2	133	10	6	257	3.1	1.7	227	65	28

2.7.2 Ajka, Veszprém County, western Hungary

On the 4th October 2010, the failure of the north-western corner of Cell X of the Ajkai Timfoldgyar Zrt alumina plant red mud repository caused the release of ~1 million m^3 of caustic red mud suspension down the Torna and Upper Marcal valleys near Ajka, western Hungary. A red mud release of this magnitude was unprecedented, the waste inundated homes causing 10 deaths and around 150 serious injuries (Adam et al., 2011a). An estimated 40 km^2 of low lying agricultural and riparian wetlands were affected and red mud was transported over 120 km downstream eventually reaching the Danube (Reeves et al., 2011).

The alumina plant is situated to the south-west of the town of Ajka, in Veszprém County. The affected area is characterised by a shallow valley where the Torna Creek flows in a westerly direction. The most severely impacted villages were Kolontár (1 km from the breach), Devecser (5 km from the breach) and Somlóvásàrhely (10 km from the breach) (Reeves et al., 2011). Figure 2.8 shows the extent of the red mud release down the Torna and Upper Marcel valleys.

The Kolontár Report commissioned by the Hungarian authorities following the disaster, states a combination of several factors leading to the failure of the dam and how the impact of the failure significantly exceeded those in the disaster management plan (Adam et al., 2011a). It is clear from the report that there was not one single cause for the disaster but many failings over several levels of plant management and the competent authorities. Some of the contributing factors are briefly summarised below:

- Outdated disposal technology. The devastation caused by the dam breach was largely due to the high water content and volume of the red mud waste stored in Cell X. Prior to the accident, untreated red mud stored in Cell X was between 20-25% w/w solids and the materials released in the spill contained around 8-10% w/w solids (Burke et al., 2013). However, dry stacking a much safer practice of red mud disposal, was available when the licence for Cell X was granted which would, in hindsight, have considerably reduced the impact of a dam breach (Adam et al., 2011a).

- Incorrect classification of red mud waste. The composition and pH of the red mud slurry was not known at the time of the disaster thus impeding the response of the emergency services. When the environmental permit for Cell X was granted the red mud was not classified as hazardous. Red mud with a pH of above 11.5 is deemed hazardous by the (Basel Convention, 2011), the pH of the red mud at Ajka has since been determined to be ~pH 13 (Mayes et al., 2011).

- Sinking of the Cell X dam wall. Satellite images of Cell X clearly show that the barrier of Cell X was sinking and at a rate of 1 cm $year^{-1}$ in some places. However, there were no structural engineering inspections of Cell X nor were satellite images inspected until the investigation after the cell wall breach (Adam et al., 2011a).

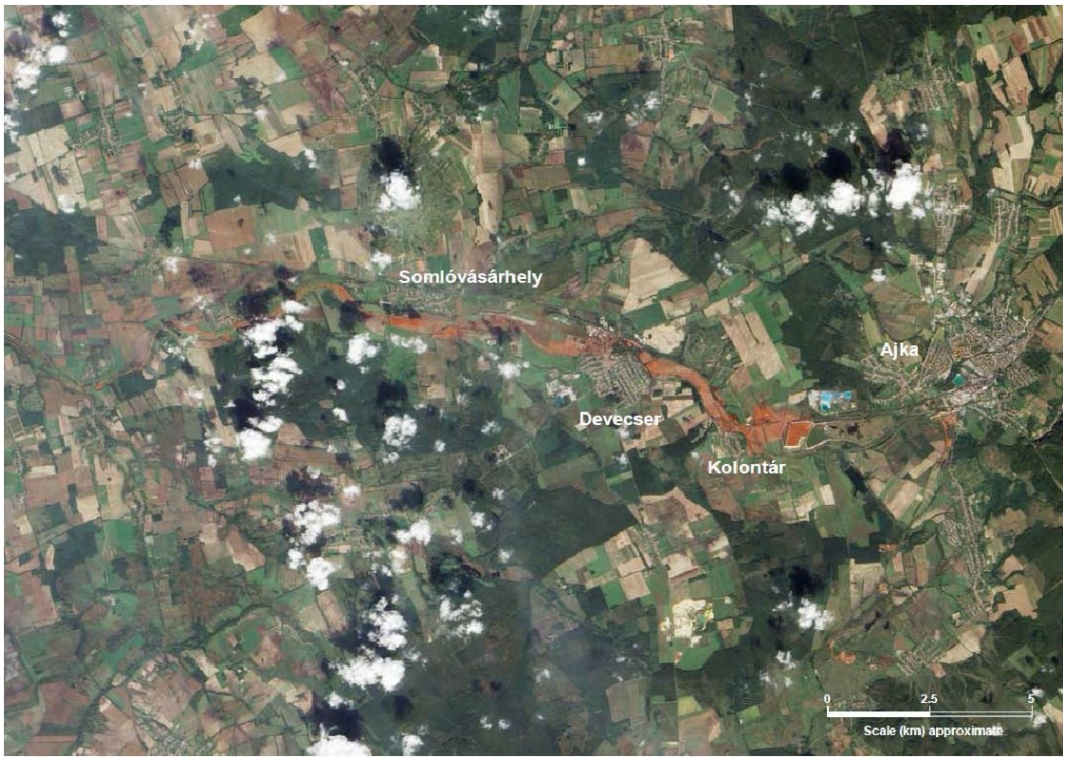

Figure 2.8 – Distribution of the red mud release, Ajka western Hungary (Image Source ALI/EO-1/Nasa via Reeves et al. (2011)

Figure 2.9 - Digital photograph of house in Devecser awaiting demolition (May 2011)

Emergency environmental procedures began almost immediately following the spill. Calcium and magnesium nitrates, gypsum and acids (acetic and sulfuric) were deployed in the affected rivers to reduce pH and prevent red mud pollution reaching the Danube (Adam et al., 2011a; Reeves et al., 2011; Nagy et al., 2013). The addition of gypsum to alkaline solutions provides free aqueous Ca^{2+} promoting the precipitation of calcite (in the presence of CO_2), which consumes hydroxyl ions thus reducing pH (see Equations 2.6 and 2.7 above) (Renforth et al., 2012). Precipitated calcite may also provide additional sorption sites for the uptake of red mud contaminants (Burke et al., 2013). The effectiveness of gypsum in the remediation effort has been investigated (Renforth et al., 2012; Burke et al., 2013). Renforth et al. (2012) noted a modest uptake of As, Cr and Mn on secondary carbonate deposits found downstream of the spill. A detailed investigation of the neutralization of red mud leachates found that gypsum precipitation removed a significant proportion (>80%) of both Al and As from red mud leachates but that very little V was removed from solution in the neutralization process (Burke et al., 2013).

Shortly after the spill, Mayes et al. (2011) sought to identify the extent of the spill within the affected river systems. They found that the geochemical signature of the red mud was apparent throughout the Marcal river system with elevated aqueous concentrations of As and V (> 50 $\mu g\ L^{-1}$) in the Torna Creek and Upper Marcal (Mayes et al., 2011). High concentrations of As, Cr, Ni and V were found in fluvial sediments, however, sequential extraction data suggested that the bulk of these elements were associated with residual phases (Mayes et al., 2011). Another area of concern following the spill was of fine red mud dust being emitted into the atmosphere and the effects of inhalation of these alkaline dusts. Studies showed that inhalation was unlikely to affect the lungs but that the resuspension of red mud dust may cause irritation in the upper

respiratory tract and eyes (Gelencser et al., 2011). In order to prevent any complications from the inhalation of red mud dust and to lessen effects to soil, removal of thick red mud deposits (>5cm) commenced a few weeks after the spill whereas thin red mud deposits (<5cm) were ploughed into soils (Klebercz et al., 2012). The average thickness of red mud on soil surfaces was 5-10 cm (min. = 3 cm max = 45cm) (Rekasi et al., 2013). There have since been several studies investigating the effects of red mud addition to soils. The main risks associated with red mud addition to agricultural soils and toxicity to plants was the increased concentrations of Na^+ and alkalinity, especially over a 5% red mud addition (Ruyters et al., 2011; Anton et al., 2012; Gruiz, 2012).

Red mud addition to soil was also found to cause changes in characteristic such as; changes in particle size, increased pH and solubility of DOC (Anton et al., 2012; Rekasi et al., 2013). An increase in toxic and potentially toxic elements such as Al, As, Co, Cr, Cu, Ni, Mo, Pb and Zn was also observed (Anton et al., 2012; Milacic et al., 2012; Rekasi et al., 2013). Other studies have indicated that red mud could act as a mobile source of V (Burke et al., 2012a).

It is worth noting that all of the studies mentioned above justify the expensive remediation efforts employed by the Hungarian authorities in removing red mud from affected land. Follow up studies, assessing the water quality of the Marcal river before and after the Ajka red mud spill found higher concentrations of As and Ni, two years after the spill when compared to pre-spill conditions (Nagy et al., 2013).

2.8 References

ADAM, J., BANVOLGYI, G., DURA, G., GRENERCZY, G., GUBECK, N., GUPTER, I., SIMON, G., SZEGFALVI, Z., SZEKACS, A., SZEPVOLGYI, J. & UJLAKY, E. 2011. The Kolontar report: Causes and Lessons from the Red Mud Disaster. In: B, J. (ed.). Budapest: Sustainable Development Committee of the Hungarian Parliament.

AFONSO, M. D. & STUMM, W. 1992. Reductive Dissolution of Iron(III) (Hydr)oxides by Hydrogen Sulfide. Langmuir, 8, 1671-1675.

ANTON, A., REKASI, M., UZINGER, N., SZEPLABI, G. & MAKO, A. 2012. Modelling the Potential Effects of the Hungarian Red Mud Disaster on Soil Properties. Water Air and Soil Pollution, 223, 5175-5188.

APPELO, C. A. J., VAN DER WEIDEN, M. J. J., TOURNASSAT, C. & CHARLET, L. 2002. Surface Complexation of Ferrous Iron on Ferrihydrite and the Mobilization of Arsenic. Environmental Science & Technology, 36 3096-3103.

ASHWORTH, D. J. & ALLOWAY, B. J. 2004. Soil mobility of sewage sludge-derived dissolved organic matter, copper, nickel and zinc. Environmental Pollution, 127, 137-144.

BAKER, B. J. & BANFIELD, J. F. 2006. Microbial Communities and Acid Mine Drainage. FEMS Microbiology Ecology, 44(2), 139-152.

BARCELOUX, D. G. 1999a. Copper. Journal of Toxicology-Clinical Toxicology, 37, 217-230.

BARCELOUX, D. G. 1999b. Nickel. Journal of Toxicology-Clinical Toxicology, 37, 239-258.

BARCELOUX, D. G. 1999c. Vanadium. Journal of Toxicology-Clinical Toxicology, 37, 265-278.

BASEL CONVENTION 2011. Basel Convention on the control of transboundary movements of hazardous waste and their disposal. In: UNITED NATIONS ENVIRONMENT PROGRAMME (ed.) Annex IX. Switzerland: Secretariat of the Basel Convention,.

BAUER, M. & BLODAU, C. 2006. Mobilization of arsenic by dissolved organic matter from iron oxides, soils and sediments. Science of the Total Environment, 354, 179-190.

BAUER, M. & BLODAU, C. 2009. Arsenic distribution in the dissolved, colloidal and particulate size fraction of experimental solutions rich in dissolved organic matter and ferric iron. Geochimica Et Cosmochimica Acta, 73, 529-542.

BAYLESS, E. R. & SCHULZ, M. S. 2003. Mineral precipitation and dissolution at two slag-disposal sites in northwestern Indiana, USA. Environmental Geology, 45, 252-261.

BONENFANT, D., KHAROUNE, L., SAUVE, S., HAUSLER, R., NIQUETTE, P., MIMEAULT, M. & KHAROUNE, M. 2008. CO_2 Sequestration Potential of Steel Slags at Ambient Pressure and Temperature. Industrial & Engineering Chemistry Research, 47, 7610-7616.

BORCH, T., KRETZSCHMAR, R., KAPPLER, A., VAN CAPPELLEN, P., GINDER-VOGEL, M., VOEGELIN, A. & CAMPBELL, K. 2010. Biogeochemical Redox Processes and their Impact on Contaminant Dynamics. Environmental Science & Technology, 44, 15-23.

BREIT, G. N. & WANTY, R. B. 1991. VANADIUM ACCUMULATION IN CARBONACEOUS ROCKS - A REVIEW OF GEOCHEMICAL CONTROLS DURING DEPOSITION AND DIAGENESIS. Chemical Geology, 91, 83-97.

BREMNER, I. 1998. Manifestations of copper excess. American Journal of Clinical Nutrition, 67, 1069S-1073S.

BROWN, G. E., FOSTER, A. L. & OSTERGREN, J. D. 1999. Mineral surfaces and bioavailabity of heavy metals: A molecular-scale perspective. National Academy of Scienes colloquium on Geology, Mineralogy, and Human Welfare. Irvine, California, U. S.: National Academy of Sciences.

BROWN, G. E. & PARKS, G. A. 2001. Sorption of trace elements on mineral surfaces: Modern perspectives from spectroscopic studies, and comments on sorption in the marine environment. International Geology Review, 43, 963-1073.

BURKE, I. T., MAYES, W. M., PEACOCK, C. L., BROWN, A. P., JARVIS, A. P. & GRUIZ, K. 2012a. Speciation of arsenic, chromium, and vanadium in red mud samples from the ajka spill site, hungary. Environmental Science & Technology, 46, 3085-92.

BURKE, I. T., MORTIMER, R. J. G., PALANIYANDI, S., WHITTLESTON, R. A., LOCKWOOD, C. L., ASHLEY, D. J. & STEWART, D. I. 2012b. Biogeochemical Reduction Processes in a Hyper-Alkaline Leachate Affected Soil Profile. Geomicrobiology Journal, 29, 769-779.

BURKE, I. T., PEACOCK, C. L., LOCKWOOD, C. L., STEWART, D. I., MORTIMER, R. J. G., WARD, M. B., RENFORTH, P., GRUIZ, K. & MAYES, W. M. 2013. Behavior of Aluminum, Arsenic, and Vanadium during the Neutralization of Red Mud Leachate by HCl, Gypsum, or Seawater. Environmental Science & Technology, 47, 6527-6535.

BURNOL, A., GARRIDO, F., BARANGER, P., JOULIAN, C., DICTOR, M.-C., BODENAN, F., MORIN, G. & CHARLET, L. 2007. Decoupling of arsenic and iron release from ferrihydrite suspension under reducing conditions: a biogeochemical model. Geochemical Transactions, 8.

CARPENTIER, W., SANDRA, K., DE SMET, I., BRIGE, A., DE SMET, L. & VAN BEEUMEN, J. 2003. Microbial reduction and precipitation of vanadium by Shewanella oneidensis. Applied and Environmental Microbiology, 69, 3636-3639.

CASTALDI, P., SILVETTI, M., GARAU, G. & DEIANA, S. 2010. Influence of the pH on the accumulation of phosphate by red mud (a bauxite ore processing waste). Journal of Hazardous Materials, 182, 266-272.

CEMPEL, M. & NIKEL, G. 2006. Nickel: A Review of Its Sources and Environmental Toxicology. Polish Journal of Environmental Studies, 15, 375-382.

CHARLET, L., MORIN, G., ROSE, J., WANG, Y. H., AUFFAN, M., BURNOL, A. & FERNANDEZ-MARTINEZ, A. 2011. Reactivity at (nano)particle-water interfaces, redox processes, and arsenic transport in the environment. Comptes Rendus Geoscience, 343, 123-139.

CHARLET, L. & POLYA, D. A. 2006. Arsenic in shallow, reducing groundwaters in southern Asia: An environmental health disaster. Elements, 2, 91-96.

CHAURAND, P., ROSE, J., BRIOIS, V., OLIVI, L., HAZEMANN, J. L., PROUX, O., DOMAS, J. & BOTTERO, J. Y. 2007. Environmental impacts of steel slag reused in road construction: A crystallographic and molecular (XANES) approach. Journal of Hazardous Materials, 139, 537-542.

CHESHIRE, M. V., BERROW, M. L., GOODMAN, B. A. & MUNDIE, C. M. 1977. METAL DISTRIBUTION AND NATURE OF SOME CU, MN AND V COMPLEXES IN HUMIC AND FULVIC-ACID FRACTIONS OF SOIL ORGANIC-MATTER. Geochimica Et Cosmochimica Acta, 41, 1131-1138.

CORNELIS, G., JOHNSON, C. A., VAN GERVEN, T. & VANDECASTEELE, C. 2008. Leaching mechanisms of oxyanionic metalloid and metal species in alkaline solid wastes: A review. Applied Geochemistry, 23, 955-976.

CZOP, M., MOTYKA, J., SRACEK, O. & SZUWARZYNSKI, M. 2011. Geochemistry of the Hyperalkaline Gorka Pit Lake (pH > 13) in the Chrzanow Region, Southern Poland. Water Air and Soil Pollution, 214, 423-434.

DAVIS, J. A. 1984. Complexation of trace metals by adsorbed natural organic matter. Geochimica Et Cosmochimica Acta, 48, 679-691.

DEAKIN, D., WEST, L. J., STEWART, D. I. & YARDLEY, B. W. D. 2001. Leaching behaviour of a chromium smelter waste heap. Waste Management, 21, 265-270.

DIXIT, S. & HERING, J. G. 2003. Comparison of arsenic(V) and arsenic(III) sorption onto iron oxide minerals: Implications for arsenic mobility. Environmental Science & Technology, 37, 4182-4189.

FEIGL, V., ANTON, A., UZIGNER, N. & GRUIZ, K. 2012. Red Mud as a Chemical Stabilizer for Soil Contaminated with Toxic Metals. Water Air and Soil Pollution, 223, 1237-1247.

FIERER, N., BREITBART, M., NULTON, J., SALAMON, P., LOZUPONE, C., JONES, R., ROBESON, M., EDWARDS, R. A., FELTS, B., RAYHAWK, S., KNIGHT, R., ROHWER, F. & JACKSON, R. B. 2007. Metagenomic and small-subunit rRNA analyses reveal the genetic diversity of bacteria, archaea, fungi, and viruses in soil. Applied and Environmental Microbiology, 73, 7059-7066.

FLEMMING, C. A. & TREVORS, J. T. 1989. COPPER TOXICITY AND CHEMISTRY IN THE ENVIRONMENT - A REVIEW. Water Air and Soil Pollution, 44, 143-158.

FRANK, A., MADEJ, A., GALGAN, V. & PETERSSON, L. R. 1996. Vanadium poisoning of cattle with basic slag. Concentrations in tissues from poisoned animals and from a reference, slaughterhouse material. Science of the Total Environment, 181, 73-92.

FREDRICKSON, J. K., ZACHARA, J. M., BALKWILL, D. L., KENNEDY, D., LI, S. W., KOSTANDARITHES, H. M., DALY, M. J., ROMAINE, M. F., BROCKMAN, F. J. 2004. Geomicrobiology of high-level nuclear waste- contaminated vadose sediments at the Hanford site, Washington State. Applied and Environmental Microbiology, 70(7), 4230-4241.

FRIESL, W., HORAK, O. & WENZEL, W. W. 2004. Immobilization of heavy metals in soils by the application of bauxite residues: pot experiments under field conditions. Journal of Plant Nutrition and Soil Science-Zeitschrift Fur Pflanzenernahrung Und Bodenkunde, 167, 54-59.

FULDA, B., VOEGELIN, A., EHLERT, K. & KRETZSCHMAR, R. 2013a. Redox transformation, solid phase speciation and solution dynamics of copper during soil reduction and reoxidation as affected by sulfate availability. Geochimica Et Cosmochimica Acta, 123, 385-402.

FULDA, B., VOEGELIN, A., MAURER, F., CHRISTL, I. & KRETZSCHMAR, R. 2013b. Copper Redox Transformation and Complexation by Reduced and Oxidized Soil Humic Acid. 1. X-ray Absorption Spectroscopy Study. Environmental Science & Technology, 47, 10903-10911.

GAMALETSOS, P., GODELITSAS, A., MERTZIMEKIS, T. J., GOTTLICHER, J., STEININGER, R., XANTHOS, S., BERNDT, J., KLEMME, S., KUZMIN, A. & BARDOSSY, G. 2011. Thorium partitioning in Greek industrial bauxite investigated by synchrotron radiation and laser-ablation techniques. Nuclear Instruments and Methods in Physics Research B, 269, 3067-3073.

GAO, Y. & MUCCI, A. 2001. Acid base reactions, phosphate and arsenate complexation and their competitive adsorption at the surface of goethite in 0.7 M NaCl solution. Geochimica Et Cosmochimica Acta, 65, 2361-2378.

GARAU, G., SILVETTI, M., DEIANA, S., DEIANA, P. & CASTALDI, P. 2011. Long-term influence of red mud on As mobility and soil physico-chemical and microbial parameters in a polluted sub-acidic soil. Journal of Hazardous Materials, 185, 1241-1248.

GEISELER, J. 1996. Use of steelworks slag in Europe. Waste Management, 16, 59-63.

GELENCSER, A., KOVATS, N., TUROCZI, B., ROSTASI, A., HOFFER, A., IMRE, K., NYIRO-KOSA, I., CSAKBERENYI-MALASICS, D., TOTH, A., CZITROVSZKY, A., NAGY, A., NAGY, S., ACS, A., KOVACS, A., FERINCZ, A., HARTYANI, Z. & POSFAI, M. 2011. The Red Mud Accident in Ajka (Hungary): Characterization and Potential Health Effects of Fugitive Dust. Environmental Science & Technology, 45, 1608-1615.

GONCALVES, M. L. S. & MOTA, A. M. 1987. Complexes of vanadyl and uranyl ions with chealting groups of humic matter. Talanta, 34, 839-847.

GRAFE, M. & KLAUBER, C. 2011. Bauxite residue issues: IV. Old obstacles and new pathways for in situ residue bioremediation. Hydrometallurgy, 108, 46-59.

GRAFE, M., POWER, G. & KLAUBER, C. 2011. Bauxite residue issues: III. Alkalinity and associated chemistry. Hydrometallurgy, 108, 60-79.

GRUIZ, K., FEIGL, V., KLEBERCZ, O., ANTON, A., AND VASZITA, E. Environmental Risk Assessment of Red Mud Contaminated Land in Hungary. Geocongress 2012: State of the

Art and Practice in Geotechnical Engineering, 2012. American Society of Civil Engineers, 4156-4165.

GRYBOS, M., DAVRANCHE, M., GRUAU, G. & PETITJEAN, P. 2007. Is trace metal release in wetland soils controlled by organic matter mobility or Fe-oxyhydroxides reduction? Journal of Colloid and Interface Science, 314, 490-501.

GUPTA, V. K., GUPTA, M. & SHARMA, S. 2001. Process development for the removal of lead and chromium from aqueous solutions using red mud - an aluminium industry waste. Water Research, 35, 1125-1134.

HAYNES, R. J., BELYAEVA, O. N. & KINGSTON, G. 2013. Evaluation of industrial wastes as sources of fertilizer silicon using chemical extractions and plant uptake. Journal of Plant Nutrition and Soil Science, 176, 238-248.

HIND, A. R., BHARGAVA, S. K. & GROCOTT, S. C. 1999. The surface chemistry of Bayer process solids: a review. Colloids and Surfaces a-Physicochemical and Engineering Aspects, 146, 359-374.

HOLLIBAUGH, J. T., CARINI, S., GURLEYUK, H., JELLISON, R., JOYE, S. B., LECLEIR, G., MEILE, C., VASQUEZ, L. & WALLSCHLAGER, D. 2005. Arsenic speciation in Mono lake, California: Response to seasonal stratification and anoxia. Geochimica Et Cosmochimica Acta, 69, 1925-1937.

HORIKOSHI, K. 1999. Alkaliphiles: Some applications of their products for biotechnology. Microbiology and Molecular Biology Reviews, 63, 735-+.

ISLAM, F. S., GAULT, A. G., BOOTHMAN, C., POLYA, D. A., CHARNOCK, J. M., CHATTERJEE, D. & LLOYD, J. R. 2004. Role of metal-reducing bacteria in arsenic release from Bengal delta sediments. Nature, 430, 68-71.

ITO, M., GUFFANTI, A. A., ZEMSKY, J., IVEY, D. M. & KRULWICH, T. A. 1997. Role of the nhaC-encoded Na+/H+ antiporter of alkaliphilic *Bacillus firmus OF4*. Journal of Bacteriology, 179, 3851-3857.

JEONG, Y., MAOHONG, F., VAN LEEUWEN, J. & BELCZYK, J. F. 2007. Effect of competing solutes on arsenic(V) adsorption using iron and aluminium oxides. Journal of Environmental Sciences, 19, 910-919.

JONES, B. E., GRANT, W. D., DUCKWORTH, A. W. & OWENSON, G. G. 1998. Microbial diversity of soda lakes. Extremophiles, 2, 191-200.

KAPPLER, A. A. S., K. L. 2005. Geomicrobiological Cycling of Iron. In: BANFIELD, J. F., CERVINI-SILVA, J., NEALSON, K. H (ed.) Molecular Geomicrobiology. Chantilly, Virginia: The Mineralogical Society of America.

KIRK, M. F., HOLM, T. R., PARK, J., JIN, Q. S., SANFORD, R. A., FOUKE, B. W. & BETHKE, C. M. 2004. Bacterial sulfate reduction limits natural arsenic contamination in groundwater. Geology, 32, 953-956.

KLAUBER, C., GRAFE, M. & POWER, G. 2011. Bauxite residue issue: II. options for residue utilization. Hydrometallurgy, 108, 11-32.

KLEBERCZ, O., MAYES, W. M., ANTON, A. D., FEIGL, V., JARVIS, A. P. & GRUIZ, K. 2012. Ecotoxicity of fluvial sediments downstream of the Ajka red mud spill, Hungary. Journal of environmental monitoring : JEM, 14, 2063-71.

KRULWICH, T. A. & GUFFANTI, A. A. 1989. ALKALOPHILIC BACTERIA. Annual Review of Microbiology, 43, 435-463.

LANGMUIR, D. 1997. Aqueous environmental geochemistry, Upper Saddle River, N. J., Prentice Hall.

LANZEN, A., SIMACHEW, A., GESSESSE, A., CHMOLOWSKA, D., JONASSEN, I. & OVREAS, L. 2013. Surprising Prokaryotic and Eukaryotic Diversity, Community Structure and Biogeography of Ethiopian Soda Lakes. Plos One, 8.

LEHMAN, R. M. & MILLS, A. L. 1994. FIELD EVIDENCE FOR COPPER MOBILIZATION BY DISSOLVED ORGANIC-MATTER. Water Research, 28, 2487-2497.

LLOYD, J. R. 2003. Microbial reduction of metals and radionuclides. Fems Microbiology Reviews, 27, 411-425.

LLOYD, J. R. & OREMLAND, R. S. 2006. Microbial transformations of arsenic in the environment: From soda lakes to aquifers. Elements, 2, 85-90.

LOMBI, E., ZHAO, F. J., ZHANG, G. Y., SUN, B., FITZ, W., ZHANG, H. & MCGRATH, S. P. 2002. In situ fixation of metals in soils using bauxite residue: chemical assessment. Environmental Pollution, 118, 435-443.

LOVLEY, D. R. 1997. Microbial Fe(III) reduction in subsurface environments. Fems Microbiology Reviews, 20, 305-313.

LU, X., JOHNSON, W. D. & HOOK, J. 1998. Reaction of Vanadate with Aquatic Humic Substances: An ESR and ^{51}V NMR Study. Environmental Science & Technology, 32, 2257-2263.

MATOCHA, C. J., KARATHANASIS, A. D., RAKSHIT, S. & WAGNER, K. M. 2005. Reduction of Copper(II) by Iron(II). Journal of Environmental Quality, 34, 1539-1546.

MAYES, W. M., JARVIS, A. P., BURKE, I. T., WALTON, M., FEIGL, V., KLEBERCZ, O. & GRUIZ, K. 2011. Dispersal and Attenuation of Trace Contaminants Downstream of the Ajka Bauxite Residue (Red Mud) Depository Failure, Hungary. Environmental Science & Technology, 45, 5147-5155.

MAYES, W. M., YOUNGER, P. L. & AUMONIER, J. 2006. Buffering of alkaline steel slag leachate across a natural wetland. Environmental Science & Technology, 40, 1237-1243.

MAYES, W. M., YOUNGER, P. L. & AUMONIER, J. 2008. Hydrogeochemistry of alkaline steel slag leachates in the UK. Water Air and Soil Pollution, 195, 35-50.

MILACIC, R., ZULIANI, T. & SCANCAR, J. 2012. Environmental impact of toxic elements in red mud studied by fractionation and speciation procedures. Science of the Total Environment, 426, 359-365.

MORTIMER, R. J. G., HARRIS, S. J., KROM, M. D., FREITAG, T. E., PROSSER, J. I., BARNES, J., ANSCHUTZ, P., HAYES, P. J. & DAVIES, I. M. 2004. Anoxic nitrification in marine sediments. Marine Ecology-Progress Series, 276, 37-51.

NAGY, A. S., SZABO, J. & VASS, I. 2013. Trace metal and metalloid levels in surface water of the Marcal River before and after the Ajka red mud spill, Hungary. Environmental Science and Pollution Research, 20, 7603-7614.

NAVARRO, C., DIAZ, M. & VILLA-GARCIA, M. A. 2010. Physico-Chemical Characterization of Steel Slag. Study of its Behavior under Simulated Environmental Conditions. Environmental Science & Technology, 44, 5383-5388.

NIELSEN, F. H. 1991. Nutritional requirements for boron, silicon, vanadium, nickel and arsenic: current knowledge and speculation. The FASEB Journal, 5, 2661-2667.

O'DAY, P. & VLASSOPOULOS, D. 2010. Mineral-Based Amendments for Remediation. Elements, 6, 375-381.

OREMLAND, R. S., DOWDLE, P. R., HOEFT, S. E., SHARP, J. O., SCHAEFER, J. K., MILLER, L. G., BLUM, J. S., SMITH, R. A., BLOOM, N. S. & WALLSCHLAGER, D. 2000. Bacterial dissimilatory reduction of arsenate and sulfate in meromictic Mono Lake, California. Geochimica Et Cosmochimica Acta, 64, 3073-3084.

OREMLAND, R. S., KULP, T. R., BLUM, J. S., HOEFT, S. E., BAESMAN, S., MILLER, L. G. & STOLZ, J. F. 2005. A microbial arsenic cycle in a salt-saturated, extreme environment. Science, 308, 1305-1308.

OREMLAND, R. S. & STOLZ, J. F. 2003. The ecology of arsenic. Science, 300, 939-944.

OREMLAND, R. S., STOLZ, J. F. & HOLLIBAUGH, J. T. 2004. The microbial arsenic cycle in Mono Lake, California. Fems Microbiology Ecology, 48, 15-27.

ORTIZ-BERNAD, I., ANDERSON, R. T., VRIONIS, H. A. & LOVLEY, D. R. 2004. Vanadium respiration by *Geobacter metalireducens*: Novel strategy for in situ removal of vanadium from groundwater. Applied and Environmental Microbiology, 70, 3091-3095.

PIGA, L., POCHETTI, F. & STOPPA, L. 1993. Recovering Metals from Red Mud Generated during Alumina Production. JOM, 45, 54-59.

POLLOCK, J., WEBER, K. A., LACK, J., ACHENBACH, L. A., MORMILE, M. R. & COATES, J. D. 2007. Alkaline iron(III) reduction by a novel alkaliphilic, halotolerant, Bacillus sp isolated from salt flat sediments of Soap Lake. Applied Microbiology and Biotechnology, 77, 927-934.

POSTMA, D. & JAKOBSEN, R. 1996. Redox zonation: Equilibrium constraints on the Fe(III)/SO_4^-reduction interface. Geochimica Et Cosmochimica Acta, 60, 3169-3175.

POWER, G., GRAFE, M. & KLAUBER, C. 2011. Bauxite residue issues: I. Current management, disposal and storage practices. Hydrometallurgy, 108, 33-45.

PROCTOR, D. M., FEHLING, K. A., SHAY, E. C., WITTENBORN, J. L., GREEN, J. J., AVENT, C., BIGHAM, R. D., CONNOLLY, M., LEE, B., SHEPKER, T. O. & ZAK, M. A.

2000. Physical and chemical characteristics of blast furnace, basic oxygen furnace, and electric arc furnace steel industry slags. Environmental Science & Technology, 34, 1576-1582.

RATNAIKE, R. N. 2003. Acute and chronic arsenic toxicity. Postgraduate Medical Journal, 391-396.

REEVES, H. J., WEALTHALL, G. & YOUNGER, P. L. 2011. Advisory visit to the bauxite processings tailings dam near Ajka, Vesprem County, western Hungary. . Keyworth, UK: British Geological Survey.

REHDER, D. 1991. THE BIOINORGANIC CHEMISTRY OF VANADIUM. Angewandte Chemie-International Edition in English, 30, 148-167.

REKASI, M., FEIGL, V., UZINGER, N., GRUIZ, K., MAKO, A. & ANTON, A. 2013. Effects of leaching from alkaline red mud on soil biota: modelling the conditions after the Hungarian red mud disaster. Chemistry and Ecology, 29, 709-723.

RENFORTH, P., MAYES, W. M., JARVIS, A. P., BURKE, I. T., MANNING, D. A. C. & GRUIZ, K. 2012. Contaminant mobility and carbon sequestration downstream of the Ajka (Hungary) red mud spill: The effects of gypsum dosing. The Science of the total environment, 421-422, 253-9.

RICHTER, R. O. & THEIS, T. L. 1980. Nickel Speciation in a Soil/Water System. In: NRIAGU, J. O. (ed.) Nickel in the Environment.

RITTER, K., AIKEN, G. R., RANVILLE, J. F., BAUER, M. & MACALADY, D. L. 2006. Evidence for the aquatic binding of arsenate by natural organic matter-suspended Fe(III). Environmental Science & Technology, 40, 5380-5387.

ROADCAP, G. S., KELLY, W. R. & BETHKE, C. M. 2005. Geochemistry of extremely alkaline (pH > 12) ground water in slag-fill aquifers. Ground Water, 43, 806-816.

ROADCAP, G. S., SANFORD, R. A., JIN, Q. S., PARDINAS, J. R. & BETHKE, C. M. 2006. Extremely alkaline (pH > 12) ground water hosts diverse microbial community. Ground Water, 44, 511-517.

RUBINOS, D. A. & BARRAL, M. T. 2013. Fractionation and mobility of metals in bauxite red mud. Environmental science and pollution research international, 20, 7787-802.

RUYTERS, S., MERTENS, J., VASSILIEVA, E., DEHANDSCHUTTER, B., POFFIJN, A. & SMOLDERS, E. 2011. The Red Mud Accident in Ajka (Hungary): Plant Toxicity and Trace Metal Bioavailability in Red Mud Contaminated Soil. Environmental Science & Technology, 45, 1616-1622.

SAUVE, S., MCBRIDE, M. B., NORVELL, W. A. & HENDERSHOT, W. H. 1997. Copper solubility and speciation of in situ contaminated soils: Effects of copper level, pH and organic matter. Water Air and Soil Pollution, 100, 133-149.

SCHIPPERS, A., NERETIN, L. N., KALLMEYER, J., FERDELMAN, T. G., CRAGG, B. A., PARKES, R. J., JORGENSEN, B. B. 2005. Prokaryotic cells of the deep sub-sea floor biosphere identified as living bacteria. Nature, 433(7028), 861-864.

SCHWAB, A. P., HICKEY, J., HUNTER, J. & BANKS, M. K. 2006. Characteristics of blast furnace slag leachate produced under reduced and oxidized conditions. J Environ Sci Health A Tox Hazard Subst Environ Eng, 41, 381-95.

SHARMA, P., OFNER, J. & KAPPLER, A. 2010. Formation of Binary and Ternary Colloids and Dissolved Complexes of Organic Matter, Fe and As. Environmental Science & Technology, 44, 4479-4485.

SHEFFIELD, P. M. 1996. Investigation and remediation of alkaline leachate from the former Consett Steelworks Site Unpublished MSc, The University of Sheffield.

SHIBA, H., YAMAMOTO, H. & HORIKOSHI, K. 1989. ISOLATION OF STRICTLY ANAEROBIC HALOPHILES FROM THE AEROBIC SURFACE SEDIMENTS OF HYPERSALINE ENVIRONMENTS IN CALIFORNIA AND NEVADA. Fems Microbiology Letters, 57, 191-195.

SMEDLEY, P. L. & KINNIBURGH, D. G. 2002. A review of the source, behaviour and distribution of arsenic in natural waters. Applied Geochemistry, 17, 517-568.

SPARKS, D. L. 2005. Toxic Metals in the Environment: The Role of Surfaces. Elements, 1, 193-197.

STEVENSON, F. J. 1994. Humus chemistry: genesis, composition, reactions, John Wiley and Sons Inc.

STURR, M. G., GUFFANTI, A. A. & KRULWICH, T. A. 1994. Growth and Bioenergetics of Alkaliphilic *Bacillus-Firmus OF4* in continuous-culture at high pH. Journal of Bacteriology, 176, 3111-3116.

SUMMERS, R. N., GUISE, N. R. & SMIRK, D. D. 1993. BAUXITE RESIDUE (RED MUD) INCREASES PHOSPHORUS RETENTION IN SANDY SOIL CATCHMENTS IN WESTERN-AUSTRALIA. Fertilizer Research, 34, 85-94.

SZALAY, A. & SZILAGYI, M. 1967. ASSOCIATION OF VANADIUM WITH HUMIC ACIDS. Geochimica Et Cosmochimica Acta, 31, 1-&.

TAKAI, K., MOSER, D. P., ONSTOTT, T. C., SPOELSTRA, N., PFIFFNER, S. M., DOHNALKOVA, A. & FREDRICKSON, J. K. 2001. *Alkaliphilus transvaalensis* gen. nov., sp nov., an extremely alkaliphilic bacterium isolated from a deep South African gold mine. International Journal of Systematic and Evolutionary Microbiology, 51, 1245-1256.

TAKAI, K., MOYER, C. L., MIYAZAKI, M., NOGI, Y., HIRAYAMA, H., NEALSON, K. H. & HORIKOSHI, K. 2005. *Marinobacter alkaliphilus* sp nov., a novel alkaliphilic bacterium isolated from subseafloor alkaline serpentine mud from Ocean Drilling Program Site 1200 at South Chamorro Seamount, Mariana Forearc. Extremophiles, 9, 17-27.

THE EUROPEAN SLAG ASSOCIATION. 2014. Ferrous Slag - general information [Online]. Germany. Available: http://www.euroslag.com/products/ [Accessed 27.03.2014].

TIAGO, I., CHUNG, A. P. & VERISSIMO, A. 2004. Bacterial diversity in a nonsaline alkaline environment: Heterotrophic aerobic Populations. Applied and Environmental Microbiology, 70, 7378-7387.

TUNNACLIFFE, V. 1991. The Biology of hydrothermal vents - Ecology and Evolution. Oceanography and Marine Biology, 29, 319-407.

U.S. GEOLOGICAL SURVEY 2013. Mineral commodity summaries 2013. In: U.S. GEOLOGICAL SURVEY (ed.). Reston Virginia: U.S.Geological Survey,.

UNITED STATES ENVIRONMENTAL PROTECTION AGENCY 1992. Toxicity Characteristic Leaching Procedure. Method 1311.

VAN MARWIJK, J., OPPERMAN, D. J., PIATER, L. A. & VAN HEERDEN, E. 2009. Reduction of vanadium(V) by *Enterobacter cloacae EV-SA01* isolated from a South African deep gold mine. Biotechnology Letters, 31, 845-849.

WANTY, R. B. & GOLDHABER, M. B. 1992. THERMODYNAMICS AND KINETICS OF REACTIONS INVOLVING VANADIUM IN NATURAL SYSTEMS - ACCUMULATION OF VANADIUM IN SEDIMENTARY-ROCKS. Geochimica Et Cosmochimica Acta, 56, 1471-1483.

WARD, D. M., BATESON, M. M., FERRIS, M. J., KUHL, M., WIELAND, A., KOEPPEL, A. & COHAN, F. M. 2006. Cyanobacterial ecotypes in the microbial mat community of Mushroom Spring (Yellowstone National Park, Wyoming) as species-like units linking microbial community composition, structure and function. Philosophical Transactions of the Royal Society B-Biological Sciences, 361, 1997-2008.

WEHRLI, B. & STUMM, W. 1989. VANADYL IN NATURAL-WATERS - ADSORPTION AND HYDROLYSIS PROMOTE OXYGENATION. Geochimica Et Cosmochimica Acta, 53, 69-77.

WHITTLESTON, R. A., STEWART, D. I., MORTIMER, R. J. G., ASHLEY, D. J. & BURKE, I. T. 2011. Effect of Microbially Induced Anoxia on Cr(VI) Mobility at a Site Contaminated with Hyperalkaline Residue from Chromite Ore Processing. Geomicrobiology Journal, 28, 68-82.

WILKIE, M. P. & WOOD, C. M. 1996. The adaptations of fish to extremely alkaline environments. Comparative Biochemistry and Physiology B-Biochemistry & Molecular Biology, 113, 665-673.

WORLD HEALTH ORGANISATION. 2008. Guidelines for Drinking-water Quality. [Accessed 8th April 2014].

WU, J., WEST, L. J. & STEWART, D. I. 2001. Copper(II) humate mobility in kaolinite soil. Engineering Geology, 60, 275-284.

YE, Q., ROH, Y., CARROLL, S. L., BLAIR, B., ZHOU, J. Z., ZHANG, C. L. & FIELDS, M. W. 2004. Alkaline anaerobic respiration: Isolation and characterization of a novel alkaliphilic and metal-reducing bacterium. Applied and Environmental Microbiology, 70, 5595-5602.

YIN, Y. J., IMPELLITTERI, C. A., YOU, S. J. & ALLEN, H. E. 2002. The importance of organic matter distribution and extract soil : solution ratio on the desorption of heavy metals from soils. Science of the Total Environment, 287, 107-119.

ZACHARA, J. M., FREDRICKSON, J. K., SMITH, S. C. & GASSMAN, P. L. 2001. Solubilization of Fe(III) oxide-bound trace metals by a dissimilatory Fe(III) reducing bacterium. Geochimica Et Cosmochimica Acta, 65, 75-93.

ZHILINA, T. N., ZAVARZINA, D. G., KOLGANOVA, T. V., LYSENKO, A. M. & TOUROVA, T. P. 2009. *Alkaliphilus peptidofermentans* sp nov., a new alkaliphilic bacterial soda lake isolate capable of peptide fermentation and Fe(III) reduction. Microbiology, 78, 445-454.

ZOBRIST, J., DOWDLE, P. R., DAVIS, J. A. & OREMLAND, R. S. 2000. Mobilization of arsenite by dissimilatory reduction of adsorbed arsenate. Environmental Science & Technology, 34, 4747-4753.

Chapter 3 Materials and Methods

This chapter describes in detail the sample collection, and methods used for the experimental and analytical work presented in this thesis, including some theoretical background to the instrumental analysis and techniques used where appropriate.

3.1 Sample Collection

3.1.1 Hownsgill Valley Site

Groundwater and soil were sampled from the Hownsgill Valley, near Consett, Co. Durham on 4th November 2010. A small trial pit was excavated on the calcite banks of the leachate pond. Once the pit had filled with groundwater (this occurred rapidly), preliminary readings of the pH (~12) and Eh (~100mV) of the groundwater were measured with a portable Hanna HI 98129 Combo meter, calibrated using pH 7.01 and 10.01 buffer solutions. 5 L of groundwater was then extracted from the pit, stored in a polypropylene container and was refrigerated upon return to the lab.

Another small pit was excavated approximately 10 m from the original. The soil in the second pit showed definite layering of surface and deeper soil (Figure 3.1). Both soil layers were sampled, and stored in 2 L plastic container. The deeper soil was homogenised on site with a 1 cm sieve. The soil samples were refrigerated (2°C) upon return to the laboratory until required.

Laboratory measurements of the sample water pH were measured the following day (pH 11.83). 100 ml of the water samples and ~150g samples of both soil types were

frozen for later analysis. The remaining soil and water samples were refrigerated for use in microcosm experiment at a later date (18 days after sampling).

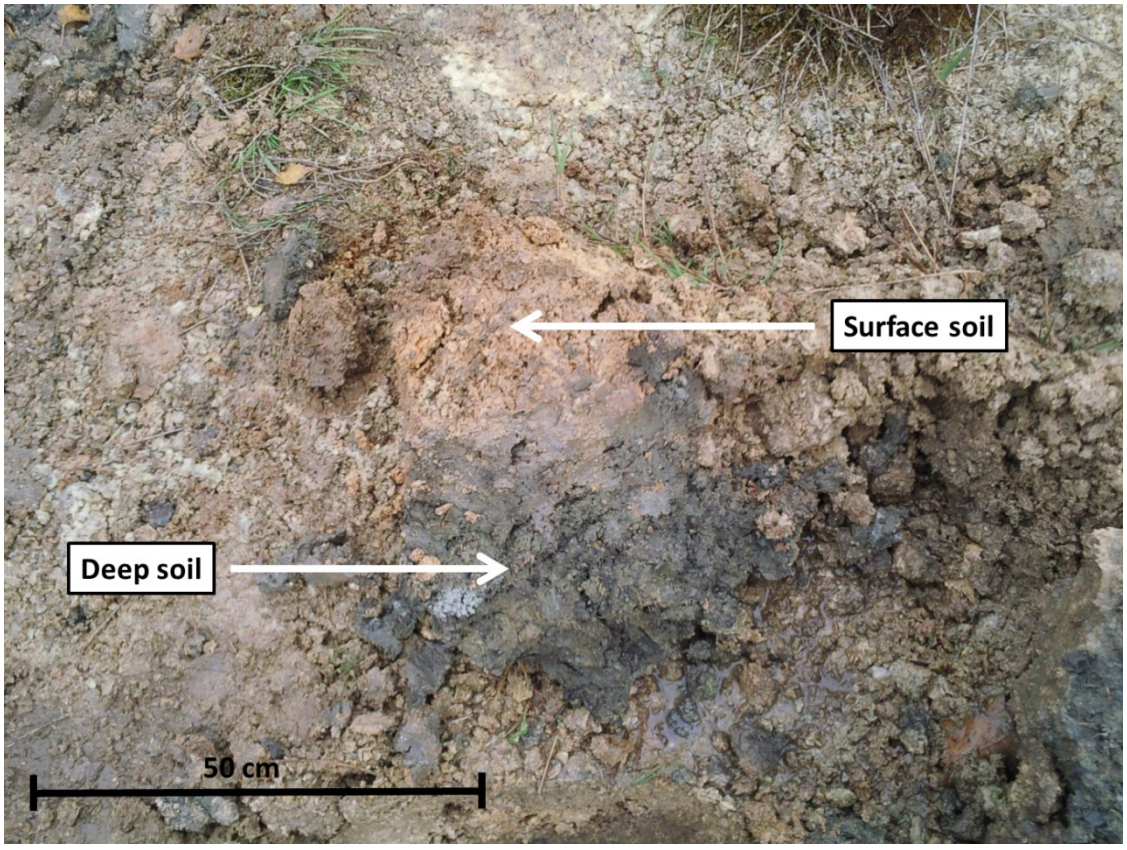

Figure 3.1 – Digital photograph of the soil excavated at the Hownsgill Valley site, showing the two distinct soil layers of surface and deeper soil

3.1.2 Veszprém County, western Hungary

Soil unaffected by red mud from the tailings dam breach was sampled from three different sites (Figure 3.2).

3.1.2.1 Sandy Soil (SS)

Reference soil as previously sampled by the Department of Applied Biotechnology and Food Science at Budapest University of Technology and Economics was sampled. The site is agricultural farmland that is situated on the roadside between

the villages of Devecser and Somlóvásárhely (47°6’38.01” N, 17°23’43.03” E). The site is approximately 8km from source and the ‘clean up’ operation of the agricultural field scraping was visible in the surrounding fields. The ditch soil was sampled without perturbation and was stored and sealed in a 2 L plastic container.

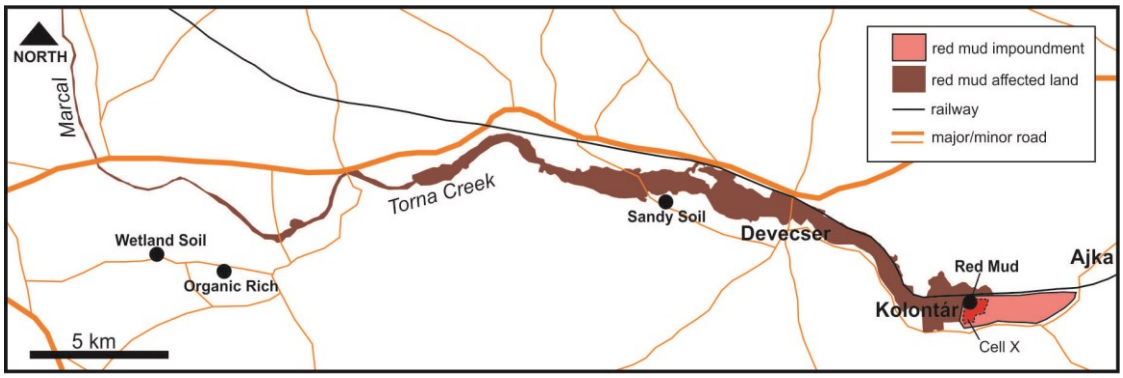

Figure 3.2 - Map showing the affected area and sample locations

3.1.2.2 Organic-rich Soil (OR)

Top soil was sampled from a field, with non-agricultural use in the area between Veszprémgalsa and Zalaszegvàr (47° 5’46.49” N, 17° 15’1.33” E). The site is approximately 18.5km from source. There were no signs of any red mud contamination in the field or the surrounding area. Dark top soil from immediately beneath the rootlet layer was sampled (between 10 - 30cm depth) without perturbation and was stored and sealed in a 2 L plastic container.

3.1.2.3 Wetland Soil (WL)

An anaerobic site was sampled in an area of wetland at the roadside on the outskirts of Zalaszegvàr (47° 5’56.39” N, 17° 13’40.90” E). The site is approximately 20.5km from source and there were no signs of any red mud contamination in the field

or surrounding area. Dark anaerobic soil was sampled from a reed bed at a depth of ~40cm. The soil was stored in several small plastic containers without further perturbation. The smaller containers were held inside one large container together with Anaerogen™ sachets. The large container was double bagged and sealed. Readings of pH (6.98), Eh (50 mV), total dissolved solids (902 mg L^{-1}) and conductivity (1281 µS) were taken from mixed surface and ground water at the site.

3.1.2.4 Tailings Pond (X), MAL Zrt

Red mud and affected leachate were sampled from inside the breached dyke at Ajkai Timfoldgyar Zrt alumina plant on 11th May 2011. Red mud was easily accessible as it was still present on site in large piles which had been left to dry since the dyke breach when the majority of the slurry waste had been released. The top layer of the red mud was very dry and this was removed with a spade to reveal a soft clay-like material. Both types of red mud were sampled and were stored and sealed in 1 L plastic containers labelled: Red Mud Dry and Red Mud Clay-like.

Hyper-alkaline leachate was sampled from a leachate pond that had accumulated behind a 12m deep concrete barrier which had been designed to reach the bottom of the red mud waste deposits. Preliminary readings of pH (12.2), Eh (-31 mV) and total dissolved solids (31 ng L^{-1}) and conductivity (31 mS) were measured with a portable Myron L Ultrameter II 6PSi, that was calibrated using pH 7.01 and 10.01 buffer solutions. 2 L of leachate was extracted from the pond and stored in 2x 1 L plastic containers. The samples were stored at ambient temperature until they were returned to the lab where they were refrigerated at 2°C.

3.1.3 Principle Component Analysis

Principle component analysis (PCA) is a statistical tool used to reduce the number of dimensions of a data set with large numbers of interrelated variables, whilst retaining as much of the set's variation as is possible. In computational terms, a new set of uncorrelated variables are found and ordered so that the first few keep most of the variation present in all the original set of variables. The first of these newly ordered variables is the principle component of the new set (Joliffe, 2002). PCA was used for the samples collected from Ajka to show them in the broader context of large scale soil and sediment sampling efforts across a 100 km reach of the Torna-Marcal-Raba River system in the immediate aftermath of the spill (Mayes et al., 2011). The theory behind the use of PCA in this study is that it will allow for the distinction between soils samples affected by the red mud spill, as sampled by Mayes et al. (2011) and the unaffected reference soils sampled at Ajka, in May 2011 (section 3.1.2).

Reference soils and red mud sampled on the site visit to Hungary in May 2011 were plotted alongside the larger scale study (Mayes et al., 2011). Each point represents a single sampling event from this study and Mayes et al. (2011). PCA was generated using Minitab v.15 software using XRF and other geochemical data (pH, ORP) from the red mud and Hungarian soils, as variables (see Figure 5.1).

3.2 Sample Characterisation

3.2.1 Sample pH

All soil sampled and red mud pH was determined following the ASTM (2006) standard method for pH in soils. 10 g of sample was suspended in a 1:1 ratio with DIW

and left to equilibrate for 1 hour before measurements were taken using an Orion benchtop pH meter with combination pH electrode (VWR International). The pH meter was calibrated using pH 4.01, 7.01 and 10.01 buffers. The measurements were carried out in triplicate (≤0.1 SD).

3.2.2 % 0.5 M Acid extractable Iron as Fe(II)

The percentage of microbially available iron (as Fe(II)) in soils, red mud and at microcosms sampling points was determined with a UV/Vis spectrophotometry method using 'ferrozine' (3-(2-pyridyl)5,6-bis(4-phenylsulfonic acid)-1,2,4-triazine). When dissolved in ammonium acetate, ferrozine reacts with ferrous iron forming a magenta coloured solution (λ_{max} = 562 nm). The method can be further adapted by using hydroxylamine hydrochloride as a reducing agent and an ammonium acetate buffer (pH 9.5) to reduce any ferric iron in solution to Fe(II) thus allowing for the determination of total Fe in solution. Measuring the change in Fe(II) relative to total Fe (Fe_T) over time can be used to monitor microbial Fe(III) reduction. The ratio of Fe(II):Fe(III) increases as bacterial oxidation of organic material is coupled with Fe(III) reduction of insoluble iron oxides (Lovley, 1997). The forms of iron considered readily available to bacteria in the subsurface are poorly crystalline, amorphous iron phases and it is possible to extract these phases using 0.5 M HCl under a 1 hour extraction time (Lovley and Phillips, 1986b). Therefore determining the change in ratio of Fe(II) to Fe_T over time in these phases can be use to monitor the progression of microbial iron reduction.

In order to assess the percentage of reduced iron in samples, 0.5M HCl acid extractable Fe(II) was measured against the Fe_T (adapted method from (Lovley and Phillips, 1986b; Viollier et al., 2000). A 'pea sized' amount of soil/red mud was added

to a 12.5 mL tube together with 0.5M HCl (5 mL). In the case of microcosm samples, a pellet of sediment recovered after centrifugation (3 min, 16,000g) was re-suspended with 0.5 M HCl (1 mL) and transferred to a 12.5 mL tube containing 0.5 M HCl (4 mL). The tubes were sealed, shaken and left for exactly 60 minutes on an orbital shaker (150 rpm). After 60 minutes the samples were filtered through a 0.2 μm syringe filter into a clean 12.5 mL tube. Five repeats of each soil sample were analysed and microcosm samples were in triplicate (% RSD 3.5% microcosm samples, 14% soil samples 12% red mud).

Cuvette 1 - test for Fe(II): The following reagents were added to a 4 mL cuvette: sample (100 μL), DIW (2900 μL), ferrozine solution (300 μL, 0.01 M).Cuvette 2 - test for Fe_T: The following reagents were added to a 4 mL cuvette: sample (100 μL), DIW (2000 μL), ferrozine solution (300μL, 0.01 M), hydroxylammonium hydrochloride solution (600 μL, 1.4 M) and buffer solution (300 μL, 9.8 M, pH 9.5 (adjusted with ammonium hydroxide).

The cuvettes were sealed with parafilm ™, shaken by hand and left for 10 minutes for a colour to develop. The absorbance was measured against matrix matched blanks at 562 nm. If high concentrations of iron were seen which resulted in saturation (Abs >2), the test was repeated using 50 μL of sample and additional DIW. If concentrations were low (Abs < 0.5) the test was repeated using 200 μL of sample and less DIW. The percentage of Fe(II) against total Fe was then calculated.

3.2.3 X-ray powder diffraction (XRD)

X-ray powder diffraction is used to identify bulk mineral phases present in samples. A beam of x-rays is directed at the solid and the photons of the x-ray beam are scattered by atoms as they strike the surface. Any unscattered x-rays pass through to the next layer of atoms and so forth, thus resulting in a diffraction pattern that is characteristic to that solid. A diffraction pattern is seen, in accordance with Bragg's Law, when

$$\sin\theta = \frac{n\lambda}{2d} \tag{3.1}$$

λ = wavelength (Å)

d = spacing between atomic layers (Å)

θ = angle of incidence

n = an integer,

Powder XRD analysis was performed on all soil samples together with the red mud samples. The soil samples were oven dried at 60°C. The soil was then ground to a fine talc like powder in a pestle and mortar. Fine red mud powder was crushed lightly in a pestle and mortar after air drying for several days under a protective cover. The wet clay-like red mud was smeared in a fine layer across several glass plates and left to air dry under a protective cover. After several days the dried red mud was removed and crushed lightly by pestle and mortar. Bulk soil and red mud diffraction patterns were collected using a Bruker D8 powder X-ray diffractometer with a Ge(111) monochromator, (CuK alpha = 1.54 Å̊; 2Θ = 5 - 70° divergence and antiscatter slits set to variable 20 mm; patterns were recorded at 0.01 step at 0.5 seconds/step).

3.2.4 X-ray fluorescence

X-ray fluorescence provides information on the elemental composition of a sample. When x-rays are directed at a sample, an electron is removed from a low energy inner-shell, leaving a vacancy. In order to return to the original configuration, an electron from a higher energy level shell fills the vacant site. The process of this electron replacements results in the emission of secondary x-rays, which is measured as fluorescence. The energy of the emitted x-rays is dependent upon the difference in energy between the two shells and is unique to individual elements. The intensity of the secondary x-ray emitted corresponds to the concentration of that element in the sample, and can be determined by comparison against known standards (Brouwer, 2010).

Homogenised soil and red mud samples were characterised for major and trace elements using a PANalytical Axios Advanced XRF spectrometer. Major elements were determined on fused glass beads prepared from ignited powders. Sample to flux ratio 1 : 5, 80% Li metaborate: 20% Li tetraborate flux. Trace elements were analysed on 32 mm diameter pressed powder pellets produced from mixing 7.5g fine ground sample with 12 – 15 drops of 7% PVA solution (Moviol 8-88) pressed at 10 tons per square inch.

(Analysis carried out by Department of Geology, University of Leicester).

3.2.5 BET specific surface area

Specific surface area is calculated using BET theory (Brunauer et al., 1938) from gas adsorption isotherm data. It is an expansion of the Langmuir equation of single layer sorption taking into account multi-layered adsorption. The BET model assumes that i) 1st layer adsorption occurs at strong uniform sites of energy; ii) that the 2nd layer adsorbs

to 1st and 3rd to 2nd etc; iii) at equilibrium the rate of condensation is equal to the rate of evaporation for each layer and iv) when the number of adsorbed layers is greater or equal to 2, then equilibrium constants are equal.

The surface area of all soil samples and red mud was determined by measurement of the BET surface area by gas adsorption with helium at 77K. Dried soil and red mud were gently disaggregated by hand prior to weighing into pre-weighed sample tubes. Samples were degassed with N_2 on a Micromeritics FlowPrep 060 sample degas system prior to analysis with a Micromeritics Gemini V BET surface area analyser (%RSD = 3%).

3.2.6 Total carbon, organic and inorganic carbon

Homogenised samples were oven dried at 105°C and disaggregated with a pestle and mortar. A portion of each sample was washed with 10% HCl to remove any carbonates following the method of Schumacher (2002) for total organic carbon determination. Total carbon together with total organic carbon was determined using a Carlo Erba NA 2500 Elemental Analyser. Total inorganic carbon was deemed to be the difference between total carbon and total organic carbon.

(Analysis carried out by School of GeoSciences, University of Edinburgh).

3.2.7 Inorganic phosphate in samples

Inorganic phosphate was determined by the molybdenum blue method (Murphy and Riley, 1962; Aspila et al., 1976) on soil and red mud samples. Dried sample (0.1g)

was weighed into a 15 mL centrifuge tube and the weight to 4 decimal places was recorded. HCl (1 M, 10 mL) was added. The tubes were sealed and left shaking on an orbital shaker overnight. The samples were then filtered with 0.45 μm syringe filter and the filtrate was diluted 10x with MilliQ. A mixed reagent solution (50 mL) was made up using H_2SO_4 (25 mL, 2.5 M), ammonium molybdate (7.5 mL, 0.2 M), antimony K-tartrate (2.5 mL, 4.34 x 10^{-3} M) and ascorbic acid (15 mL, 0.1 M).

Diluted sample (2 mL) and mixed reagent (0.5 mL) were pipetted into a 4 mL cuvette and left for 15 minutes for a colour to develop. The absorbance was measured at 880 nm against a matrix matched blank. Standards were prepared from a 1000 ppm, PO_4^{3-} solution in HCl (0.1 M) between 0.25 μM and 20 μM and treated as the samples above (R^2 = 0.999). A certified reference sample (LGC6020) was used to check the accuracy and precision of the measurements (%RSD 5%, relative error 4%)

3.3 Batch microcosm experiments

Individual batch microcosm experiments are described in detail in the methods section of the results chapters (Chapters 4, 6, 7 and 8). Below is a description of general methods used for microcosm sterilisation, and the technique used for sampling the microcosms

3.3.1 Microcosm Sterilisation

The use of control experiments using sterile microcosms is required in order to establish background conditions and the abiotic processes that occur in microcosms without influence from microbially mediated transactions. It is therefore important that the method of sterilisation chosen is able to inhibit or eliminate organisms without

changing chemical and physical soil characteristics (Tuominen et al, 1994). There are several different methods of soil sterilisation, the most widely used methods include forms of; heat sterilisation, chemical sterilisation and irradiation. Each method of sterilisation can affect the soil in different ways, and therefore the chosen method will depend upon the specificities of the research; i.e. length of incubation period, geochemical determinations required etc. A brief description of common sterilisation techniques are described below.

3.3.1.1 Gamma (γ-) irradition

The use of gamma (γ-) irradiation from cobalt-60 has been recommended in several studies over other soil sterilisation techniques, as minimal soil disturbance occurs during the sterilisation process (Trevors, 1996, McNamara et al, 2003). However, this technique can only be carried out at an appropriate irradiation facility, where soil samples are placed in sealed polythene bags and irradiated at 2.5 Mrad at the rate of 2 Mrad $hour^{-1}$ (Trevors, 1996). The main problems associated with γ-irradiation are the increased release of soil nutrients (e.g. nitrogen species, manganese and phosphorous) and damage to soil organic matter (Wolf et al, 1989; McNamara et al, 2003).

3.3.1.2 Chemical Sterilisation

Chemical sterilisation can be achieved by either fumigation by gaseous chemicals or by the addition of chemicals to the soil directly. Common chemical agents for fumigation are chloroform ($CHCl_3$), propylene oxide (CH_3CHCH_2) and methyl bromide (CH_3Br) (Trevors, 1996). Chemicals routinely added to soils for sterilisation are formaldehyde (CH_2O), mercuric chloride ($HgCl_2$) and sodium azide (NaN_3) (Trevors, 1996). One of the main problems associated with chemical sterilisation is the

toxicity and disposal problems relating to the chemicals required, particularly with regards to Hg contaminated samples (Trevors, 1996). However, there are other disadvantages to using chemical sterilisation: for example, Wolf et al., (1989) found that soil pH increased with the use of propylene oxide and sodium azide. It is worth noting that sodium azide is an inhibitor and does not sterilise the soil, therefore further additions of NaN_3 are required over the incubation period of the experiments. High concentrations of NaN_3 can also result in Na leaching (Trevors, 1996).

3.3.1.3 Heat Sterilisation

Heat sterilisation of soils by autoclaving is a widely used method, mainly due to the ease of use and instrument availability. Usually, soil is autoclaved in a glass beaker at 121°C for 30 - 60 minutes. It is important that the layer of soil in the beaker is not too deep to allow for the steam to fully penetrate the soil (Trevors, 1996). Heat sterilisation by autoclaving is more effective after it is repeated for several widely spaced cycles, as a rest period between cycles allows for the recovery of spore forming bacteria which are then destroyed in the next cycle (Lotrario et al, 1995). Studies have shown that the use of autoclaving can decrease the surface area of clays and alter the surface charge of sandstone (Jenneman et al, 1986; Lotrario et al, 1995), but that it has little effect on soil pH, organic matter content and cation exchange capacity (Lotrario et al, 1995). It should be noted that dry soil sterilisation can also be used, but spore-forming bacteria are more resistant to dry heat than autoclaving (Trevors, 1996).

Heat sterilisation was used in all microcosm experiments in the absence of a suitable irradiation facility. It was decided that one cycle of 121°C would be adequate to eliminate the majority of organisms in the soil and red mud slurries. However, the main reasons for using heat sterilisation was the lack of chemical interference (increase in

nutrient leaching from soils, Na^+ and Cl^- leaching) and to avoid any change to soil pH which was considered to be crucial to these experiments.

3.3.2 Microcosm sampling technique

Slurry (~3 ml) was extracted with a sterile needle (19G x 2" 1.1mm x 50 mm) from sealed microcosm bottles with OFN and equally distributed between two 1.5 ml Eppendorf centrifuge tubes. The tubes were centrifuged for 3 minutes at 14,000 rpm in Sigma Microcentrifuge 1-14ED. Supernatant from tube 1 was filtered (0.2 μm) into a clean centrifuge tube and half was acidified with 2% HNO_3 for ICP-MS analysis, the other half was frozen along with the soil residue, for future anion analysis and potential microbial work.

The supernatant from tube 2 was decanted into a 15 ml blood tube. 100 μL of each sample was pipetted into 3x 1.5mL micro cuvettes for V(V) analysis if required (see Section 3.4.1 below). The remaining sample was then used for pH and ORP measurements using a Thermo Scientific Orion DualStar pH/ISE benchtop meter with a Hamilton Polyplast ORP BNC electrode and a VWR 662-1759 pH electrode. The remaining soil was used for % 0.5M HCl acid extractable iron (as Fe(II)) analysis (Section 3.2.2 above).

3.4 Geochemical Analysis

3.4.1 Determination of Vanadium (V)

Aqueous V(V) was determined by a reaction with 4-(2-pyrodylazo)-resorcinol (PAR) to produce a very sensitive violet colouration (λ_{max} = 550 nm). The optical density of the reaction is highest between pH 5 – 8. In the past, PAR has also been used as a reagent for the colorimetric determination of many other metal ions, e.g. Co, Ga, In, Nb, Pd, Sc, Th and U. However, the selectivity of the PAR/V(V) reaction can be much improved by the addition of 1,2-diaminocyclohexanetetra acetic acid (DCTA). The presence of DCTA prevents the reaction of many metals with PAR making it a very selective method for determining V(V) except in the presence of high concentrations of Nb, Ti and U. The method obeys the Beer Lambert law between 10 – 1000 µM (Budevsky, 1965; Ortiz-Bernad et al., 2004).

Sample (100µL) was pipetted into a cuvette (1.5mL). The following reagents were then added: mixed DCTA (0.011 M) and ammonium acetate (0.088 M) buffer solution (900µL, pH adjusted to 5.5 with acetic acid) and PAR indicator reagent (100 µL, 0.001 M). The solution was then left for 30 minutes for any colour to develop. The absorbance was then measured at 550 nm. Standards between 0.01 and 0.5 mM were prepared from a 10 mM stock solution of V(V) (R^2 = ≥0.999, %RSD 1.8%)

3.4.2 Anion analysis by Ion Chromatography

Aqueous concentrations of chloride, nitrate, nitrite and sulfate were determined using ion chromatography. An aqueous sample is loaded onto a stationary phase column which is packed with a material that has a high affinity for anionic species. An ionic

eluent (e.g. a carbonate solution) is then passed through the column which displaces the anions. The time interval between the sample injection and anion detection is known as the retention time. Retention times vary for each anion due to the affinity of the anion to the stationary column. The anion can be identified by matching elution peaks at given retention times by comparison to known standard materials. The concentration of the anions is determined by the definite integral of the elution peak together with comparisons against a calibration curve with standards at known concentrations.

Analysis was performed for the Hownsgill Valley samples on a Dionex DX600 AS16 column and hydroxide gradient elution with supressed conductivity and UV detection which was fitted for absorption at 225 nm. Ajka samples were analysed on a Dionex DX500 AS9 column and sodium carbonate (0.009 M) elution with supressed conductivity and UV detection which was fitted for absorption at 225 nm. Blanks and 25 mg L^{-1} standard were checked after every 10 samples to check for drift over the time of the analysis. Mixed anion standards were prepared from 500 mg L^{-1} stock solutions of NaCl, Na_2NO_3 and Na_2SO_4 and from a 46 mg L^{-1} stock for $NaNO_2$. Accuracy was checked by using certified reference materials (CRM) (LGC6020 and Hamilton-20). (R^2 = ≥0.99, % RSD = Cl^- = 2.7%, NO_3^- = 6.2%, SO_4^{2-} = 3.4%, NO_2^- = 7.0%, % relative error to CRM Cl^- = <8%, $SO4_2^-$ = <7% NO_3 = <7% (n = 26).

3.4.3 Aqueous trace metal/loid analysis by Inductively Coupled Plasma Mass Spectrometry (ICP-MS)

Aqueous concentrations main elements of interest; As, Cd, Co, Cu, Cr, Mn, Mo, Ni and V were determined using a Perkin-Elmer Elan DRCII inductively coupled

plasma-mass spectrometer. Acidified aqueous samples are introduced to an argon plasma as an aerosol via a nebulizer and spray chamber to ensure an aerosol with homogeneous particle size. The plasma removes an electron from the components to form single-charged ions. The single-charged ions are directed into the mass spectrometer, which is under a high vacuum, through a pumped double platinum cone interface. The mass spectrometer filters the components according to their mass, where only one mass to charge ratio is allowed through the spectrometer at a time. Upon exiting the quadrupole mass spectrometer, the ions strike an electron multiplier which acts as the detector. The impact of ions on the electron multiplier causes a cascade release of electrons depending upon the intensity of the component. The intensities of each component are then compared to those of known standards which are used to determine the concentration of the element from a calibration line.

Mixed standards were prepared from stock 1000 mg L^{-1} standard solutions (Romil Ltd, Cambridge UK) between 1 µg L^{-1} and 100 µg L^{-1} (R^2 = ≥0.9999, %RSD < 1%). After every 10 samples, blanks and the 50 ppb standard was measured to detect any drift over the time of the analysis. All samples were diluted 10x with 2% HNO_3^-. Ga and In were used as internal standards, which were mixed 1:1 with the sample stream online.

ICP-MS is a highly sensitive analytical technique and has been primarily used in this study due the capability for multi-elemental analysis and low detection limits (ng L^{-1} level for many elements). However, there can be problems with interferences which need to be addressed. Generally, interferences occur when polyatomic ions are generated by the plasma that have a mass to charge ratio that is identical to that of an analyte (PerkinElmerSCIEX, 2003) when measured with a quadrupole mass spectrometer such as the Elan DRCII instead of a high resolution instrument. Arsenic, a

key element in this study, has one single isotope, ^{75}As and this is overlapped by a ^{40}Ar ^{35}Cl peak. It is possible to correct for this interference using an interference equation, as follows:

I (As75) = I(75) – I (Ar 40 Cl 35) (3.2)

I (Ar 40 Cl 35) = I (75) – [abundance (Cl 35) / abundance (Cl 37) x I (77)]

Where I = intensity of a specified mass

abundance = natural abundance of the isotope

Which can be combined and rewritten as:

I (As75) = I (75) – [abundance (Cl 35) / abundance (Cl 37)] x I (77) (3.3)

Substituting the abundance for the chlorine isotopes yields the following result

I (As 75) = I (75) – [(0.7577 / 0.2423) x I (77)] = I (75) – 3.127 x I (77) (3.4)

The above equation is then incorporated in the program method and corrects for the interference (PerkinElmerSCIEX, 2003).

3.4.4 Aqueous trace metal/loid analysis by Inductively Coupled Plasma Optical Emission Spectroscopy

The concentrations of all other trace metal/loids, other than those mentioned in Section 3.4.5 above (and Al, in Chapter 5 which was determined by flame atomic absorption spectroscopy) were determined using an Optima 5300 DV inductively coupled plasma-optical emission spectrometer. This was a broad spectrum analysis to

look at 69 elements. All elements were calibrated with a 10 ppm standard and a blank solution and a CRM/10 solution was used as an external reference material. It is a 10x diluted digest of commercial estuarine sediment. It contains the following in undiluted digest; Al 700.0 mg L^{-1}, Ca 80.0 mg L^{-1}, Fe 350.0 mg L^{-1}, Mg 100.0 mg L^{-1}, K 150.0 mg L^{-1}, Na 200.0 mg L^{-1}, Cr 0.8 mg L^{-1}, Cu 0.20 mg L^{-1}, Co 0.10 mg L^{-1}, Mn 4.0 mg L^{-1}, P 5.0 mg L^{-1}, V 1.0 mg L^{-1}, Zn 1.5 mg L^{-1} (instrument % RSD +/- 1-5% depending on the element, some certified elements being more stable in solution than others).

The detection limit for both the ICP-MS and OES is 3 times the mean standard deviation of 3 blanks, and all measurements were made in triplicate to obtain this data.

3.4.5 Aqueous arsenic speciation analysis by High Performance Liquid Chromatography, Inductively Coupled Plasma Mass Spectrometry

High performance liquid chromatography is an improvement on simple column chromatography where high pressure is used to force a mobile phase through a stationary phase column. The high pressure allows for the use of a stationary phase with a high surface area which gives for a much better separation of analytes. As with other forms of chromatography it is the retention time and the use of known standards which allows for sample determination. It is important to note that the retention time is highly dependent upon; pressure, the stationary phase, the type of solvent and the temperature. Once detected by HPLC, a small amount of sample can be diverted to an ICP-MS. Coupling HPLC with ICP-MS allows for the analytes to be detected by their mass/charge ratio making identification of analytes much more simple. This coupling of techniques also allows for the separation of different species of the same element and has been used in relating to As, Cr and Se speciation (Wolf et al., 2008).

Arsenic speciation from 0.2 μM filtered end point solutions was analysed by HPLC-ICP-MS. As(V) and As(III) were separated using a Hamilton PRP-X100 250 x 4.6mm column at 30°C, using an Agilent 1260 infinity HPLC system interfaced with an Agilent 7500 ICP-MS at 30°C. The aqueous mobile phase was ammonium carbonate (50 mM) at a flow rate of 1.5 mL min-1 and a standard injection volume, 50 μL.

(Analysis carried out by School of Earth, Atmospheric and Environment Sciences, University of Manchester).

3.5 Organic Geochemistry

3.5.1 Dissolved Organic Carbon Analysis

The aqueous phase sampled at the end point of the Ajka batch experiments were filtered (0.2 μM, Whatman GD/XP filter) diluted with MilliQ (2x or 5x depending upon the sample) for dissolved organic carbon analysis (DOC). DOC was determined using an Analytikjena Multi N/C 2100® using thermocatalytic oxidation, MC-NDIR detection analysis.

The type of filter used for samples prior to DOC analysis is very important due to contamination from organic leaching which can impact the results (Khan and Subramania-Pillai, 2007). Any contamination can be determined through blank MilliQ samples that are filtered using the same type of filter. Filtered MilliQ blanks from this analysis were all below detection for DOC.

3.5.2 Solid Phase Extraction by C18 Resin Filters

Solid phase extraction (SPE) is a sample preparation technique used to separate a selected analyte from a mobile phase. The selected analyte is retained in a solid phase, keeping it isolated from the remaining sample which can then be eluted (Poole, 2003). C18 resin is a type of low-specificity sorbent which is commonly used in SPE for the extraction of contaminants from environmental, biological or chemical samples (Poole, 2003). C18 resin is a silica bonded with an octadecyl functional group (Fontanals et al., 2005). The analyte is isolated from the sample via hydrophobic interactions between analyte and the resin. The main disadvantage of the use of silica based resins is that the structure can decompose at pH extremes so pH control is essential (Fontanals et al., 2005; Dittmar et al., 2008). Despite this, C18 resin filters have been successfully used for the extraction of dissolved organic matter (DOM) from freshwater (Kim et al., 2003) and seawater systems (Dittmar et al., 2008). In these studies, the amount of DOM retained by the resin was between 40 (Dittmar et al., 2008) and 70% (Kim et al., 2003). Method development using C18 resin filters retained >90% of Fe(II) bound to both ferrozine and 2,2'-Bipyridine (Ferrozine and BIPY used as analogues for organically complexed metals in an aqueous matrix) (Thomas, 2000). Following isolation of DOM by the C18 resin, it is then possible to extract DOM from the resin using an organic solvent (e.g. methanol) (Biotage, 2006).

Solutions (5 mL) extracted from the end sampling point of the Ajka batch experiments were passed through ISOLUTE® C18 1g / 6 mL non polar SPE filters in order to retain any organic substances (and thereby any organically bound metals). The filters were conditioned according to the manufacturers protocol (Biotage, 2006) using 1 mL MilliQ then a further 1 mL of methanol. The samples were acidified prior to

extraction to pH 5.5 (±0.5) using HNO_3 (the optimum pH for maximum organic retention by ISOLUTE® C18 filters (Thomas, 2000). The acidified samples were then loaded on C18 filters which were fitted to a vacuum-block. The flow rate of the sample through the filters did not exceed 1 mL / min. The filtrates were then further diluted with 2% HNO_3 (to a final 10x dilution) for ICP-MS analysis (see section 3.4.3) to determine the inorganic/free aqueous metal concentrations. The concentration of the organically bound metals was calculated as the difference from the difference in aqueous metals concentrations measured before (total $[M^+]$) and after SPE (inorganic/free $[M^+]$). Further extraction of the isolated DOM phase by methanol from the filters was not attempted as a desolvating nebuliser (required for ICP-MS samples where an organic solvent is present) was not available on the ICP-MS instrument used.

3.6 X-Ray Absorption Spectroscopy

X-ray absorption spectroscopy (XAS) is an x-ray analytical technique that is used for determining the formal oxidation state, co-ordination chemistry and species of the neighbouring atoms of a selected element in a sample. Modern XAS analysis uses synchrotron radiation, an intense and energy tuneable source of x-rays, which is generated by accelerating electrons to near the speed of light (Newville, 2004). Electrons are emitted from an electron gun and accelerated, first in a linear accelerator and then to a circular accelerator where they reach a very high energy level, typically in the GeV range. The high energy electrons are then injected into a closed storage ring and are forced to travel in a circular trajectory by strong dipole magnetic fields (Zubavichus and Slovokhotov, 2001). As the electrons travel round the storage ring they

emit an intense electromagnetic radiation which is channelled along ‘beamlines’ to spectroscopy stations. (Zubavichus and Slovokhotov, 2001).

When the incident x-ray matches the energy of the binding energy of a core electron in the selected element of a sample, there is a rise in absorption. The rise in absorption, known as the absorption edge, corresponds to the promotion of the core electron out of the atom into the continuum (Newville, 2004). The absorption edge energy is characteristic of each element and the x-rays can be tuned to the appropriate absorption edge of the selected element (e.g. As = 11867 eV and V = 5465 eV). The ejected electron is called a photoelectron and has the properties of both a particle and a wave (Vlaic and Olivi, 2004). Following the removal of the photoelectron, the ‘core hole’ is filled by an electron from a higher energy level which emits fluorescent secondary x-rays upon de-excitation. These fluorescent secondary x-rays are also characteristic of the selected atom (Newville, 2004).

The occurrence of fluorescent x-rays allows for the use of XAS in fluorescence mode, allowing for more sensitive analysis than simple transmission mode and is used where there are low concentrations of the absorbing atom.

$$\mu(E) \propto I_f / I_0 \qquad (3.5)$$

Where, $\mu(E)$ = is the absorption coefficient

and, I_f is the intensity of fluorescence

In transmission mode, the intensity of the x-rays is measured before and after the sample.

$$\mu(E) = \log(I_0 / I) \qquad (3.6)$$

The x-ray absorption spectrum can be divided into two parts: x-ray absorption near-edge spectroscopy (XANES) and extended x-ray absorption fine-structure spectroscopy (EXAFS). The XANES region comprises of the area just before the absorption edge, the edge itself and ~30 eV above the edge (Newville, 2004). XANES spectra are used to determine the oxidation state and co-ordination chemistry of the absorbing atom. The remainder of the spectrum is the EXAFS region. EXAFS is used to determine co-ordination number, interatomic distances and species of neighbouring atoms. EXAFS spectra arise from the interactions of ejected photoelectron with neighbouring atoms. A backscattering effect is created when the photoelectrons interact with neighbouring atoms producing wave interferences within the spectra. The interference for a given photoelectron depends upon the distance of the neighbouring atoms and their respective atomic numbers (Vlaic and Olivi, 2004).

Samples were prepared for XAS analysis by mounting under an argon atmosphere into in Perspex holders with Kapton™ windows. Samples were frozen (-20°C) and transported to the synchrotron on dry ice. Standards were prepared as 1000 mg L^{-1} solutions and held in polythene bags for analysis.

As K-edge spectra (11867 eV) and V K-edge spectra (5465 eV) were collected on beamline I18 at the Diamond Light Source operating at 3 GeV with a typical current of 200 mA, using a nitrogen cooled Si(111) double crystal monochromator and focussing optics. A pair of plane mirrors was used to reduce the harmonic content of the beam and Kirkpatrick-Baez mirrors were used to produce a relatively unfocused beam (approximately 0.5 mm diameter at the sample). For standards prepared as pressed pellets, K-edge spectra were collected in transmission mode at room temperature (~295 °K). For samples and solutions, data were collected in fluorescence mode using a 9 element solid state Ge detector at room temperature. To prevent beam damage

presenting as an apparent change in speciation (Morin et al., 2008; Charlet et al., 2011) only single spectra were collected (~20 mins) from a spot within the sample and the sample stage automatically moved to expose an unaffected part of the sample before subsequent scans.

Multiple scans were then averaged to improve the signal to noise ratio using Athena version 0.8.061 (Ravel and Newville, 2005b). For XANES spectra absorption was also normalised in Athena over the full data range and plotted from approximately -15 eV to +30 eV relative to the edge position with no correction required for drift in E_0.

3.6.1 EXAFS modelling

EXAFS data was background subtracted using PySpline v1.1 (Tenderholt et al., 2007) and analysed in DLexcurv v1.0 (Tomic, 2005) using full curved wave theory (Gurman et al., 1984). Phaseshifts were derived from *ab initio* calculations using Hedin-Lundqvist potentials and von-Barth ground states (Binsted, 1998). Multiple scattering was allowed for as coded in DLexcurv (Binsted, 1998; Tomic, 2005). Fourier transforms of the EXAFS spectra were used to obtain an approximate radial distribution function around the absorber atom; the peaks of the Fourier transform can be related to "shells" of surrounding backscattering ions characterised by atom type, number of atoms, absorber-scatterer distance, and the Debye-Waller factor (± 25%), $2\sigma^2$. Atomic distances calculated by DLexcurv have an error of approximately ± 0.02 and ± 0.05 Å in the first and outer shells respectively (Burke et al., 2005). Debye-Waller factors are typically 0.002 – 0.02 $2\sigma^2$ for the first shell and 0.02 – 0.04 $2\sigma^2$ for the outer shells (Binsted, 1998).

3.7 Microbial Community Analysis

3.7.1 DNA Extraction, Sequencing and Analysis

DNA was extracted using a FastDNA spin kit (Qbiogene, Inc.) and FastPREP instrument (unless explicitly stated, the manufacturer's protocol as supplied with the kits, were followed precisely). DNA fragments in the size range 3kb ~20kb were isolated on a 1% agarose, "1x" Tris-borate-EDTA (TBE) gel stained with ethidium bromide to enable viewing under UV light (10x TBE solution from Invitrogen Ltd., UK). The DNA was extracted from the gel using a QIAquick gel extraction kit (QIAGEN Ltd., UK). The purified DNA was then used for subsequent analysis.

3.7.2 16S rRNA gene sequencing

A fragment of the 16S rRNA gene of approximately 500bp was PCR amplified using broad-specificity bacterial primers 8f (5′–AGAGTTTGATCCTGGCTCAG-3′) (Eden et al., 1991) and 519r (5′–GWATTACCGCGGCKGCTG-3′) where K =G or T, W = A or T (Lane et al., 1985). The PCR was carried out using an Eppendorf Mastercycler gradient thermal cycler. The PCR reaction mixture contained: DIW (10μL), purified DNA solution (25μL), GoTaq DNA polymerase (1μL), PCR reaction buffer, $MgCl_2$ (1.5mM, 10μL), PCR nucleotide mix (10mM, 1μL) and 8f and 519r primers (20μM, 1.5μL). The final reaction volume was 50μL. The reaction mixtures were incubated at 95°C for 2 min and then cycled 30 times through three steps; denaturing (95°C, 30s), annealing (50°C, 30s), primer extension (72°C, 45s). This was then followed by a final extension step at 72°C for 7 minutes. The PCR product was purified using a QIAquick PCR purification kit and amplification product sizes were

verified by electrophoresis of 10µL of PCR product and 2µL of 6x loading dye in a 1% agarose TBE gel with ethidium bromide staining. DNA concentration was determined using by UV/Vis spectroscopy on a Biomate 3 spectrophotometer.

The PCR product was ligated into the standard cloning vector pGEM-T Easy (Promega Corp., USA). The ligation mixture contained: DIW (2.6µL), 2X Rapid ligation buffer (5µL), pGEM-T Easy Vector (50ng, 1µL), PCR product (0.4µL), T4 DNA Ligase (3 Weiss units/µL, 1µL). The final ligation volume was 10µL. The ligated product was then transformed into E.Coli XL1-Blue supercompetent cells (Stratagene). The transformed cells were then grown on LB-agar plates containing ampicillin (100µg mL^{-1}) at 37°C for ~17 hours. The plates were dressed with IPTG and X-gal (as per Stratgene protocol) for blue-white colour screening. 60 colonies containing an insert were restreaked on LB-ampicillin agar plates and incubated at 37°C overnight. Single colonies from the restreaked plates were transferred to a 96 well ampicillin plate (GATC Biotech Ltd) and were sent for sequencing (GATC Biotech, Germany).

3.7.3 Phylogenetic assignment

The quality of each 16S rRNA sequence recovered from GATC Biotech Ltd was evaluated with Mallard (version 1.02) (Ashelford et al., 2006) in order to exclude any putative chimeras from further analysis. The sequences were then assigned to bacterial phyla using the online Ribosomal Database Project (RDP) naive Bayesian classifier version 2.2, (available online http://rdp.cme.msu.edu/classifier/classifier.jsp) in February 2011. The sequences were assigned to the taxonomical hierarchy: RDP training set 6, based on nomenclatural taxonomy and Bergey's Manual, with a

confidence threshold of 95% (Wang et al., 2007). Good quality sequences were uploaded to the EMBL Genbank database.

3.7.4 Phylogenetic tree building

Sequences were grouped into operational taxonomic units (OTU's) using MOTHUR software (Schloss et al., 2009) using a >98% furthest neighbour sequence similarity cut off. The Seqmatch tool from RDP was used to identify 16S rRNA gene sequences from type strains similar to the sequences from this study. The 16S rRNA gene sequences from these type strains were downloaded from the EMBL database and aligned with new sequences using Clustal X software package (version 2.0.11) and phylogenetic trees were constructed from the distance matrix by neighbour joining. Bootstrap analysis was performed by 1000 replicates and resulting phylograms were drawn using Treeview (version 1.6.6) software package.

3.8 Statistical Analysis

3.8.1 Standard deviation, relative standard deviation and relative error.

Standard deviation (SD or σ) is a measure of the deviation of a set of data from the arithmetic mean of the data. If all the measured values across a sample set are the same then, σ = 0: if there is a wide spread of values across samples then σ >0. SD is calculated as the square root of the variance in a data set. The standard deviation was calculated for each set of chemical determinations (where n = 3) using the equation below (see equation 3.7).

$$\sigma = \sqrt{\frac{\sum(x-\bar{x})^2}{n-1}} \quad (3.7)$$

Relative standard deviation (RSD) is calculated from SD. In this thesis it was used to express the precision and repeatability of analytical methods described during the research (especially where data was collected over a number of different days) by using the equation below (see equation 3.8). A lower percentage represents a lower variability in the data set.

$$\%RSD = \frac{\sigma}{\bar{x}} \times 100 \quad (3.8)$$

3.8.2 Pearson's correlation measures (r and p-values)

The Pearsons correlation co-efficient (r) measures the strength of linearity between two variables. It can be in a range of numbers between +1 and -1 (inclusive). A value of 0 would indicate that no linearity exists but +1 or -1 would indicate a definite positive correlation or negative correlation respectively. The p-value, on the other hand looks at the probability of a result, if the correlation co-efficient was 0. It works on the basis of rejecting one of two competing hypothesis, in this case the probability that the release of metal ions is or is not related to increased concentrations of DOC, for example. Generally speaking, if the probability determined is lower than 5% (i.e. p = <0.05) then the correlation is said to be statistically significant. Correlation tables are used to determine p-values. In this thesis, r and p-values were calculated using statistical on-line software (Wessa, P. 2014) and a two sided p-value was quoted in all cases.

3.9 References

ASHELFORD, K. E., CHUZHANOVA, N. A., FRY, J. C., JONES, A. J. & WEIGHTMAN, A. J. 2006. New screening software shows that most recent large 16S rRNA gene clone libraries contain chimeras. Applied and Environmental Microbiology, 72, 5734-5741.

ASPILA, K. I., AGEMIAN, H. & CHAU, A. S. Y. 1976. SEMIAUTOMATED METHOD FOR DETERMINATION OF INORGANIC, ORGANIC AND TOTAL PHOSPHATE IN SEDIMENTS. Analyst, 101, 187-197.

ASTM 2006. D4972.01: standard test method for pH of soils. Annual Book of ASTM standards, 4, 963-965.

BINSTED, N. 1998. CLRC Daresbury Laboratory EXCURV98 program. Warrington, UK: CLRC Daresbury Laboratory.

BIOTAGE 2006. Method Development in Solid Phase Extraction using Non-polar ISOLUTE (R) SPE Columns for the Extraction of Aqueous Samples (TN-101.06).

BROUWER, P. 2010. Theory of XRF: Getting acquainted with the principles, Almelo, The Netherlands, PANalytical B.V.

BRUNAUER, S., EMMETT, P. H. & TELLER, E. 1938. Adsoprtion of Gases in Multimolecular Layers. Journal of the American Chemical Society, 60.

BUDEVSKY, O. A. J., L. 1965. Colorimetric determination of vanadium(V) with 4-(2-pyridylazo)-resorcinol. Talanta, 12, 291 to 301.

BURKE, I. T., BOOTHMAN, C., LLOYD, J. R., MORTIMER, R. J. G., LIVENS, F. R. & MORRIS, K. 2005. Effects of progressive anoxia on the solubility of technetium in sediments. Environmental Science & Technology, 39, 4109-4116.

CHARLET, L., MORIN, G., ROSE, J., WANG, Y. H., AUFFAN, M., BURNOL, A. & FERNANDEZ-MARTINEZ, A. 2011. Reactivity at (nano)particle-water interfaces, redox processes, and arsenic transport in the environment. Comptes Rendus Geoscience, 343, 123-139.

DITTMAR, T., KOCH, B., HERTKORN, N. & KATTNER, G. 2008. A simple and efficient method for the solid-phase extraction of dissolved organic matter (SPE-DOM) from seawater. Limnology and Oceanography-Methods, 6, 230-235.

EDEN, P. A., SCHMIDT, T. M., BLAKEMORE, R. P. & PACE, N. R. 1991. PHYLOGENETIC ANALYSIS OF AQUASPIRILLUM-MAGNETOTACTICUM USING POLYMERASE CHAIN REACTION-AMPLIFIED 16S RIBOSOMAL-RNA-SPECIFIC DNA. International Journal of Systematic Bacteriology, 41, 324-325.

FONTANALS, N., MARCE, R. M. & BORRULL, F. 2005. New hydrophilic materials for solid-phase extraction. Trac-Trends in Analytical Chemistry, 24, 394-406.

GURMAN, S. J., BINSTED, N. & ROSS, I. 1984. A RAPID, EXACT CURVED-WAVE THEORY FOR EXAFS CALCULATIONS. Journal of Physics C-Solid State Physics, 17, 143-151.

JENNEMAN, G. E., McINERNEY, M. J., CROCKER, M. E. & KNAPP, R. M. 1986. Effect of sterilization by dry heat or autoclaving on bacterial penetration through Berea sandstone. Applied and Environmental Microbiology, 51, 39-43.

JOLIFFE, I. T. 2002. Principle Component Analysis New York, Springer-Verlag

KHAN, E. & SUBRAMANIA-PILLAI, S. 2007. Interferences contributed by leaching from filters on measurements of collective organic constituents. Water Research, 41, 1841-1850.

KIM, S., SIMPSON, A. J., KUJAWINSKI, E. B., FREITAS, M. A. & HATCHER, P. G. 2003. High resolution electrospray ionization mass spectrometry and 2D solution NMR for the analysis of DOM extracted by C-18 solid phase disk. Organic Geochemistry, 34, 1325-1335.

LANE, D. J., PACE, B., OLSEN, G. J., STAHL, D. A., SOGIN, M. L. & PACE, N. R. 1985. RAPID-DETERMINATION OF 16S RIBOSOMAL-RNA SEQUENCES FOR PHYLOGENETIC ANALYSES. Proceedings of the National Academy of Sciences of the United States of America, 82, 6955-6959.

LOVLEY, D. R. 1997. Microbial Fe(III) reduction in subsurface environments. Fems Microbiology Reviews, 20, 305-313.

LOTRARIO, J. B., STUART, B. J., LAM, T., ARANDS, R. R., O'CONNOR, O. A. & KOSSON, D. S. 1995. Effects of Sterilization methods on the Physical Characteristics of Soil: Implications for Sorption Isotherm Analyses. Bulletin of Environmental Contamination and Toxicology, 54, 668-675.

LOVLEY, D. R. & PHILLIPS, E. J. P. 1986. ORGANIC-MATTER MINERALIZATION WITH REDUCTION OF FERRIC IRON IN ANAEROBIC SEDIMENTS. Applied and Environmental Microbiology, 51, 683-689.

McNAMARA, N. P., BLACK, H. I. J., BERESFORD, N. A. & PAREKH, N. R. 2003. Effects of acute gamma irradiation on chemical, physical and biological properties of soils. Applied Soil Ecology, 24, 117-132.

MAYES, W. M., JARVIS, A. P., BURKE, I. T., WALTON, M., FEIGL, V., KLEBERCZ, O. & GRUIZ, K. 2011. Dispersal and Attenuation of Trace Contaminants Downstream of the Ajka Bauxite Residue (Red Mud) Depository Failure, Hungary. Environmental Science & Technology, 45, 5147-5155.

MORIN, G., ONA-NGUEMA, G., WANG, Y. H., MENGUY, N., JUILLOT, F., PROUX, O., GUYOT, F., CALAS, G. & BROWN, G. E. 2008. Extended X-ray absorption fine structure analysis of arsenite and arsenate adsorption on maghemite. Environmental Science & Technology, 42, 2361-2366.

MURPHY, J. & RILEY, J. P. 1962. A MODIFIED SINGLE SOLUTION METHOD FOR DETERMINATION OF PHOSPHATE IN NATURAL WATERS. Analytica Chimica Acta, 26, 31-&.

NEWVILLE, M. 2004. Fundamentals of XAFS, Chicago, U.S., Consortium for Advanced Radiation Sources, University of Chicago.

ORTIZ-BERNAD, I., ANDERSON, R. T., VRIONIS, H. A. & LOVLEY, D. R. 2004. Vanadium respiration by *Geobacter metalireducens*: Novel strategy for in situ removal of vanadium from groundwater. Applied and Environmental Microbiology, 70, 3091-3095.

PERKINELMERSCIEX 2003. ELAN Version 3.0 Software Guide.

POOLE, C. F. 2003. New trends in solid-phase extraction. Trac-Trends in Analytical Chemistry, 22, 362-373.

RAVEL, B. & NEWVILLE, M. 2005. ATHENA, ARTEMIS, HEPHAESTUS: data analysis for X-ray absorption spectroscopy using IFEFFIT. Journal of Synchrotron Radiation, 12, 537-541.

SCHLOSS, P. D., WESTCOTT, S. L., RYABIN, T., HALL, J. R., HARTMANN, M., HOLLISTER, E. B., LESNIEWSKI, R. A., OAKLEY, B. B., PARKS, D. H., ROBINSON, C. J., SAHL, J. W., STRES, B., THALLINGER, G. G., VAN HORN, D. J. & WEBER, C. F. 2009. Introducing mothur: Open-Source, Platform-Independent, Community-Supported Software for Describing and Comparing Microbial Communities. Applied and Environmental Microbiology, 75, 7537-7541.

SCHUMACHER, B. A. 2002. Methods for the Detemination of Total Organic Carbon (TOC) in Soils and Sediments. In: UNITED STATES ENVIRONMENTAL PROTECTION AGENCY (ed.). Las Vegas, U.S.: United States Environmental Protection Agency,.

TENDERHOLT, A., HEDMAN, B. & HODGSON, K. O. 2007. PySpline: A modern, cross-platform program for the processing of raw averaged XAS edge and EXAFS data. In: HEDMAN, B. & PAINETTA, P. (eds.) X-Ray Absorption Fine Structure-XAFS13.

THOMAS, B. 2000. Solid phase extraction for the removal of organic-iron complexes in contaminated groundwater. MSc MSc The University of Leeds.

TOMIC, S. S., B. G.; WANDER, A.; HARRISON, N. M.; DENT, A. J.; MOSSELMANS, J. F. W.; INGLESFIELD, J. E. 2005. New Tools for the Analysis of EXAFS: The DL_EXCURV Package. CCLRC Technical Report DL-TR-2005-01. Daresbury, UK.

TREVORS, J. T. 1996. Sterilization and inhibition of microbial activity in soil. Journal of Microbiological Methods, 26, 53-59.

TUOMINEN, L., KAIRESALO, T. & HARTIKAINEN, H. 1994. Comparison of Methods for Inhibiting Bacterial Activity in Sediments. Applied and Environmental Microbiology, 60(9), 3454-3457.

VIOLLIER, E., INGLETT, P. W., HUNTER, K., ROYCHOUDHURY, A. N. & VAN CAPPELLEN, P. 2000. The ferrozine method revisited: Fe(II)/Fe(III) determination in natural waters. Applied Geochemistry, 15, 785-790.

VLAIC, G. & OLIVI, L. 2004. EXAFS Spectroscopy: a Brief Introduction. Croatica Chemica ACTA, 77, 427-433.

WANG, Q., GARRITY, G. M., TIEDJE, J. M. & COLE, J. R. 2007. Naive Bayesian classifier for rapid assignment of rRNA sequences into the new bacterial taxonomy. Applied and Environmental Microbiology, 73, 5261-5267.

WESSA, P. 2014. Free Statistics Software, Office for Research Development and Education, version 1.1.23-r7, URL http://www.wessa.net/ [Accessed on-line 10th April 2014]

WOLF, D. C., DAO, T. H., SCOTT, H. D., LAVY, T. L. 1989. Influence of Sterilization Methods on Selected Soil Microbiological, Physical and Chemical Properties. Journal of Environmental Quality, 18, 39-44.

WOLF, R. E., MORMAN, S. A., MORRISON, J. A. & LAMONTHE, P. J. 2008. Simultaneous Speciation of Arsenic, Selenium and Chromium by HPLC-ICP-MS. In: U.S. GEOLOGICAL SURVEY OPEN-FILE REPORT 2008-1334 (ed.). Virginina, U. S.

ZUBAVICHUS, Y. V. & SLOVOKHOTOV, Y. L. 2001. X-Ray synchrotron radiation in physicochemical studies. Russian Chemical Reviews, 70, 373-403.

Chapter 4 Biogeochemical processes controlling the fate of vanadium at a legacy steel slag disposal site.

Abstract

Alkaline leachates from weathering of a steel slag waste site in the north of England, have affected the surrounding natural soil over many years. The leachates can transport potentially toxic oxyanion forming elements (e.g. As, Cr, Mo and V) from the steel slag which are more mobile at high pH. The soil underneath a layer of calcite dominated soil (that has formed around an alkaline leachate pond) has a pH of 12, 170 mg kg^{-1} V and 36 – 40% of the microbially available iron as Fe(II). XAS analysis of the soil indicated that the V is present as the less mobile V(IV) suggesting that V had been reduced after transport in the leachate as V(V). V(V) spiked anaerobic microcosms indicated that abiotic processes were responsible for the removal of V(V) from solution, and the microcosms were not able to support nitrate or Fe(III)-reduction. However, despite the elevated pH, a microbial consortium dominated by β-Proteobacteria and Deinococcus thermos was found in soil the under calcite crust. A single OTU of a Trupera-like species was found that was very closely related to a Trupera-like species, which has been previously isolated from a different alkaline waste site. The results and interpretations in this chapter introduce the possible site processes controlling the fate and transport of V mobilised from steel slag leachates to a surrounding soil profile with a view to developing a further more in depth study.

4.1 Introduction

The disposal of waste from industrial activities can have a profound effect on surrounding environment and water systems. It is estimated that the worldwide steel industry generates between 150 – 230 million tonnes of steel slag each year (U.S. Geological Survey, 2013). Historically, the majority was openly dumped in 'slag heaps' and left to weather over long periods of time (Proctor et al., 2000; Navarro et al., 2010). Steel slag recycling is becoming increasingly popular and it is currently used in a number of industries such as: road construction (Chaurand et al., 2007a); as fertilizers or soil conditioners (Haynes et al., 2013); and recent research suggests that it may be useful for CO_2 sequestration (Bonenfant et al., 2008).

There are two main methods of steel production in the UK: 1) basic oxygen furnace (BOF) which uses hot iron from blast furnace production or steel scraps and 2) Electric arc furnace (EAF) which uses cold scrap steel only. The composition of the slag produced from each method is generally very similar and the main components of steel slag are oxides of calcium, magnesium silicon, iron, manganese, aluminium and various sulfates and phosphates (Proctor et al., 2000). It can also contain, in varying concentrations, toxic elements such as As, Cr, Cd, Mo, Pb and V (Roadcap et al., 2005; Chaurand et al., 2007a). Steel production is a high lime process, where lime (CaO) is used to increase heat transfer and remove impurities. Although, slag is generally considered to be a non-hazardous material there is some environmental concern about the highly alkaline leachates produced from slag weathering (Schwab et al., 2006; Chaurand et al., 2007a; Navarro et al., 2010).

When lime (CaO) in the slag comes in contact with water it undergoes a cascade of reactions that produce a high pH leachate. These reactions are listed previously in

Chapter 2 (see reaction sequence 2.1 to 2.7). Firstly, solid lime mixes with water to produce aqueous $Ca(OH)_2$ (2.1). Once in contact with water, portlandite dissociates into its component ions and thus the alkalinity of the resulting solution is increased by the presence of hydroxide ions (2.2).

Together with high pH leachates, the precipitation of calcite ($CaCO_3$) can also be cause for environmental concern. When the alkaline leachate comes into contact with atmospheric CO_2, as it does at the surface or a groundwater spring, then carbonate precipitates (see Chapter 2 for the reaction sequence, equations 2.3 – 2.7). (Schwab et al., 2006; Mayes et al., 2008). Calcite precipitation can be very rapid in affected areas and the formation of calcite hardpans can smother benthic habitats and reduce the light penetration to benthic primary producers (Bayless and Schulz, 2003; Mayes et al., 2006).

Other typical problems from steel slag weathering include; high total dissolved solids (> 5000 mg L^{-1}), increased salinity and elevated aqueous metal and metalloid concentrations such as; As, Ba, Co Hg, Pb and V (Bayless and Schulz, 2003; Roadcap et al., 2005; Chaurand et al., 2007a; Cornelis et al., 2008) which can all affect water and soil profiles after coming into contact with steel slag leachates.

Chromium and vanadium are metals that are regularly found at high concentrations in steel slags (up to 30,000 mg kg^{-1} and up to 10,000 mg kg^{-1} respectively) (Cornelis et al., 2008). Both Cr and V are used as additives in steel production to increase strength, and resistance to corrosion and metal fatigue. In particular, the demand for vanadium in steel is growing. This is most evident in China where stronger steel is required to meet new building regulations since the Sichuan earthquakes in 2008 (Horn, 2010). Both metals are considered to be potentially toxic

(Barceloux, 1999a; Barceloux, 1999d) and can be mobilised at high pH due to the formation of oxyanions [CrO_4^{2-}, VO_4^{3-}] (Langmuir, 1997). Vanadium in slag is known to be toxic to farm animals; in 1990 23 heifers from a herd of 98 died from acute vanadium poisoning when basic slag containing ~3% vanadium was used as a soil fertilizer (Frank et al., 1996).

Chaurand et al. (2007a) investigated leaching of Cr and V from BOF slags via leaching tests at pH 5 and long term field simulations, but found that low concentrations of Cr were mobilised whilst V release was significantly higher. The difference in the leaching behaviour between Cr and V here is due to the differences in the geochemical behaviour of the two metals. In the environment, chromium exists as Cr(III), which is mostly insoluble and Cr(IV), which is very toxic and readily transported, especially under oxic conditions (Fendorf, 1995). The pH 5 leaching tests and long term field simulations found that chromium was found as the less mobile Cr(III) and that the speciation of Cr did not evolve during either process, thus retarding Cr mobility (Chaurand et al., 2007a). Vanadium, however, was found as V(IV) in the slags but was oxidised to V(V) during the leaching process, thus enhancing vanadium mobility (Chaurand et al., 2007a).

The transport mechanisms of V from steel slag are strongly influenced by pH, Eh, concentration of V and competing ions, aqueous complexation and surface complexation to surrounding mineral surfaces (Apul et al., 2005; Chaurand et al., 2007a; Cornelis et al., 2008). Vanadium has oxidation states ranging from –1 to 5+, although 3+ 4+ and 5+ are most common in natural environments. The toxicity and mobility of vanadium increases with valence state and therefore pentavalent V compounds are the most toxic and most common in natural waters (Wehrli and Stumm, 1989; Wanty and Goldhaber, 1992; Crans, 1998). Vanadium(V) also has a tendency to

polymerise at concentrations in excess of 100 μM (5.1 mg L^{-1}) (Peacock and Sherman, 2004b). At lower concentrations V(V) forms mononuclear oxyanionic species which tend to be mobilised at high pH (Langmuir, 1997; Cornelis et al., 2008). However, sorption processes have been shown to play a large part in the retardation of V(V) as the vanadate anions act as a phosphate analogue and bind via ligand exchange (Peacock and Sherman, 2004b). Sorption processes are also very important for the vanadyl cation [V(IV), usually as VO^{2+}] (Wehrli and Stumm, 1989). Microbial reduction of V(V) to less mobile forms V(IV) has also been reported (Lyalikova and Yurkova, 1992; Carpentier et al., 2003; Lloyd, 2003; Ortiz-Bernad et al., 2004; Carpentier et al., 2005) which may be another important mechanism involved in the fate of vanadium in steel slag affected soils.

Soils affected by steel slag leachates have a characteristically high pH. However, many microorganisms have adapted to life at high pH and 'alkaliphiles' grow optimally when pH is >9. The main challenge for alkaliphiles is how to maintain a neutral intracellular pH, when the extracellular pH can be up to 2 pH units higher (Krulwich and Guffanti, 1989; Horikoshi, 1999). One mechanism for maintaining internal pH homeostasis by alkaliphiles is by the selective exchange of sodium and hydronium ions across plasma membranes via a Na^+/H^+ and K^+/H^+ antiporter system. Here, Na^+ or K^+ ions from within the cell are exchanged with external H^+ ions, thus decreasing internal pH (Ito et al., 1997; Horikoshi, 1999). Diverse microbial communities have been described from many high pH industrial waste sites (Horikoshi, 1999; Takai et al., 2001; Ye et al., 2004; Burke et al., 2012b; Whittleston et al., 2013). Roadcap et al. (2006) specifically describe a microbial community from a legacy steel slag site at Lake Calumet, Illinois, USA.

Due to the high mobility of vanadium from steel slags it is important to establish what controls the fate and transport of V into surrounding soils. This chapter reports on a pilot study into the possible mechanisms controlling vanadium transport from a legacy steel slag site in the north of England, to the surrounding soil profile. It uses a multidisciplinary approach to gain insight into the processes controlling V leached from steel slags. It also investigates redox indicators and the microbial community that exists in alkaline soils altered by steel slag leachates.

4.2 Material and Methods

4.2.1 Site Description

The Grove Heaps, in the Hownsgill Valley, near Consett, Co. Durham were used for over a century to dump blast furnace and steel slag until the closure of the Consett steelworks works in 1980. The heaps are situated in a valley that was a glacial melt water channel. Rainwater that enters the slag re-emerges in the valley bottom, where a large alkaline leachate pond has formed (pH 11-12) (Mayes et al., 2006). There is reduced vegetation around the leachate pond due to high pH and an area of calcite has formed around the pond. Vegetation in the surrounding area is much denser, with reeds, rushes and grasses. The hydrochemistry across the wetland has been previously described by Mayes et al. (2008) and trace metal analysis showed elevated concentrations of vanadium at some areas across the site, with concentrations breaching Environment Agency guidance levels for freshwater of 20μg L^{-1} (The Environment Agency, 2011).

4.2.2 Site Sampling

Groundwater and soil were sampled from the Hownsgill Valley site on 4th November 2010. A small trial pit was excavated on the calcite banks of the leachate pond from which ground water was extracted (see Figure 4.1). Another small pit was excavated approximately 10 m from the original (54°50'15" N, 1°51'22" W). In the second pit the soil showed definite layering of surface and deeper soil. The surface soil layer (hence forth referred to as 'surface soil') was ~ 30 cm thick and differed in both colour and texture from the deeper soil. Surface soil was brown/beige in colour and very gravelly in texture. The deeper soil (hence forth referred to as 'deep soil') was dark grey in colour and had much smaller grain size. Deep soil was sampled for characterisation and microcosm experiments. Surface soil was sampled for soil characterisation analysis only as a comparison to deep soil. Soil and water samples were placed in sealed polythene containers. Preliminary readings of the pH (~12) and Eh (~100mV) of the groundwater were measured with a portable Hanna HI 98129 Combo meter, calibrated using pH 7.01 and 10.01 buffer solutions. Laboratory measurements of the sample water pH were measured the following day. 100 mL of the water samples were frozen for analysis at a later date together with 150g samples soil. The remaining soil and water samples were refrigerated for use in microcosm experiments.

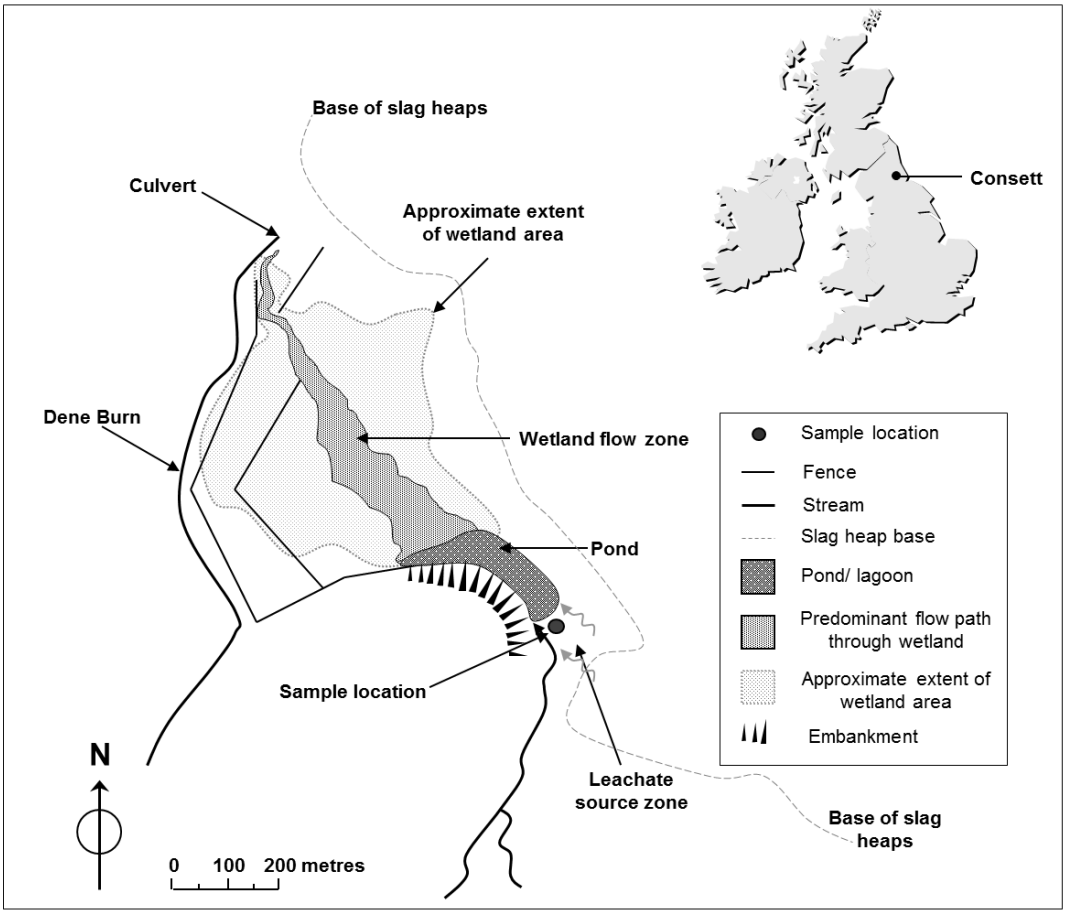

Figure 4.1 – Schematic diagram of the Hownsgill Valley sites, showing sample location edited from Mayes et al. (2006)

4.2.3 Sample Characterisation

The soil was oven dried at 60°C and finely ground for X-ray powder diffraction (XRD) and X-ray fluorescence measurements (XRF). XRD analysis was performed on a Bruker D8 powder X-ray diffractometer with a Ge(111) monochromator. XRF analysis was performed on a PANalytical Axios Advanced XRF spectrometer. Soil pH measurements were carried out using standard method for pH of soils (ASTM, 2006). The 0.5M HCl extractable Fe(II) was measured by Ferrozine assay and the total amount of 0.5M HCl extractable Fe was measured by reaction with hydroxylammonium

hydrochloride and ammonium acetate buffer solution prior to Ferrozine assay (Lovley and Phillips, 1986a; Viollier et al., 2000). The acid volatile sulfide (AVS) method for soil sulfide content was also carried out using an extraction with cold 6M HCl followed by a precipitation step with CuCl (adapted see (Morse and Cornwell, 1987)). Inorganic phosphate was determined using the molybdate blue method (Aspila et al., 1976). Total inorganic carbon (TIC) and total organic carbon (TOC) contents were determined from samples that had been dried and finely ground, using a Carlo Erba NA 2500 Elemental Analyser. BET specific surface area was also determined. Samples for BET were degassed with N_2 on a Micromeritics FlowPrep 060 sample degas system prior to analysis with a Micromeritics Gemini V BET surface area analyser.

Groundwater analysis was carried using an Optima 5300 DV inductively coupled plasma-optical emission spectrometer for all elements mentioned except V. Groundwater V concentration was measured using a Perkin-Elmer DRCII inductively coupled plasma-mass spectrometer.

4.2.4 Reduction Microcosm Experiments

Triplicate reduction microcosms spiked with V(V) were prepared as follows: 11g (±0.2g) of homogenised soil was added to a 120 mL glass serum bottle together with 100 mL of groundwater and V(V) spike from a $NaVO_3$ solution (100 µL, 100 mM, therefore microcosm concentration was 100µM and no polymerisation of V(V) should occur). Control experiments were prepared as above and then heat treated by autoclaving (120°C for 30 mins). A sterile groundwater control was also prepared by filtering 100 mL groundwater with a V(V) spike (100 µL, 100 mM) through a 0.2 µm filter and then heat treating by autoclave (120°C for 30 mins). The headspaces of all the

experiments were purged with oxygen free nitrogen (OFN) before capping and crimp sealing. All experiments were incubated in the dark at 21°C for the duration of the experiments. The microbially-active experiments and heat treated controls were sampled periodically for geochemical analysis to produce a progressive time series. At each sample point, microcosms were shaken and 3 mL of slurry was extracted using aseptic technique with sterile and OFN-flushed needles and syringes (Burke et al., 2006). Samples were centrifuged (3 min, 16,000 g) and soil and water was analysed for a range of redox indicators, V(V) and microbiology.

4.2.5 Geochemical Analysis

The pH was measured using a Thermo Scientific Orion DualStar pH/ISE benchtop meter with calibrated electrodes (the pH electrodes were calibrated daily with pH 4, 7 and 10 standard buffer solutions). The ORP (as an indicator for Eh) was measured using a Hamilton Polyplast ORP BNC electrode. Aqueous chloride, sulfate, nitrate and nitrite concentrations were determined by ion chromatography on a Dionex DX600 AS16 column and hydroxide gradient elution with supressed conductivity and UV detection which was fitted for absorption at 225 nm. Aqueous V(V) concentrations were determined using UV-vis spectroscopy method on a Cecil CE 3021 spectrophotometer using 4-(2-pyrodylazo)-resorcinol (PAR) (Budevsky, 1965; Ortiz-Bernad et al., 2004) indicator. Fe(II) in solids was also determined using UV/vis spectroscopy after extraction by 0.5M HCl and reaction with ferrozine (Lovley and Phillips, 1986a; Viollier et al., 2000). Standards and calibrations were routinely checked for accuracy and precision. All calibrations had good linearity (typically $r^2 \geq 0.99$).

4.2.6 X-ray Absorption Near Edge Structure Spectroscopy (XANES)

XANES spectra from the soil were collected at the V K-edge (5465 eV) on beamline I18 at the Diamond Light Source in May 2012. Approximately 100 mg of moist soil (day zero) was prepared for XANES analysis by mounting under argon atmosphere into Perspex holders with Kapton™ windows. Samples were frozen (-20°C) and transported to the synchrotron on dry ice and kept frozen until analysed. Standard spectra were collected from various V(III), V(IV) and V(V) aqueous solutions (1000 mg L^{-1}), and from vanadate adsorbed to $Al(OH)_3$. The V-$Al(OH)_3$ was prepared by suspension of 1 g $Al(OH)_3$ in 1 L DIW and adding 1 ml of 1000 mg L^{-1} Na_3VO_4 (made up in 0.01 mol L^{-1} NaOH at pH 12). The mixed suspension was stirred for 48 hours and the final pH was 7.0. The V-$Al(OH)_3$ solid was recovered by centrifugation (600 g) and prepared for analysis as a moist paste as above. For each sample and standard multiple XANES spectra were then averaged and normalised using Athena version 0.8.061 (Ravel and Newville, 2005b). The V pre-edge peak energy was determined by calculation of the area normalised centroid energy position following the method of Chaurand et al. (2007b)

4.2.7 DNA Extraction, Sequencing and Analysis

DNA was extracted from the deep soil (0.4307g) using a FastDNA spin kit (Qbiogene, Inc.) and FastPREP instrument (unless explicitly stated, the manufacturer's protocol were followed precisely). DNA fragments in the size range 3kb ~20kb were isolated on a 1% agarose, "1x" Tris-borate-EDTA (TBE) gel stained with ethidium bromide to enable viewing under UV light (10x TBE solution from Invitrogen Ltd.,

UK). The DNA was extracted from the gel using a QIAquick gel extraction kit (QIAGEN Ltd., UK). The purified DNA was then used for subsequent analysis.

4.2.8 16S rRNA gene sequencing

A fragment of the 16S rRNA gene of approximately 500bp was PCR amplified using broad-specificity bacterial primers 8f (5′–AGAGTTTGATCCTGGCTCAG-3′) (Eden et al., 1991) and 519r (5′–GWATTACCGCGGCKGCTG-3′) where K =G or T, W = A or T (Lane et al., 1985). The PCR reaction mixture contained: DIW (10µL), purified DNA solution (25µL), GoTaq DNA polymerase (1µL), PCR reaction buffer, $MgCl_2$ (1.5mM, 10µL), PCR nucleotide mix (10mM, 1µL) and 8f and 519r primers (20µM, 1.5µL). The final reaction volume was 50µL. The reaction mixtures were incubated at 95°C for 2 min and then cycled 30 times through three steps; denaturing (95°C, 30s), annealing (50°C, 30s), primer extension (72°C, 45s). This was then followed by a final extension step at 72°C for 7 minutes. The PCR product was purified using a QIAquick PCR purification kit and amplification product sizes were verified by electrophoresis of 10 µL of PCR product and 2 µL of 6x loading dye in a 1% agarose TBE gel with ethidium bromide staining.

The PCR product was ligated into the standard cloning vector pGEM-T Easy (Promega Corp., USA). The ligation mixture contained: DIW (2.6 µL), 2X Rapid ligation buffer (5 µL), pGEM-T Easy Vector (50ng, 1µL), PCR product (0.4 µL), T4 DNA Ligase (3 Weiss units/µL, 1 µL). The final ligation volume was 10 µL. The ligated product was then transformed into E.Coli XL1-Blue supercompetent cells (Stratagene). The transformed cells were then grown on LB-agar plates containing ampicillin (100 µg mL^{-1}) at 37°C for ~17 hours. The plates were dressed with IPTG and

X-gal (as per Stratgene protocol) for blue-white colour screening. 60 colonies containing an insert were restreaked on LB-ampicillin agar plates and incubated at 37°C overnight.

60 single colonies from the restreaked plates were transferred to a 96 well ampicillin plate (GATC Biotech Ltd) and were sent for sequencing (GATC Biotech, Germany). The sequences were uploaded to the Ribosomal Database Project (RDP) naive Bayesian classifier version 2.2 (Wang et al., 2007), in February 2011. The quality of each 16S rRNA sequence was then evaluated with Mallard (version 1.02) (Ashelford et al., 2006) and probable chimeras were excluded from any further analysis. Non-chimeric sequences were then submitted to the Genbank database (accession numbers HE584610 – HE584610, see Appendix A, Table A1 for full details. Sequences were grouped into operational taxonomic units (OTU's) using MOTHUR software (Schloss et al., 2009) (>98% furthest neighbour sequence similarity cut off).

4.2.9 Phylogenetic tree building

The Seqmatch tool from the Ribosomal Database project was used to identify 16S rRNA gene sequences from type strains similar to the sequences from this study. The 16S rRNA gene sequences from these type strains were downloaded from the EMBL database and aligned with new sequences using Clustal X software package (version 2.0.11) and phylogenetic trees were constructed from the distance matrix by neighbour joining. Bootstrap analysis was performed by 1000 replicates and resulting phylograms were drawn using Treeview (version 1.6.6) software package.

Bootstrap analysis is a form of statistical analysis that determines the accuracy of a phylogenetic relationship by matching subsets of data (Baldauf, 2003). It is generally accepted that a figure of >70% indicates reliable phylogenetic grouping (Hillis and Bull, 1993).

4.3 Results

4.3.1 Soil Characterisation and Groundwater Analysis

Soil characterisation is presented in Tables 4.1 and 4.2. Briefly, the soils were dominated by quartz (SiO_2) and calcite ($CaCO_3$) and with small amounts of layered silicates and feldspars. The main difference between the surface and deep soils was the amount of calcite. The XRD patterns indicated that there was much more calcite in the surface soil (see appendix A Figures A1 and A2 for XRD patterns). Also, there was a single small characteristic peak indicating a trace of hematite in the deep soil, which was not present in the surface soil. XRF analysis (Table 4.1) reveals that there are elevated concentrations of Cr and Pb in the soil (The Environment Agency, 2011).Acid volatile sulfide analysis was carried out on the soil sample. There was only a very small amount of sulfide visible on the filter paper (weighing 0.00078g). Due to these minor quantities the Copper/EDTA titration step for quantification was not carried out. In order for the quantification step to be viable there must be a sufficient quantity of sulfide precipitate present to distinguish any difference over the detection limit (Morse and Cornwell, 1987).

Analysis of the groundwater sampled is summarised in Table 4.3. Briefly the groundwater has a characteristically high pH (pH 11.8) and a relatively low concentrations of aqueous Ca^{2+} when compared to other geochemical data from the site

(Mayes et al., 2008). The aqueous V concentration was 15 μg L^{-1} (0.294 μM, therefore the total concentration of V in the spiked microcosm was 100.294μM ≈ 100μM). The groundwater also has a concentration of aqueous Al in excess of the UK and EU freshwater standards of 200 ug L^{-1} (The Environment Agency, 2011).

Table 4.1 – Major (%) and minor (mg kg^{-1}) elemental composition of the Consett soils

Determinand	**Deep Soil**	**Surface Soil**
Major elements (oxides %)		
SiO_2	62	22
TiO_2	0.6	0.2
Al_2O_3	11	3.6
Fe_2O_3	6.8	2.9
MnO	0.2	0.1
MgO	0.6	0.5
CaO	4.7	37
Na_2O	0.3	0.1
K_2O	1.2	0.4
P_2O_5	0.1	0.1
SO_3	0.2	<0.1
LOI	11	33
Trace Elements (mg kg^{-1})		
As	9.1	4.7
Ba	597	283
Ce	84	34
Co	14	2.1
Cr	210	50
Cu	47	13
Ga	16	5.3
La	42	20
Mo	3.0	2.3
Ni	38	8.3
Pb	360	160
Sb	2.8	<1.0
Sr	83	142
Th	12.2	3.8
U	2.6	0.5
V	170	94
W	<1.0	<1.2
Zn	314	113
Zr	273	99

Table 4.2 – Consett soils characterisation (data in parentheses is the standard error of the mean, where n=3).

Soil Sample	Total V (mg kg^{-1})	pH	0.5 M HCl extractable iron as Fe(II) (%)	0.5 M HCl extractable iron as Total Fe (mg L^{-1})	Major minerals present	TOC (%)	BET Surface Area ($m^2 g^{-1}$)
Surface	94	9.9 (±0.5)	26 (±1)	1.59 (±0.3)	Quartz, Calcite, Kaolinite	1.98	3.4 (±0.02)
Deep	170	11.5 (±0.1)	38 (±2)	2.98 (±0.5)	Quartz, Calcite, Kaolinite	4.83	8.4 (±0.06)

Table 4.3 - Groundwater analysis

Determinand	
pH (in lab)	11.8
pH (on site)	12
Eh (on site)	-100 mV
Major cations (mg L^{-1})	
Ca^{2+}	84
K^{+}	8.5
Mg^{2+}	0.1
Na^{+}	7.7
Other aqueous metals (µg L^{-1})	
Al	270
Ba	74
Cd	1.6
Cr	2.5
Cu	3.7
Fe	140
Hg	14
La	31
Li	50
Mn	17
Mo	6.0
Ni	2.1
Pb	12
Se	12
Sr	150
U	2.6
V	15
Zn	6

4.3.2 Reduction microcosm experiments

Figure 4.2 shows geochemical responses for the deep soil, sterile and groundwater control experiments. The initial pH of all experiments was pH 11.0 which then increased in all experiments to pH 11.5. The trend for pH of all experiments was very closely matched over the incubation period. Aqueous V(V) removal from solution commenced straight away in the deep soil and sterile experiments, with concentrations dropping from 100 μM to ~60 μM in both experiments. Once again, the trend of removal was very closely matched for both the soil and sterile control and final concentrations were 24 (±5.5) μM and 16 μM respectively. Aqueous V(V) concentrations in the groundwater remained relatively constant throughout the incubation period (with the exception of an uncharacteristic dip at day 7), with concentrations only dropping from 100 μM to 95 μM.

There was no significant change in either of the soil or sterile experiments in the percentage 0.5 M HCl extractable Fe(II), although there was a slight increase in the sterile control. There is a large difference in initial sulfate concentration between the soil and groundwater experiments compared with the sterile control. All replicates of the soil experiments had a concentration of ~ 217 (±55.4) μM at day zero, which remained relatively constant throughout the incubation period. The groundwater control had an initial sulfate concentration of 190 μM and an average concentration of 168 (± 37.8) μM. The sterile control had initial sulfate concentration of 885 μM, although this decreased over the first 10 days of incubation, final concentrations were still ~ 640 μM. The high concentration of sulfate in the sterile control could be as a result of heat treatment but without repeats of the sterile controls it is difficult to say. It is possible

that the soil used was not sufficiently homogenised prior to preparing the microcosm experiments.

Nitrate concentrations in the soil and sterile control were also very low (≤ 5 μM). There was no real evidence of nitrate removal in any of the experiments and concentrations fluctuate in all experiments. Nitrite concentrations in both the soil experiments and both sterile and groundwater controls follow a similar trend. Initial concentrations are both ~ 5 μM, the concentration then increased sharply which was followed by a period of gradual removal.

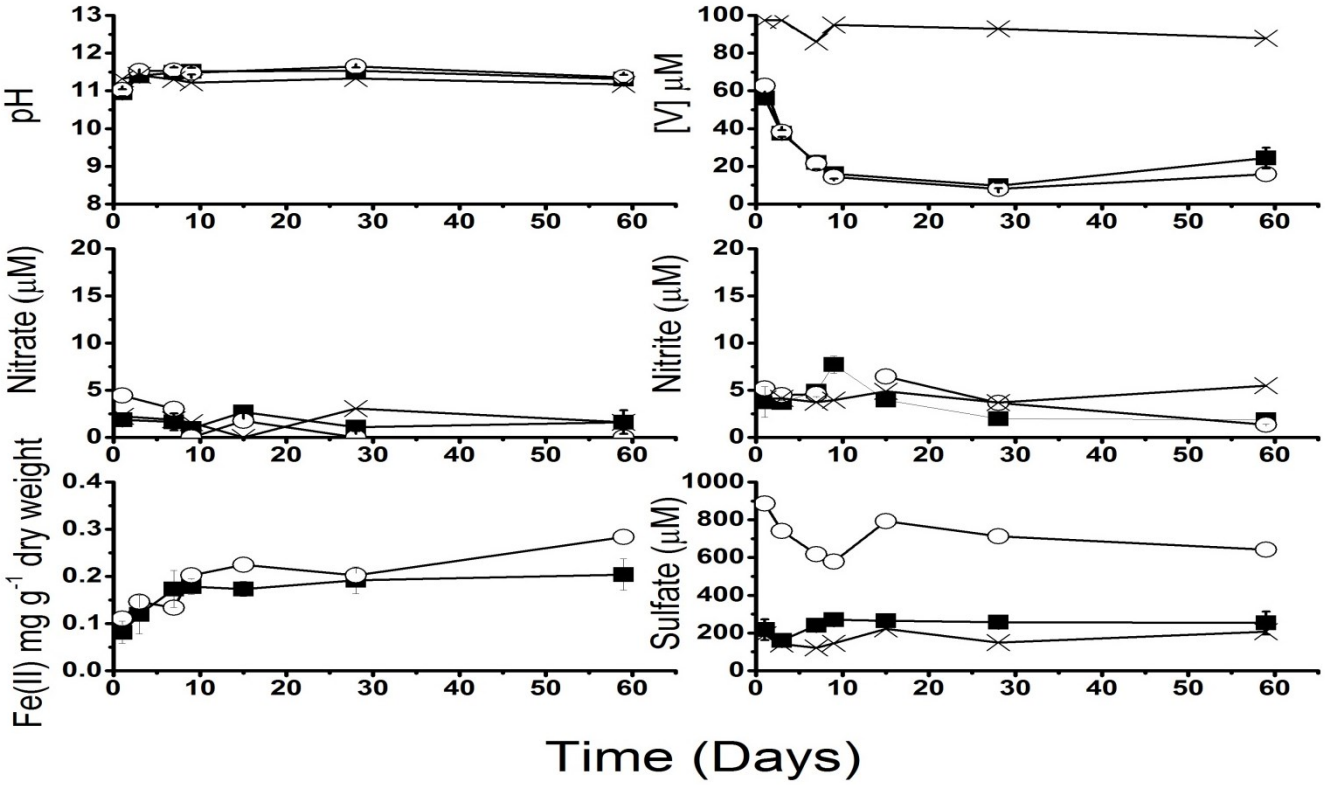

Figure 4.2 – Geochemical responses for the soil (black squares), equivalent sterile control (empty circles) and sterile groundwater control (crosses).Only the soil experiments were carried out in triplicate. Errors bars shown are 1 σ of triplicate results for the soil microcosms only (where not shown, errors are within the symbol size).

4.3.3 XANES spectroscopy

The V K-edge XANES spectra has been interpreted using the system proposed by Chaurand et al. (2007b). This system is based upon the detailed observation of pre-edge peak intensity and energy position. V K-edge XANES spectra (Figure 4.3) collected from the deep soil sample has a prominent pre-edge peaks at 5470 eV. The main absorption edges ($E_{1/2}$ = point where absorption reaches 50% of the normalised absorption) was 5480.0 eV and the pre-edge peak intensity was 0.3 indicating an oxidation state of V(IV) and is identical to the vanadyl standard used in this study. A summary of the spectral information extracted from the sample and standards is shown in Table 4.4. Figure 4.4 shows a plot of normalised pre-edge peak intensity vs Pre-edge peak energy (eV) for the sample and standards.

Table 4.4 - Pre-edge peak position, normalised pre-edge peak intensity and main edge position determined from the V K-edge XANES spectra shown in Figure 4.3. Energy values are quoted ± 0.2 eV; normalised intensity values are quoted ± 0.1.

Sample/ Compound	Valence	Pre-edge Peak (eV)	Normalised Intensity	Main Edge, $E_{1/2}$ (eV))
V_2O_3	3+	5468.0	0.1	5476.4
$VOSO_4 \cdot xH_2O$	4+	5470.0	0.3	5478.8
Consett deep soil sample	4+	5470.0	0.3	5480.0
Vanadate sorbed to $Al(OH)_3$	5+	5470.2	0.6	5480.3
V_2O_5	5+	5470.9	0.8	5480.4
Calcium meta-vanadate	5+	5470.2	1.1	5482.2

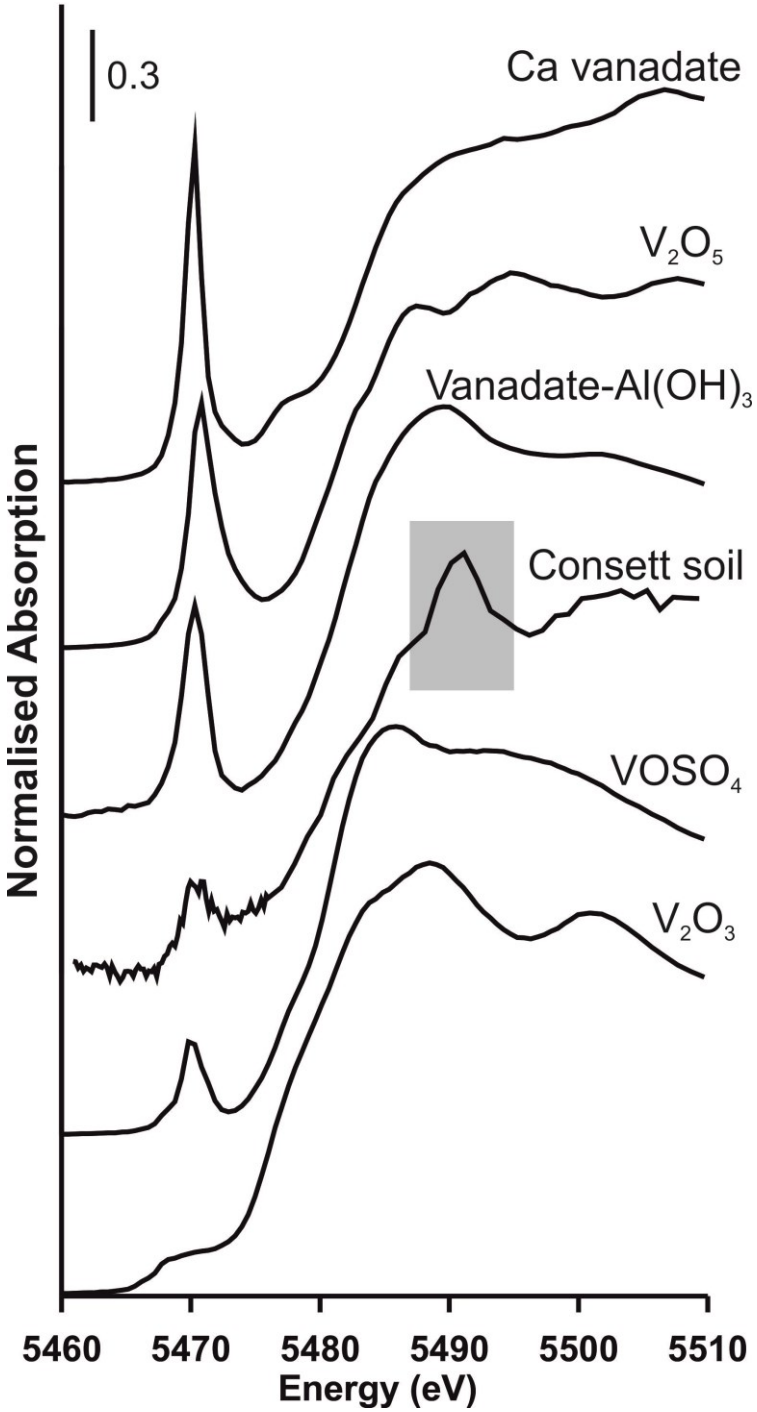

Figure 4.3 - Normalised V K-edge XANES spectra collected from Consett deep soil sample and V(III), V(IV) and V(V) containing standards. The grey box denotes where the white line peak of the La L_3-edge is visible in sample spectra.

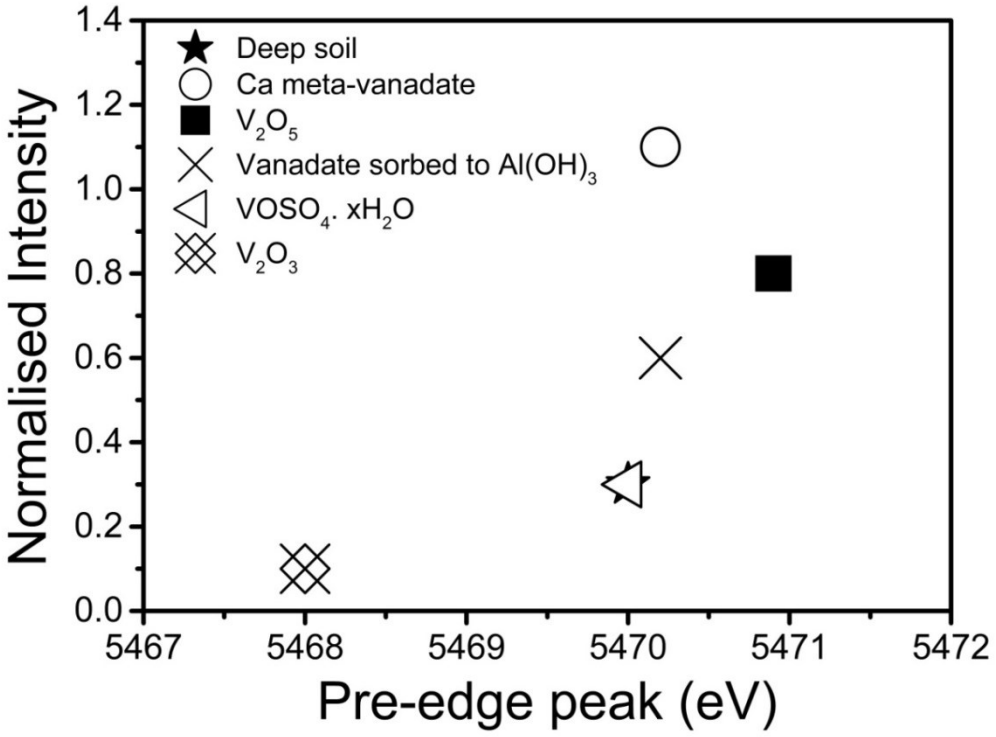

Figure 4.4 – Plot of normalised intensity vs Pre-edge peak energy derived from V K-edge XANES spectra for the deep soil sample and standards from this study and Burke et al. (2013).

4.3.4 DNA extraction, amplification and sequencing

Fifty-six 16S rRNA gene sequences were successfully recovered from the soil, however Mallard evaluation (Ashelford et al., 2006) identified two probable chimeras which were excluded from any further analysis. Rarefaction analysis of the sequences (Figure 4.5) indicates that there are 12 OTU's in the deep soil sample. Figure 4.6 shows phylogenetic affiliation of the remaining fifty-four sequences, including ten sequences that could not be assigned to a phylum with ≥95% confidence and are listed as unidentified bacteria (see Appendix A, Table A1, for full assignment details). The dominant species, indicated by a single OTU for the Deinococcus-Thermus was found to be a Trupera-like species. A phylogenetic tree showing a characteristic member of the

Trupera-like OTU is shown in Figure 4.6.

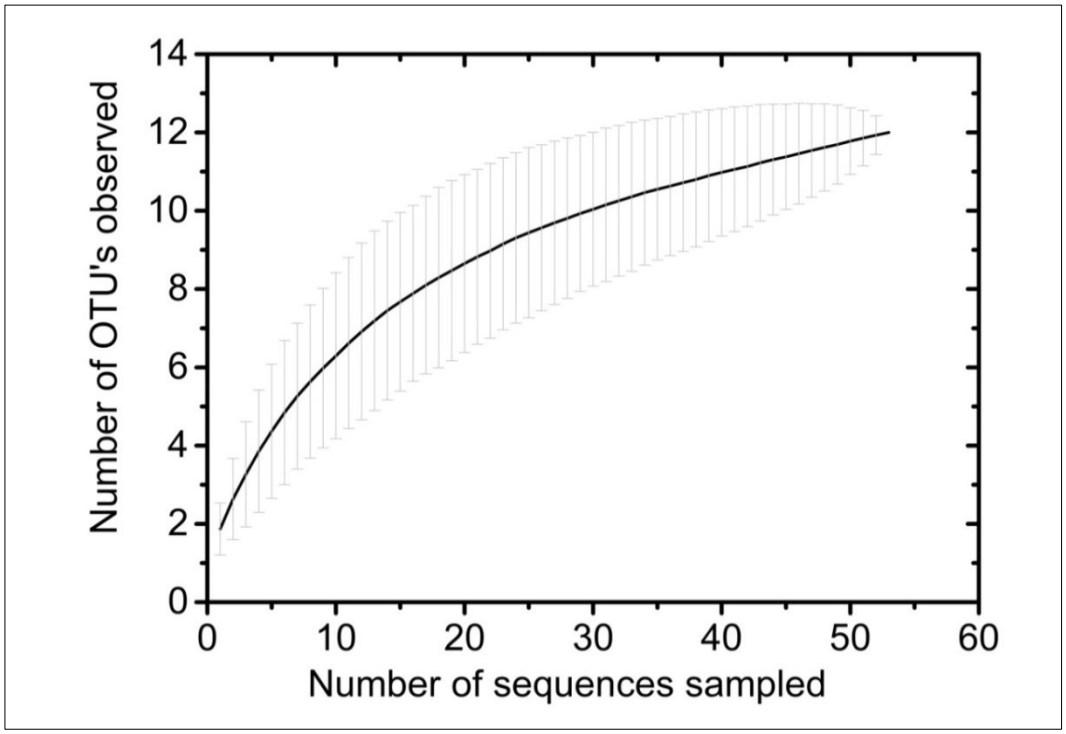

Figure 4.5 – Rarefaction curves from MOTHUR analysis using furthest neighbour with 98% similarity cut-off

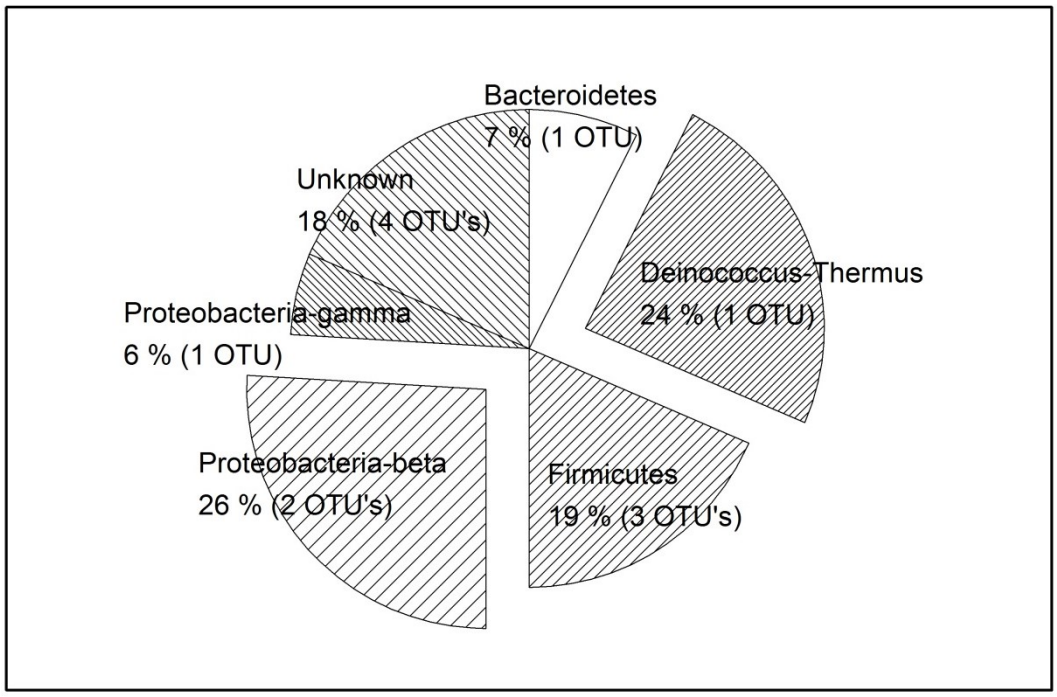

Figure 4.6 – Microbial community of the soil at day zero (54 sequences). Chart shows phylogenetic and OTU assignment from RDP and MOTHUR analysis using 95% and 98% confidence threshold and similarity respectively.

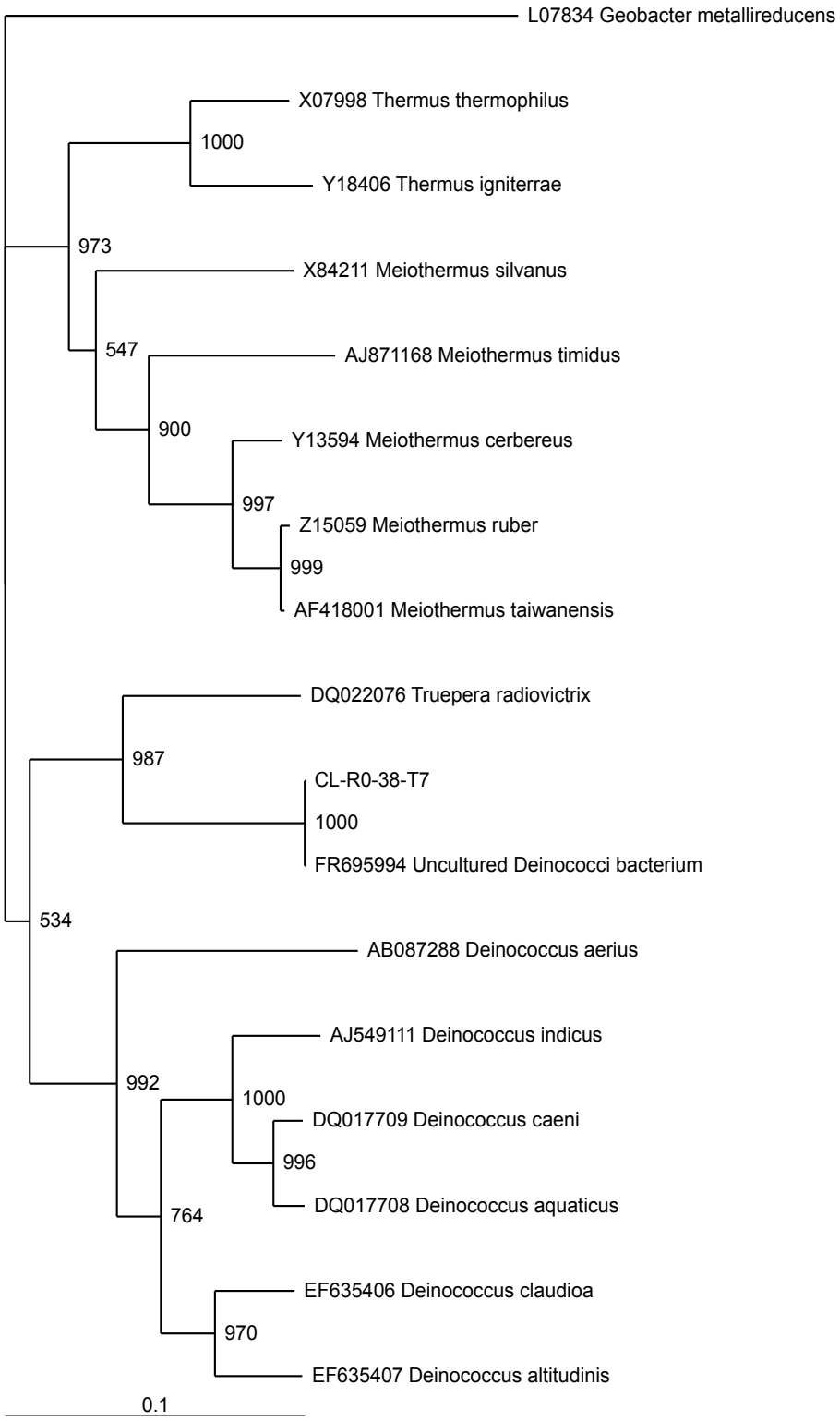

Figure 4.7 – Phylogenetic tree showing relationship between representative from Trupera-like sequence from this study (CL-R0-38) and a 16S rRNA gene sequence of a previously described Trupera-like OTU (FR695994) (Whittleston et al., 2013) (see discussion). *Geobacter metallireducens* was included as an out-group. The scale bar corresponds to 0.1 nucleotide substitutions per site. Bootstrap values (from 1000 replications) are shown at the branch point.

4.4 Discussion

4.4.1 Extent of Soil Alteration by highly alkaline steel slag leachates

XRD analysis of the surface soil revealed that it largely consisted of calcite. This was due to the ingress of atmospheric CO_2 from the surface to form calcite from dissolved Ca^{2+} and CO_3^{2-} ions (see equations 4.1 to 4.7, section 4.1). XRD patterns on the deep soil used in this study indicate that some calcite was present but there were also other primary soil minerals. This indicates that calcite formation becomes less important with depth, probably due to lower CO_2 ingress. The presence of primary minerals in the soil and not just remaining refractory minerals indicates that the deep soil had not been as highly altered by leachate from the steel slag when compared to the surface soil. Literature values for vanadium concentrations in natural soils vary considerably (10 – 400 mg kg^{-1}, average = 150 mg kg^{-1}) (Poledniok and Buhl, 2003; Panichev et al., 2006). Vanadium concentration in the deep soil was 170.1 mg kg^{-1} and 94 mg kg^{-1} in the surface soil, however the soil concentration of V from a reference site upstream of the slag leachate was 8 mg kg^{-1} (Mayes et al., 2008) indicating that the higher concentrations of V had most likely been transported from slag heaps via slag leachates. The soil also had a high pH (pH 11.5) also indicating alteration via slag leachates.

4.4.2 Microcosm experiments

There is no real evidence of any microbially mediated Fe(III), nitrate or sulfate reduction occurring in the reduction microcosms. However, the increase in nitrite concentration in the soil experiment at day 10, could be an indication of nitrate

reduction. This slight peak in nitrite was concomitant with a reduction in nitrate but this trend is matched in both the sterile and groundwater controls. For each redox indicator measured, the trend for the soil experiment and sterile and groundwater controls matched (with the exception of sulfate). This could be an indication that the sterile sample had not been sufficiently heat treated, however there is not any real evidence in the data to support microbially mediated Fe(III) or sulfate reduction in either the soil or sterile systems. The sterile system is also somewhat unreliable due to the lack of replicates. In order to assess if the patterns determined are 'real', then further replicates are required to rule out any artefacts from sampling or analysis.

Abiotic processes also control the removal of V(V) from solution. Up to 90% removal had occurred in both the soil and sterile control by day 30, whereas concentrations remained at ~95% of the original spike in the groundwater control. Vanadium in steel slag can be found in a number of oxidation states but due to reducing conditions predominately as; V(0), V(III) and V(IV) (Cornelis et al., 2008). Chaurand et al. (2007a) found V predominately as V(IV) in BOF slag which was then oxidised to V(V) during the ageing and weathering process. Vanadium K-edge XANES indicated that V in the Consett soil was predominantly as V(IV) before commencement of reduction experiments. This indicates that if V was transported as V(V) in the leaching process that a further reduction has occurred in the soil profile. Removal of the V(V) spike from the aqueous phase in the microcosm experiments could be due to adsorption to solids, V(V) is known to sorb weakly at pH > 10.5 (Peacock and Sherman, 2004b; Langmuir, 1997). Therefore, a reductive precipitation reaction (where the added vanadate is reduced to a vanadyl species that strongly sorbs to surfaces at high pH (Peacock and Sherman, 2004b)) within the reduced soils cannot be excluded.

Vanadium (IV) is readily formed from V(V) in the presence of any reducing agent. Hydrogen sulphide is known to be a strong reducer of V and the affinity for vanadium and organically bound sulfur and sulfates are well known (Breit and Wanty, 1991; Wanty and Goldhaber, 1992). Vanadium(IV) is most commonly present as the vanadyl cation [as VO^{2+}] which is known to adsorb more strongly to solid phases than V(V) oxyanions and will preferentially adsorb to oxides except under high ligand concentrations (Wehrli and Stumm, 1989). The vanadyl cation is not thermodynamically stable above pH 7 but the complexation to organic and inorganic ligands can considerably increase its stability (Szalay and Szilagyi, 1967; Breit and Wanty, 1991; Wehrli and Stumm, 1989). Several studies report high V concentrations in areas with an associated dissolved organic carbon content (Alberic et al., 2000; Pourret et al., 2012). Vanadate can form complexes with organic compounds, but studies using electron spin resonance and ^{51}V NMR indicated that the OM-V(V) complexes may not be stable above pH 9 (Lu et al., 1998). Humic and fulvic acids such as those found in soils are known to reduce V(V) to V(IV) to form stable complexes (Szalay and Szilagyi, 1967; Cheshire et al., 1977; Breit and Wanty, 1991).

An Eh/pH diagram (Figure 4.8) indicates that aqueous V(V) is likely to be present as VO_3OH^{2-} in the groundwater. According to Peacock and Sherman (2004b), there may be some sorption of VO_3OH^{2-} to Fe oxyhydroxide surfaces at pH 10.5, which may account for the removal of some of the V^{5+} from solution. We tentatively suggest that a more likely mechanism is V(V) reduction with increasingly anaerobic conditions and removal from the aqueous phase occurs as V(IV) is as adsorbed to mineral surfaces (Fe/Al oxyhydroxides) or that the VO^{2+} cation is taken up by calcite (vanadate sorbs weakly to calcite (Burke et al., 2013)). A decrease in Eh of only 0.1V would reach the

aqueous V(V)/V(IV) boundary at pH 11.3 (average microcosm pH over the incubation period) (Figure 4.8).

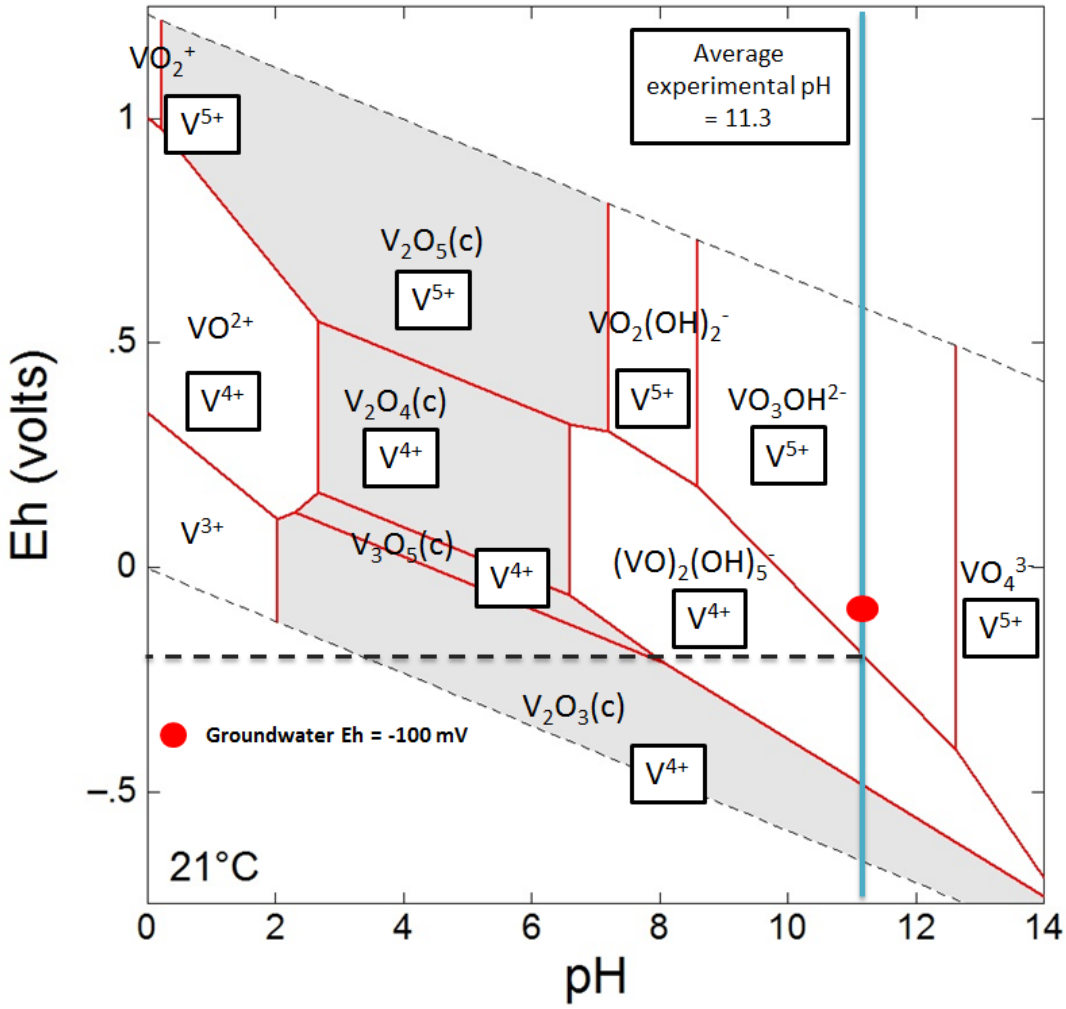

Figure 4.8 – Eh/pH V species predominance and relative mineral stability diagram calculated using Geochemists Workbench® for t = 21°C / P = 1 atmos. for the system V-O-H with log ∑V/m – 0.9194 and a [H_2O(aq)] = 1.

4.4.3 Microbial Community Analysis

The rarefaction curve (Figure 4.5) indicates that the total microbial diversity of the soil has not been sequenced as the curve does not quite reach an asymptote (Fierer et al., 2007). However, there is some flattening off of the curve which may indicate that the microbial population is not very diverse compared to other soils (Fierer et al., 2007). The successful sequences indicate that the microbial population of the deep soil appears to be dominated by three phyla; β-Proteobacteria (25.9%), Deinicoccus-Thermus (24.1%) and to a lesser extent Firmcutes (18.5%). Firmicutes had 3 OTU's, 2 of which were assigned to the order Natranaerobiales and were probably a Dethiobacter species. The other OTU was not assigned above the class of Clostridia. The β-Proteobacteria had 2 OTU's, which were both assigned to the order Burkholderiales. β-Proteobacteria in the order Burkholderiales have been found in other alkaline environments (Burke et al., 2012b).

The Deinococcus-Thermus had only 1 OTU assigned to the order of Deinococcales and were Truepera-like species. The phylogenetic tree (Figure 4.6) confirms this classification. Included in the phylogenetic tree is sequence FR695994, this sequence was isolated from soil sampled from beneath a chromite ore processing residue (COPR) disposal site (Whittleston et al., 2013). The maximum bootstrap value (1000 matches from 1000 repetitions) indicates that the grouping between CL-R0-38-T7 and FR695994 is very reliable (Hillis and Bull, 1993). Very little is known about the Truepera species. *Truepera radiovictrix* is the only Truepera species that has been studied in any depth and has been recently sequenced as part of the Genomic Encyclopedia of Bacteria and Archaea project (Ivanova et al., 2011). *Truepera radiovictrix* was first sampled in 2005 from a hot spring in a geothermal area

(Albuquerque et al., 2005). The bacteria is an aerobe known to grow under multiple extreme conditions; it is alkaliphilic, can tolerate high temperatures, moderate saline conditions and is also resistant to ionizing radiation (Albuquerque et al., 2005).

The presence of alkaliphiles in the soils does seem to indicate that some microbial processes (such as Fe(III) reduction, the deep soil shows some Fe(II) present in the soil, see table 4.1) may be supported in situ despite not being observed in microcosms. The pH of the microcosms is ~11.3, which is towards the upper limit of most alkaliphilic bacteria (Horikoshi, 1999). Previous studies have shown that microcosm experiments where the pH was buffered from pH 11.2 to 9.3 have elicited a microbial response with regards to nitrate and iron reduction whereas unamended microcosms were only able to support nitrate reduction (Whittleston et al., 2013).

4.5 Conclusions

A population of alkaliphilic bacteria dominated by a single unidentified species within the Truepera family of Deinococcus-Thermus and two species of Burkholderiales of β-Proteobacteria were established in the deep soil prior to the incubation experiments. A phylogenetic tree confirmed that the Truepera-like species was related (with high confidence) to another Truepera-like species sequenced from a COPR disposal site (Whittleston et al., 2013).

The V(V) spiked microcosms indicated that the key processes to the attenuation of vanadium at the Hownsgill Valley site are abiotic. Despite anaerobic incubation for 60 days, there was no real evidence of any biologically mediated redox processes occurring in the Consett soil experiments. There was ~80% removal of aqueous V(V)

from both the experiment and sterile control also indicating that abiotic processes had removed V(V) from solution, which might be due to the reduction of V(V) and the sorption of V(IV) to mineral surfaces and the possible uptake of the VO^{2+} cation by calcite present in the soil under reducing conditions.

Several issues with the data set relating to the lack of replicates in the sterile controls make it difficult to determine between artefacts of sampling and real trends in the data. However these data act as an interesting pilot study into the attenuation of V in steel slag affected soils. There are several ways in which this study could be extended to further our understanding of the microbial processes and processes controlling vanadium transport at this site; 1) replication of microcosms at a range of different pH, to span the upper limit of microbial activity; 2) detailed analysis of soil to investigate the existence of micro-niches of lower pH where microbial Fe(III) reduction might occur; 3) oxidation experiments to determine if V(IV) can be remobilised during oxidation and, 4) an extensive site investigation to determine the interaction of the leachate plume with natural soils.

4.6 References

ALBERIC, P., VIOLLIER, E., JEZEQUEL, D., GROSBOIS, C. & MICHARD, G. 2000. Interactions between trace elements and dissolved organic matter in the stagnant anoxic deep layer of a meromictic lake. Limnology and Oceanography, 45, 1088-1096.

ALBUQUERQUE, L., SIMOES, C., NOBRE, M. F., PINO, N. M., BATTISTA, J. R., SILVA, M. T., RAINEY, F. A. & DA COSTA, M. S. 2005. *Truepera radiovictrix* gen. nov., sp nov., a new radiation resistant species and the proposal of Trueperaceae fam. nov. Fems Microbiology Letters, 247, 161-169.

APUL, D. S., GARDNER, K. H., EIGHMY, T. T., FALLMAN, A. M. & COMANS, R. N. J. 2005. Simultaneous application of dissolution/precipitation and surface complexation/surface precipitation modeling to contaminant leaching. Environmental Science & Technology, 39, 5736-5741.

ASHELFORD, K. E., CHUZHANOVA, N. A., FRY, J. C., JONES, A. J. & WEIGHTMAN, A. J. 2006. New screening software shows that most recent large 16S rRNA gene clone libraries contain chimeras. Applied and Environmental Microbiology, 72, 5734-5741.

ASPILA, K. I., AGEMIAN, H. & CHAU, A. S. Y. 1976. SEMIAUTOMATED METHOD FOR DETERMINATION OF INORGANIC, ORGANIC AND TOTAL PHOSPHATE IN SEDIMENTS. Analyst, 101, 187-197.

ASTM 2006. D4972.01: standard test method for pH of soils. Annual Book of ASTM standards. Amer Soc Test Mater.

BALDAUF, S. L. 2003. Phylogeny for the faint of heart: a tutorial. TRENDS in Genetics, 19(6), 345-351.

BARCELOUX, D. G. 1999a. Chromium. Journal of Toxicology-Clinical Toxicology, 37, 173-194.

BARCELOUX, D. G. 1999b. Vanadium. Journal of Toxicology-Clinical Toxicology, 37, 265-278.

BAYLESS, E. R. & SCHULZ, M. S. 2003. Mineral precipitation and dissolution at two slag-disposal sites in northwestern Indiana, USA. Environmental Geology, 45, 252-261.

BONENFANT, D., KHAROUNE, L., SAUVE, S., HAUSLER, R., NIQUETTE, P., MIMEAULT, M. & KHAROUNE, M. 2008. CO2 Sequestration Potential of Steel Slags at Ambient Pressure and Temperature. Industrial & Engineering Chemistry Research, 47, 7610-7616.

BREIT, G. N. & WANTY, R. B. 1991. VANADIUM ACCUMULATION IN CARBONACEOUS ROCKS - A REVIEW OF GEOCHEMICAL CONTROLS DURING DEPOSITION AND DIAGENESIS. Chemical Geology, 91, 83-97.

BUDEVSKY, O. A. J., L. 1965. Colorimetric determination of vanadium(V) with 4-(2-pyridylazo)-resorcinol. Talanta, 12, 291 to 301.

BURKE, I. T., BOOTHMAN, C., LLOYD, J. R., LIVENS, F. R., CHARNOCK, J. M., MCBETH, J. M., MORTIMER, R. J. G. & MORRIS, K. 2006. Reoxidation behavior of technetium, iron, and sulfur in estuarine sediments. Environmental Science & Technology, 40, 3529-3535.

BURKE, I. T., MORTIMER, R. J. G., PALANIYANDI, S., WHITTLESTON, R. A., LOCKWOOD, C. L., ASHLEY, D. J. & STEWART, D. I. 2012. Biogeochemical Reduction Processes in a Hyper-Alkaline Leachate Affected Soil Profile. Geomicrobiology Journal, 29, 769-779.

BURKE, I. T., PEACOCK, C. L., LOCKWOOD, C. L., STEWART, D. I., MORTIMER, R. J. G., WARD, M. B., RENFORTH, P., GRUIZ, K. & MAYES, W. M. 2013. Behavior of Aluminum, Arsenic, and Vanadium during the Neutralization of Red Mud Leachate by HCl, Gypsum, or Seawater. Environmental Science & Technology, 47, 6527-6535.

CARPENTIER, W., DE SMET, L., VAN BEEUMEN, J. & BRIGE, A. 2005. Respiration and growth of *Shewanella oneidensis MR-1* using vanadate as the sole electron acceptor. Journal of Bacteriology, 187, 3293-3301.

CARPENTIER, W., SANDRA, K., DE SMET, I., BRIGE, A., DE SMET, L. & VAN BEEUMEN, J. 2003. Microbial reduction and precipitation of vanadium by *Shewanella oneidensis*. Applied and Environmental Microbiology, 69, 3636-3639.

CHAURAND, P., ROSE, J., BRIOIS, V., OLIVI, L., HAZEMANN, J. L., PROUX, O., DOMAS, J. & BOTTERO, J. Y. 2007a. Environmental impacts of steel slag reused in road construction: A crystallographic and molecular (XANES) approach. Journal of Hazardous Materials, 139, 537-542.

CHAURAND, P., ROSE, J., BRIOIS, V., SALOME, M., PROUX, O., NASSIF, V., OLIVI, L., SUSINI, J., HAZEMANN, J.-L. & BOTTERO, J.-Y. 2007b. New methodological approach for the vanadium K-edge X-ray absorption near-edge structure interpretation: Application to the speciation of vanadium in oxide phases from steel slag. Journal of Physical Chemistry B, 111, 5101-5110.

CHESHIRE, M. V., BERROW, M. L., GOODMAN, B. A. & MUNDIE, C. M. 1977. METAL DISTRIBUTION AND NATURE OF SOME CU, MN AND V COMPLEXES IN HUMIC AND FULVIC-ACID FRACTIONS OF SOIL ORGANIC-MATTER. Geochimica Et Cosmochimica Acta, 41, 1131-1138.

CORNELIS, G., JOHNSON, C. A., VAN GERVEN, T. & VANDECASTEELE, C. 2008. Leaching mechanisms of oxyanionic metalloid and metal species in alkaline solid wastes: A review. Applied Geochemistry, 23, 955-976.

CRANS, D. C., AMIN, S. S. AND KERAMIDAS, A. D. 1998. Chemistry of Relevance to Vanadium in the Environment. In: NRIAGU, J. O. (ed.) Vanadium in the Environment, Part One: Chemistry and Biochemistry. New York: John Wiley and Sons, Inc.

EDEN, P. A., SCHMIDT, T. M., BLAKEMORE, R. P. & PACE, N. R. 1991. PHYLOGENETIC ANALYSIS OF AQUASPIRILLUM-MAGNETOTACTICUM USING POLYMERASE CHAIN REACTION-AMPLIFIED 16S RIBOSOMAL-RNA-SPECIFIC DNA. International Journal of Systematic Bacteriology, 41, 324-325.

FENDORF, S. E. 1995. SURFACE-REACTIONS OF CHROMIUM IN SOILS AND WATERS. Geoderma, 67, 55-71.

FIERER, N., BREITBART, M., NULTON, J., SALAMON, P., LOZUPONE, C., JONES, R., ROBESON, M., EDWARDS, R. A., FELTS, B., RAYHAWK, S., KNIGHT, R., ROHWER, F. & JACKSON, R. B. 2007. Metagenomic and small-subunit rRNA analyses reveal the genetic diversity of bacteria, archaea, fungi, and viruses in soil. Applied and Environmental Microbiology, 73, 7059-7066.

FRANK, A., MADEJ, A., GALGAN, V. & PETERSSON, L. R. 1996. Vanadium poisoning of cattle with basic slag. Concentrations in tissues from poisoned animals and from a reference, slaughterhouse material. Science of the Total Environment, 181, 73-92.

HAYNES, R. J., BELYAEVA, O. N. & KINGSTON, G. 2013. Evaluation of industrial wastes as sources of fertilizer silicon using chemical extractions and plant uptake. Journal of Plant Nutrition and Soil Science, 176, 238-248.

HILLIS, D. M. & BULL, J. J. 1993. AN EMPIRICAL-TEST OF BOOTSTRAPPING AS A METHOD FOR ASSESSING CONFIDENCE IN PHYLOGENETIC ANALYSIS. Systematic Biology, 42, 182-192.

HORIKOSHI, K. 1999. Alkaliphiles: Some applications of their products for biotechnology. Microbiology and Molecular Biology Reviews, 63, 735-+.

HORN, D. 2010. Vanadium: Going Green. Mining Journal, 19/02/2010, p.2.

ITO, M., GUFFANTI, A. A., ZEMSKY, J., IVEY, D. M. & KRULWICH, T. A. 1997. Role of the nhaC-encoded Na+/H+ antiporter of alkaliphilic *Bacillus firmus OF4*. Journal of Bacteriology, 179, 3851-3857.

IVANOVA, N., ROHDE, C., MUNK, C., NOLAN, M., LUCAS, S., DEL RIO, T. G., TICE, H., DESHPANDE, S., CHENG, J.-F., TAPIA, R., HAN, C., GOODWIN, L., PITLUCK, S., LIOLIOS, K., MAVROMATIS, K., MIKHAILOVA, N., PATI, A., CHEN, A., PALANIAPPAN, K., LAND, M., HAUSER, L., CHANG, Y.-J., JEFFRIES, C. D., BRAMBILLA, E., ROHDE, M., GOEKER, M., TINDALL, B. J., WOYKE, T., BRISTOW, J., EISEN, J. A., MARKOWITZ, V., HUGENHOLTZ, P., KYRPIDES, N. C., KLENK, H.-P. & LAPIDUS, A. 2011. Complete genome sequence of *Truepera radiovictrix* type strain (RQ-24(T)). Standards in Genomic Sciences, 4, 91-99.

KRULWICH, T. A. & GUFFANTI, A. A. 1989. ALKALOPHILIC BACTERIA. Annual Review of Microbiology, 43, 435-463.

LANE, D. J., PACE, B., OLSEN, G. J., STAHL, D. A., SOGIN, M. L. & PACE, N. R. 1985. RAPID-DETERMINATION OF 16S RIBOSOMAL-RNA SEQUENCES FOR PHYLOGENETIC ANALYSES. Proceedings of the National Academy of Sciences of the United States of America, 82, 6955-6959.

LANGMUIR, D. 1997. Aqueous environmental geochemistry, Upper Saddle River, N. J., Prentice Hall.

LLOYD, J. R. 2003. Microbial reduction of metals and radionuclides. Fems Microbiology Reviews, 27, 411-425.

LOVLEY, D. R. & PHILLIPS, E. J. P. 1986. AVAILABILITY OF FERRIC IRON FOR MICROBIAL REDUCTION IN BOTTOM SEDIMENTS OF THE FRESH-WATER TIDAL POTOMAC RIVER. Applied and Environmental Microbiology, 52, 751-757.

LU, X., JOHNSON, W. D. & HOOK, J. 1998. Reaction of Vanadate with Aquatic Humic Substances: An ESR and 51V NMR Study. Environmental Science & Technology, 32, 2257-2263.

LYALIKOVA, N. N. & YURKOVA, N. A. 1992. ROLE OF MICROORGANISMS IN VANADIUM CONCENTRATION AND DISPERSION. Geomicrobiology Journal, 10, 15-26.

MAYES, W. M., YOUNGER, P. L. & AUMONIER, J. 2006. Buffering of alkaline steel slag leachate across a natural wetland. Environmental Science & Technology, 40, 1237-1243.

MAYES, W. M., YOUNGER, P. L. & AUMONIER, J. 2008. Hydrogeochemistry of alkaline steel slag leachates in the UK. Water Air and Soil Pollution, 195, 35-50.

MORSE, J. W. & CORNWELL, J. C. 1987. ANALYSIS AND DISTRIBUTION OF IRON SULFIDE MINERALS IN RECENT ANOXIC MARINE-SEDIMENTS. Marine Chemistry, 22, 55-69.

NAVARRO, C., DIAZ, M. & VILLA-GARCIA, M. A. 2010. Physico-Chemical Characterization of Steel Slag. Study of its Behavior under Simulated Environmental Conditions. Environmental Science & Technology, 44, 5383-5388.

ORTIZ-BERNAD, I., ANDERSON, R. T., VRIONIS, H. A. & LOVLEY, D. R. 2004. Vanadium respiration by *Geobacter metalireducens*: Novel strategy for in situ removal of vanadium from groundwater. Applied and Environmental Microbiology, 70, 3091-3095.

PANICHEV, N., MANDIWANA, K., MOEMA, D., MOLATLHEGI, R. & NGOBENI, P. 2006. Distribution of vanadium(V) species between soil and plants in the vicinity of vanadium mine. Journal of Hazardous Materials, 137, 649-653.

PEACOCK, C. L. & SHERMAN, D. M. 2004. Vanadium(V) adsorption onto goethite (alpha-FeOOH) at pH 1.5 to 12: A surface complexation model based on ab initio molecular geometries and EXAFS spectroscopy. Geochimica Et Cosmochimica Acta, 68, 1723-1733.

POLEDNIOK, J. & BUHL, F. 2003. Speciation of vanadium in soil. Talanta, 59, 1-8.

POURRET, O., DIA, A., GRUAU, G., DAVRANCHE, M. & BOUHNIK-LE COZ, M. 2012. Assessment of vanadium distribution in shallow groundwaters. Chemical Geology, 294-295, 89-102.

PROCTOR, D. M., FEHLING, K. A., SHAY, E. C., WITTENBORN, J. L., GREEN, J. J., AVENT, C., BIGHAM, R. D., CONNOLLY, M., LEE, B., SHEPKER, T. O. & ZAK, M. A. 2000. Physical and chemical characteristics of blast furnace, basic oxygen furnace, and electric arc furnace steel industry slags. Environmental Science & Technology, 34, 1576-1582.

RAVEL, B. & NEWVILLE, M. 2005. ATHENA, ARTEMIS, HEPHAESTUS: data analysis for X-ray absorption spectroscopy using IFEFFIT. Journal of Synchrotron Radiation, 12, 537-541.

ROADCAP, G. S., KELLY, W. R. & BETHKE, C. M. 2005. Geochemistry of extremely alkaline (pH > 12) ground water in slag-fill aquifers. Ground Water, 43, 806-816.

ROADCAP, G. S., SANFORD, R. A., JIN, Q. S., PARDINAS, J. R. & BETHKE, C. M. 2006. Extremely alkaline (pH > 12) ground water hosts diverse microbial community. Ground Water, 44, 511-517.

SCHLOSS, P. D., WESTCOTT, S. L., RYABIN, T., HALL, J. R., HARTMANN, M., HOLLISTER, E. B., LESNIEWSKI, R. A., OAKLEY, B. B., PARKS, D. H., ROBINSON, C. J., SAHL, J. W., STRES, B., THALLINGER, G. G., VAN HORN, D. J. & WEBER, C. F. 2009. Introducing mothur: Open-Source, Platform-Independent, Community-Supported Software for Describing and Comparing Microbial Communities. Applied and Environmental Microbiology, 75, 7537-7541.

SCHWAB, A. P., HICKEY, J., HUNTER, J. & BANKS, M. K. 2006. Characteristics of blast furnace slag leachate produced under reduced and oxidized conditions. J Environ Sci Health A Tox Hazard Subst Environ Eng, 41, 381-95.

SZALAY, A. & SZILAGYI, M. 1967. ASSOCIATION OF VANADIUM WITH HUMIC ACIDS. Geochimica Et Cosmochimica Acta, 31, 1-&.

TAKAI, K., MOSER, D. P., ONSTOTT, T. C., SPOELSTRA, N., PFIFFNER, S. M., DOHNALKOVA, A. & FREDRICKSON, J. K. 2001. *Alkaliphilus transvaalensis* gen. nov., sp nov., an extremely alkaliphilic bacterium isolated from a deep South African gold mine. International Journal of Systematic and Evolutionary Microbiology, 51, 1245-1256.

THE ENVIRONMENT AGENCY. 2011. Chemical Standards Report [Online]. Available: http://evidence.environment-agency.gov.uk/ChemicalStandards/report.aspx?cid=282 [Accessed 11th April 2014].

U.S. GEOLOGICAL SURVEY 2013. Mineral commodity summaries 2013. In: U.S. GEOLOGICAL SURVEY (ed.). Reston Virginia: U.S.Geological Survey,.

VIOLLIER, E., INGLETT, P. W., HUNTER, K., ROYCHOUDHURY, A. N. & VAN CAPPELLEN, P. 2000. The ferrozine method revisited: Fe(II)/Fe(III) determination in natural waters. Applied Geochemistry, 15, 785-790.

WANG, Q., GARRITY, G. M., TIEDJE, J. M. & COLE, J. R. 2007. Naive Bayesian classifier for rapid assignment of rRNA sequences into the new bacterial taxonomy. Applied and Environmental Microbiology, 73, 5261-5267.

WANTY, R. B. & GOLDHABER, M. B. 1992. THERMODYNAMICS AND KINETICS OF REACTIONS INVOLVING VANADIUM IN NATURAL SYSTEMS - ACCUMULATION OF VANADIUM IN SEDIMENTARY-ROCKS. Geochimica Et Cosmochimica Acta, 56, 1471-1483.

WEHRLI, B. & STUMM, W. 1989. VANADYL IN NATURAL-WATERS - ADSORPTION AND HYDROLYSIS PROMOTE OXYGENATION. Geochimica Et Cosmochimica Acta, 53, 69-77.

WHITTLESTON, R. A., STEWART, D. I., MORTIMER, R. J. G. & BURKE, I. T. 2013. Enhancing microbial iron reduction in hyperalkaline, chromium contaminated sediments by pH amendment. Applied Geochemistry, 28, 135-144.

YE, Q., ROH, Y., CARROLL, S. L., BLAIR, B., ZHOU, J. Z., ZHANG, C. L. & FIELDS, M. W. 2004. Alkaline anaerobic respiration: Isolation and characterization of a novel alkaliphilic and metal-reducing bacterium. Applied and Environmental Microbiology, 70, 5595-5602.

Chapter 5 Gypsum addition to soils contaminated by red mud: Implications for aluminium, arsenic, molybdenum and vanadium solubility.

Abstract

Red mud is highly alkaline (pH 13), saline and can contain elevated concentrations of several potentially toxic elements (e.g. Al, As, Mo and V). Release of up to 1 million m^3 of bauxite residue (red mud) suspension from the Ajka repository, western Hungary, caused large scale contamination of downstream rivers and floodplains. There is now concern about the potential leaching of toxic metal/loids from the red mud as some have enhanced solubility at high pH. This chapter investigates the impact of red mud addition to three different Hungarian soils with respect to trace element solubility and soil geochemistry. The effectiveness of gypsum amendment for the rehabilitation of red mud-contaminated soils was also examined. Red mud addition to soils caused a pH increase, proportional to red mud addition, of up to 4 pH units (e.g. pH 7 $\rightarrow$ 11). Increasing red mud addition also led to significant increases in salinity, dissolved organic carbon (DOC) and aqueous trace element concentrations. However, the response was highly soil specific and one of the soils tested buffered pH to around pH 8.5 even with the highest red mud loading tested (33% w/w); experiments using this soil also had much lower aqueous Al, As, and V concentrations. Gypsum addition to soil / red mud mixtures, even at relatively low concentrations (1% w/w) was sufficient to buffer experimental pH to 7.5 - 8.5. This effect was attributed to the reaction of Ca^{2+} supplied by the gypsum with OH^- and carbonate from the red mud to precipitate calcite. The lowered pH enhanced trace element sorption and largely inhibited the release of Al, As and V. Mo concentrations, however, were largely unaffected by gypsum induced

pH buffering due to the greater solubility of Mo (as molybdate) at circumneutral pH. Gypsum addition also leads to significantly higher porewater salinities and column experiments demonstrated that this increase in total dissolved solids persisted even after 25 pore volume replacements. Gypsum addition could therefore provide a cheaper alternative to recovery (dig and dump) for treatment of red mud affected soils. The observed inhibition of trace metal release within red mud affected soils was relatively insensitive to either the percentage of red mud or gypsum present, making the treatment easy to apply. However, there is risk that over-application of gypsum could lead to detrimental long term increases in soil salinity.

5.1 Introduction

Fine fraction bauxite residue (red mud) is a by-product of alumina refining, with up to 120 million tonnes produced worldwide each year (Grafe and Klauber, 2011). Red mud typically comprises residual iron oxides, quartz, sodium aluminosilicates, titanium dioxide, calcium carbonate/aluminate and sodium hydroxide which raises the pH up to 13 (Grafe et al., 2011; Gelencser et al., 2011; Burke et al., 2012a). The failure of the bauxite residue dam at the Ajkai Timfoldgyar Zrt alumina plant, western Hungary, on the 4th October 2010 resulted in the release of up to 1 million m^3 of caustic red mud suspension (Reeves et al., 2011). The waste inundated homes and land downstream causing 10 deaths and over 150 serious injuries. Approximately 40 km^2 of agricultural and urban land was affected and the red mud was transported over 120 km downstream (Reeves et al., 2011; Mayes et al., 2011). This was the largest recorded environmental release of red mud and, as such, studies on the after-effects of the spill have both improved the knowledge-base on risks associated with red mud (Gruiz et al., 2012) and informed broader management strategies for stockpiled red mud. At Ajka, Hungary, red mud samples contained elevated concentrations of potentially toxic trace elements such as Al (75000 mg kg^{-1}), As (150 mg kg^{-1}) and V (900 mg kg^{-1}) (Mayes et al., 2011; Ruyters et al., 2011). Red mud leachates are also hyperalkaline (pH 13), and can be directly toxic to aquatic life (Wilkie and Wood, 1996). Equally important is the enhanced mobility of several oxyanionic forming trace elements at high pH (Langmuir, 1997). Water in contact with Ajka red mud had dissolved Al concentration of 800 mg L^{-1}, and dissolved As, V, and Mo concentrations of 4 - 6 mg L^{-1} (Mayes et al., 2011).

The initial response to the accident was to dose affected rivers with weak acids and gypsum (up to 23,500 t (Rédey, 2012)) to neutralise the water, and (in some cases)

to plough the red mud into the fields to prevent dust formation (Gelencser et al., 2011; Renforth et al., 2012). Longer term strategies included the building of new containment dams and the large scale recovery of red mud deposits from affected land, although thin deposits of red mud (< 5 cm) were not routinely recovered (Klebercz et al., 2012). Studies on the effect of the red mud in soils conducted in the weeks following the spill suggested that the high NaOH present inhibits plant growth (Ruyters et al., 2011), however, little is known about the longer term leaching and potential for bioaccumulation of metal/loids into plants grown in soils affected by the Ajka red mud spill.

Acid dosing and gypsum addition to rivers were both effective in lowering pH values and metal/loid concentrations in river waters downstream of the spill (Burke et al., 2012a; Mayes et al., 2011; Renforth et al., 2012). Lack of Ca^{2+} in red mud leachate (Renforth et al., 2012) limits the natural pH reduction mechanism (Equations 5.1 and 5.2). Providing excess free Ca^{2+} is therefore the main effect of gypsum addition. The reaction, which involves CO_2 in-gassing to form calcite with net OH^- removal, can be rapid in high pH systems (Renforth et al., 2012).

$$OH^-_{(aq)} + CO_{2(aq)} \leftrightarrow HCO_3^-{}_{(aq)} \quad (5.1)$$

$$2OH^-_{(aq)} + CaSO_4.2H_2O_{(s)} + 2CO_{2(g)} \leftrightarrow$$

$$CaCO_{3(s)} + SO_4^{2-}{}_{(aq)} + 2H_2O_{(l)} + H_2CO_{3(aq)} \quad (5.2)$$

The Ca^{2+} provided by gypsum addition can also displace Na^+ from exchange complexes and potentially reduces salt stress to vegetation (Grafe and Klauber, 2011;

Grafe et al., 2011). Although gypsum addition has also been shown to be very effective in the rehabilitation of stock-piled red mud (Courtney and Timpson, 2004; Courtney and Timpson, 2005; Courtney and Kirwan, 2012), studies have focussed primarily on soil sodicity and availability of major ions (e.g. Al, Na, Ca: (Courtney et al., 2009; Courtney and Kirwan, 2012; Courtney and Harrington, 2012) and less on the mobility of potentially toxic trace elements (e.g. As, Mo and V). At Ajka, gypsum addition to affected soils was not attempted, but it is therefore possible that gypsum addition may have been a useful tool for soil stabilisation and negated the need for such extensive recovery of marginally-contaminated soils. This was highlighted as a more appropriate and cost-effective alternative approach for dealing with red mud-contaminated floodplain areas in official reviews of the disaster response (Adam et al., 2011b).

The primary objective of this chapter is a preliminary investigation into the potential geochemical effects of red mud mixing with different soils collected from the Torna and upper Marcal catchments. Batch experiments were used to determine the evolution of chemical properties (e.g. pH, salinity) when soil was mixed with red mud. The solubility of several potentially problematic elements (Al, As, Mo and V) was investigated as a function of red mud loading and the resultant perturbation in soil pH over short time incubation periods. Finally, gypsum was added to soil / red mixtures in batch and column tests to determine the effectiveness of gypsum addition for treatment of red mud-contaminated soils. As such, this chapter provides information not only on potential remedial strategies for environmental release of red mud but also provides some basic analogue data on the soil and leachate quality that would be anticipated in amended red mud in bauxite residue disposal areas (BDRAs).

5.2 Materials and Methods

5.2.1 Sample Collection

Samples were collected in May 2011. Red mud was collected from inside the breached Ajka repository (Lat. 47°4'58"N, Long.17°29'34"E) and three soil samples (that did not receive red mud during the 2010 spill) were collected from sites representative of the varying land uses and landforms in the affected Torna and Upper Marcal catchment, western Hungary. Soil SS was an agricultural topsoil (Lat. 47°6'38"N, Long. 17°23'43"). Soil OR was a non-agricultural topsoil sampled from below the rootlet layer at 10-50 cm (Lat. 47° 5'46"N, 17° 15'1"E). Soil WL was a wetland soil from within a reed bed area (Lat. 47°5'56"N, Long. 17°13'41"E). The Hungarian soils were used in the batch experiments described below. The column experiments (also described below) required significantly greater amount of soil than was originally sampled. Therefore, a well characterised sandy silt loam (Soil E1), collected from north western England in May 2009, was used in column experiments. All red mud and soils were stored at 4°C ±2°C in polypropylene containers until used. Soil WL was stored anaerobically using Anaerogen™ sachets.

5.2.2 Sample Characterisation

The red mud and soil samples (after oven drying (105 ^{0}C) and grinding in a mortar and pestle) were characterised by X-ray powder diffraction using a Bruker D8 Advance XRD, X-ray fluorescence using a PANalytical Axios Advanced XRF spectrometer (data corrected for loss on ignition; % weight loss after furnace treatment at 1050 ^{0}C), total organic carbon analysis using a Carlo Erba NA 2500 Elemental

Analyser. The pH was determined (using homogenised field moist soils) after 10 g : 10 mL suspension in deionised water [ASTM method D4972-01]. The BET surface area was determined (on oven dried samples) after degassing with N_2 on a Micromeritics FlowPrep 060 sample degas system prior to analysis with a Micromeritics Gemini V BET surface area analyser. Principal Component Analysis (PCA) of the red mud and soil samples was under-taken on standardized elemental concentration data and compared against other published samples from the red mud contaminated catchment (Mayes et al., 2011).

5.2.3 Batch Experiments

All soils and the red mud were homogenised by hand before establishing experiments, but otherwise were used as collected. Batch experiments were established by mixing soils OR, SS and WL with red mud to achieve final concentrations of 0, 1, 5, 9, 20, and 33% red mud on a dry weight basis. (After the Ajka spill, red mud deposits in fields varied from <1cm to, at most, ~20cm; and all deposits >5cm were routinely recovered (Klebercz et al., 2012). If red mud was ploughed into soils to a typical depth of ~40-50 cm, an approximate 5:50 mixing ratio (~9%), would therefore, be an important condition for study. Larger additions, up to 33% red mud, were only considered as worst case scenario.) The soil / red mud mixtures where suspended at 200 g L^{-1}, in deionised water in 15 ml polypropylene centrifuge tubes, and continuously shaken on an orbital shaker (100 rpm) for 30 days. In order to maintain an aerobic headspace, each tube was opened daily (5 days per week, for <1 minute). Additional batch experiments were established with the same red mud conditions as above but with 4% (w/w) addition of gypsum ($CaSO_4 \cdot 2H_2O$). Finally a set of batch experiments was

established which contained 9% (w/w) red mud, with varying quantities of gypsum to achieve 0, 1, 4, 8, 12, and 15% gypsum additions on a dry weight basis. After 30 days equilibration, all tubes were centrifuged (6000 g) for 5 minutes to separate aqueous and solid phases. All aqueous samples were then membrane filtered (0.2 μm). Duplicate experiments were performed at two key conditions (9% red mud, and, 9% red mud +4% gypsum) in all three soil types as a check on data reproducibility (duplicate data is reported in Appendix A, Table A2).

5.2.4 Column Experiments

500 g of Soil E1 (< 2 mm fraction) was homogenised and mixed with red mud (8% w/w) with and without gypsum addition (also 8% w/w). The amended soils were hand packed into glass Omnifit™ columns (400 mm length, 50 mm diameter) with Teflon end pieces and 50 μm filters at both the influent and effluent ends. Columns were saturated with deionised water and left to equilibrate overnight. Thereafter, deionised water was pumped vertically upwards through the columns using an isocratic pump at (0.06 mL min^{-1}; 86.4 mL day^{-1}), with influent at the column bottom and effluent at the top. This rate of pumping equated to approximately 1 pore volume per day (determined as the weight difference of dry and saturated columns). Pumping was continued until approximately 25 pore volumes had passed through each column. At each sampling point, the volume of effluent was recorded and water samples were collected and filtered (0.2 μm).

5.2.5 Geochemical Analysis

Sample pH was measured using a Microprocessor pH meter with electrodes calibrated at pH 7 and 10 using standard buffer solutions; Total Dissolved Solids (TDS) was determined using a Myron Ultrameter calibrated with a KCl solution. Solution colour was determined by measuring the absorbance at 254 nm using an Uvikon XL spectrophotometer and a quartz cell. Dissolved organic carbon (DOC) was measured on a multi N/C® 2100 using thermocatalytic oxidation, MC-NDIR detection analysis. In these experiments, absorbance at 254 nm and DOC concentrations were found to be significantly correlated (Pearson's correlation: $r = 0.93$, $p = <0.001$, $n = 27$), therefore, absorbance at 254 nm was used routinely to estimate sample DOC concentration (DOC analysis was performed on 40% of the samples). As, V and Mo concentrations were determined in aqueous samples (after acidification with 2% HNO_3) on a Perkin–Elmer Elan DRCII inductively coupled plasma-mass spectrometer (ICP-MS) (LoD = 0.49, 0.25, and 0.86 μg L^{-1} respectively). Aluminium concentrations were determined by using Flame Atomic Absorption Spectroscopy (FAAS) on an Analytic Jena ContrAA 700 (after acidification with 2% HCl; LoD = 200 μg L^{-1})

5.3 Results

5.3.1 Sample Characterization

The red mud mineral content is dominated by hematite, calcite, magnetite, cancrinite and hydrogarnet (with some residual boehmite and gibbsite), which is very similar to other red mud analysed from the Ajka spill (Gelencser et al., 2011; Burke et al., 2012a). Sample characterisation data for the red mud, the three Hungarian soils and

soil E1 are summarised in Table 5.1. Principal Component Analysis compared the elemental composition of the red mud sample and the three Hungarian soil samples (see Table 5.2) to other surface and fluvial samples from the affected region (Mayes et al., 2011). Results (Figure 5.1) show that the soil sample compositions were consistent with other unaffected reference samples from the area and the red mud composition was consistent with other source term red mud samples from the Ajka repository.

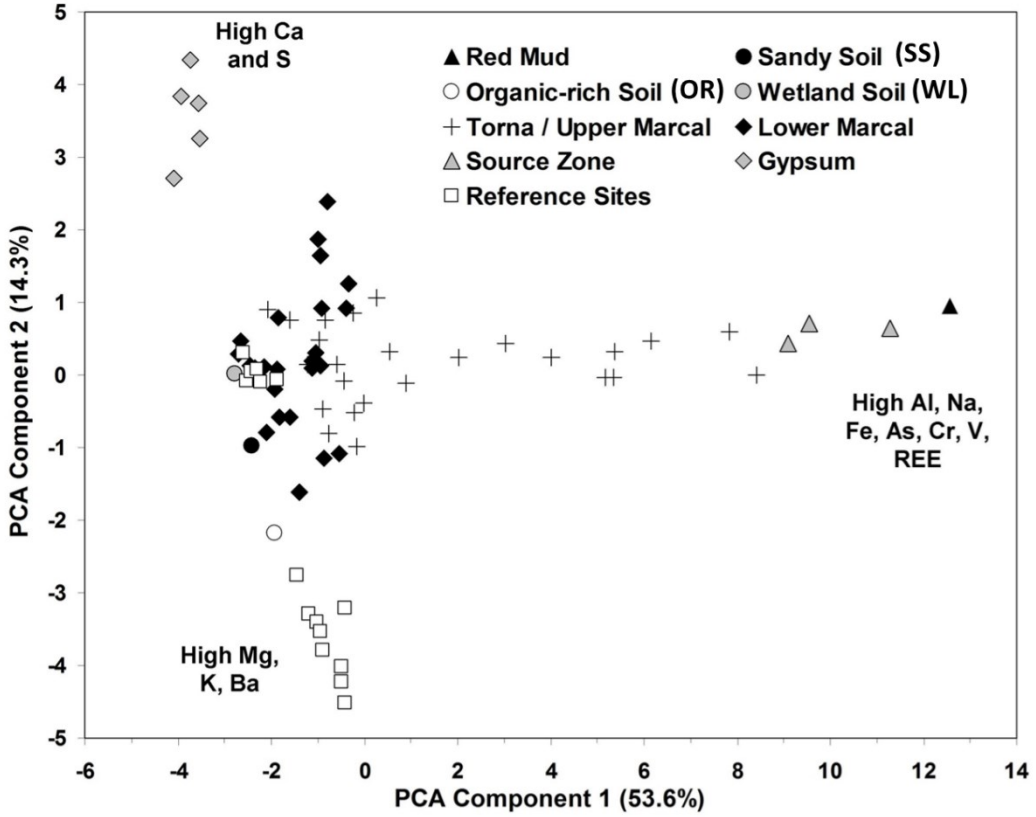

Figure 5.1 - Principal Component Analysis based on major and minor elemental abundance in the red mud and soil samples using data from background and red mud affected sites in the Torna and Marcal catchments. Note that the red mud data ('Red Mud') plots at the extreme right hand side with other source term materials ('Source'); the soil samples used in this study all plot in a group on the left hand side with unaffected sites from the lower Marcal River and unaffected reference ('REF') samples (see text and Mayes et al. 2011, for detail). REE = rare earth elements.

Table 5.1 - Summary of red mud and soil characterisation data collected from the materials used in this study (*data from (Law et al., 2010; Thorpe et al., 2012; Wallace et al., 2012). (NA = data not available)

	Red Mud	**SS**	**OR**	**WL**	**E1***
pH	13.1	7.2	6.7	7.7	5.5
Dominant minerals	hematite cancrinite, calcite magnetite hydrogarnet boehmite gibbsite	quartz albite microcline chlorite muscovite	quartz albite microcline chlorite muscovite	quartz albite microcline chlorite muscovite	quartz albite microcline chlorite muscovite
C_{org} (% w/w)	0.2	0.74	4.15	1.14	0.60
SSA_{BET} (m^2 g^{-1})	14.0 ±0.1	0.94 ±0.01	1.8 ±0.2	2.6 ±0.01	3.4 ±0.6
PO_4 (mg kg^{-1})	1019	520	297	355	NA
0.5 M HCl Acid extractable iron as % Fe(II)	22 ±3	5 ±2	10 ±2	87 ±14	NA
as Total [Fe] (mg L^{-1})	0.14 ±0.1	1.16 ±0.2	4.29 ±1.0	1.46 ±0.2	NA
Munsell™ soil colour	dark red (10R 3/6)	light olive brown (2.5Y 5/6)	dark brown (7.5Y 3/2)	very dark grey (10Y 3/1)	reddish brown (2.5YR 4/8)
Texture	clay (100% clay)	sandy loam (70% sand, 30% silt and 0% clay)	clay loam (65% sand, 28% silt and 7% clay)	clay loam (69% sand, 24% silt and 7% clay)	sandy loam (52% sand, 43% silt and 5% clay)

Table 5.2 - Concentrations of selected elements present in the red mud sample and soil samples. Soils OR, WL and SS were collected in Western Hungary. Soil E1 was collected in North Western England (*data from Law et al., 2010).

Major Elements (Weight %)	**Red Mud**	**Soil SS**	**Soil OR**	**Soil WL**	**Soil E1***
Si	6.0	42	38	34	35
Al	4.2	1.1	1.7	2.4	5.8
Fe	13.4	0.6	0.6	1.0	3.1
K	0.04	0.4	0.5	0.7	2.7
Na	3.0	0.3	0.3	0.4	1.0
Mg	0.4	0.2	0.6	0.5	0.5
Ti	3.1	0.2	0.2	0.3	0.4
Ca	5.7	0.4	1.6	0.8	0.2
Mn	0.2	0.04	0.02	0.03	0.1
P	0.04	0.02	0.02	0.02	0.02
S	0.1	0.002	0.01	0.01	-
Ba	0.007	0.014	0.04	0.03	0.04
Loss on Ignition	*1.0*	*1.8*	*5.1*	*1.2*	*4.1*
Minor Elements ($mg\ kg^{-1}$)					
As	196	2	11	8	-
Ce	607	17	47	34	-
Co	59	3	11	5	<10
Cr	864	50	68	62	30
Cu	104	2	12	6	<30
Ga	26	4	10	6	-
La	283	10	26	18	23
Mo	15	1	1	1	-
Ni	361	5	23	14	17
Pb	215	9	25	12	42
Sb	22	1	1	2	-
Sr	318	47	78	94	58
Th	98	2	6	4	-
U	21	1	3	2	-
V	1132	30	72	51	81
W	17	<1	<1	<1	-
Zn	162	21	52	26	51
Zr	1223	88	122	102	251

< denotes less than given level of detection
- denotes not determined.

5.3.2 Red Mud Addition to Soils

The addition of alkaline red mud caused an increase in experimental pH that increased with red mud loadings (Figure 5.2a). At low red mud additions (< 10%) pH increases were limited to 1 - 1.5 pH units for all three soils. At the highest red mud loadings (33%) pH increases of 3 - 4 pH units from pH 7 - 8 to around pH 11 occurred in experiments using Soil SS and WL, however, Soil OR buffered pH more effectively and pH increases were limited to 2 pH units (pH 6.5 to 8.5). TDS increased modestly in all experiments with increasing red mud addition (Figure 5.2b) with TDS increasing by around 500 mg L^{-1} to ~1500 mg L^{-1} in experiments receiving the highest red mud loading. DOC concentrations also increased with increasing red mud addition (Figure 5.2c) but the response was soil specific; experiments containing Soil WL had relatively lower aqueous DOC concentrations at higher red mud loadings. Concentrations of Al, As, V, and Mo in experiments also increase with increasing red mud addition (Figure 5.3a-d). Experiments containing Soil OR had relatively lower aqueous concentrations of Al, As and V compared to Soil SS or WL, but Mo concentrations were comparable in all three soils.

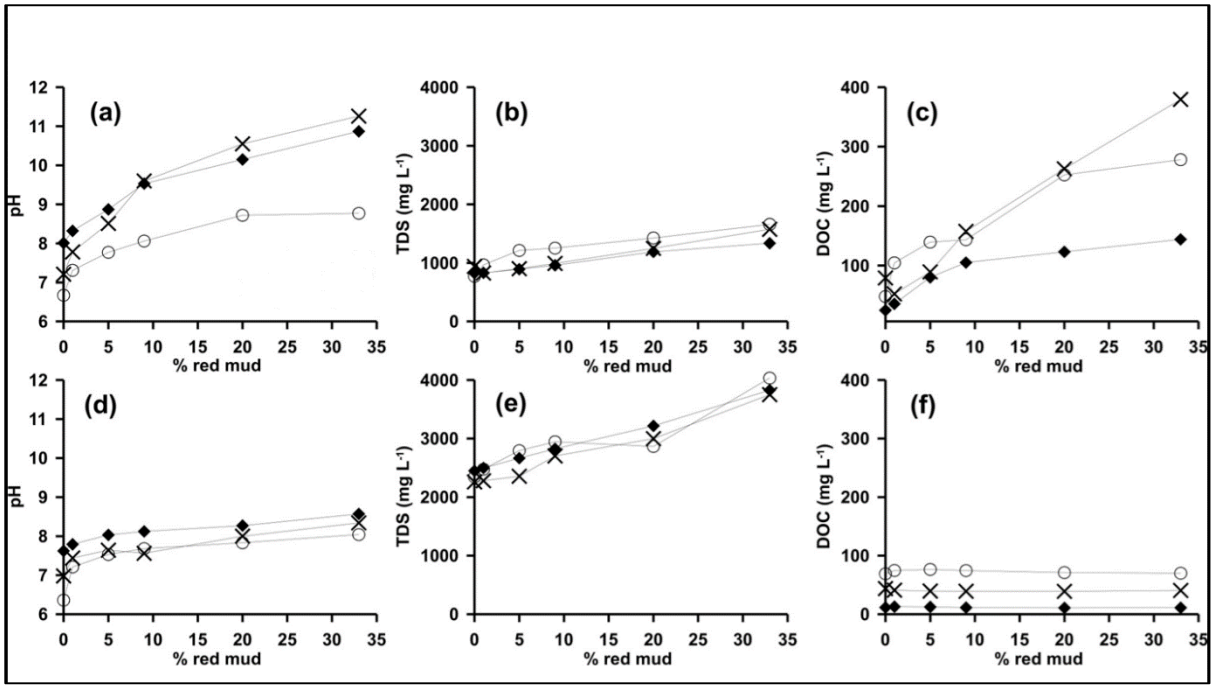

Figure 5.2 - The effect of increasing red mud addition to three Hungarian soils on experimental pH, total dissolved solids (TDS) and dissolved organic carbon (DOC). Results are shown in both the absence (upper three panels) and presence (lower three panels) of 4% (w/w) gypsum addition. Key: Crosses = Soil SS, Circles = Soil OR and Diamonds = Soil WL.

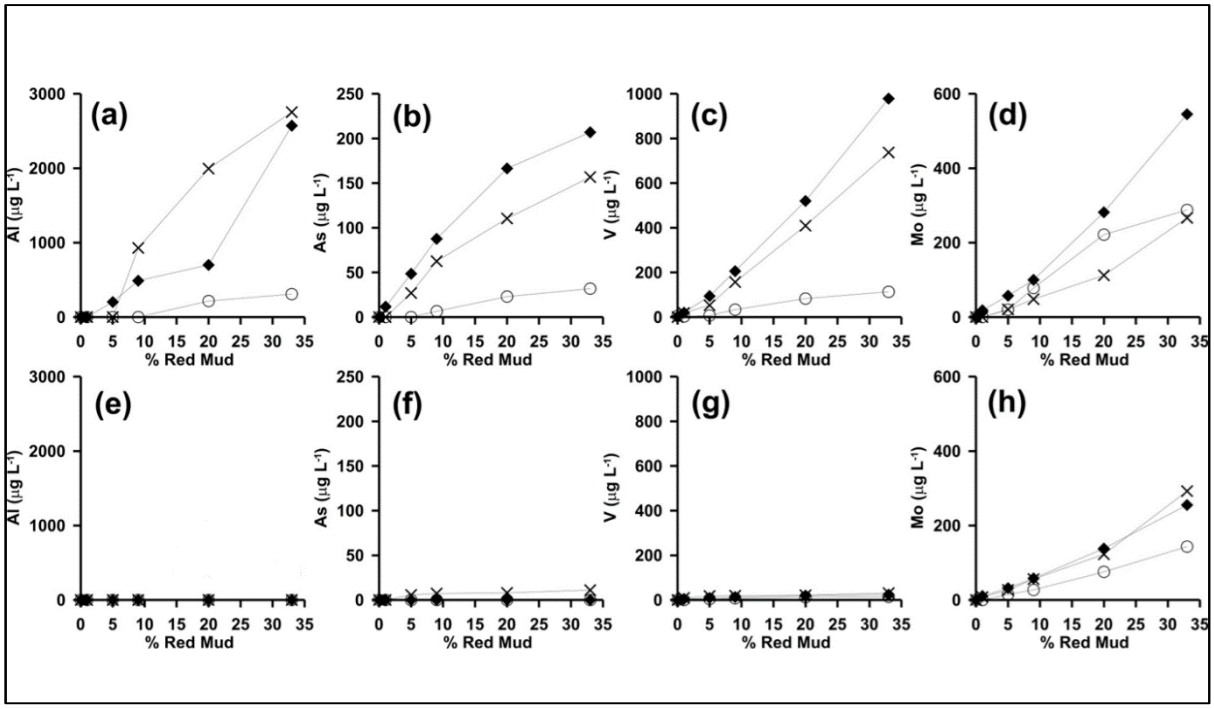

Figure 5.3 - The effect of increasing red mud addition to three Hungarian soils on experimental trace element concentrations. Results are shown in both the absence (upper four panels) and presence (lower four panels) of 4% (w/w) gypsum addition. Key: Crosses = Soil SS, Circles = Soil OR and Diamonds = Soil WL.

5.3.3 Gypsum Addition to Red Mud / Soil Mixtures

When 4% gypsum was added to experiments the observed pH increases were much lower compared to experiments without gypsum (Figure 5.2d). There was a smaller increase of pH (up to 1 pH unit) observed with increasing red mud loadings and no experiments had pH values above 8.5 even with 33% red mud addition. TDS, however, was much higher in gypsum containing experiments (Figure 5.2e). Also the gradient of TDS increases with increasing red mud addition was greater, with TDS increasing by nearly 2000 mg L^{-1} to around 4000 mg L^{-1} as red mud addition increased from 0 to 33%. Aqueous DOC concentrations in gypsum amended experiments were significantly lower compared to experiments without gypsum (Figure 5.2f) and there was no observed change in DOC concentrations with increasing red mud addition. Aqueous Al, As and V concentrations in gypsum amended experiments (Figure 5.3e-g) were also much lower than in unamended experiments. Aqueous Mo concentrations, however, were only slightly lower in gypsum amended experiments (Figure 5.3h).

In experiments where the amount of gypsum added was varied (from 0 to 15%) and red mud addition was constant (9%), it was discovered that the soils tested were relatively insensitive to increasing gypsum addition (Figure 5.4). Approximately equal reductions in pH and aqueous DOC, Al, As and V values were observed with 1 to 15% gypsum addition. The observed TDS increase (Figure 5.4b) was about 1000 mg L^{-1} between 0 and 1% addition and further increased to about 2800-3000 mg L^{-1} with 4% gypsum present. No further increase in TDS was observed for gypsum addition above 4%. Aqueous Mo concentrations do not show any reduction at any level of gypsum addition (Figure 5.4g).

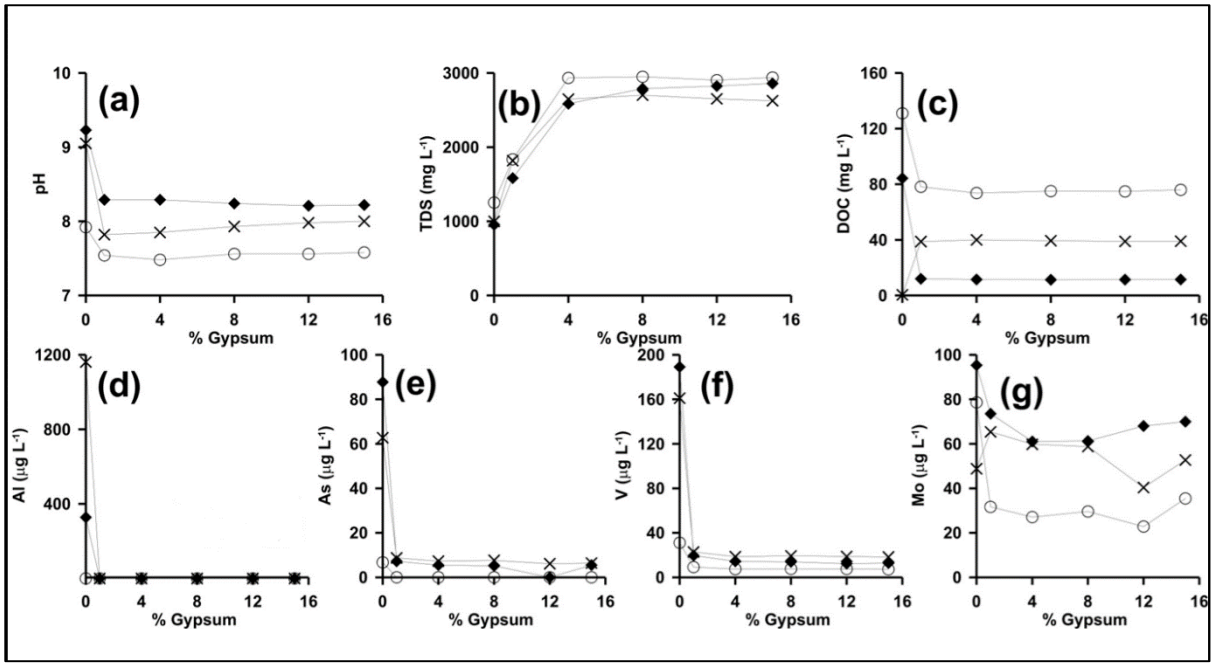

Figure 5.4 - The effect of increasing gypsum addition to soil / red mud mixtures (9% red mud w/w) on experimental pH, total dissolved solids (TDS), dissolved organic carbon (DOC) and trace element concentrations. Key: Crosses = Soil SS, Circles = Soil OR and Diamonds = Soil WL.

5.3.4 Column Experiments

The pumped column experiments compared the changes with column volume in effluent pH and TDS, DOC and Al concentrations (Figure 5.5), in tests containing soil /red mud mixtures (8%), both with and without the presence of gypsum (at 8%). Addition of gypsum induces a reduction in effluent pH of about 1 pH unit compared to the unamended column. Both DOC and Al concentrations are lower in effluent from the gypsum amended column. Over the course of the experiment the difference in DOC and Al concentrations in amended and unamended columns decreases, however, the overall export of aqueous DOC and Al in particular is attenuated. TDS spiked at over 40 g L^{-1} in the first sample collected from the gypsum amended column, but reduced quickly to around 2-3 g L^{-1}, which was maintained until the end of the test. Total TDS export in the unamended column was much lower.

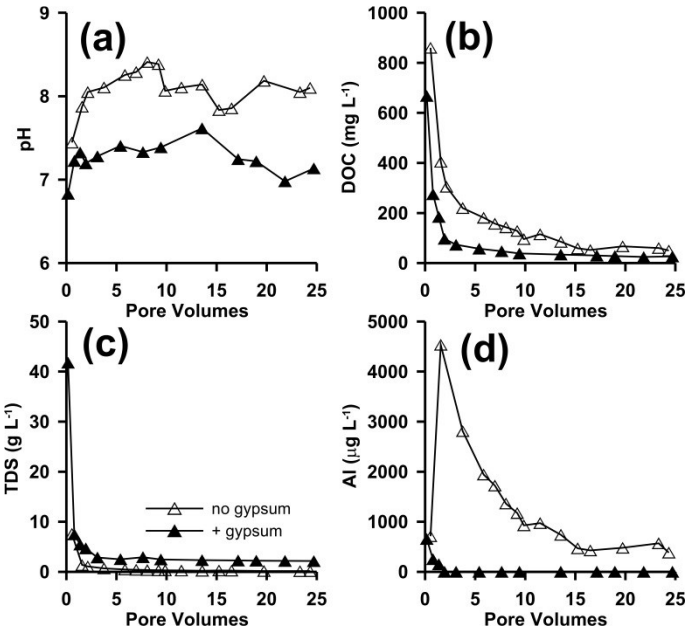

Figure 5.5 - Evolution of effluent pH, total dissolved solids (TDS), dissolved organic carbon (DOC) and aluminium concentrations in column experiments, containing soil / red mud mixtures (8% red mud w/w) both with and without gypsum addition (also 8% w/w). Key Empty triangles = no gypsum, Full triangles = with gypsum

5.4 Discussion

5.4.1 Effect of red mud contamination on Hungarian soils

Addition of red mud to soils induced the following effects, increasing proportionally to the amount of red mud added: 1) increase in pH, 2) increase in aqueous DOC concentrations, 3.) increase in aqueous metal/loids concentrations, and 4) increase in salinity (TDS). The red mud suspension released on the 4th October 2010 was highly alkaline (pH 13), contained elevated concentrations of potentially soluble trace elements such as Al As Mo and V, and was highly saline ; therefore, the results observed in these experiments are to some extent expected. Soil specific behaviour, however, was observed. One of the soils tested (Soil OR) more effectively buffered the

alkalinity added with the red mud, possibly due to the higher organic carbon content of this soil. This resulted in more modest increases in pH and trace element concentrations in experiments using Soil OR compared to those using Soil SS and WL. Interestingly, the higher pH buffering capacity observed for soil OR was very similar to that of the single Hungarian soil sample used by Ruyters et al. (2011) who also reported relatively small pH increases and no significant increase in trace metal concentrations in experiments using soil / red mud mixtures (up to 17% w/w red mud). In the present study significant increases in pH and trace element concentration were observed at red mud loadings less than 10% w/w using two of the three soils studied.

The pattern of increasing DOC concentrations with increasing red mud addition has not been reported previously, but can be explained by the reaction between the alkalinity present in the red mud and organic matter present in the soils. Red mud contains elevated concentrations of NaOH and Na_2CO_3, both of which have been used in alkaline extractions designed to solubilise natural organic matter (Séby et al., 1997; Macleod and Semple, 2000). Furthermore, in other studies increases in DOC under analogous hyperalkaline conditions associated with a steel slag / wood shavings mix have been ascribed to alkaline hydrolysis that releases low molecular weight carboxylic acids (Karlsson et al., 2011). Therefore, red mud addition to soils produces an unintended alkaline extraction liberating organic matter to solution. Along with clay mineral dissolution (Deng et al., 2006; Fernandez et al., 2009) and sorption reactions (Konan et al., 2012), the reaction of alkalinity with natural organic matter will therefore be one of the main short term mechanisms for pH buffering in red mud / soil mixtures. Also, at higher red mud loadings, where alkalinity may be present in excess, the supply of extractable organic matter may limit DOC concentrations. The increased DOC loss from red mud affected soils in itself has potential for wider environmental impacts in

terms of degradation of soil fertility and quality, loss of carbon storage and impacts on downstream water quality.

5.4.2 Effectiveness of Gypsum for the Treatment of Red Mud contaminated soils

Gypsum addition is highly effective in controlling soil pH even under high red mud loading (maximum pH observed in experiments was 8.5). Gypsum addition to red mud affected soils buffers pH by providing a source of available Ca^{2+} that can react with soluble alkalinity (both carbonate and hydroxide) to produce calcite and a pH reduction (see equation 5.2). The formation of calcite also provides solid alkalinity that helps buffer the system to any further changes in pH. The consumption of alkalinity prevents the alkaline extraction of natural organic matter and thus produces lower DOC concentrations in gypsum amended experiments. The Ca^{2+} produced by gypsum dissolution can displace Na^{+} from exchange complexes in the red mud (Grafe et al., 2011). It is also possible that the reduction in pH might enhance the dissolution of high pH phases that are present in the red mud (Hind et al., 1999; Hillier et al., 2007). These effects combined with the sulfate that is released during gypsum dissolution will all contribute to the increased amount of salinity generation observed in gypsum amended batch experiments (i.e. there is a greater relative increase in TDS observed as red mud loading is increased in experiments with gypsum present compared to experiments without gypsum). This is consistent with an observation made during the initial response to the Ajka incident that gypsum dosing of directly affected rivers resulted in an increase in sulfate concentration long distances downstream of the spill (Mayes et al., 2011). Batch experiments designed to test the effect of varying the concentration of

gypsum used found no difference in TDS between 4 and 15% additions. This implies that once gypsum is added in excess an equilibrium (controlled by the solubility of gypsum) is established that limits TDS release. Interestingly the same equilibrium TDS concentration was observed in batch and column tests where gypsum was added (Figures, 5.4b and 5.5c), implying that gypsum containing soils will continue to export salinity until the gypsum is depleted. Overall the column tests also demonstrate that the positive effects of 8% gypsum addition (i.e. reduction in pH, Al and DOC concentrations) are maintained over many porewater exchanges.

In order to understand the effect of gypsum addition on trace element concentrations, aqueous Al, As, Mo and V concentrations from all the batch experiments have been plotted as a function of the measured pH (Figure 5.6). In experiments without gypsum present, higher red mud loadings lead to both higher additions of trace elements to the soil and higher pH. At the pH of the red mud, As, V, Al and Mo are all predicted to be present as soluble oxyanions (as arsenate, vanadate, aluminate and molybdate (Langmuir, 1997)). Strong adsorption of both arsenate and vanadate to mineral surfaces at circumneutral pH is widely documented (Wehrli and Stumm, 1989; Genc et al., 2003; Sherman and Randall, 2003; Peacock and Sherman, 2004b). Aluminate becomes highly insoluble below about pH 10.5 and precipitates as an amorphous oxyhydroxide phase (Langmuir, 1997; Burke et al., 2012a). The solubility of oxyanion-forming elements is, therefore, highly affected by pH, with sorption / precipitation reactions limiting solution concentrations at low pH (Langmuir, 1997; Ladeira et al., 2001; Genc-Fuhrman et al., 2004; Peacock and Sherman, 2004b). In these experiments significant increases in aqueous Al, As and V concentrations are observed above approximately pH 8.5. Addition of gypsum to the soil / red mud mixtures substantially reduces pH, in many cases to below 8.5. Therefore, the pH

reduction associated with gypsum addition results in both an enhancement in sorption (As and V) or precipitation (Al) that effectively inhibits metal/loid release to solution. This pH control also explains the behaviour observed for Soil OR, where greater pH buffering leads to lower overall experimental pH and lower aqueous Al, As and V concentrations in those tests. Mo, however, only weakly interacts with soil minerals at circumneutral pH (Goldberg et al., 1996; Goldberg and Forster, 1998; Buekers et al., 2010), and therefore, remains highly soluble at the pH values observed in experiments where gypsum was present.

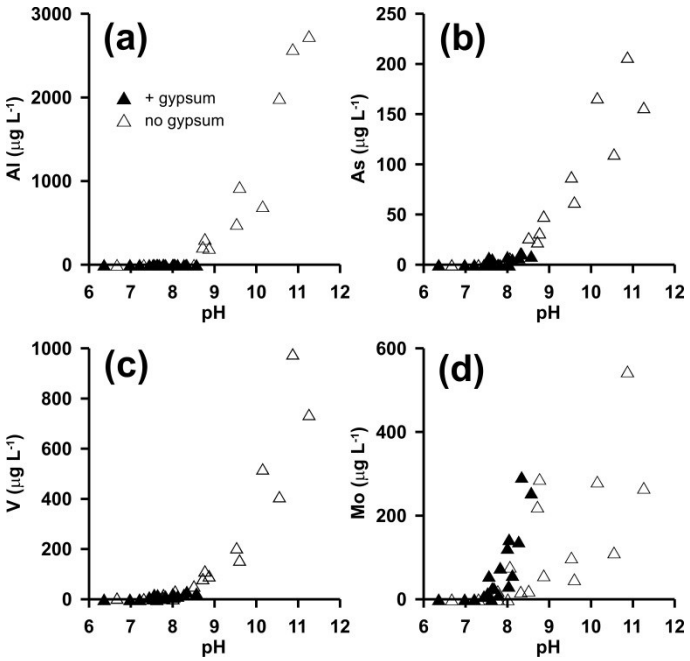

Figure 5.6 - Plots of trace element concentrations vs final pH in batch experiments containing soil / red mud mixtures (N.B. highest pH and trace element concentrations were observed in experiments with highest red mud loadings), both with and without gypsum addition (4% w/w). Key, Empty triangles = no gypsum, Full triangles = with gypsum

5.5 Conclusions and implications for remediation

Addition of red mud to soils causes an increase in pH, TDS, DOC and aqueous concentrations of oxyanion-forming trace elements. The extent of the increases observed is ultimately controlled by the amount of red mud present; however, the intrinsic ability of the soils to buffer pH is also important. Soils with low organic matter and clay content, also have lower buffering capacities, and therefore, are more at risk of suffering larger relative increases in pH, Al, As and V concentrations. In these experiments, there appeared to be threshold pH value between pH 8.5 - 9, above which significant increases in Al, As and V concentrations occurred. Therefore soil pH measurements could be used as a simple screening method to identify red mud affected soils where significant deleterious effects might be expected, with pH values higher than 8.5 equating to greater risk.

Gypsum addition resulted in soil pH values below 8.5 in all experiments and inhibited Al, As, V and DOC release. The immobilisation of As, V and Al is related to their enhanced adsorption at circumneutral pH. Although adsorption is reversible (e.g. at high pH; Langmuir (1997), the associated precipitation of calcite will typically buffer soil pH. However, sorbed oxyanions may be remobilised by anion exchange reactions, particularly with phosphate (and to a lesser extent carbonate), at circumneutral pH (Altundogan et al., 2000; Genc-Fuhrman et al., 2004). Mo concentrations were not affected by gypsum addition as sorption of the molybdate ion to soil minerals is low at circumneutral pH. These results indicate that gypsum addition to soils receiving red mud could be used as an emergency measure to consume the associated excess alkalinity and reduce porewater concentrations of several toxic elements, including Al, As and V. Although some long term potential for partial remobilisation may remain, the

results also highlight the potential benefits that may arise in BDRAs with lower concentrations of potentially problematic trace elements where residue undergoes organic matter and gypsum amendment. The effectiveness of the treatment was found to be relatively insensitive to both the amounts of gypsum or red mud present, making this approach easy to administer. At Ajka, up to 1 million m^3 red mud slurry was released with an estimated solids content of ~8% (w/w) and density of ~1.20 g mL^{-1} (Szépvölgyi, 2011) this equates to approximately 100,000 t red mud. Using the ~2:1 red mud to gypsum ratio (i.e. 9% red mud + 4% gypsum) used in many of our experiments, we calculate that around 50,000 t of gypsum would be required to treat of all the released material (cf. ~23,500 t gypsum was added to rivers following the spill; Rédey (2012)). However, lower gypsum dosing ratios were also affective in our experiments (up to ~8:1 red mud: gypsum) and many thinner red mud deposits may require no treatment if the intrinsic pH buffering capacity of the soil is not exceeded. Also, much of the red mud released was transported out of the system by rivers and not deposited on land (Mayes et al., 2011); therefore, in reality much lower amounts of gypsum may actually be required (~5-10,000 t) to treat red mud / soil mixtures. There is also the potential advantage of preventing dust formation by ploughing in the gypsum during application. However, caution is also required when drawing conclusions at the field scale from laboratory experiments, as for example, the ability to achieve large scale homogenous mixing may be difficult, reducing the effectiveness of treatment.

Although addition of gypsum to soils can improve soil structure (e.g. by increasing hydraulic conductivity Chen and Dick (2011)), increased salinity (TDS) is the major disadvantage associated with gypsum addition. Indeed, for larger gypsum loadings, these salinity increases persisted for over 25 pore water exchanges (as did the beneficial effects). Increased soil salinity can cause damage to plant growth and soil

microbes (Ruyters et al., 2011), therefore, gypsum addition should be carefully limited to that required to produce pH values between 8.5 and 9 in affected soils. Long terms trials of plant germination, and trace metal uptake would be a useful extension to this work to determine the effects of gypsum addition to red mud affected soils on plant growth. Alternate treatments such as soil washing and increasing dilution (of the red mud) may also significantly reduce the risk of trace metal leaching, without the associated risk of increased salinity due to gypsum addition; however, these methods are likely to be expensive and slower to administer.

5.6 References

ADAM, J., BANVOLGYI, G., DURA, G., GRENERCZY, G., GUBEK, N., GUTPER, I., SIMON, G., SZEGFALVI, Z., SZEKACS, A., SZEPVOLGYI, J. & UJLAKY, E. 2011. The Kolontár Report. Causes and lessons from the red mud disaster. In: JAVOR, B. & HARGITAI, M. (eds.). Budapest: Greens / European Free Alliance Parliamentary Group in the European Parliament and LMP - Politics Can Be Different.

ALTUNDOGAN, H. S., ALTUNDOGAN, S., TUMEN, F. & BILDIK, M. 2000. Arsenic removal from aqueous solutions by adsorption on red mud. Waste Management, 20, 761-767.

BUEKERS, J., MERTENS, J. & SMOLDERS, E. 2010. Toxicity of the molybdata anion in soil is partially explained by effects of the accompanying cation or by soil pH. Environmental Toxicology and Chemistry, 29, 1274-1278.

BURKE, I. T., MAYES, W. M., PEACOCK, C. L., BROWN, A. P., JARVIS, A. P. & GRUIZ, K. 2012. Speciation of arsenic, chromium, and vanadium in red mud samples from the ajka spill site, hungary. Environmental Science & Technology, 46, 3085-92.

CHEN, L. & DICK, W. A. 2011. Gypsum as an agricultural ammendment:General use guidelines, Wooster OH, Ohio State University Extension

COURTNEY, R. G. & HARRINGTON, T. 2012. Growth and nutrition of Holcus lanatus in bauxite residue amended with combinations of spent mushroom compost and gypsum. Land Degradation & Development, 23, 144-149.

COURTNEY, R. G., JORDAN, S. N. & HARRINGTON, T. 2009. Physico-chemical changes in bauxite residue following application of spent mushroom compost and gypsum. Land Degradation & Development, 20, 572-581.

COURTNEY, R. G. & KIRWAN, L. 2012. Gypsum amendment of alkaline bauxite residue - Plant available aluminium and implications for grassland restoration. Ecological Engineering, 42, 279-282.

COURTNEY, R. G. & TIMPSON, J. P. 2004. Nutrient status of vegetation grown in alkaline bauxite processing residue amended with gypsum and thermally dried sewage sludge - A two-year field study. Plant and Soil, 266, 187-194.

COURTNEY, R. G. & TIMPSON, J. P. 2005. Reclamation of fine fraction bauxite processing residue (red mud) amended with coarse fraction residue and gypsum. Water Air and Soil Pollution, 164, 91-102.

DENG, Y. J., HARSH, J. B., FLURY, M., YOUNG, J. S. & BOYLE, J. S. 2006. Mineral formation during simulated leaks of Hanford waste tanks. Applied Geochemistry, 21, 1392-1409.

FERNANDEZ, R., MADER, U. K., RODRIGUEZ, M., DE LA VILLA, R. V. & CUEVAS, J. 2009. Alteration of compacted bentonite by diffusion of highly alkaline solutions. European Journal of Mineralogy, 21, 725-735.

GELENCSER, A., KOVATS, N., TUROCZI, B., ROSTASI, A., HOFFER, A., IMRE, K., NYIRO-KOSA, I., CSAKBERENYI-MALASICS, D., TOTH, A., CZITROVSZKY, A., NAGY, A., NAGY, S., ACS, A., KOVACS, A., FERINCZ, A., HARTYANI, Z. & POSFAI, M. 2011. The Red Mud Accident in Ajka (Hungary): Characterization and Potential Health Effects of Fugitive Dust. Environmental Science & Technology, 45, 1608-1615.

GENC-FUHRMAN, H., TJELL, J. C. & MCCONCHIE, D. 2004. Adsorption of arsenic from water using activated neutralized red mud. Environmental Science & Technology, 38, 2428-2434.

GENC, H., TJELL, J. C., MCCONCHIE, D. & SCHUILING, O. 2003. Adsorption of arsenate from water using neutralized red mud. Journal of Colloid and Interface Science, 264, 327-334.

GOLDBERG, S. & FORSTER, H. S. 1998. Factors affecting molybdenum adsorption by soils and minerals. Soil Science, 163, 109-114.

GOLDBERG, S., FORSTER, H. S. & GODFREY, C. L. 1996. Molybdenum adsorption on oxides, clay minerals, and soils. Soil Science Society of America Journal, 60, 425-432.

GRAFE, M. & KLAUBER, C. 2011. Bauxite residue issues: IV. Old obstacles and new pathways for in situ residue bioremediation. Hydrometallurgy, 108, 46-59.

GRAFE, M., POWER, G. & KLAUBER, C. 2011. Bauxite residue issues: III. Alkalinity and associated chemistry. Hydrometallurgy, 108, 60-79.

GRUIZ, K., FEIGL, V., KLEBERCZ, O., ANTON, A. & VASZITA, E. Environmental Risk Assessment of Red Mud Contaminated Land in Hungary. In: HRYCIW, R. D., ATHANASOPOULOS-ZEKKOS, A. & YESILLER, N., eds. GeoCongress 2012: State of the Art and Practice in Geotechnical Engineering, 2012. American Society of Civil Engineers, 4156-4165.

HILLIER, S., LUMSDON, D. G., BRYDSON, R. & PATERSON, E. 2007. Hydrogarnet: A host phase for Cr(VI) in chromite ore processing residue (COPR) and other high pH wastes. Environmental Science & Technology, 41, 1921-1927.

HIND, A. R., BHARGAVA, S. K. & GROCOTT, S. C. 1999. The surface chemistry of Bayer process solids: a review. Colloids and Surfaces a-Physicochemical and Engineering Aspects, 146, 359-374.

KARLSSON, S., SÖBERG, V. & GRANDIN, A. 2011. Hetertrophic leaching of LD-slag - formation of organic ligands. In: RÜDE, T. R., FREUND, A. & C., W. (eds.) 1th IMWA congress, Mine Water - Managing the Challenges. Aachen, Germany.

KLEBERCZ, O., MAYES, W. M., ANTON, A. D., FEIGL, V., JARVIS, A. P. & GRUIZ, K. 2012. Ecotoxicity of fluvial sediments downstream of the Ajka red mud spill, Hungary. Journal of environmental monitoring : JEM, 14, 2063-71.

KONAN, K. L., PEYRATOUT, C., SMITH, A., BONNET, J. P., MAGNOUX, P. & AYRAULT, P. 2012. Surface modifications of illite in concentrated lime solutions investigated by pyridine adsorption. Journal of Colloid and Interface Science, 382, 17-21.

LADEIRA, A. C. Q., CIMINELLI, V. S. T., DUARTE, H. A., ALVES, M. C. M. & RAMOS, A. Y. 2001. Mechanism of anion retention from EXAFS and density functional calculations: Arsenic (V) adsorbed on gibbsite. Geochimica Et Cosmochimica Acta, 65, 1211-1217.

LANGMUIR, D. 1997. Aqueous environmental geochemistry, Upper Saddle River, N. J., Prentice Hall.

LAW, G. T. W., GEISSLER, A., BOOTHMAN, C., BURKE, I. T., LIVENS, F. R., LLOYD, J. R. & MORRIS, K. 2010. Role of Nitrate in Conditioning Aquifer Sediments for Technetium Bioreduction. Environmental Science & Technology, 44, 150-155.

MACLEOD, C. J. A. & SEMPLE, K. T. 2000. Influence of contact time on extractability and degradation of pyrene in soils. Environmental Science & Technology, 34, 4952-4957.

MAYES, W. M., JARVIS, A. P., BURKE, I. T., WALTON, M., FEIGL, V., KLEBERCZ, O. & GRUIZ, K. 2011. Dispersal and Attenuation of Trace Contaminants Downstream of the Ajka Bauxite Residue (Red Mud) Depository Failure, Hungary. Environmental Science & Technology, 45, 5147-5155.

PEACOCK, C. L. & SHERMAN, D. M. 2004. Vanadium(V) adsorption onto goethite (alpha-FeOOH) at pH 1.5 to 12: A surface complexation model based on ab initio molecular geometries and EXAFS spectroscopy. Geochimica Et Cosmochimica Acta, 68, 1723-1733.

RÉDEY, A. 2012. The red mud disaster of Ajka in Hungary and its consequences. 4th EUCHeMS Chemistry Congress. Prague, Czech Republic.

REEVES, H. J., WEALTHALL, G. & YOUNGER, P. L. 2011. Advisory visit to the bauxite processings tailings dam near Ajka, Vesprem County, western Hungary. . Keyworth, UK: British Geological Survey.

RENFORTH, P., MAYES, W. M., JARVIS, A. P., BURKE, I. T., MANNING, D. A. C. & GRUIZ, K. 2012. Contaminant mobility and carbon sequestration downstream of the Ajka (Hungary) red mud spill: The effects of gypsum dosing. The Science of the total environment, 421-422, 253-9.

RUYTERS, S., MERTENS, J., VASSILIEVA, E., DEHANDSCHUTTER, B., POFFIJN, A. & SMOLDERS, E. 2011. The Red Mud Accident in Ajka (Hungary): Plant Toxicity and Trace Metal Bioavailability in Red Mud Contaminated Soil. Environmental Science & Technology, 45, 1616-1622.

SÉBY, F., POTIN GAUTIER, M., LESPÉS, G. & ASTRUC, M. 1997. Selenium speciation in soils after alkaline extraction. Science of The Total Environment, 207, 81-90.

SHERMAN, D. M. & RANDALL, S. R. 2003. Surface complexation of arsenie(V) to iron(III) (hydr)oxides: Structural mechanism from ab initio molecular geometries and EXAFS spectroscopy. Geochimica Et Cosmochimica Acta, 67, 4223-4230.

SZÉPVÖLGYI, J. 2011. A Chemical Engineer's View of the Red Mud Disaster. Nachrichten aus der Chemie, 59, 5-7.

THORPE, C. L., LLOYD, J. R., LAW, G. T. W., BURKE, I. T., SHAW, S., BRYAN, N. D. & MORRIS, K. 2012. Strontium sorption and precipitation behaviour during bioreduction in nitrate impacted sediments. Chemical Geology, 306, 114-122.

WALLACE, S. H., SHAW, S., MORRIS, K., SMALL, J. S., FULLER, A. J. & BURKE, I. T. 2012. Effect of groundwater pH and ionic strength on strontium sorption in aquifer sediments: Implications for Sr-90 mobility at contaminated nuclear sites. Applied Geochemistry, 27, 1482-1491.

WEHRLI, B. & STUMM, W. 1989. VANADYL IN NATURAL-WATERS - ADSORPTION AND HYDROLYSIS PROMOTE OXYGENATION. Geochimica Et Cosmochimica Acta, 53, 69-77.

WILKIE, M. P. & WOOD, C. M. 1996. The adaptations of fish to extremely alkaline environments. Comparative Biochemistry and Physiology B-Biochemistry & Molecular Biology, 113, 665-673.

Chapter 6 Mobilisation of arsenic from bauxite residue (red mud) affected soils: Effect of pH and redox conditions.

Abstract

Fine fraction bauxite residue (red mud) has a characteristically alkaline pH and contains several potentially toxic elements, including arsenic. The tailings dam breach at the Ajka alumina plant, western Hungary in 2010 introduced ~1 million m^3 of red mud suspension into the surrounding area. Aerobic and anaerobic batch experiments were prepared using Hungarian soils in order to investigate the effects of red mud addition on soil biogeochemistry and arsenic mobility in soil-water experiments representative of land affected by the red mud spill. XAS analysis showed that As was present in the red mud as As(V) in the form of arsenate. The solubility of red mud associated arsenate was highly pH dependant and the addition of phosphate (and to a lesser extent carbonate) to red mud suspensions greatly enhanced As solubility. In aerobic batch experiments, where red mud was mixed with soils, As release to solution was highly dependent on experimental pH. With increasing incubation time carbonation of the experiments occurred (as atmospheric CO_2 dissolved in the alkaline solutions) and lower pH resulted in lower aqueous As concentrations. However, this did not result in complete removal of aqueous As in any of the experiments. In anaerobic experiments carbonation reactions were prevented and pH remained high. Under these conditions, microbial populations from three different soils were able to support both Fe(III) and SO_4^{2-} reduction in soil water systems with moderate pH increases (up to ~pH 10.5) following red mud addition. Aqueous As concentrations increased in all the anaerobic red mud amended experiments, however, both XANES and HPLC-ICP-MS

showed that no As reduction processes occurred and that only As(V) species were present. These experiments show that when red mud is mixed with a range of Hungarian soils the resultant increases in soil pH promote the release of As(V) to solution under a range of alkaline pH and under both aerobic and anaerobic conditions. Therefore, there is the potential for increased As mobility / bioavailability in soil-water systems affected by red mud addition and recovery of red mud deposits from land is recommended.

6.1 Introduction

Bauxite residue (red mud) is the fine fraction waste remaining after Al extraction from bauxite using the Bayer Process. The composition of red mud varies depending upon the quality of the ore and processing methods (Hind et al., 1999; Liu et al., 2007; Somlai et al., 2008). Typically, it comprises residual iron oxides, quartz, sodium aluminosilicates, titanium dioxide, calcium carbonate/aluminate and sodium hydroxide (Hind et al., 1999; Brunori et al., 2005; Grafe et al., 2011; Gelencser et al., 2011). Red mud can also contain problematic concentrations of potentially toxic metals and metalloids, including As, Cr, Ni, Pb, Mo and V (Brunori et al., 2005; Grafe et al., 2011; Klebercz et al., 2012). Water in contact with red mud is saline and highly alkaline (between 1.4 - 28.4 mS m^{-1}, up to pH 13 (Mayes et al., 2011; Grafe et al., 2011) due to the presence of NaOH. Under these conditions there is potential for enhanced mobility of oxyanion forming trace elements (e.g. Al, As, Cr, Mo and V) (Langmuir, 1997; Smedley and Kinniburgh, 2002; Cornelis et al., 2008) due to their higher solubility and reduced adsorption to surfaces at high pH. These issues aside, the abundance of red mud as a waste product (up to 120 million tonnes are produced annually (Power et al., 2011)) has led to much research into possible uses. These include: recovery of Al, Fe, trace and rare earth metals (Hind et al., 1999; Hammond, 2013); a low cost sorbent for water decontamination (Altundogan et al., 2002; Bhatnagar et al., 2011; Liu et al., 2011); in CO_2 sequestration (Yadav et al., 2010); and as an additive to ceramics and building materials (Somlai et al., 2008; Liu and Zhang, 2011) or as a soil amendment (Lombi et al., 2002; Friesl et al., 2004; Gray et al., 2006; Feigl et al., 2012).

On 4th October 2010 the tailings dam of Cell X at the Ajkai Timfoldgyar Zrt alumina plant was breached, releasing ~1 million m^3 of red mud suspension (Adam et

al., 2011a; Reeves et al., 2011). The surge of red mud down the Torna and upper Marcal valleys inundated homes and land, killing 10 people and injuring over 150 (Adam et al., 2011a; Enserink, 2010). An estimated 40 km^2 of low-lying agricultural land and riparian wetlands were affected (Mayes et al., 2011; Reeves et al., 2011) and red mud was transported 120 km downstream by rivers, eventually reaching the Danube (Enserink, 2010; Adam et al., 2011a; Reeves et al., 2011). The immediate emergency environmental response sought to neutralise the affected rivers and streams by the addition of acid and/or gypsum (Adam et al., 2011a; Renforth et al., 2012). Further remediation efforts removed red mud from the affected land (Adam et al., 2011a) but at some locations thin red mud deposits (<5cm) were ploughed in to soils to prevent dust formation and further dispersal (Gelencser et al., 2011; Adam et al., 2011a; Anton et al., 2012). It was not possible to recover red mud deposited in low lying riparian wetlands.

This addition of red mud to soils introduced several potential contaminant trace elements (Ruyters et al., 2011; Mayes et al., 2011), including the highly toxic and redox sensitive metalloid arsenic. Ajka red mud contains ~200 mg kg^{-1} As, primarily as inorganic arsenate phases (Burke et al., 2012a). Adsorption of As to red mud is known to be enhanced at circumneutral pH (as opposed to very high (>11.5) and very low (<4.5) pH) (Altundogan et al., 2000; Genc-Fuhrman et al., 2004) and previous tests have found As leaching from Ajka red mud/soil mixtures (up to 16% red mud w/w) does not occur readily under aerobic conditions (Ruyters et al., 2011). These and similar findings have led researchers to conclude that fears of toxic metal/loid leaching from red mud to soils have been overstated and that the main short-term issues from red mud addition to soils relate to increased pH and salinity (Ruyters et al., 2011; Gelencser et al., 2011; Klebercz et al., 2012; Anton et al., 2012; Gruiz, 2012).

Redox conditions in natural soils and sediments are prone to seasonal variations, particularly with fluctuations in groundwater levels. This can have a profound influence on the transport of As in the environment. Soils containing only modest As concentrations (< 7 mg kg^{-1}) can produce unacceptably high concentrations of aqueous As in soil porewaters under reducing conditions (Charlet and Polya, 2006; Hery et al., 2010). One of the key mechanisms responsible for high As concentrations is the reduction of arsenate to more soluble arsenite species during microbially mediated processes and the mobilisation of further As during the reductive dissolution of arsenate-bearing Fe(III) oxides (Islam et al., 2004; Lloyd and Oremland, 2006). Thus, if red mud deposits that have been mixed with soils in floodplain settings become exposed to anaerobic conditions, there is an increased possibility of microbial processes leading to As release, and very high porewater As concentrations might be expected (Smedley and Kinniburgh, 2002; O'Day et al., 2004).

The specific objectives of this study were: 1) To use aerobic and anaerobic batch experiments to investigate the potential for arsenic mobilisation from Ajka red muds and representative soil-red mud mixtures. 2) To use a combination of X-ray absorption spectroscopy and high performance liquid chromatography-ion coupled plasma-mass spectroscopy to determine changes in solid or aqueous phase As speciation induced by long term anaerobic incubation. 3) To determine the effects of red mud addition on biogeochemical processes in soil-water systems and relate soil geochemistry to mechanisms controlling As mobilisation in red mud amended soils.

6.2 Materials and Methods

6.2.1 Field Sampling and Sample Handling

Samples were collected in May 2011. A red mud sample (RM) was collected from within Cell X of the Ajka impoundment (Location 47°0'18.48"N, 17°29'46.77"E). Soil was sampled from three locations in the Torna and upper Marcal floodplains that did not receive red mud during the 2010 dam breach (see Figure 3.2, for sampling locations). The sampling locations were chosen to capture local variations in composition, total organic carbon (TOC) and initial redox conditions. Two of the soils were agricultural top soils and the third sample was collected from below the rootlet layer 50 cm below the surface of a wetland. Samples were stored at 4°C in polythene containers, (sub-samples were stored for XAS analysis at -80 ^{0}C). The wetland soil was stored anaerobically using Anaerogen™ sachets.

6.2.2 Sample Characterization

Red mud and soil samples were characterised by X-ray powder diffraction using a Bruker D8 Advance XRD, X-ray fluorescence using a PANalytical Axios Advanced XRF spectrometer; TOC using a Carlo Erba NA 2500 Elemental Analyser; pH was determined after 1 g : 1 ml suspension in deionised water (ASTM, 2006); and 0.5 N HCl extractable Fe(II) was determined by ferrozine assay (Lovley and Phillips, 1986a). Inorganic phosphate was determined using molybdate blue method (Aspila et al., 1976).

6.2.3 Red mud batch leaching tests

2 g red mud were suspended in 10 mL of 0.1 M salt solutions (NaCl Na_2SO_4, Na_2CO_3 or $NaHPO_4$) as a background electrolyte or deionised water for the 'no amendment' system. The pH values were adjusted to between 5.5 and 12.5 by addition of HCl or NaOH. After 7 days agitation on an orbital shaker (100 rpm), pH was determined and the aqueous phase was removed by filtration (0.45 μm) and As concentrations were determined using a Perkin-Elmer Optima 5300 DV ICP-OES.

6.2.4 Aerobic batch experiments

Triplicate aerobic microcosms for each soil type were prepared under three different conditions (all weights given as dry weight equivalents): (1) *Unamended* - 6.0 g of homogenised soil with 30 ml of deionised water in 50 mL polypropylene centrifuge tubes; (2) *9% RM addition* (representing a thin red mud deposit (~5 cm) mixed with 40-50 cm soil by ploughing) – the same as the unamended system with addition of 0.6 g RM; (3) *33% RM addition* (representing a thick red mud deposit (~15 cm) mixed with ~30 cm soil by ploughing or as a worst case scenario for wetland areas) - the same as the unamended system with addition of 3.0 g RM. Microcosms were incubated in the dark at 21 °C. The headspace was regularly exchanged with air (1 hour each weekday) over a period of 100 days. During sampling microcosms were shaken and 3 mL aliquots of soil/RM slurry was extracted. Samples were centrifuged (3 min, 6000 *g*) and the soil analysed for 0.5 N HCl extractable Fe(II). Water was analysed for pH, oxidation/reduction potential (ORP) and aliquots were filtered (0.2 μM) and acidified for ICP-MS analysis.

6.2.5 Anaerobic batch experiments

Triplicate anaerobic microcosms for each soil type were prepared under three different conditions, equivalent to the aerobic experiments (all weights given as dry weight equivalents): (1) *Unamended* - 20.0 g of homogenised soil with 100 ml of deionised water in 120 mL glass serum bottles; (2) *9% RM addition* – the same as the unamended system with addition of 2.0 g RM; (3) *33% RM addition* - the same as the unamended system with addition of 10.0 g RM. All bottles were purged with nitrogen before capping and crimp sealing and sampled periodically ~180 days. Triplicate anaerobic heat treated controls were also established as anaerobic experiments as, above but using autoclaved soils and red mud (120 °C, 1 hour) and were sampled over 120 days. All microcosms were incubated in the dark at 21 °C. During sampling microcosms were shaken and 4.5 mL aliquots of soil/RM slurry was extracted using aseptic technique. Samples were centrifuged (3 min, 6000 *g*) and the soil analysed for 0.5 N HCl extractable Fe(II). Water was analysed for pH, ORP and aliquots were filtered (0.2 μM) and acidified for ICP-MS analysis or frozen (-20 °C) for anion analysis. At the end point of each experiment 15 mL of slurry was extracted and centrifuged, the solution and the solids were frozen (-80 °C) until required for HPLC-ICP-MS analysis and XAS.

These experiments were designed primarily to investigate biogeochemical effects of red mud addition to the soils, therefore, the same inoculation of uncontaminated soil was used in all microcosms, however, the solid : liquid ratio varied by red mud loading. All experiments were initially sampled over a 100-120 day period, however the anaerobic experiments were sampled again at 180 days as some biogeochemical reactions were still ongoing at 120 days in some tests.

(Note – henceforth the experiments and controls will be referred to as 'aerobic experiments' 'anaerobic experiments', 'heat treated controls'.)

6.2.6 Geochemical Methods

pH and ORP (as an indicator for Eh) were measured using a Thermo Scientific Orion Dualstar pH benchtop meter (calibrated daily at pH values of 4, 7 and 10 and a new factory calibrated ORP electrode was used). Acid extractable Fe(II) was determined by ferrozine assay (Lovley and Phillips, 1986a). Arsenic concentrations were determined using a Perkin Elmer Elan DRCII ICP-MS. Anion concentrations were determined by ion chromatography using a Dionex DX500 and AS9 column. Arsenic speciation in 0.2 μm filtered end point solutions was analysed by HPLC-ICP-MS. As(V) (as arsenate) and As(III) (as arsenite) were separated using a Hamilton PRP-X100 250 x 4.6 mm column at 30°C, using an Agilent 1260 Infinity HPLC system interfaced with an Agilent 7500 ICP-MS.

6.2.7 X-ray Absorption Spectroscopy (XAS)

As K-edge (11867 eV) XANES and EXAFS spectra were collected on station I18 at the Diamond Light Source, UK, in May, 2012. Approximately 100 mg of sample was prepared under anaerobic conditions for analysis as moist pastes in Perspex holders with Kapton™ windows. Standard spectra were collected from aqueous As(III) and As(V) solutions (1000 mg L^{-1}). For each sample and standard multiple XANES spectra were averaged and normalised using Athena v0.8.061. Arsenic K-edge EXAFS spectra were background subtracted using PySpline v1.1. EXAFS spectra were then fit in DLexcurv v1.0 (Tomic, 2005) to model clusters.

6.3 Results

6.3.1 Sample Characterization

Sample characterization of the red mud and soils has been summarised (see Tables 5.1 and 5.2) (See Appendix A Figure A3 and A4 for XRD patterns). Briefly; XRD analysis showed that the red mud was dominated by hematite (Fe_2O_3), calcite ($CaCO_3$), magnetite (Fe_3O_4), cancrinite ($Na_6CaAl_6Si_6(CO_3)O_{24}{\cdot}2H_2O$) and hydrogarnet ($Ca_3AlFe(SiO_4)(OH_8)$ with residual boehmite (γ-AlOOH) and gibbsite ($Al(OH_3)$) phases. This assemblage is very similar to that of other red mud samples taken from the breach area (Gelencser et al., 2011; Burke et al., 2012a). The pH value of the three soils was between pH 7 and 8. The dominant mineral in all three soil samples was quartz: feldspars and clays were also present. The first topsoil was a sandy clay loam and had 4.15% organic carbon content (hereafter referred to as *Soil OR*). The wetland sample was a very dark grey sandy clay loam with 1.14% organic carbon (hereafter referred to as *Soil WL*). The third soil was sandy loam topsoil with 0.74% organic carbon (hereafter referred to as *Soil SS*). Principle component analysis of red mud and the 3 soils shows that the soils have similar composition to other unaffected soils from the region and that the red mud sampled here is of a similar composition to other red mud samples from the Ajka source (Mayes et al., 2011) (see Figure 5.1).

6.3.2 Arsenic in red mud

XANES spectra collected from red mud shows that As is present as As(V) (Figure 6.1). Arsenic K-edge EXAFS spectra from the same red mud sample (Figures 6.2) could be fitted with a co-ordination environment of 4 oxygen backscatterers at 1.67

– 1.69 Å (Table 6.1) consistent with a tetrahedral arsenate structure. The fit of the data could not be improved by including any additional shells of Al or Fe backscatterers and there is no evidence to suggest there is any contribution from atoms at longer distances.

Red mud batch leaching tests (Figure 6.3) show that As is mobilised from red mud at high pH. The no amendment system (without a background electrolyte) indicates that As is mobilised above pH 9. This effect was greatly enhanced when PO_4 and CO_3^{2-} were used as background electrolytes, where mobilisation started to occur at pH 8 and 8.5 respectively. When PO_4 was used, there was a maximum As desorption at ~pH 10 resulting in ~6.5 mg L^{-1} in solution representing ~15% of total As present in red mud.

Table 6.1 - Red mud As K-edge EXAFS Fits Where *N* is the Occupancy (± 25%), R is Interatomic Distance (± 0.02 Å for the First Shell, ±0.05 Å for Outer Shells), $2\sigma^2$ is the Debye-Waller Factor (± 25%) and R and Reduced χ^2 are the Least Squares Residual and the Reduced Chi^2 Goodness of Fit Parameters, respectively[a]

				goodness of fit	
			$2\sigma^2$	R	Reduced
shell	*N*	R (Å)	(Å^2)	(%)	χ^2
O	1	1.67	0.010	29	4.1
O	1	1.68	0.007		
O	1	1.68	0.006		
O	1	1.69	0.007		

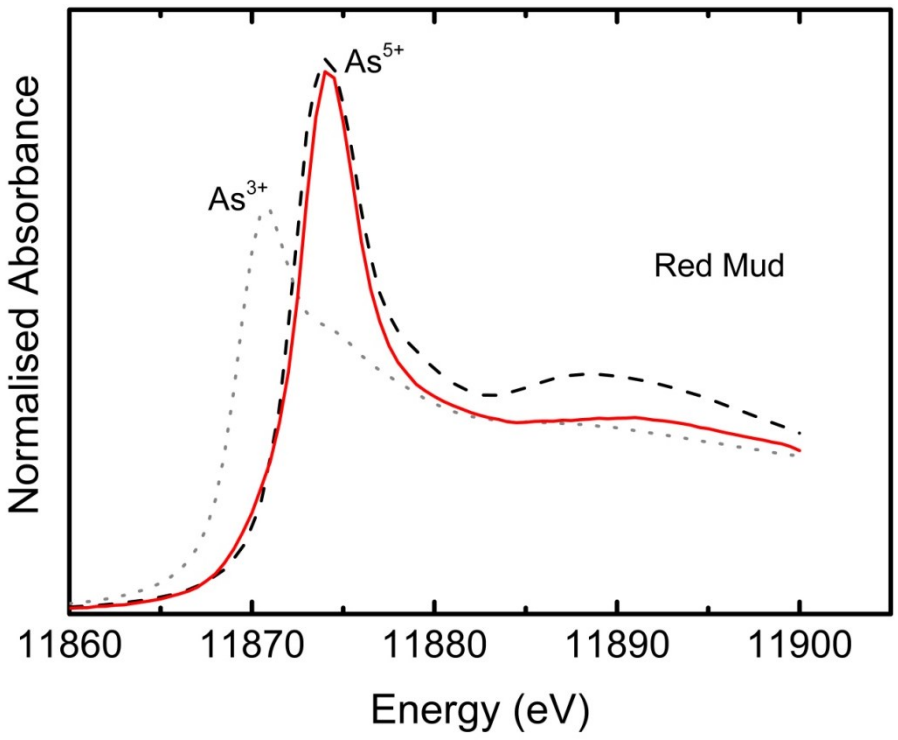

Figure 6.1 - Normalised arsenic K-edge XANES spectra collected from standards and Red Mud (collected from within Cell X of the Ajka impoundment, May 2011). Grey dotted line = arsenite standard (As^{3+}). Black dashed line = arsenate standards (As^{5+}). Red Line = Red mud sample (RM).

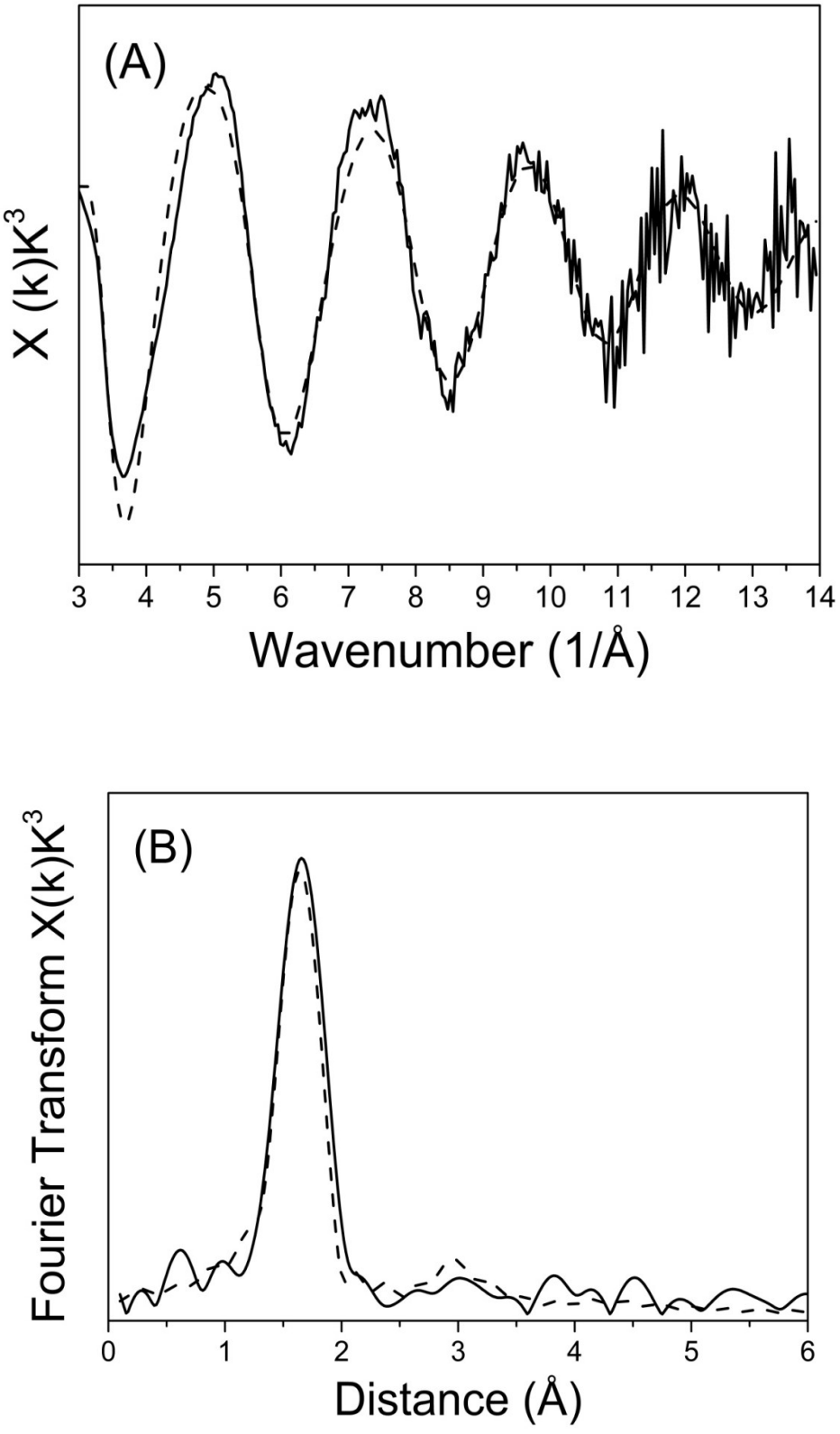

Figure 6.2 - (A) Background subtracted As K-edge EXAFS spectra of Red Mud (collected from within Cell X of the Ajka impoundment, May 2011). (B) Corresponding Fourier transforms calculated from EXAFS spectra. Dashed lines represent DLexcurv V1.0 model fits using the parameters listed in Table 6.1.

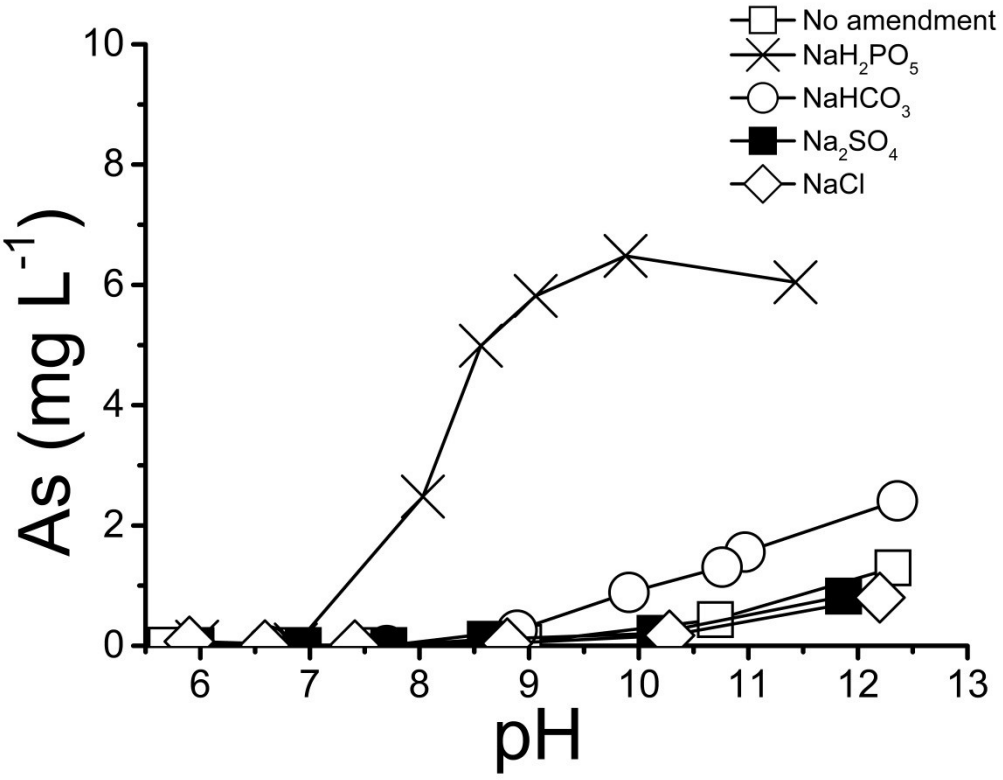

Figure 6.3 - Red mud leaching batch tests showing increased aqueous concentration of aqueous As with a background electrolyte of 0.1 M PO_4 and CO_3^{2-} when compared against a no amendment system with distilled water.

6.3.3 Effect of red mud addition on experimental pH and ORP

The initial pH of all equivalent experiments was very similar. Experiments with a red mud addition showed an increase in pH which was in line with red mud loading. The Soil SS experiments were most affected by red mud addition and initially the pH increased from pH 8 in the unamended systems to pH 10 with 9% RM addition and to pH 11.5 with 33% RM addition.

The pH in the unamended aerobic experiments remained relatively constant over the incubation period (Figure 6.4 a-c). The pH in the aerobic experiments with red mud addition gradually decreased over the incubation period (Figure 6.4 a-c) in all

experiments except for Soil OR experiment with 9% RM addition (Figure 6.4 a). In this experiment, there was an initial increase in pH from pH 7 to 8, which then remained constant. In both the anaerobic experiments and heat treated controls the pH remained relatively constant after an initial equilibration period of 5 days, (Figure 6.5 a-c and Figure 6.6 a-c.).

ORP measurements in the aerobic experiments rose over the first 20 days from +50 to +150 mV to reach values around +250 mV in all experiments indicating that generally oxic conditions were maintained throughout the incubation (Figure 6.4 d-f). In the anaerobic microcosms ORP values show the opposite trend, reducing to negative values (between 0 and -400 mV) indicating progressively more reducing conditions occurred with time (Figure 6.5d-f).

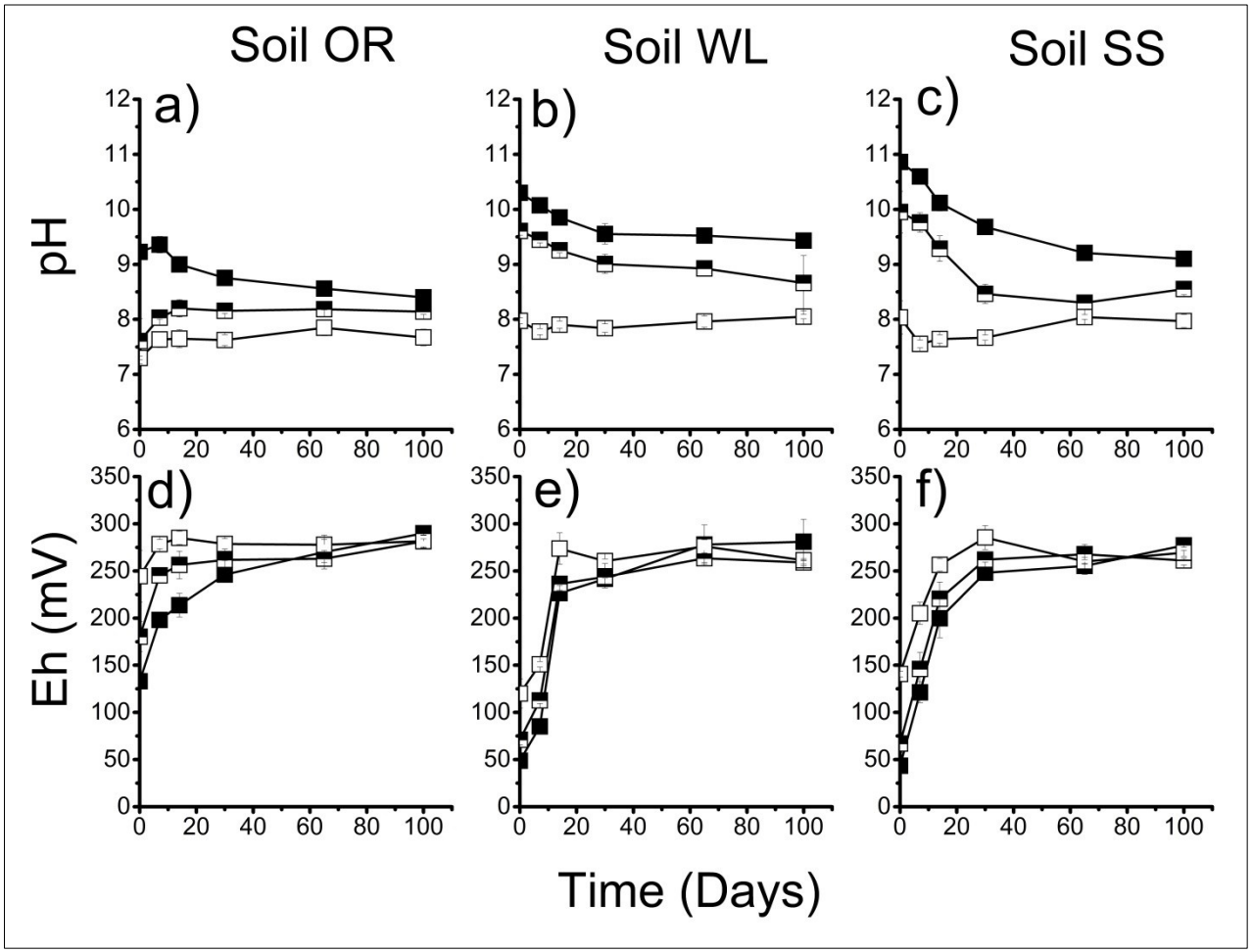

Figure 6.4 - Geochemical analysis time plots from aerobic experiments showing pH and ORP (as an indicator for Eh). Empty squares = unamended, Half squares = 9% RM addition, Full squares = 33% RM addition. Error bars are 1 σ of triplicate results (where not shown, errors are within the symbol size).

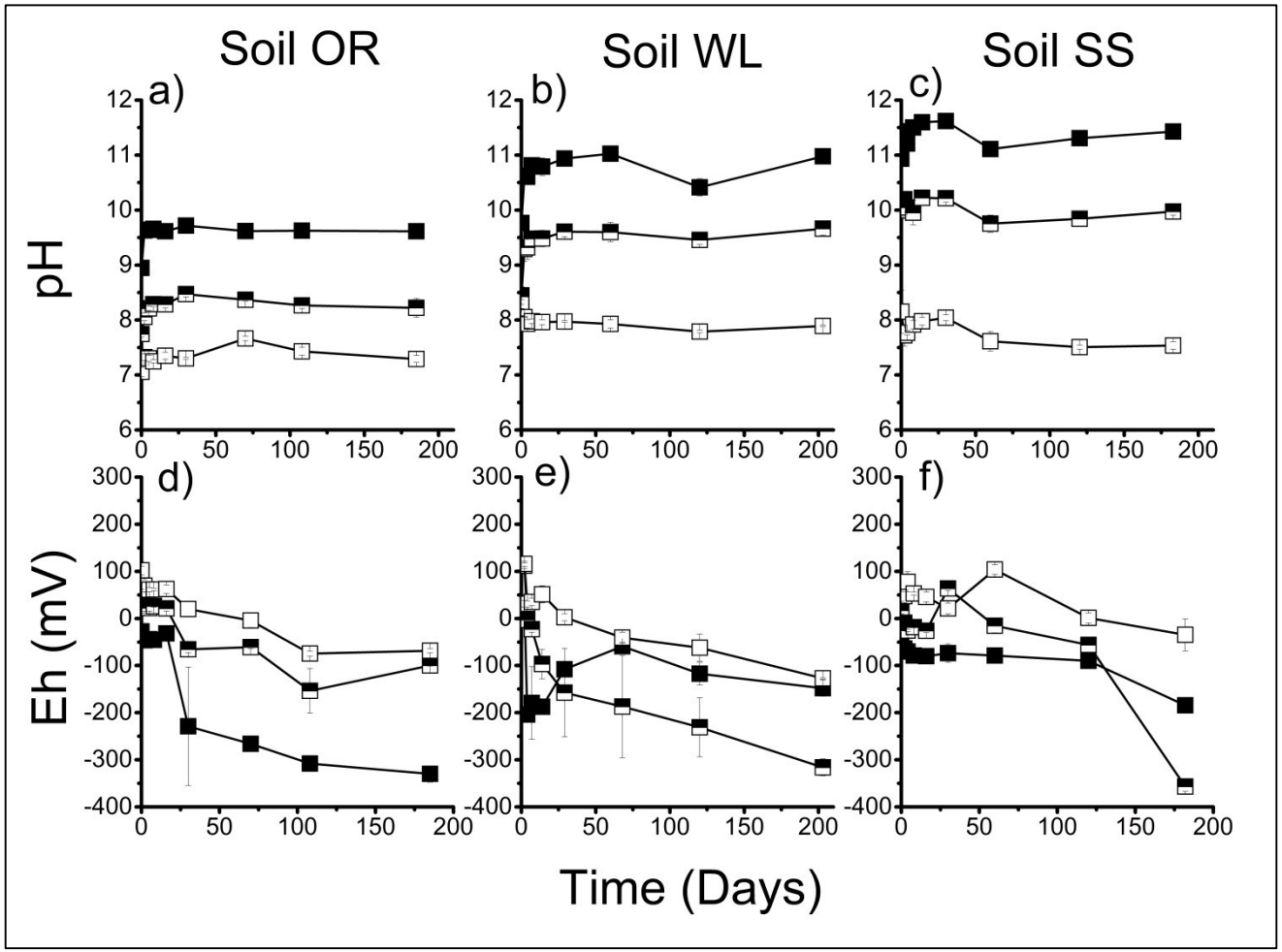

Figure 6.5 - Geochemical analysis time plots from anaerobic experiments showing pH and ORP (as an indicator for Eh). Empty squares = unamended, Half squares = 9% RM addition, Full squares = 33% RM addition. Error bars are 1 σ of triplicate results (where not shown, errors are within the symbol size).

6.3.4 Biogeochemical Redox Indicators

There was no evidence of any increase in acid extractable Fe(II) in the aerobic experiments. Concentrations in all the aerobic experiments were < 1 mg g^{-1} dry weight (Figure 6.7 d-f). Acid extractable Fe(II) was monitored in the aerobic experiments as a check on whether bioreduction processes occurred that might affect As mobilisation (i.e. there is a strong link expected between Fe(III)-reduction and enhanced As solubility (Islam et al., 2004)). Aqueous phase electron acceptors such as nitrate and sulphate were not monitored as a combination of high ORP and negligible Fe(II) accumulation was considered a sufficient negative control.

In the anaerobic experiments, there was some evidence of rapid nitrate removal occurring in Soil OR and Soil SS anaerobic experiments at the beginning of the incubation period (Figure 6.6). The amount of 0.5 N HCl extractable Fe(II) in the solid phase increased significantly with incubation time in most anaerobic experiments from initial values ≤ 1 mg g^{-1} (Figure 6.8 d-f). For each soil type the largest increases in acid extractable Fe(II) were observed in the unamended experiments, although in the Soil OR system, the unamended and 9% RM addition experiments had a similar overall increase in acid extractable Fe(II). The greatest increase in acid extractable Fe(II) was observed in the Soil SS unamended experiments, with progressively less acid extractable Fe(II) found in the 9% RM and 33% RM microcosms at the end of the experiments. The rate of accumulation of acid extractable Fe(II) varied with soil type. The Soil OR and Soil WL systems showed increases after only short incubation times (before 30 days), but the Soil SS experiments responded much more slowly. Heat treated controls showed no significant increases in acid extractable Fe(II) in the wetland or the sandy soil systems (Figure 6.9). Acid extractable Fe(II) does increase in heat

treated Soil OR controls, but the increases are smaller than those observed in the equivalent anaerobic experiments.

In the unamended anaerobic experiments the aqueous SO_4^{2-} concentration was ~25 mg L^{-1} in the Soil OR, and negligible in the Soil WL and Soil SS experiments (Figure 6.8 g-i). The 33% RM addition anaerobic experiments had the highest SO_4^{2-} concentrations for all the soil types. The pattern of SO_4^{2-} removal was different for each soil system. In the Soil OR anaerobic experiments complete removal of SO_4^{2-} occurred after 100 days under all conditions (no removal occurred in corresponding heat treated controls, Figure 6.9 g-i). The Soil WL system exhibited a rapid increase in SO_4^{2-} concentrations between 30 and 60 days in the 9% RM and 33% RM additions which was followed by a gradual removal. Again, no removal occurred in corresponding heat treated controls. In the Soil SS system the SO_4^{2-} concentrations were proportional to the amount of RM addition and remained relatively constant throughout the incubation period for both the anaerobic experiments and heat treated controls.

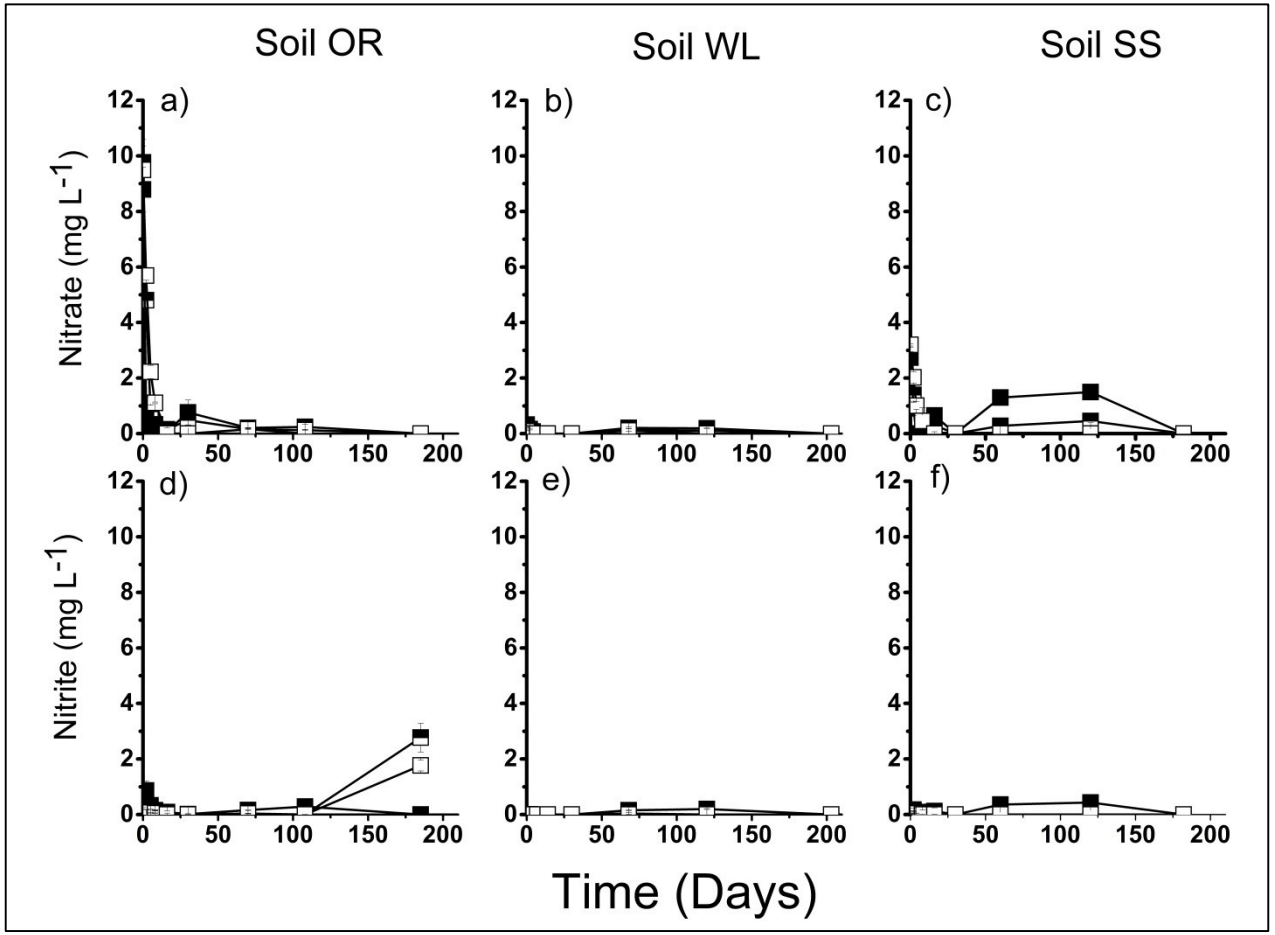

Figure 6.6 - Evolution of Nitrate and Nitrite in anaerobic red mud affected soil-water systems and unamended controls. Empty squares = unamended, Half squares = 9% RM addition, Full squares = 33% RM addition. Error bars are 1 σ of triplicate results (where not shown, errors are within the symbol size).

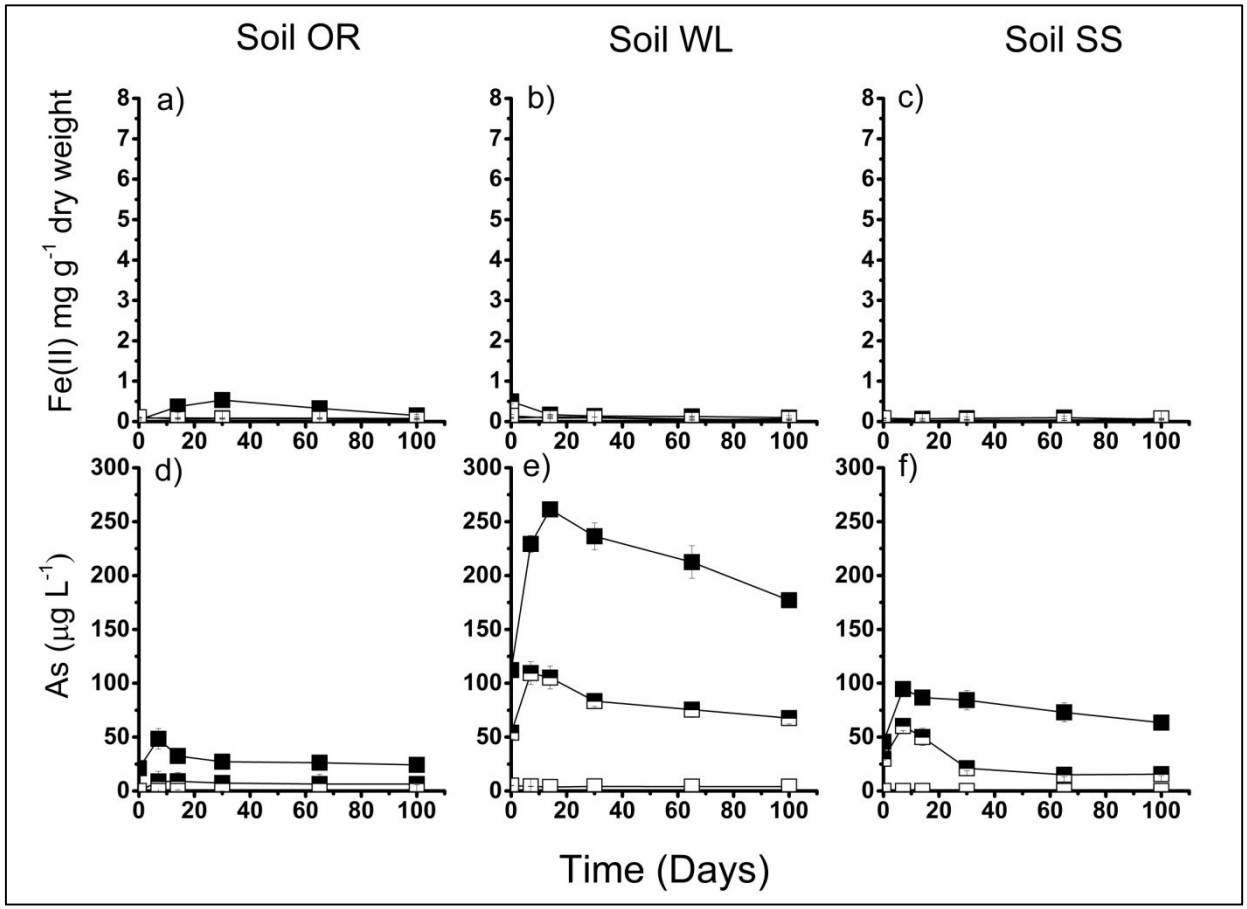

Figure 6.7 - Evolution of acid extractable Fe(II), and As concentrations in aerobic red mud affected soil-water systems and unamended controls. Empty squares = unamended, Half squares = 9% RM addition, Full squares = 33% RM addition. Error bars are 1 σ of triplicate results (where not shown, errors are within the symbol size).

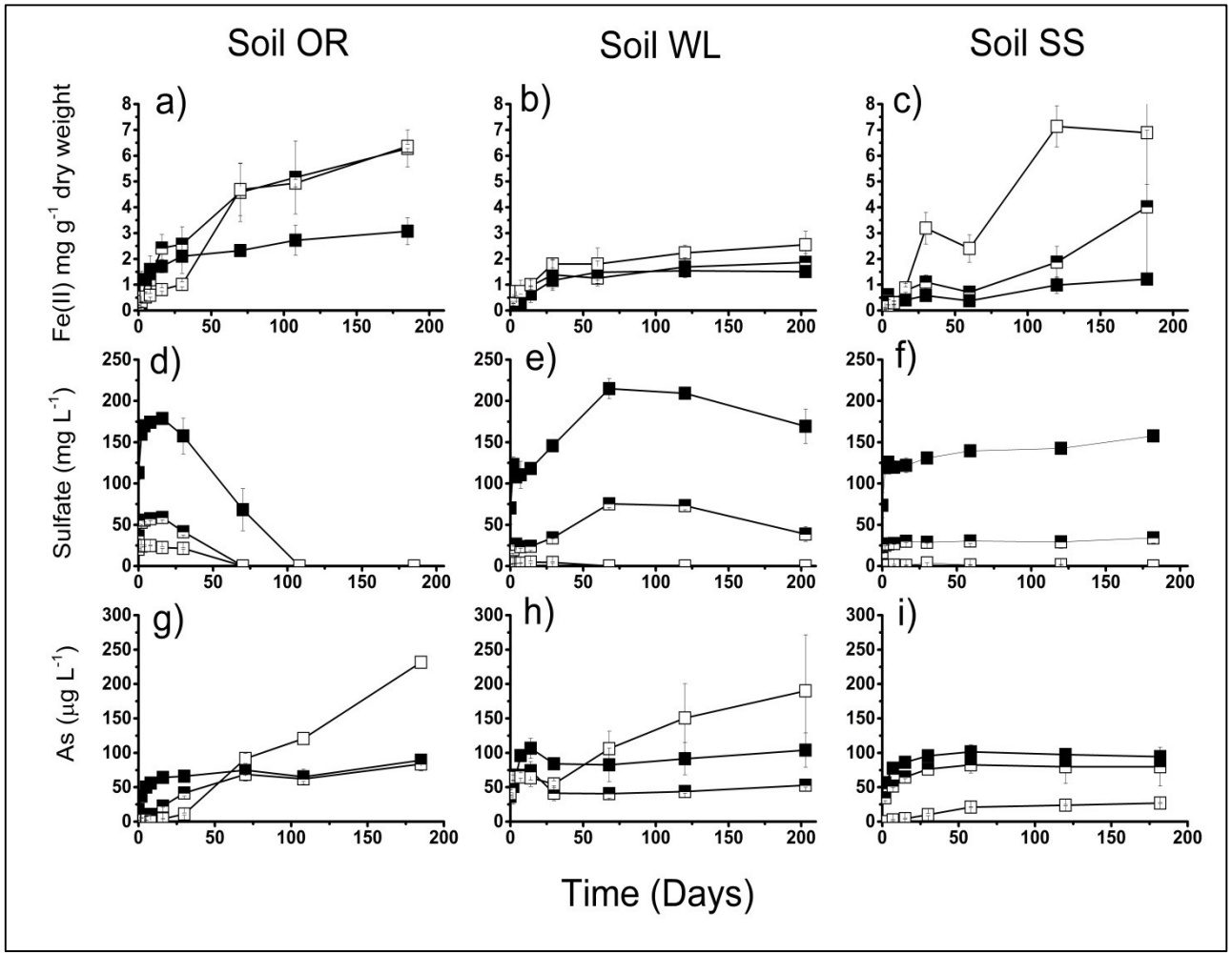

Figure 6.8 - Evolution of acid extractable Fe(II), aqueous SO_4^{2-} and As concentrations in anaerobic red mud affected soil-water systems and unamended controls. Empty squares = unamended, Half squares = 9% RM addition, Full squares = 33% RM addition. Error bars are 1 σ of triplicate results (where not shown, errors are within the symbol size).

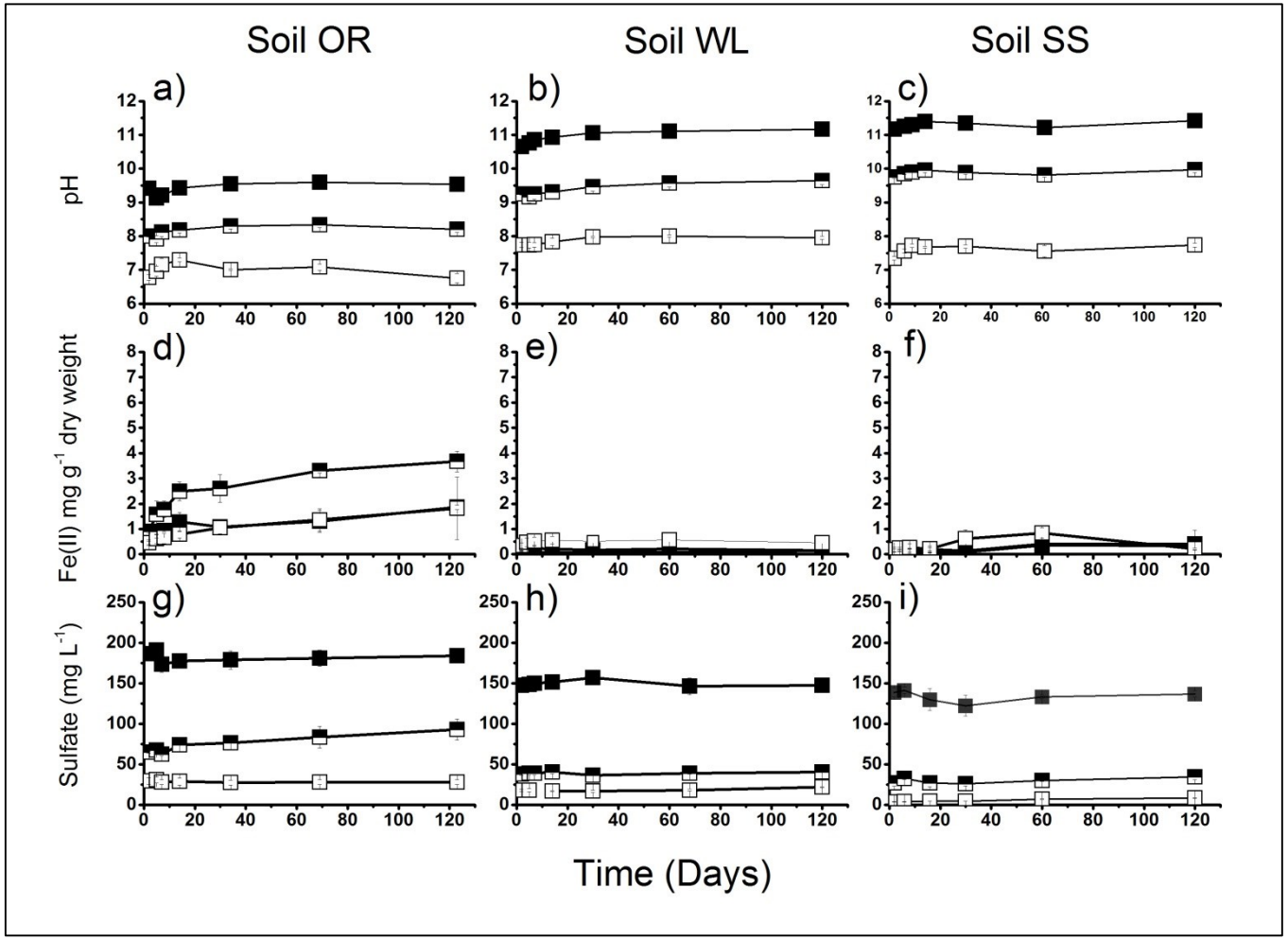

Figure 6.9 - Geochemical analysis time plots from heat treated controls showing pH, Fe(II) mg g^{-1} dry weight and SO_4^{2-} . Empty squares = unamended, Half squares = *9% RM addition*, Full squares = *33% RM addition*. Error bars are 1 σ of triplicate results (where not shown, errors are within the symbol.

6.3.5 Arsenic in microcosm experiments

At the initial sampling points the unamended aerobic experiments all had no detectable aqueous As present. However, in the experiments with a red mud addition, there was detectable aqueous As in all the aerobic experiments, with the exception of the Soil OR experiment with a 9% RM addition. The initial aqueous As concentration was highest (~ 100 μg L^{-1}) in the Soil WL experiment with a 33% RM addition of (Figure 6.7 d-f).

There was no increase in aqueous As concentrations in unamended aerobic experiments over the incubation period. When red mud was added to the aerobic experiments aqueous As concentrations increased in line with red mud loading to between 50 and 250 μg L^{-1} with lowest concentrations in the Soil OR system and highest in the Soil WL system (Figure 6.7 d-f). Each aerobic experiment with red mud addition followed a similar trend of rapid release over the first 10 day followed by a long period of removal.

At the initial sampling point the unamended anaerobic experiments (Figure 6.8 g-i) containing the Soil SS and OR had no detectable aqueous As present. However, the Soil WL anaerobic experiments contained ~40 μg L^{-1} As. The aqueous As concentrations in all three unamended anaerobic experiments had increased above their initial values by day 30, and continued to rise for the remainder of the experiments. Concentrations reached >200 μg L^{-1} in the Soil OR and WL microcosms, but did not exceed 25 μg L^{-1} in the Soil SS experiments. HPLC-ICP-MS analysis performed on the aqueous phase sampled a end point solutions showed that ~50% of aqueous As was present as As(III) in all three soil-only systems (Table 6.2).

Table 6.2 - Percentages of As(V) (as arsenate) and As(III) (as arsenite) present in the solutions taken at the end points of the anaerobic experiments.

Soil	Red Mud %	Total As µg L^{-1}	% As(III)	% As(V)
Soil OR	0%	232 (±9)	50 (±0)	50 (±0)
	9%	84 (±10)	1 (±1)	99 (±1)
	33%	89 (±5)	4 (±4)	96 (±4)
Soil WL	0%	190 (±81)	53 (±2)	47 (±2)
	9%	53 (±3)	0 (±1)	100 (±1)
	33%	104 (±25)	0 (±1)	100 (±1)
Soil SS	0%	27 (±1)	47 (±9)	53 (±9)
	9%	80 (±28)	1 (±1)	99 (±1)
	33%	95 (±8)	0 (±1)	100 (±1)

When red mud was added to the anaerobic experiments there was an increase in the initial aqueous As concentrations that directly related to red mud loading (Figure 6.8 g-i). The As concentration increased over the first 30 - 60 days of incubation with all three soils but then remained relatively constant thereafter. The final As concentration in all the anaerobic experiments with red mud addition was between 50 – 125 µg L^{-1}. HPLC-ICP-MS analysis performed on the aqueous phase sampled at the end of the incubation period showed that <5% of aqueous As was present as As(III) in all anaerobic experiments with a red mud addition (Table 6.2).

Arsenic K-edge XANES spectra (Figure 6.10) collected from the Hungarian soils all have absorption edge positions and white line peaks at the same energy as the arsenate standard indicating that As in the soils is primarily present As(V). The spectra collected from the Soil WL experiments have a shoulder on the As(V) absorption edge at the same energy as the white line peak of the arsenite standard, indicating a small contribution from As(III) to this spectra. The spectra from unamended anaerobic experiments at the incubation period end-point showed an As(III) shoulder for the Soil WL and Soil SS, and an increase in the shoulder for the Soil OR suggesting that some of the As present in the unamended anaerobic experiments was reduced to As(III) during incubations.

Sediment from the incubation end point from anaerobic experiments that contained red mud and either Soil WL or Soil SS have very similar As XANES spectra to the equivalent heat treated controls. The edge position and white line peaks are at the same energy as the arsenate standard, indicating that the majority of As is present as As(V). XANES spectra collected from samples taken from the Soil OR anaerobic experiments with either 9% or 33% RM have small shoulders at the same energy as the arsenite standard. This shoulder is not apparent in samples from corresponding heat treated controls indicating that some of the As present had been reduced to As(III) in these experiments.

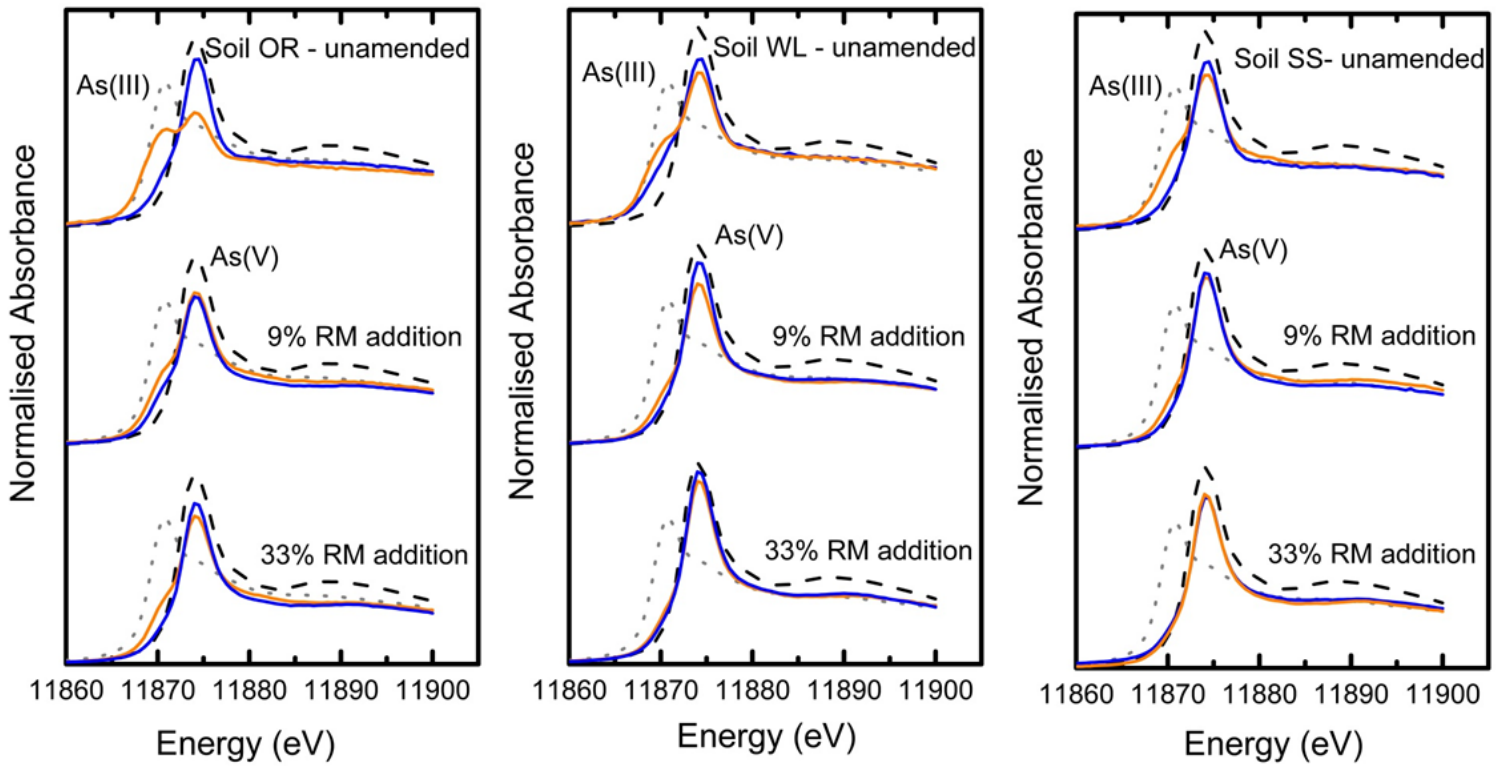

Figure 6.10 - Normalised arsenic K-edge XANES spectra collected from standards, soil samples and solids recovered anaerobic experiments and heat treated controls. All graphs: Grey dotted line = arsenite, As(III), Black dashed line = arsenate, As(V). Top graphs: blue line = soil as sampled, orange line = soil at end point of unamended anaerobic experiments. Middle and bottom graphs: blue line = samples taken from heat treated controls at end point, orange line = samples taken from anaerobic experiments at end point.

6.4 Discussion

6.4.1 The occurrence of As in red mud and the effect of pH / completing ions on As solubility

XAS analysis determined that As in the red mud sampled is present primarily as an inorganic arsenate phase (Figure 6.2), most of which could only be extracted by HF/aqua regia in sequential extractions (Mayes et al., 2011) suggesting that it is mostly associated with residual phases. However, alkaline leaching tests indicate that a potentially mobile source of surface bound exchangeable As exists in red mud. Although, sequential extraction data shows that ~0.3% of As in red mud is extractable by $MgCl_2$ at pH 7 (Mayes et al., 2011) (~0.6 mg kg^{-1}), alkaline leaching tests (Figure 6.3) indicated that up to 15 % of the red mud associated arsenic can be desorbed particularly when phosphate is present as a competing ion at pH values >8. Therefore, there is significant potential for surface bound As to be released from red mud by competitive desorption processes involving OH^-, phosphate or carbonate ion.

6.4.2 Controls on As release during aerobic incubation

In aerobic experiments containing red mud, there was a large variation in the concentrations of aqueous As which varied depending upon red mud loading and soil type. All the aerobic experiments showed an overall decrease in solution pH with time. This is attributed to the ingress of atmospheric CO_2 to the experiments. Dissolution of CO_2, in alkaline solutions results in a pH reduction as alkalinity is consumed (see Chapter 2, for the reaction sequence 2.3 - 2.7).

In the presence of M^{2+} ions (such as Ca^{2+} and Mg^{2+}, which may be exchanged from the soil by Na^{+} present in the red mud, or; alternatively sourced from dissolution of Ca aluminosilicate minerals (e.g. cancrinite / hydrogarnet; (Hind et al., 1999; Rubinos and Barral, 2013) present in red mud that are unstable below pH 12 (Castaldi et al., 2010), carbonate phases can precipitate (e.g., $Ca^{2+}_{(aq)} + CO_3^{2-}{}_{(aq)} \rightarrow CaCO_{3(s)}$), promoting the further dissolution of atmospheric CO_2 as carbonate is removed from solution (Renforth et al., 2012; Burke et al., 2013).

Thus, As release from the aerobic experiments is largely controlled by solution pH (Figure 6.11a). There was a positive correlation between high aqueous As concentrations and higher pH at the experimental end point for all the aerobic experiments containing red mud. Although the observed reduction in pH with time tended to also result in a trend towards lower As concentrations with time, the final pH was buffered in all systems to pH values (pH 8.5-9.5) where small amounts of arsenate is expected to become desorbed from red mud. It is also possible that in these aerobic experiments, CO_2 ingress lead to higher aqueous carbonate concentrations (where pH buffers > 9) which acted as a competing ion for available sorption sites, further promoting As solubility.

6.4.3 Effects of red mud addition on biogeochemical redox processes

Unamended anaerobic experiments using Soil WL and Soil SS showed increases in acid extractable Fe(II) that were not observed in either the equivalent heat treated controls or equivalent aerobic experiments, suggesting that microbially mediated Fe(III) reduction occurred during anaerobic incubation. In the case of the unamended anaerobic experiments using Soil OR, an increase in acid extractable Fe(II) was observed in both

the heat-treated controls and anaerobic experiments (but not in equivalent aerobic experiments). The Fe(II) increase observed in heat-treated controls may be related to recovery of microbial activity in these tests e.g. involving the survival of bacterial spores (Esty and Williams, 1924). However, the concentration of acid extractable Fe(II) detected in the heat-treated controls was much lower than in the unamended anaerobic experiments (i.e. an increase of <1.5 mg g^{-1} compared with >6 mg g^{-1}).

When comparing the heat treated controls (Figure 6.9) with the anaerobic experiments (Figure 6.8) there is evidence to suggest that microbial Fe(III) reduction also occurred in both red mud amended anaerobic experiments using the Soil OR amended with red mud (pH 8.5 and 9.5 respectively); the Soil WL amended with red mud (pH 9.5 and 10.5 respectively), and the Soil SS amended with 9% red mud (pH 10). Microbial Fe(III) reduction was probably inhibited in the Soil SS amended with 33% red mud due to the high pH (pH 11.5). These results are consistent with thermodynamic calculations indicating that Fe(III) reduction is not generally favoured above pH 11 (Burke et al., 2012b; Rizoulis et al., 2012). Although several groups of alkaliphilic bacteria are capable of Fe(III)-reduction at pH values up to pH 11(Ye et al., 2004; Pollock et al., 2007; Zhilina et al., 2009; Whittleston et al., 2011; Burke et al., 2012b), these bacteria have adapted to high pH conditions by prolonged exposure. It is, therefore, unlikely that any microbes present in the sample soils have quickly adapted to life at high pH. However, these data indicate that the microbial communities present in these soils contain species capable of Fe(III)-reduction that are tolerant of the increase in pH and other challenges (e.g. increased salinity and toxic metal loadings) caused by red mud addition.

Despite the large amounts of Fe(III)-oxides present in Ajka red mud (~40-50% hematite determined previously by Gelencser et al., (2011)), the increases in acid

extractable Fe(II) detected in the red mud amended anaerobic microcosms is equivalent (or less than) unamended anaerobic microcosms. The hematite present in red mud is nanoparticulate (50-200 nm) (Gelencser et al., 2011; Mayes et al., 2011; Burke et al., 2012a) . Although smaller hematite nanoparticles (<10 nm in size) are potentially bioavailable (Dehner et al., 2011), hematite is much less bioavailable than poorly ordered iron oxyhydroxides (Cutting et al., 2009). Therefore the low bioavailability of hematite can account for the lack of additional Fe(II) production observed in red mud amended experiments. The lack of reactive Fe is further evidenced from sequential extraction data indicating that all Fe in red mud was associated with residual phases (Mayes et al., 2011). Any increases in Fe(II) seen in the experiments containing red mud were, therefore, most likely the result of bioreduction of the reactive Fe(III)-oxides already present in the soils.

Addition of red mud to microcosms increases initial sulfate concentrations compared to soil only systems. Rapid removal of SO_4^{2-} was seen in Soil OR anaerobic experiments amended with both 9% and 33 % red mud. The Soil WL anaerobic experiments containing red mud appear to following a similar trend to the red mud amended organic-rich experiments (initially rising concentrations, followed by removal) but SO_4^{2-} removal occurred at a much slower rate in these experiments. No removal of SO_4^{2-} occurred in any of the Soil SS anaerobic experiments where red mud was present. In the heat treated controls SO_4^{2-} concentrations were similar to the peak concentrations seen in the anaerobic experiments. There was no SO_4^{2-} removal observed in any of the heat treated controls. This difference in behaviour between anaerobic experiments and heat treated controls suggests that SO_4^{2-} removal was a result of microbial sulfate reduction.

Microbial sulfate reduction is observed in some alkaline soda lakes (with an average pH up to 11) (Foti et al., 2007), but more generally sulfate reduction is not thermodynamically favoured much above pH 9 (Burke et al., 2012b; Rizoulis et al., 2012). In these experiments, three anaerobic experiments that all equilibrated between pH 9.5 - 10 had entirely different responses (i.e. Soil OR + 33% red mud = complete removal; Soil WL + 9% red mud addition = partial removal; and Soil SS + 9% red mud = no removal), suggesting that trends in SO_4^{2-} removal in the different systems appear to be soils specific, as they cannot be completely explained by the impact of the pH change or amount of red mud present.

6.4.4 As release in anaerobic experiments with no red mud addition

The concentration of As in unamended anaerobic experiments were minimal at the start of incubation. However, large increases in aqueous As concentrations were seen in both the Soil OR and Soil WL unamended anaerobic experiments which were found to be ~50% As(III). Although increases of aqueous As were much lower in the Soil SS unamended anaerobic experiment (this is consistent with the lower native As content of this soil); aqueous As was also found to be ~50% As(III). The reduction of As(V) to As(III) in the unamended anaerobic experiments could be an indication that microbial arsenic reduction was occurring. Microbial As(V)-reduction in natural soils is well documented (Dowdle et al., 1996; Oremland and Stolz, 2003; Lloyd and Oremland, 2006) and is a key mechanism contributing to high As concentrations in naturally contaminated waters (Islam et al., 2004; Oremland and Stolz, 2005; Charlet and Polya, 2006). As(III) is generally more soluble than As(V) at circumneutral pH (Smedley and Kinniburgh, 2002) thus accounting for the increased concentrations seen

in unamended anaerobic experiments. Further evidence of As reduction is present in the XANES spectra from these experiments. XANES spectra revealed that As in each of the soils was initially present primarily as As(V) but small increases in the contribution of As(III) to XANES spectra were observed as a result of the microcosm incubation.

6.4.5 As release in anaerobic experiments with red mud addition

XANES and HPLC-ICP-MS analysis of the anaerobic experiments containing red mud found that As was almost entirely present as As(V) with no evidence of As(III) accumulation in either solution or in the solids. Therefore, As reduction did not occur in any of the experiments with a red mud addition despite having supported microbial Fe(III)- and sulfate reduction in several of the experiments. In addition microbial mediated As reduction occurred in all the unamended anaerobic experiments, demonstrating that both bioavailable As(V) and a microbial community capable of As-reduction was present in the soils used. Arsenic reduction is a common biological process in soda lakes, which are both alkaline and saline like red mud contaminated systems (Oremland et al., 2004; Oremland et al., 2005). However, the population of As reducing bacteria present in these soils was not able to tolerate the additional stresses caused by red mud addition and did not support As(V) reduction processes even when pH increases observed were relatively modest (e.g. in the experiments using the organic rich soil).

In the absence of microbial induced changes of As speciation, experimental pH should be the primary control of surface bound arsenate associated with red mud. In the anaerobic experiments, pH values were higher than equivalent aerobic experiments (as CO_2 ingress was prevented) but As concentrations were similar (or slightly lower) than

in the aerobic experiments (Figure 6.11b). However, in the anaerobic experiments using Soil OR with a 9% RM addition (at pH 8-8.5), As concentrations were between 5-10 times higher than the equivalent aerobic experiments. Fe(III)-reducing conditions developed in the anaerobic experiments (Figure. 6.7a). The reductive dissolution of iron oxides minerals is expected to promote the release of surface bound arsenate into solution (Zachara et al., 2001; Islam et al., 2004), which might explain the increased As(V) concentrations observed in this experiment (and the overall lack of relationship between As concentration and pH observed in Fig 6.11b). However, the addition of non-reactive nanoparticulate hematite particles associated with the red mud, should reduce the overall extent of this effect by providing additional surfaces for arsenate adsorption.

6.5 Conclusions

Arsenic in red mud is present as As(V) as arsenate species where up to 15% is present in phosphate exchangeable surface bound complexes that have the potential to be remobilised. Arsenate solubility from red mud is enhanced at high pH and also in the presence of competing ions such as phosphate and carbonate. In aerobic soil systems, As release is related to red mud loading and the pH value that occurs due to soil buffering reactions. Under aerobic conditions, carbonation reactions also produced lower pH with time resulting in a trend towards lower aqueous As concentrations. However, dissolved CO_2 (speciated as carbonate at pH >9) may also provide a source of competing ions thus increasing As concentrations in some cases. In anaerobic experiments, carbonation reactions do not occur and experimental pH is determined by red mud loading and the buffering capacity of the soils used. As(V) release is not

strongly dependent on experimental pH, and some As release is observed in all experiments. Although no reduction of As(V) to As(III) occurs, Fe(III)-reduction occurred in several experiments, and dissolution of high surface area iron (oxy)hydroxides may play a role in As release by reducing the overall sorption capacity present.

The results of this study, suggest that the pH of all the red mud affected soil systems studied (during both aerobic and anaerobic incubation) was typically sufficiently high (>pH 8.5) that release of small amounts of surface bound As from red mud occurred to some extent. Leaching of As from red mud affected soils may have contributed to the moderate increases in As concentrations found in river waters up to two years after the spill (Nagy et al., 2013). These data, therefore, vindicate the decision by Hungarian authorities to recover most of the red mud from affected land as arsenic leaching is likely to have been much greater without this intervention.

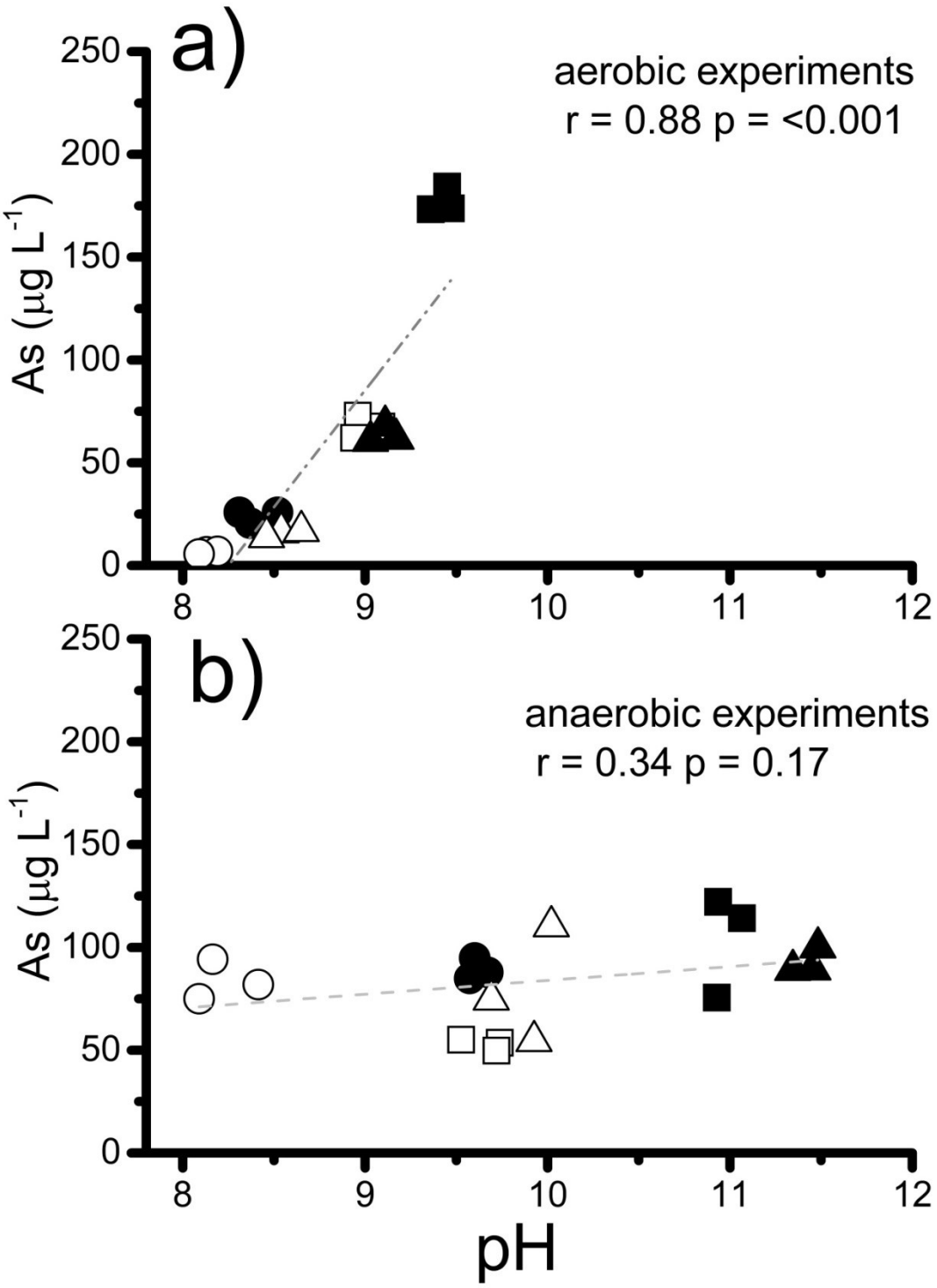

Figure 6.11 - As concentration vs pH at the both the aerobic (a) and anaerobic (b) red mud experiments at the incubation end point. There is no significant correlation present (Pearson's correlation) in the anaerobic experiments but there is a positive correlation present in the aerobic experiments. Full symbols = *33% RM addition*, Empty symbols = *9% RM addition*, Circles = Soil OR, Squares = Soil WL and Triangles = Soil SS.

6.6 References

ADAM, J., BANVOLGYI, G., DURA, G., GRENERCZY, G., GUBECK, N., GUPTER, I., SIMON, G., SZEGFALVI, Z., SZEKACS, A., SZEPVOLGYI, J. & UJLAKY, E. 2011. The Kolontar report: Causes and Lessons from the Red Mud Disaster. In: B, J. (ed.). Budapest: Sustainable Development Committee of the Hungarian Parliament.

ALTUNDOGAN, H. S., ALTUNDOGAN, S., TUMEN, F. & BILDIK, M. 2000. Arsenic removal from aqueous solutions by adsorption on red mud. Waste Management, 20, 761-767.

ALTUNDOGAN, H. S., ALTUNDOGAN, S., TUMEN, F. & BILDIK, M. 2002. Arsenic adsorption from aqueous solutions by activated red mud. Waste Management, 22, 357-363.

ANTON, A., REKASI, M., UZINGER, N., SZEPLABI, G. & MAKO, A. 2012. Modelling the Potential Effects of the Hungarian Red Mud Disaster on Soil Properties. Water Air and Soil Pollution, 223, 5175-5188.

ASPILA, K. I., AGEMIAN, H. & CHAU, A. S. Y. 1976. SEMIAUTOMATED METHOD FOR DETERMINATION OF INORGANIC, ORGANIC AND TOTAL PHOSPHATE IN SEDIMENTS. Analyst, 101, 187-197.

ASTM 2006. D4972.01: standard test method for pH of soils. Annual Book of ASTM standards. Amer Soc Test Mater.

BHATNAGAR, A., VILAR, V. J. P., BOTELHO, C. M. S. & BOAVENTURA, R. A. R. 2011. A review of the use of red mud as adsorbent for the removal of toxic pollutants from water and wastewater. Environmental Technology, 32, 231-249.

BRUNORI, C., CREMISINI, C., MASSANISSO, P., PINTO, V. & TORRICELLI, L. 2005. Reuse of a treated red mud bauxite waste: studies on environmental compatibility. Journal of Hazardous Materials, 117, 55-63.

BURKE, I. T., MAYES, W. M., PEACOCK, C. L., BROWN, A. P., JARVIS, A. P. & GRUIZ, K. 2012a. Speciation of arsenic, chromium, and vanadium in red mud samples from the ajka spill site, hungary. Environmental Science & Technology, 46, 3085-92.

BURKE, I. T., MORTIMER, R. J. G., PALANIYANDI, S., WHITTLESTON, R. A., LOCKWOOD, C. L., ASHLEY, D. J. & STEWART, D. I. 2012b. Biogeochemical Reduction Processes in a Hyper-Alkaline Leachate Affected Soil Profile. Geomicrobiology Journal, 29, 769-779.

BURKE, I. T., PEACOCK, C. L., LOCKWOOD, C. L., STEWART, D. I., MORTIMER, R. J. G., WARD, M. B., RENFORTH, P., GRUIZ, K. & MAYES, W. M. 2013. Behavior of Aluminum, Arsenic, and Vanadium during the Neutralization of Red Mud Leachate by HCl, Gypsum, or Seawater. Environmental Science & Technology, 47, 6527-6535.

CASTALDI, P., SILVETTI, M., GARAU, G. & DEIANA, S. 2010. Influence of the pH on the accumulation of phosphate by red mud (a bauxite ore processing waste). Journal of Hazardous Materials, 182, 266-272.

CHARLET, L. & POLYA, D. A. 2006. Arsenic in shallow, reducing groundwaters in southern Asia: An environmental health disaster. Elements, 2, 91-96.

CORNELIS, G., JOHNSON, C. A., VAN GERVEN, T. & VANDECASTEELE, C. 2008. Leaching mechanisms of oxyanionic metalloid and metal species in alkaline solid wastes: A review. Applied Geochemistry, 23, 955-976.

CUTTING, R. S., COKER, V. S., FELLOWES, J. W., LLOYD, J. R. & VAUGHAN, D. J. 2009. Mineralogical and morphological constraints on the reduction of Fe(III) minerals by Geobacter sulfurreducens. Geochimica Et Cosmochimica Acta, 73, 4004-4022.

DEHNER, C. A., BARTON, L., MAURICE, P. A. & DUBOIS, J. L. 2011. Size-Dependent Bioavailability of Hematite (alpha-Fe2O3) Nanoparticles to a Common Aerobic Bacterium. Environmental Science & Technology, 45, 977-983.

DOWDLE, P. R., LAVERMAN, A. M. & OREMLAND, R. S. 1996. Bacterial dissimilatory reduction of arsenic(V) to arsenic(III) in anoxic sediments. Applied and Environmental Microbiology, 62, 1664-1669.

ENSERINK, M. 2010. ENVIRONMENT After Red Mud Flood, Scientists Try to Halt Wave of Fear and Rumors. Science, 330, 432-433.

ESTY, J. R. & WILLIAMS, C. C. 1924. Heat resistance studies I A new method for the determination of heat resistance let of bacterial spores. Journal of Infectious Diseases, 34, 516-528.

FEIGL, V., ANTON, A., UZIGNER, N. & GRUIZ, K. 2012. Red Mud as a Chemical Stabilizer for Soil Contaminated with Toxic Metals. Water Air and Soil Pollution, 223, 1237-1247.

FOTI, M., SOROKIN, D. Y., LOMANS, B., MUSSMAN, M., ZACHAROVA, E. E., PIMENOV, N. V., KUENEN, J. G. & MUYZER, G. 2007. Diversity, activity, and abundance of sulfate-reducing bacteria in saline and hypersaline soda lakes. Applied and Environmental Microbiology, 73, 2093-2100.

FRIESL, W., HORAK, O. & WENZEL, W. W. 2004. Immobilization of heavy metals in soils by the application of bauxite residues: pot experiments under field conditions. Journal of Plant Nutrition and Soil Science-Zeitschrift Fur Pflanzenernahrung Und Bodenkunde, 167, 54-59.

GELENCSER, A., KOVATS, N., TUROCZI, B., ROSTASI, A., HOFFER, A., IMRE, K., NYIRO-KOSA, I., CSAKBERENYI-MALASICS, D., TOTH, A., CZITROVSZKY, A., NAGY, A., NAGY, S., ACS, A., KOVACS, A., FERINCZ, A., HARTYANI, Z. & POSFAI, M. 2011. The Red Mud Accident in Ajka (Hungary): Characterization and Potential Health Effects of Fugitive Dust. Environmental Science & Technology, 45, 1608-1615.

GENC-FUHRMAN, H., TJELL, J. C. & MCCONCHIE, D. 2004. Adsorption of arsenic from water using activated neutralized red mud. Environmental Science & Technology, 38, 2428-2434.

GRAFE, M., POWER, G. & KLAUBER, C. 2011. Bauxite residue issues: III. Alkalinity and associated chemistry. Hydrometallurgy, 108, 60-79.

GRAY, C. W., DUNHAM, S. J., DENNIS, P. G., ZHAO, F. J. & MCGRATH, S. P. 2006. Field evaluation of in situ remediation of a heavy metal contaminated soil using lime and red-mud. Environmental Pollution, 142, 530-539.

GRUIZ, K., FEIGL, V., KLEBERCZ, O., ANTON, A., AND VASZITA, E. Environmental Risk Assessment of Red Mud Contaminated Land in Hungary. Geocongress 2012: State of the Art and Practice in Geotechnical Engineering, 2012. American Society of Civil Engineers, 4156-4165.

HAMMOND, K., MISHRA, B., APELIAN, D., BLANPAIN, B. 2013. CR3 Communication: Red Mud - A Resource or a Waste. JOM, 65, 340-341.

HERY, M., VAN DONGEN, B. E., GILL, F., MONDAL, D., VAUGHAN, D. J., PANCOST, R. D., POLYA, D. A. & LLOYD, J. R. 2010. Arsenic release and attenuation in low organic carbon aquifer sediments from West Bengal. Geobiology, 8, 155-168.

HIND, A. R., BHARGAVA, S. K. & GROCOTT, S. C. 1999. The surface chemistry of Bayer process solids: a review. Colloids and Surfaces a-Physicochemical and Engineering Aspects, 146, 359-374.

ISLAM, F. S., GAULT, A. G., BOOTHMAN, C., POLYA, D. A., CHARNOCK, J. M., CHATTERJEE, D. & LLOYD, J. R. 2004. Role of metal-reducing bacteria in arsenic release from Bengal delta sediments. Nature, 430, 68-71.

KLEBERCZ, O., MAYES, W. M., ANTON, A. D., FEIGL, V., JARVIS, A. P. & GRUIZ, K. 2012. Ecotoxicity of fluvial sediments downstream of the Ajka red mud spill, Hungary. Journal of environmental monitoring : JEM, 14, 2063-71.

LANGMUIR, D. 1997. Aqueous environmental geochemistry, Upper Saddle River, N. J., Prentice Hall.

LIU, X. & ZHANG, N. 2011. Utilization of red mud in cement production: a review. Waste Management & Research, 29, 1053-1063.

LIU, Y., LIN, C. & WU, Y. 2007. Characterization of red mud derived from a combined Bayer Process and bauxite calcination method. Journal of Hazardous Materials, 146, 255-261.

LIU, Y., NAIDU, R. & MING, H. 2011. Red mud as an amendment for pollutants in solid and liquid phases. Geoderma, 163, 1-12.

LLOYD, J. R. & OREMLAND, R. S. 2006. Microbial transformations of arsenic in the environment: From soda lakes to aquifers. Elements, 2, 85-90.

LOMBI, E., ZHAO, F. J., ZHANG, G. Y., SUN, B., FITZ, W., ZHANG, H. & MCGRATH, S. P. 2002. In situ fixation of metals in soils using bauxite residue: chemical assessment. Environmental Pollution, 118, 435-443.

LOVLEY, D. R. & PHILLIPS, E. J. P. 1986. AVAILABILITY OF FERRIC IRON FOR MICROBIAL REDUCTION IN BOTTOM SEDIMENTS OF THE FRESH-WATER TIDAL POTOMAC RIVER. Applied and Environmental Microbiology, 52, 751-757.

MAYES, W. M., JARVIS, A. P., BURKE, I. T., WALTON, M., FEIGL, V., KLEBERCZ, O. & GRUIZ, K. 2011. Dispersal and Attenuation of Trace Contaminants Downstream of the Ajka Bauxite Residue (Red Mud) Depository Failure, Hungary. Environmental Science & Technology, 45, 5147-5155.

NAGY, A. S., SZABO, J. & VASS, I. 2013. Trace metal and metalloid levels in surface water of the Marcal River before and after the Ajka red mud spill, Hungary. Environmental Science and Pollution Research, 20, 7603-7614.

O'DAY, P. A., VLASSOPOULOS, D., ROOT, R. & RIVERA, N. 2004. The influence of sulfur and iron on dissolved arsenic concentrations in the shallow subsurface under changing redox conditions. Proceedings of the National Academy of Sciences of the United States of America, 101, 13703-13708.

OREMLAND, R. S., KULP, T. R., BLUM, J. S., HOEFT, S. E., BAESMAN, S., MILLER, L. G. & STOLZ, J. F. 2005. A microbial arsenic cycle in a salt-saturated, extreme environment. Science, 308, 1305-1308.

OREMLAND, R. S. & STOLZ, J. F. 2003. The ecology of arsenic. Science, 300, 939-944.

OREMLAND, R. S. & STOLZ, J. F. 2005. Arsenic, microbes and contaminated aquifers. Trends in Microbiology, 13, 45-49.

OREMLAND, R. S., STOLZ, J. F. & HOLLIBAUGH, J. T. 2004. The microbial arsenic cycle in Mono Lake, California. Fems Microbiology Ecology, 48, 15-27.

POLLOCK, J., WEBER, K. A., LACK, J., ACHENBACH, L. A., MORMILE, M. R. & COATES, J. D. 2007. Alkaline iron(III) reduction by a novel alkaliphilic, halotolerant, Bacillus sp isolated from salt flat sediments of Soap Lake. Applied Microbiology and Biotechnology, 77, 927-934.

POWER, G., GRAFE, M. & KLAUBER, C. 2011. Bauxite residue issues: I. Current management, disposal and storage practices. Hydrometallurgy, 108, 33-45.

REEVES, H. J., WEALTHALL, G. & YOUNGER, P. L. 2011. Advisory visit to the bauxite processings tailings dam near Ajka, Vesprem County, western Hungary. . Keyworth, UK: British Geological Survey.

RENFORTH, P., MAYES, W. M., JARVIS, A. P., BURKE, I. T., MANNING, D. A. C. & GRUIZ, K. 2012. Contaminant mobility and carbon sequestration downstream of the Ajka (Hungary) red mud spill: The effects of gypsum dosing. The Science of the total environment, 421-422, 253-9.

RIZOULIS, A., STEELE, H. M., MORRIS, K. & LLOYD, J. R. 2012. The potential impact of anaerobic microbial metabolism during the geological disposal of intermediate-level waste. Mineralogical Magazine, 76, 3261-3270.

RUBINOS, D. A. & BARRAL, M. T. 2013. Fractionation and mobility of metals in bauxite red mud. Environmental science and pollution research international, 20, 7787-802.

RUYTERS, S., MERTENS, J., VASSILIEVA, E., DEHANDSCHUTTER, B., POFFIJN, A. & SMOLDERS, E. 2011. The Red Mud Accident in Ajka (Hungary): Plant Toxicity and Trace

Metal Bioavailability in Red Mud Contaminated Soil. Environmental Science & Technology, 45, 1616-1622.

SMEDLEY, P. L. & KINNIBURGH, D. G. 2002. A review of the source, behaviour and distribution of arsenic in natural waters. Applied Geochemistry, 17, 517-568.

SOMLAI, J., JOBBAGY, V., KOVACS, J., TARJAN, S. & KOVACS, T. 2008. Radiological aspects of the usability of red mud as building material additive. Journal of Hazardous Materials, 150, 541-545.

TOMIC, S. S., B. G.; WANDER, A.; HARRISON, N. M.; DENT, A. J.; MOSSELMANS, J. F. W.; INGLESFIELD, J. E. 2005. New Tools for the Analysis of EXAFS: The DL_EXCURV Package. CCLRC Technical Report DL-TR-2005-01. Daresbury, UK.

WHITTLESTON, R. A., STEWART, D. I., MORTIMER, R. J. G., ASHLEY, D. J. & BURKE, I. T. 2011. Effect of Microbially Induced Anoxia on Cr(VI) Mobility at a Site Contaminated with Hyperalkaline Residue from Chromite Ore Processing. Geomicrobiology Journal, 28, 68-82.

YADAV, V. S., PRASAD, M., KHAN, J., AMRITPHALE, S. S., SINGH, M. & RAJU, C. B. 2010. Sequestration of carbon dioxide (CO_2) using red mud. Journal of Hazardous Materials, 176, 1044-1050.

YE, Q., ROH, Y., CARROLL, S. L., BLAIR, B., ZHOU, J. Z., ZHANG, C. L. & FIELDS, M. W. 2004. Alkaline anaerobic respiration: Isolation and characterization of a novel alkaliphilic and metal-reducing bacterium. Applied and Environmental Microbiology, 70, 5595-5602.

ZACHARA, J. M., FREDRICKSON, J. K., SMITH, S. C. & GASSMAN, P. L. 2001. Solubilization of Fe(III) oxide-bound trace metals by a dissimilatory Fe(III) reducing bacterium. Geochimica Et Cosmochimica Acta, 65, 75-93.

ZHILINA, T. N., ZAVARZINA, D. G., KOLGANOVA, T. V., LYSENKO, A. M. & TOUROVA, T. P. 2009. *Alkaliphilus peptidofermentans* sp nov., a new alkaliphilic bacterial soda lake isolate capable of peptide fermentation and Fe(III) reduction. Microbiology, 78, 445-454.

Chapter 7 Leaching of copper and nickel in soil-water systems contaminated by red mud from Ajka, Hungary: The importance of soil organic matter.

Abstract

The red mud spill at Ajka, Hungary released 1 million m^3 of caustic red mud into the surrounding area with devastating results. Red mud is a highly alkaline (pH >12) waste product from bauxite ore processing. It contains elevated concentrations of oxyanion forming elements such as As and V that are mobilised at high pH but also trace metals that form stable complexes with organic matter (OM), such as Cu and Ni. Land remediation after the spill sought to remove red mud from affected areas or plough thinner deposits (< 5 cm) to prevent dust formation whereas wetland areas were left untreated. The addition of red mud to soils increases aqueous dissolved organic carbon (DOC) concentrations due to soil alkalisation. The mobilisation of Cu and Ni from red mud affected soil-water systems was investigated using aerobic and anaerobic batch microcosms together with solid phase extraction techniques to assess the amount of organically bound metals. The results showed that if the red mud loading and TOC content is sufficient there will be increased mobilisation of Cu and Ni through OM complexation, when compared to unaffected soils. This mechanism was found to be more prevalent under anaerobic conditions. These data indicate that the extensive remediation efforts by the Hungarian authorities were justified but that red mud should be used with caution as a soil amendment, especially in soils with a high TOC content. These data also highlight the problematic leaching of other oxyanion forming elements such as Mo, Se and Ti under anaerobic conditions and concerns over the water quality of unremediated wetland areas.

7.1 Introduction

The accidental release of ~1 million m^3 (Reeves et al., 2011; Adam et al., 2011a) of bauxite processing residue (red mud) from the Ajkai Timfoldgyar Zrt alumina plant in Ajka, western Hungary in October 2010 focused world attention on the potential public health and environmental hazards associated with red mud. The spill had devastating effects; causing damage to property, serious injuries and killing 10 people (Enserink, 2010; Adam et al., 2011a). An estimated 40km^2 of low lying agricultural land and riparian wetlands were affected and the red mud was transported 120 km downstream by rivers eventually reaching the Danube (Reeves et al., 2011; Mayes et al., 2011).

Red mud is the name given to the fine fraction residue that remains after alumina is extracted from bauxite ore during the Bayer process. The composition of red mud is highly dependent upon the bauxite ore used (Hind et al., 1999; Liu et al., 2007), but is typically comprised of; residual iron oxides, quartz, sodium aluminosilicates, titanium dioxide, calcium carbonate/aluminate and sodium hydroxide (Hind et al., 1999; Grafe et al., 2011; Gelencser et al., 2011). There has been considerable attention drawn to the potential hazards of red mud since the disaster, mainly in relation to its caustic nature (Grafe et al., 2011) which can be toxic to plants and some freshwater biota (Wilkie and Wood, 1996). The use of NaOH during the Bayer process means that unless neutralisation steps are taken during the refining process the red mud produced is very alkaline (Grafe et al., 2011; Power et al., 2011). At Ajka it had a pH>12 (Adam et al., 2011a) making it a hazardous substance as defined by the Basel Convention (Basel Convention, 2011).

Red mud also is known to contain elevated concentrations of toxic and potentially toxic metals and metalloids. The majority of these problematic elements are associated with sparingly soluble red mud minerals (Mayes et al., 2011; Rubinos and Barral, 2013) but research since the disaster has highlighted oxyanion forming elements such as; Al, As, Cr, Mo and V as persistently mobile (Milacic et al., 2012; Burke et al., 2013). The red mud leachate from Ajka had high levels of dissolved salts (up to 160 mS cm^{-2}) and contained up to 350 mg L^{-1} Al, 8 mg L^{-1} As, 12 mg L^{-1} Mo and 16 mg L^{-1} V (these oxyanion forming elements are very soluble at high pH) (Mayes et al., 2011; Burke et al., 2013).

Several studies since the spill have investigated the effects of red mud on human health (Gelencser et al., 2011); soil toxicity (Anton et al., 2012); freshwater and soil ecology (Klebercz et al., 2012; Rekasi et al., 2013); the mobility of red mud associated trace metals in the wider environment (Mayes et al., 2011; Burke et al., 2012a); and the effects dosing of rivers and streams with acid and gypsum to reduce pH (Renforth et al., 2012; Burke et al., 2013). After the Ajka disaster, the affected land was treated in two different ways: 1) removal of red mud where deposits were >5cm and 2) ploughing any red mud into land where deposits were <5cm. The land clean-up began a few weeks after the disaster but in some areas the red mud covered the soils for several months (Rekasi et al., 2013), and removal of red mud from fields was still continuing in May 2011. The clean-up operation focussed on recovering farmland, and, any affected wetland areas remain unremediated.

Humic acids are an important component of soil organic matter (SOM) whose solubility varies with pH. They are produced by microbial degradation of plant and animal residues, and represent a range of chemically similar compounds that contain carboxyl and phenolate groups, and behave functionally as a dibasic (occasionally tri-

basic) acid (Stevenson, 1994). As a result the amount of dissolved organic matter (DOM) in soil pore water tends to increase as the pH increases (Cheshire et al., 1977; Yin et al., 2002). Indeed, addition of dilute NaOH is used as a standard method for extracting humic substances from soil (Parsons, 1988; Sparks, 1998). The addition of red mud to soil increases both the pH and DOC of soil pore-waters (Lombi et al., 2002; Rekasi et al., 2013). The degree to which a particular soil is affected by the pH increase associated with red mud addition will depend on the nature of the soil affected. For example; sandy soils will undergo a greater pH increase, as they lack the intrinsic buffering capacity of a clay soil; but soil with high SOM contents will release more DOC into soil porewaters upon soil alkalisation (see Chapter 5). DOC in soil pore-waters has a major impact on the aqueous concentrations of trace metals in circumneutral and alkaline pore-waters (Davis, 1984; Ashworth and Alloway, 2004) due to formation of complexes between metal cations and SOM functional groups (at acidic pH, SOM adsorption to soil mineral surfaces is enhanced)(Wu et al., 2002). Therefore the addition of red mud to soil can create two problems: 1) oxyanion forming elements become more soluble as soil pH increases and 2) the increase in DOC also increases the solubility of metals that form stable complexes with organic matter.

Cu and Ni have been highlighted, alongside As, as occurring in elevated concentrations in the Torna and Marcel Rivers since the spill (Nagy et al., 2013). Unlike oxyanions, Cu and Ni cations are both generally more mobile under more acidic conditions (sorption edge Cu ~pH 5.1, Ni ~ pH 6.8, (Langmuir, 1997)). However Lombi et al. (2002) found that Cu mobility increased in Cu contaminated soils with red mud amendment (2% w/w) over 100 and 200 days compared to non-amended soils although Ni mobility from the same experiments was not found to be problematic. Since the red mud spill, Rekasi et al. (2013) found that the aqueous concentration of Cu increased in

red mud affected soil experiments which they attributed to increased soil pH and DOC concentration. Wu et al. (2001) found that Cu is mobile in alkaline soil when the humate is present, but immobile when it is absent. Cu and Ni can form complexes with organic matter (Cheshire et al., 1977; Richter and Theis, 1980). Cu(II) in particular, forms strong complexes with electron donors from O, N and S with SOM functional groups (Leckie and Davis, 1979), which may explain the persistence of this metal solution in alkaline conditions.

Cu is a redox sensitive element that occurs in the (+II) state under oxic conditions and can be reduced to Cu(I) or Cu(0) in reducing environments forming insoluble oxides, sulfides and $Cu_{(s)}$ (Weber et al., 2009; Fulda et al., 2013a). The solubility of Ni is less affected by changes in redox potential but forms insoluble hydroxides (as $Ni(OH)_2$) as pH increases (above pH 9) (Richter and Theis, 1980; Bradbury and Baeyens, 2009). Sorption to Fe and especially Mn oxides are also very important in controlling aqueous Ni concentrations (Peacock and Sherman, 2007).

Here, results are presented from a series of long-term aerobic and anaerobic batch experiments designed to investigate the mobility of Cu and Ni from red mud contaminated soil-water systems analogous to soil conditions post the Ajka disaster clean-up. These data build on recent work relating to oxyanion release (see chapter 5) and As mobility (see chapter 6) in similar systems. The specific objectives of this study were 1) to determine the potential for Cu and Ni release in red mud affected soil-water systems 2) to determine the effect of complexation with soil derived DOC on metal behaviour as a function of soil type 3) Discuss the long-term implications of ploughing in red mud to soils as an emergency remediation method and the potential hazards associated with unremediated wetland areas.

7.2 Materials and Methods

7.2.1 Field Sampling and Sample Handling

Sampling was undertaken in May 2011 (see Figure 3.2 for sampling locations). Red mud (RM) was sampled from within Cell X of the Ajka impoundment (Location 47°05'18.48"N, 17°29'46.77"E) and red mud leachate was collected from an open leachate pond at the same location. Three uncontaminated soils were sampled from locations in the Torna and upper Marcal river catchments unaffected by the release of red mud in 2010. Two were agricultural top soils (one was organic-rich (OR), the other a sandy soil (SS)) and the third was collected from 50cm from below the surface (i.e. beneath the rootlet layer) of a wetland (WL). All samples were stored at 4°C in polythene containers and a small sub-sample was stored at −80°C for X-ray absorption spectroscopy. The wetland soil was stored anaerobically using Anaerogen^{TM} sachets.

7.2.2 Long-Term Batch Experiments

Batch microcosm experiments were established under both aerobic and anaerobic conditions. Two different red mud-soil mixtures were prepared for each soil type (triplicate microcosms were prepared for each condition). A 9% red mud addition (by dry weight) was chosen as an analogue for where red mud had been ploughed into fields (based on ~5cm ploughed to a typical depth of 40-50cm, an approximate 5:50 mixing ratio). The 33% addition was used as a worst case scenario for any unremediated wetlands. Deionised water was added in a 5:1 ratio to the amount of soil.

Anaerobic experiments were carried out in 120 mL glass serum bottles, which were purged with nitrogen before capping and crimp sealing. Aerobic experiments were

carried out in 50 mL polypropylene centrifuge tubes and opened every week day for an hour in order to exchange the experimental headspace with air and prevent anaerobic conditions forming due to microbial respiration. Both aerobic and anaerobic experiments were incubated in the dark at 21 °C and sampled periodically over 100 - 120 days. During sampling bottles / tubes were shaken and 2 to 4 mL aliquots of soil / RM slurry was extracted. Aseptic technique was used where appropriate. Extractions were centrifuged (3 min, 6,000 g) and water pH and oxidation/reduction potential (ORP) was determined. The aqueous phase was filtered (0.2 μm) and acidified with 2% HNO_3 for ICP-MS analysis. At the end point of each experiment between 6 - 15 ml of slurry was extracted and centrifuged, the solutions were used for dissolved organic carbon (DOC) analysis and solid phase extraction (SPE) experiments. Control experiments without red mud addition for each soil type were incubated under anaerobic and aerobic conditions as described above.

7.2.3 Geochemical Methods.

ORP (as an indicator for Eh) and pH were measured using a Thermo Scientific Orion Dualstar pH/ISE benchtop meter (pH was calibrated daily at pH 4, 7 and 10; a new factory calibrated ORP electrode was used). Aqueous As, Cd, Co, Cr, Cu, Mo, Ni and V concentrations were determined using a Perkin Elmer Elan DRCII inductively coupled plasma-mass spectrometer and an Optima 5300 DV ICP-OES was used to determine aqueous concentrations of other elements. DOC in end point solutions was determined by a multi N/C® 2100 using thermocatalytic oxidation, MC-NDIR detection analysis. Standards were used to check the accuracy and precision of the methods. Calibration regression had $R^2 \geq 0.999$. Reference materials were used where appropriate.

7.2.4 Solid Phase Extraction (SPE)

The solutions from the end points of the batch experiments were passed through Isolute™ C18 1 g / 6 mL non polar SPE filters to retain organic substances (and thereby any organically bound metals). These filters were conditioned according to the manufacturer's instructions, and the solutions acidified to pH 5.5 prior to filtration using HNO_3 (the optimum pH for maximum organic matter retention by Isolute C18 filters (Thomas, 2000). The filtrates were further diluted with 2% HNO_3 for ICP-MS analysis to determine the inorganic/free aqueous metal concentrations. The concentration of organically bound metals was calculated from the difference in aqueous metals concentrations measured before (total $[M^+]$) and after SPE (inorganic/free $[M^+]$). Please note the important caveat that this is an operationally defined extraction and it is possible that a small percentage of metals bound to organic compounds may not retained by C18 filters will therefore be included in the aqueous fraction. The percentages calculated from this method should be used only as an indicator for the amount of organically bound metals.

7.3 Results

7.3.1 Sample Characterization

The full sample characterisation of RM and the 3 different soil samples has been described previously and is presented in chapter 5 (see Table 5.1and full XRF analysis is presented in Table 5.2). Briefly, the RM mineral content was dominated by hematite (Fe_2O_3), calcite ($CaCO_3$), magnetite (Fe_3O_4), cancrinite ($Na_6CaAl_6Si_6(CO_3)O_{24}{\cdot}2H_2O$) and hydrogarnet ($Ca_3AlFe(SiO_4)(OH_8)$ with residual boehmite (γ-AlOOH) and gibbsite

($Al(OH_3)$) phases, very similar to other red mud analysed from the breach area (Gelencser et al., 2011; Burke et al., 2012a). The concentrations of Cu and Ni in red mud was 104 and 361 mg kg^{-1} respectively (see Table 5.2).

All three soils had similar mineralogy, with quartz as the dominant mineral, and feldspars and clays were also present. The principal differences between them were in the organic carbon content, and the proportion of the 0.5 N HCl extractable iron in the Fe(II) oxidation state (see Table 5.1). The OR soil had the highest concentrations of Cu (12 mg kg^{-1}) and Ni (23 mg kg^{-1}). The WL soil had 6 mg kg^{-1} Cu and 14 mg kg^{-1} Ni. The SS soil had the lowest concentrations of Cu (2 mg kg^{-1}) and Ni (5 mg kg^{-1}) (see Table 5.2). PCA analysis (see Figure 5.1) shows soils sampled are of a similar composition to other unaffected reference soils from the area (Mayes et al., 2011).

7.3.2 Effect of RM addition on microcosm pH and DOC

The effect of red mud addition to pH and ORP on these batch experiments has been discussed in detail previously (see Chapter 6, section 6.3.3). Briefly, the average pH of both the anaerobic and aerobic soil only control experiments was between 7 and 8 (Figure 6.4 and 6.5). The pH of the anaerobic and aerobic experiments developed differently over time. The pH of the RM amended anaerobic systems (Figure 6.5 a-c) remained relatively constant after an initial equilibration period. For each soil type the RM amended systems had the order Soil SS> Soil WL> Soil OR with decreasing pH. Although the starting pH values of the red mud amended aerobic experiments were very similar to those of the anaerobic experiments, pH in all experiments gradually decreased over time (Figure 6.4 a-c). The final pH values of the 9% RM tests between 8 and 9 (~pH 8 in the OR tests, and just above pH 8.5 in the WL and SS tests). The final pH

values of the 33% RM tests were slightly higher than the equivalent 9% RM tests (~pH 8.5 in the OR tests, and between pH9 and 9.5 in the WL and SS tests). In all anaerobic experiments the ORP decreased to between −100 and −300 mV (Figure 6.4 d-f). In the aerobic experiments it increased to ~+250 mV (Figure 6.4 d-f.).

There is a clear pattern to the DOC concentrations measured at the end of the incubation periods (Table 7.1). In each of the six systems (three soils in anaerobic and aerobic conditions) the amount of DOC in solution increases with the RM loading. For each soil type there is also a significantly higher DOC concentration in the anaerobic system than in the equivalent aerobic system at the end of testing (this is most apparent in the OR Soil, 33% RM experiment, where the DOC concentration is ~850mg L^{-1} in the anaerobic system, but only ~82 mg L^{-1} in the aerobic system). Comparison of the three soils indicates that the DOC concentrations in OR soil tests were higher than in the equivalent WL or SS soil tests (the WL and SS soils exhibited broadly similar DOC concentrations in equivalent tests).

Table 7.1 – DOC concentrations (mg L^{-1}) at experiment end points

Experimental Conditions	Soil OR		Soil WL		Soil SS	
	Anaerobic	Aerobic	Anaerobic	Aerobic	Anaerobic	Aerobic
Unamended Control	81 (±8)	11 (±2)	21 (±2)	8 (±5)	NR	13 (±3)
9% RM Addition	150 (±3)	31 (±4)	95 (±16)	37 (±1)	149 (±22)	22 (±4)
33% RM Addition	850 (±6)	82 (±8)	209 (±39)	67 (±3)	262 (±4)	58 (±7)

NR – not analysed

7.3.3 Mobilisation of Cu and Ni from RM affected soil-water systems

The aqueous Cu concentrations in the anaerobic soil-only controls were all ~15 μg L^{-1}, and did not vary much with time (see Figure 7.1 a-c). After an equilibration period, the aqueous Cu concentrations in the anaerobic RM amended experiments were significantly higher than in the controls (Fig. 7.2 a-c), and increased with the amount of RM added (a slight exception is the OR Soil amended with 9% RM, where the final concentration was only slightly higher than the control, <25 μg L^{-1}). The highest aqueous Cu concentration of ~1450 μg L^{-1} was recorded after 30 days with the OR Soil amended with 33% RM, although this concentration subsequently decreased with time to ~850 μg L^{-1}. The aqueous Cu concentrations in the aerobic controls (Figure 7.2 a-c) were generally higher than in the anaerobic controls (typically about 20 μg L^{-1}), and showed more variation, but no trend with time. The aqueous Cu concentrations in the aerobic RM amended experiments were generally slightly higher than in the soil-only controls (25 - 100 μg L^{-1}), but significantly lower than in the equivalent anaerobic experiments.

The aqueous Ni concentrations in the anaerobic soil-only controls were all <10 μg L^{-1} (Figure 7.1 d-f), and did not vary much with time. In the anaerobic RM amended experiments the aqueous Ni concentration was higher than in the anaerobic controls, and followed a similar pattern to the evolution of aqueous Cu (although concentrations were about 5x smaller) (Figure 7.2 d-f). In the anaerobic systems amended with 33%RM the final Ni concentrations were 150, 42 and 34 μg L^{-1} for the OR, WL and SS soils, respectively. The aqueous Ni concentrations in the aerobic controls were generally slightly lower than in the anaerobic controls (typically <7 μg L^{-1}). Aqueous Ni concentrations in the aerobic RM amended experiments were similar to those of the

equivalent controls (Figure 7.2 d-f), with the exception of the OR Soil amended with 33% RM, which was significantly higher (Figure 7.2 d-f). In the aerobic systems amended with 33%RM the final Ni concentrations were 25, 6 and 5 μg L^{-1} for the OR, WL and SS soils, respectively.

Table 7.2, shows aqueous concentrations of other potentially problematic elements at the end of the batch experiments (it reports the data ranges observed with all three soils). It shows that in addition to Cu and Ni (the focus of this chapter), Al, As, Mo, Se, Ti and V can be also mobilised by red mud addition to anaerobic soil (Ba can be mobilised from these soils without the addition of RM). Under aerobic conditions the principal concerns will be Al, As and V (the environmental behaviour of these oxyanion forming elements with respect to the Ajka red mud spill has already been considered in previous work (see Chapters 5, 6 and 8 together with (Mayes et al., 2011; Burke et al., 2012a; Burke et al., 2013)).

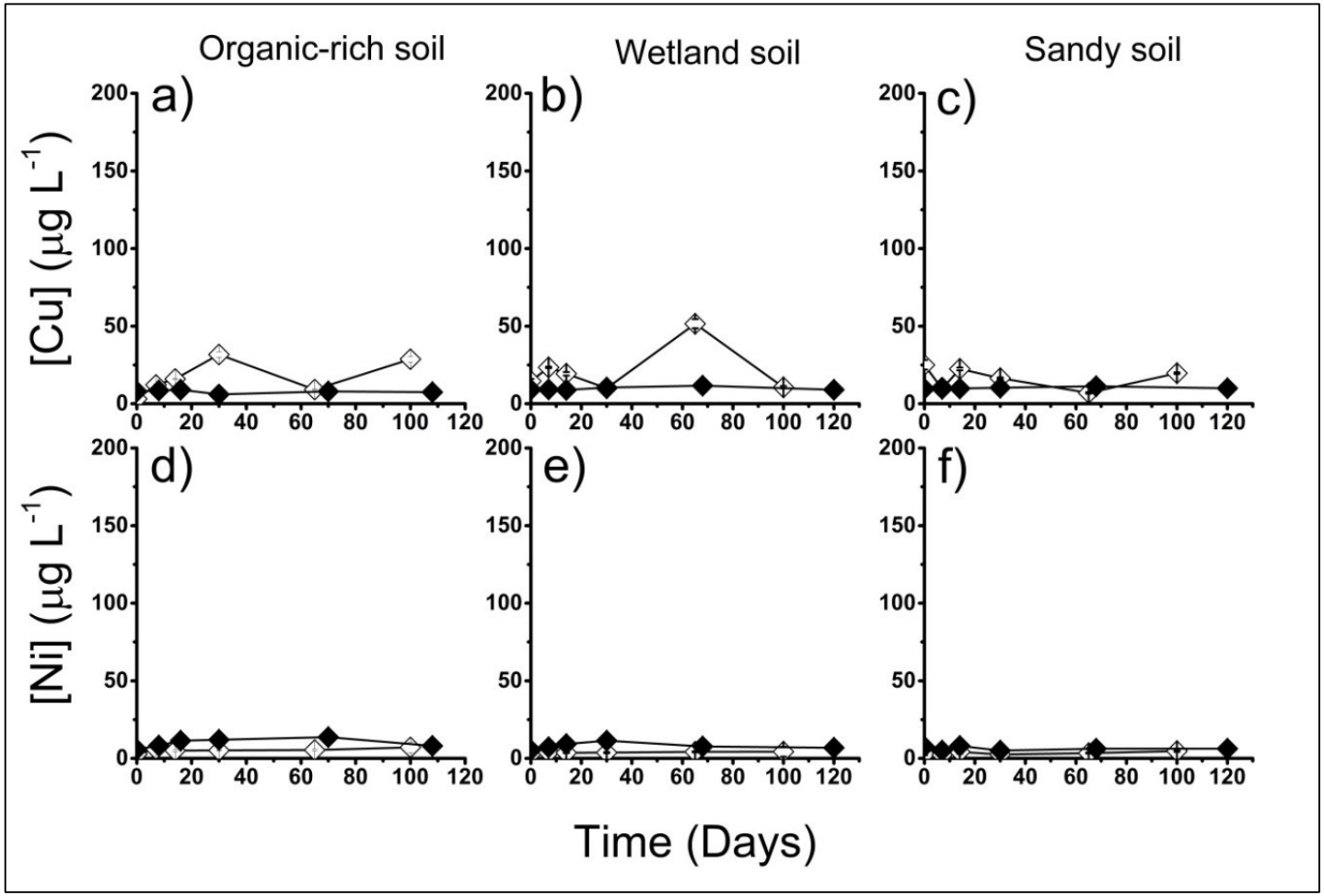

Figure 7.1 – Evolution of aqueous Cu and Ni over time in unamended control experiments. Full symbols = anaerobic, empty symbols = aerobic. Error bars are 1 σ of triplicate results (where not shown, errors are within the symbol).

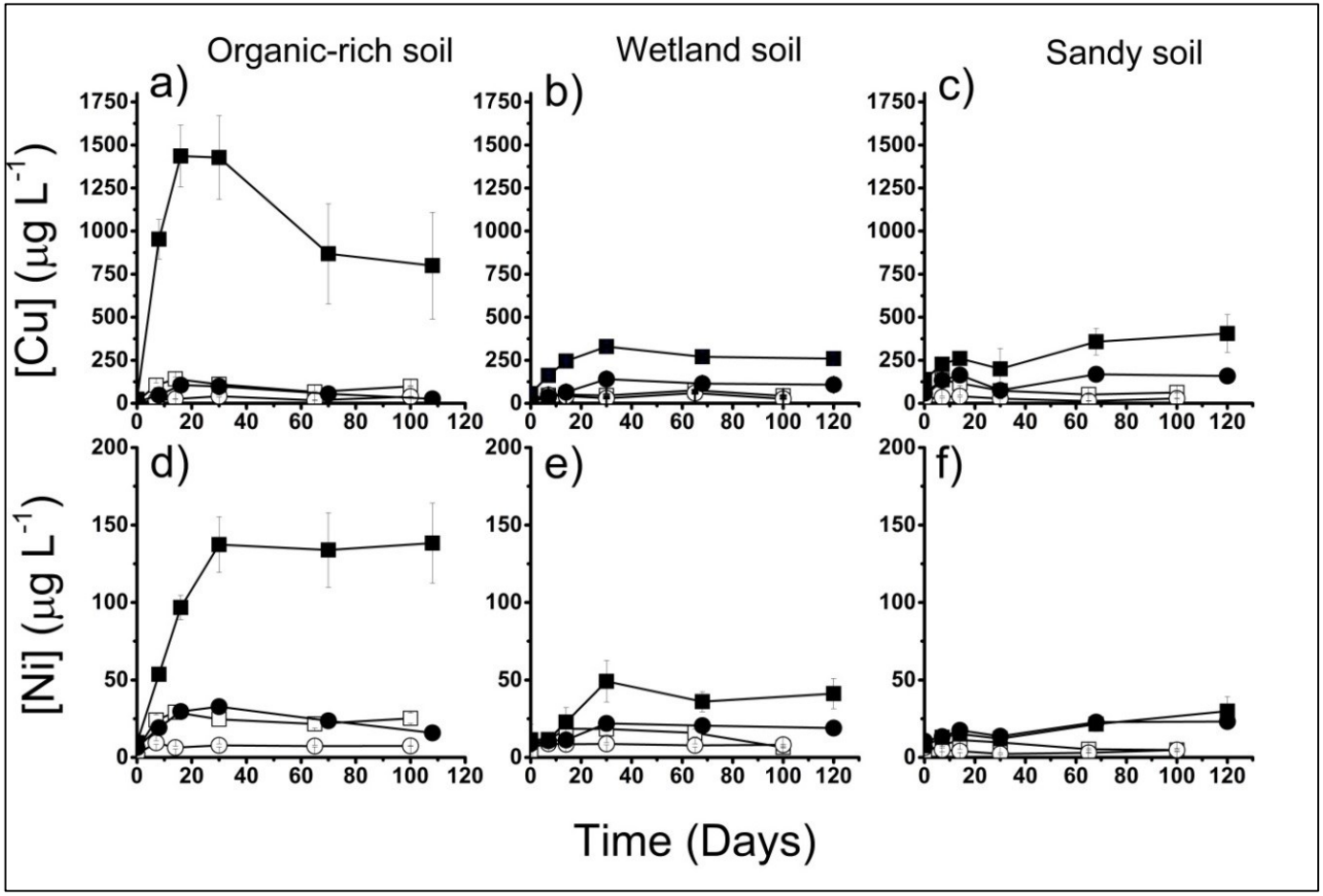

Figure 7.2 – Evolution of aqueous Cu and Ni over time in anaerobic and aerobic RM amended experiments. Black = anaerobic, white = aerobic. Square = 33% RM amended, Circle = 9% RM amended. Error bars are 1 σ of triplicate results (where not shown, errors are within the symbol).

Table 7.2 – Average metal concentrations (n =3) from batch experiments solutions taken from the experimental end point, listed in the order; Soil OR, Soil WL,Soil SS

Determinand ($\mu g\ L^{-1}$)	**Incubation conditions**	**0% red mud addition OR, WL, SS**	**9% red mud addition OR, WL, SS**	**33% red mud addition OR, WL, SS**
Al	Aerobic	7, 7, 0	25, 60, 30	344, 126, 163
	Anaerobic	14, 4, 12	80, 793, 1020	5490, 5212, 4620
As	Aerobic	bd	6, 67, 15	24, 177, 63
	Anaerobic	231, 190, 27	84, 53, 80	89, 104, 95
Ba	Aerobic	2, 0, 0	2, 2, 1	141, 1, 1,
	Anaerobic	90, 70, 71	83, 102, 87	129, 154, 125
Cd	Aerobic	0, 1, 1	0, 1, 1	1, 1, 3
	Anaerobic	0, 0, 0	0, 1, 2	11, 4, 4
Co	Aerobic	bd	Bd	2, 0, 0
	Anaerobic	1, 0, 2	1, 2, 2	24, 4, 2
Cr	Aerobic	bd	0-8 (±1)	20-40 (±8)
	Anaerobic	4, 1, 2	9, 9, 2	102, 19, 11
Cu	Aerobic	29, 10, 19	39, 26, 28	98, 43, 63
	Anaerobic	12, 10, 8	23, 102, 131	858, 249, 340
Hg	Aerobic	bd	0, 0, 3	0, 0, 4
	Anaerobic	bd	Bd	0, 0, 87
Mo	Aerobic	0, 4, 0	15, 169, 14	47, 649, 58
	Anaerobic	261, 254, 5	340, 385, 132	909, 935, 627
Ni	Aerobic	9, 4, 4	7, 8, 4	25, 6, 4
	Anaerobic	7, 6, 0	13, 20, 34	150, 42, 20
Pb	Aerobic	bd	Bd	bd
	Anaerobic	dd	Bd	0, 0, 69
Se	Aerobic	7, 0, 0	14, 8, 0	15, 11, 0
	Anaerobic	bd	167, 133, 0	134, 158, 0
Ti	Aerobic	bd	4, 6, 2	48, 7, 7
	Anaerobic	bd	7, 14, 18	143, 41, 118
V	Aerobic	bd	15-125 (±9)	108-325 (±35)
	Anaerobic	4, 0, 4	45, 62, 122	669, 128, 225
Zn	Aerobic	4, 7, 10	5, 7, 10	29, 7, 10
	Anaerobic	74, 26, 40	45, 9, 21	39, 9, 20

7.3.5 Organically bound metals

Tables 7.3a and 7.3b show the percentages of Cu and Ni from the incubation end point solution of batch experiments that were organically complexed. With the exception of the WL aerobic control experiment, a significant proportion of the aqueous Cu is organically complexed in all systems. This proportion is generally higher in the experiments where red mud was added. There was little difference between anaerobic and aerobic conditions in the OR systems but more organically complexed Cu in the anaerobic system compared to the aerobic system. No organically complexed Ni was found in either set of controls experiments. However organically complexed Ni was found in aerobic experiments with OR and WL soil where 33% RM was added, and significant amounts of organically complexed Ni was found in all the anaerobic experiments where RM was added.

Table 7.3a) - % Organically bound aqueous metals from anaerobic end point solutions

Experimental Conditions	% Cu			% Ni		
	Soil OR	Soil WL	Soil SS	Soil OR	Soil WL	Soil SS
Unamended controls	37 (±13)	64 (±2)	NR	0*	0*	NR
9% RM addition	73 (±6)	91 (±1)	57 (±9)	28 (±6)	34 (±9)	14 (±2)
33% RM addition	70 (±7)	80 (±3)	73 (±7)	46 (±10)	39 (±7)	48 (±13)

Table 7.3b) - % Organically bound aqueous metals from aerobic end point solutions

Experimental Conditions	% Cu			% Ni		
	Soil OR	Soil WL	Soil SS	Soil OR	Soil WL	Soil SS
Unamended controls	65 (±3)	4 (±4)	47 (±8)	0*	0*	0*
9% RM addition	72 (±2)	55 (±4)	60 (±3)	0*	0*	0*
33% RM addition	75 (±2)	32 (±1)	55 (±2)	55 (±5)	12 (±10)	0*

NR – not analysed

0* - inorganic/free[M^+] was ≥ total [M^+] therefore organically bound [M^+] was deemed to be zero.

7.4 Discussion

7.4.1 Effect of red mud addition on soil pH and DOC

When red mud was added to the anaerobic soil-water systems there was an immediate increase in pH which was related to the red mud loading, after which there the pH remained relatively constant throughout the incubation period. The final pH of values of these systems increased with red mud loading because red mud contains sodium hydroxide, but also varied with soil type due to differences in buffering capacity. In previous experiments the pH buffering capacity of these soils was attributed to the clay minerals and particularly to the amount of organic matter present (see Chapter 5), with buffering of alkaline perturbations resulting from deprotonation (reactions 7.1 and 7.2: (Celik, 2004) (Stevenson, 1994):

$$[\text{Clay-M-OH}] + [OH^-] \leftrightarrow [\text{Clay-M-O}^-] + H_2O \quad (7.1)$$

$$[\text{R-COOH}] + [OH^-] \leftrightarrow [\text{R-COO}^-] + H_2O \quad (7.2)$$

The dissolution of amorphous and poorly crystalline silica starts to become important in systems with a pH above 9.8 (Langmuir, 1997) so may also affect the buffering capacity of systems with a high pH and a high quartz content (reaction 7.3 (Langmuir, 1997)).

$$[SiO_2] + 2[H_2O] \leftrightarrow [H_2SiO_4^-] + [H^+] \quad (7.3)$$

Thus, at each red mud loading, the pH value of the SS system > the WL system > the OR system.

In aerobic systems there was also an initial increase in pH upon red mud addition (similar to the anaerobic systems), however there was a subsequent gradual

decrease of pH. The latter trend is explained by carbonation by atmospheric CO_2, as formation of aqueous carbonate species consumes OH^- resulting in a reduction in pH (Schwab et al., 2006). The carbonate ions can also react with any M^{2+} ions present (e.g. Ca^{2+} and Mg^{2+} from either the soils or the red mud) to precipitate carbonate minerals, therefore the final pH of all the systems is buffered to between 8.0 and 9.5 regardless of soil type.

For the anaerobic experiments, the DOC released from the organic rich soil systems was between 3 and 4 times higher than that released from the wetland or sandy soil systems at the same level of red mud loading. This suggests that the amount of soil organic matter present is the main factor controlling DOC release in these experiments (Soil OR has 4.15% TOC compared to 1.14% in Soil WL and 0.74% in Soil SS). The higher initial pH values of Soil WL and Soil SS compared with Soil OR (7.9, 7.9 and 7.0 respectively) may have meant that SOM in these soils contained a lower proportion of humic acids (humic acids are a mixture of chemically similar compounds that dissolve progressively with increasing pH). Under aerobic conditions, the DOC concentration in the batch experiment end point solutions were much lower than in the equivalent anaerobic tests (up to 10x less at the same red mud loading). This is likely to be due to the carbonation reactions described above removing OH^- from solution, resulting in lower amount of organic carbon mobilisation. Another mechanism that may have contributed to the increased DOC concentrations in the anaerobic experiments is release during microbial reduction of Fe(III) oxyhydroxides (when Fe oxydroxides dissolve they can release sorbed organic matter (Zachara et al., 2001; Grybos et al., 2009).

7.4.2 Controls on Cu release

Cu solubility in soils is often controlled by variation in pH, with high aqueous concentrations found at low pH due to reductive adsorption to positively charged mineral surfaces (Peacock and Sherman, 2004a; Peacock and Sherman, 2005). At neutral and high pH values, Cu^{2+} adsorbs strongly to negatively charged mineral surfaces and solution concentrations are low (Peacock and Sherman, 2004a). In the presence of DOC, Cu can form stable aqueous complexes thus increasing Cu concentrations in neutral and alkaline conditions (Wu et al., 2002; Fulda et al., 2013b). In the alkaline red mud amended soil experiments, there was a significant proportion of dissolved Cu (Table 7.3a and 7.3b) retained on SPE resin filters in all experiments, suggesting that organically complexed Cu formed a significant fraction of the total dissolved Cu. There was also a significant positive correlation between aqueous Cu concentrations and DOC during both anaerobic and aerobic incubations (Pearson's r = 0.82-0.87; p = <0.001; Table 7.4), suggesting that the main control of Cu solubility in these experiments was complexation of Cu with dissolved organic matter. These findings are in agreement with previous work, which found that ~ 62% of Cu mobilised from soils amended with red mud was associated primarily with OM (Lombi et al., 2002).

In the anaerobic soil-water systems there was a general trend of increasing aqueous Cu concentration with increasing DOC concentration at the end of the incubation periods. This trend is very strong when maximum aqueous Cu concentration is correlated with the DOC concentration measured in the end point solutions (Table 7.3a), but the aqueous Cu concentrations at the end of Soil OR tests fall below this trend. The pH values in these tests do not vary significantly between the point when the

maximum aqueous Cu concentration was measured and the end of the test, so the decrease in aqueous Cu concentration is unlikely to be associated with humate solubility, however there was also a decrease in the redox potential in this time period (see Fig. 6.5) that may have may affected Cu speciation and solubility.

Microbial sulfate reduction occurred in the anaerobic Soil OR tests, to a small extent in the WL tests, but not in the SS tests (see Chapter 6, section 6.3.4). Under oxidising conditions the stable Cu species in inorganic systems are Cu(II), but they are Cu(I) and Cu(0) under more reducing conditions (Leckie and Davis, 1979; Weber et al., 2009). An Eh/pH diagram for relevant inorganic Cu species is shown in Figure 7.3, with the Eh/pH states of the anaerobic tests annotated on it. This shows that the anaerobic OR tests reached an Eh/pH state where sulfide can complete for Cu. Both Cu(II) and Cu(I) form complexes with organic matter thus increasing the stability of Cu(I) under certain conditions. However, in strongly reducing sulfide-rich environments inorganic sulfide is thought to compete with OM for Cu(I) (Fulda et al., 2013b). Thus, formation of solid sulfide associated Cu following sulfate reduction may account for the trend of reducing Cu concentrations observed in the Soil OR experiments after 30 days in red mud amended experiments, although Cu concentrations in these experiment still remain relatively high (Figure 7.2 a-b).

For all the tests on the three soils, the maximum aqueous Cu concentration is less than the amount of Cu that was present in the soil prior to the addition of red mud (the highest proportion was mobilised in the anaerobic OR 33% RM addition experiment, where it is equivalent to 90% of the Cu originally associated with the soil). Thus it is not possible to determine whether it is soil associated or red mud associated Cu that is mobilised to solution. However it is entirely possible that the Cu mobilised to

solution represents organically complex Cu associated with the soils that is mobilised due to the pH increases associated with red mud addition alone.

7.4.3 Controls on Ni release

Like Cu, nickel solubility decreases with increasing pH due to increased sorption to negatively charged minerals surfaces (Richter and Theis, 1980), and above pH 9 Ni forms insoluble $Ni(OH)^+$ and $Ni(OH)_2$ species (Bradbury and Baeyens, 2009). Whilst Ni speciation is not affected by redox chemistry (it tends to form Ni(II) ions and complexes (Brookins, 1988)), it is known to form stable complexes with OM which can increase the solubility of Ni in some systems (Richter and Theis, 1980; Achterberg et al., 1997; Ashworth and Alloway, 2004).

Concentrations of Ni solubilised in red mud affected soil-water systems and the percentage of aqueous Ni retained by SPE filters was generally lower than for Cu. Only low concentrations (<25 $\mu g\ L^{-1}$) of Ni were mobilised under aerobic conditions and soluble organically bound Ni (i.e. the amount retained on SPE filters) was not measurable for most of the experiments (except for the organic rich and wetland soil systems amended with 33% red mud) (Tables 7.3a and 7.3b). Under anaerobic conditions the amount of organically bound Ni retained on SPE filters increased in line with red mud loading. However, Ni release was still relatively low (<50 μL^{-1}) in all anaerobic experiments except where DOC concentrations are elevated in the organic-rich 33% amended experiment. There is a strong positive correlation with DOC under both anaerobic and aerobic conditions (Table 7.4 r = 0.64-0.62, p value = ≤0.01). An Eh/pH diagram for relevant inorganic Ni species is shown in Fig. 7.4, with the Eh/pH states of the anaerobic tests annotated on it. This figure shows the thermodynamically

stable Ni containing phase is NiO without SOM present, except where strongly reducing conditions developed towards the end of the anaerobic OR tests, where sulfidic phase [NiS_2] should be the stable. However, unlike Cu, there is little change in the aqueous Ni concentration. This may be because a lower proportion of the Ni is organically bound, or may reflect the significantly lower aqueous nickel concentrations (Cu concentrations are 10x higher in this experiment, Figure 7.2). These data indicate that DOC is an important mechanism for controlling Ni solubility, especially when DOC concentrations are elevated, but compared to Cu, the affinity for OM to Ni is weaker (Ashworth and Alloway, 2004), which resulted in lower aqueous Ni concentrations despite all three soil-water systems containing higher total nickel concentrations.

Table 7.4 - Pearson's regression correlation values for aqueous Cu and Ni concentrations vs pH or DOC for red mud amended experiments after 100-120 days incubation

Determinand	**Experimental Conditions**	
	Anaerobic (r ; p-value)	Aerobic (r ; p-value)
[Cu] vs		
DOC	0.87; <0.001	0.82; <0.001
pH	0.34; 0.200	0.03; 0.900
[Ni] vs		
DOC	0.64; 0.004	0.62; 0.006
pH	0.05; 0.800	-0.41; 0.090

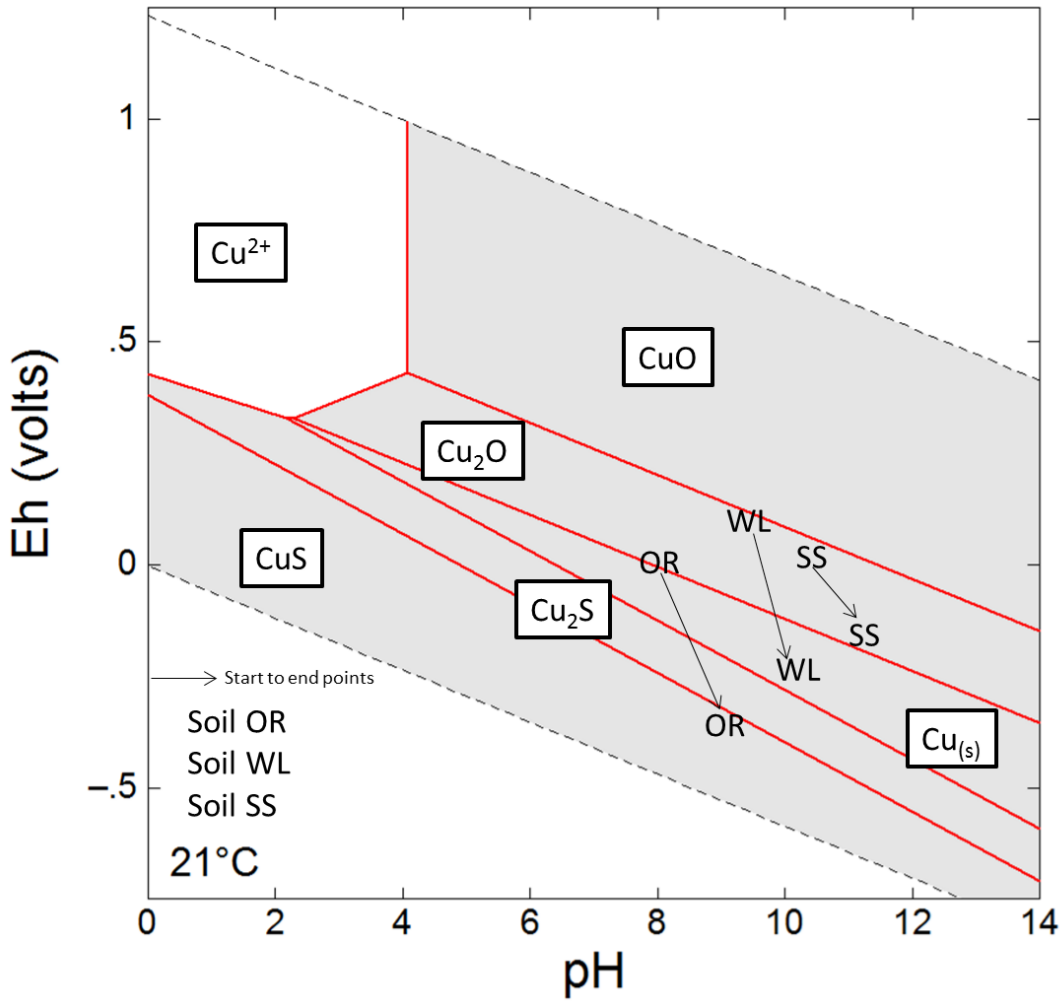

Figure 7.3 – Eh/pH conditions calculated for 33% RM amended anaerobic experiments superimposed on an Eh/pH Cu species predominance and relative mineral stability diagram calculated using Geochemists Workbench® for t = 21°C / P = 1 at, for the system Cu-O-H-SO_4^{2-} with log ∑Cu/m = -.3256, log $\sum SO_4^{2-}$/m -.3646 and a[$H_2O_{(aq)}$] = 1. Points plotted show geochemical conditions at day zero and experimental end points.

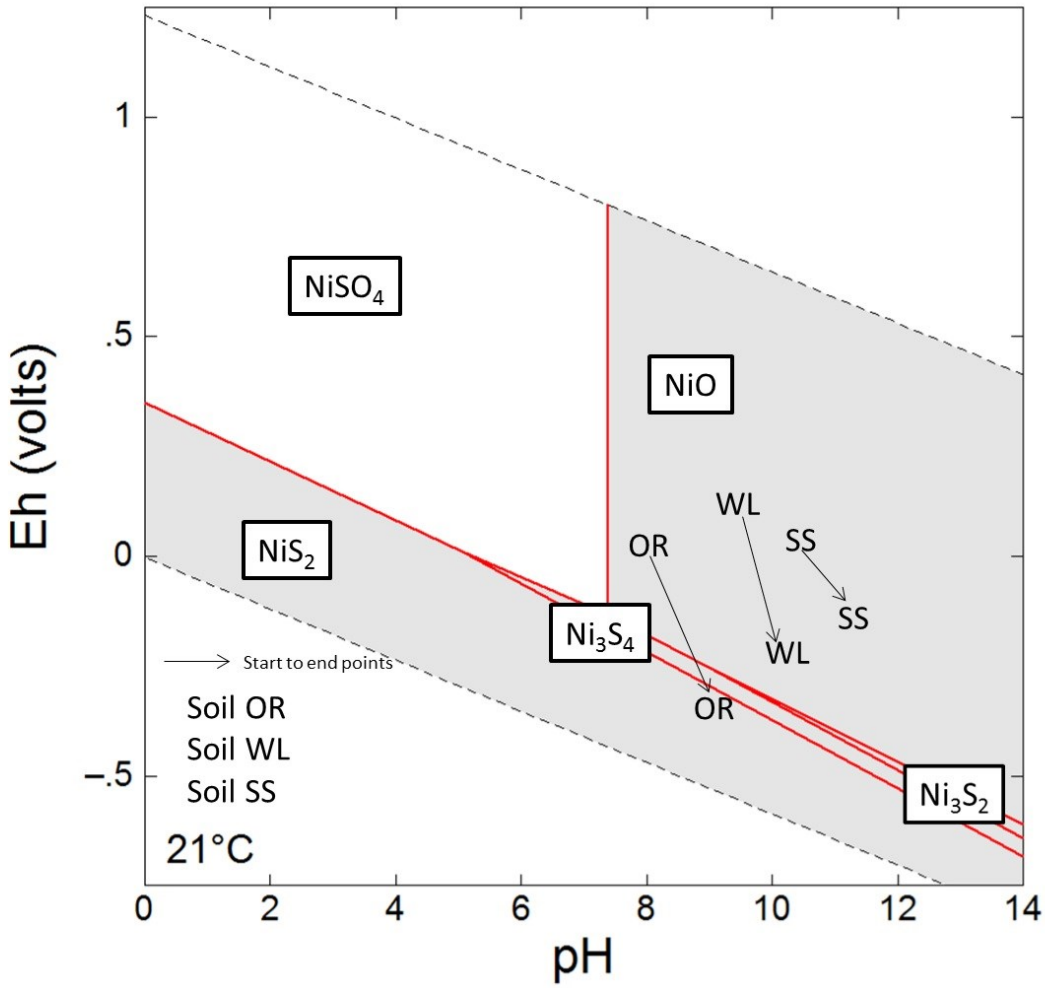

Figure 7.4 – Eh/pH conditions calculated for 33% RM amended anaerobic experiments superimposed on an Eh/pH Ni species predominance and relative mineral stability diagram calculated using Geochemists Workbench® for t = 21°C / P = 1 at, for the system Ni-O-SO_4^{2-} with log ∑Ni/m = -.3256, log ∑SO_4^{2-} -.3646 and a[$H_2O_{(aq)}$] = 1. Points plotted show geochemical conditions at day zero and experimental end points.

7.5 Conclusions

The alkalisation of soils following red mud addition increased the leaching of DOC from soils. If the red mud loading and SOM are sufficiently high this will result in increased mobilisation of Cu and Ni through OM complexation compared to unaffected soils. This mechanism is especially prevalent under anaerobic conditions, where the lack of carbonation reactions, that did occur in the aerobic experiments, that remove OH^- from solution, result in higher concentrations of aqueous organic carbon mobilisation and also reductive dissolution of mineral surfaces which releases further DOM previously bound to surfaces (Zachara et al., 2001) .

SPE extraction shows that Cu has a greater affinity for DOC compared to Ni in these experiments. The mobility of Cu may be retarded under sufficiently reducing conditions (after SO_4^{2-} reduction), where Cu removal will occur due to the formation of insoluble Cu mineral phases. Nickel mobility is not likely to be problematic. The pH increase following red mud addition means that Ni will likely form insoluble (hydr)oxides and will not be mobilised unless very high concentrations of DOC are present.

Further to previous studies following the Kolontár disaster (Mayes et al., 2011; Klebercz et al., 2012; Milacic et al., 2012; Gruiz, 2012), this study also verifies that costly large scale red mud removal from soils by Hungarian authorities was vindicated. However, as the leaching of metals is much greater under anaerobic conditions, this leads to concerns about the water quality in unremediated wetland areas, especially those that received high red mud loadings. These experiments also highlight the problematic leaching of several other elements under anaerobic conditions; Al, As, Mo,

Se, Ti and V, although only Al, As and V were found to be potentially problematic under aerobic conditions.

These data also call for caution in the use of high pH red mud as a soil ameliorant for Cu contaminated soils which are high in SOM. Soil alkalisation promotes DOC release and thus the mobilisation of complexed metals; such as Cu and to some extent Ni (and potentially other metals which are known to form stable OM complexes, such as Cd, V and Zn).

7.6 References

ACHTERBERG, E. P., VAN DEN BERG, C. M. G., BOUSSEMART, M. & DAVISON, W. 1997. Speciation and cycling of trace metals in Esthwaite Water: A productive English lake with seasonal deep-water anoxia. Geochimica Et Cosmochimica Acta, 61, 5233-5253.

ADAM, J., BANVOLGYI, G., DURA, G., GRENERCZY, G., GUBECK, N., GUPTER, I., SIMON, G., SZEGFALVI, Z., SZEKACS, A., SZEPVOLGYI, J. & UJLAKY, E. 2011. The Kolontar report: Causes and Lessons from the Red Mud Disaster. In: B, J. (ed.). Budapest: Sustainable Development Committee of the Hungarian Parliament.

ANTON, A., REKASI, M., UZINGER, N., SZEPLABI, G. & MAKO, A. 2012. Modelling the Potential Effects of the Hungarian Red Mud Disaster on Soil Properties. Water Air and Soil Pollution, 223, 5175-5188.

ASHWORTH, D. J. & ALLOWAY, B. J. 2004. Soil mobility of sewage sludge-derived dissolved organic matter, copper, nickel and zinc. Environmental Pollution, 127, 137-144.

BASEL CONVENTION 2011. Basel Convention on the control of transboundary movements of hazardous waste and their disposal. In: UNITED NATIONS ENVIRONMENT PROGRAMME (ed.) Annex IX. Switzerland: Secretariat of the Basel Convention,.

BRADBURY, M. H. & BAEYENS, B. 2009. Sorption modelling on illite Part I: Titration measurements and the sorption of Ni, Co, Eu and Sn. Geochimica Et Cosmochimica Acta, 73, 990-1003.

BROOKINS, D. 1988. Eh, pH diagrams for geochemistry, Berlin., Springer-Verlag.

BURKE, I. T., MAYES, W. M., PEACOCK, C. L., BROWN, A. P., JARVIS, A. P. & GRUIZ, K. 2012. Speciation of arsenic, chromium, and vanadium in red mud samples from the ajka spill site, hungary. Environmental Science & Technology, 46, 3085-92.

BURKE, I. T., PEACOCK, C. L., LOCKWOOD, C. L., STEWART, D. I., MORTIMER, R. J. G., WARD, M. B., RENFORTH, P., GRUIZ, K. & MAYES, W. M. 2013. Behavior of Aluminum, Arsenic, and Vanadium during the Neutralization of Red Mud Leachate by HCl, Gypsum, or Seawater. Environmental Science & Technology, 47, 6527-6535.

CELIK, M. S. 2004. Electrokinetic behaviour of clay surfaces. In: WYPYCK, F. & SATYANARAYANA, K. G. (eds.) Clay Surfaces: Fundamentals and Applications. London: Elsevier Ltd.

CHESHIRE, M. V., BERROW, M. L., GOODMAN, B. A. & MUNDIE, C. M. 1977. METAL DISTRIBUTION AND NATURE OF SOME CU, MN AND V COMPLEXES IN HUMIC AND FULVIC-ACID FRACTIONS OF SOIL ORGANIC-MATTER. Geochimica Et Cosmochimica Acta, 41, 1131-1138.

DAVIS, J. A. 1984. Complexation of trace metals by adsorbed natural organic matter. Geochimica Et Cosmochimica Acta, 48, 679-691.

ENSERINK, M. 2010. ENVIRONMENT After Red Mud Flood, Scientists Try to Halt Wave of Fear and Rumors. Science, 330, 432-433.

FULDA, B., VOEGELIN, A., EHLERT, K. & KRETZSCHMAR, R. 2013a. Redox transformation, solid phase speciation and solution dynamics of copper during soil reduction and reoxidation as affected by sulfate availability. Geochimica Et Cosmochimica Acta, 123, 385-402.

FULDA, B., VOEGELIN, A., MAURER, F., CHRISTL, I. & KRETZSCHMAR, R. 2013b. Copper Redox Transformation and Complexation by Reduced and Oxidized Soil Humic Acid. 1. X-ray Absorption Spectroscopy Study. Environmental Science & Technology, 47, 10903-10911.

GELENCSER, A., KOVATS, N., TUROCZI, B., ROSTASI, A., HOFFER, A., IMRE, K., NYIRO-KOSA, I., CSAKBERENYI-MALASICS, D., TOTH, A., CZITROVSZKY, A., NAGY, A., NAGY, S., ACS, A., KOVACS, A., FERINCZ, A., HARTYANI, Z. & POSFAI, M. 2011. The Red Mud Accident in Ajka (Hungary): Characterization and Potential Health Effects of Fugitive Dust. Environmental Science & Technology, 45, 1608-1615.

GRAFE, M., POWER, G. & KLAUBER, C. 2011. Bauxite residue issues: III. Alkalinity and associated chemistry. Hydrometallurgy, 108, 60-79.

GRUIZ, K., FEIGL, V., KLEBERCZ, O., ANTON, A., AND VASZITA, E. Environmental Risk Assessment of Red Mud Contaminated Land in Hungary. Geocongress 2012: State of the Art and Practice in Geotechnical Engineering, 2012. American Society of Civil Engineers, 4156-4165.

GRYBOS, M., DAVRANCHE, M., GRUAU, G., PETITJEAN, P. & PEDROT, M. 2009. Increasing pH drives organic matter solubilization from wetland soils under reducing conditions. Geoderma, 154, 13-19.

HIND, A. R., BHARGAVA, S. K. & GROCOTT, S. C. 1999. The surface chemistry of Bayer process solids: a review. Colloids and Surfaces a-Physicochemical and Engineering Aspects, 146, 359-374.

KLEBERCZ, O., MAYES, W. M., ANTON, A. D., FEIGL, V., JARVIS, A. P. & GRUIZ, K. 2012. Ecotoxicity of fluvial sediments downstream of the Ajka red mud spill, Hungary. Journal of environmental monitoring : JEM, 14, 2063-71.

LANGMUIR, D. 1997. Aqueous environmental geochemistry, Upper Saddle River, N. J., Prentice Hall.

LECKIE, J. O. & DAVIS, J. A. 1979. Aqueous Environmental Chemistry of Copper. In: NRIAGU, J. O. (ed.) Copper in the Environment Part 1: Ecological Cycling. New York: John Wiley & Sons Inc.

LIU, Y., LIN, C. & WU, Y. 2007. Characterization of red mud derived from a combined Bayer Process and bauxite calcination method. Journal of Hazardous Materials, 146, 255-261.

LOMBI, E., ZHAO, F. J., ZHANG, G. Y., SUN, B., FITZ, W., ZHANG, H. & MCGRATH, S. P. 2002. In situ fixation of metals in soils using bauxite residue: chemical assessment. Environmental Pollution, 118, 435-443.

MAYES, W. M., JARVIS, A. P., BURKE, I. T., WALTON, M., FEIGL, V., KLEBERCZ, O. & GRUIZ, K. 2011. Dispersal and Attenuation of Trace Contaminants Downstream of the Ajka Bauxite Residue (Red Mud) Depository Failure, Hungary. Environmental Science & Technology, 45, 5147-5155.

MILACIC, R., ZULIANI, T. & SCANCAR, J. 2012. Environmental impact of toxic elements in red mud studied by fractionation and speciation procedures. Science of the Total Environment, 426, 359-365.

NAGY, A. S., SZABO, J. & VASS, I. 2013. Trace metal and metalloid levels in surface water of the Marcal River before and after the Ajka red mud spill, Hungary. Environmental Science and Pollution Research, 20, 7603-7614.

PARSONS, J. W. 1988. Isolation of Humic Substances from Soils and Sediments. In: FRIMMEL, F. H. A. C., R. F. (ed.) Humic Substances and Their Role in the Environment. Berlin, Germany: John Wiley & Sons.

PEACOCK, C. L. & SHERMAN, D. M. 2004. Copper(II) sorption onto goethite, hematite and lepidocrocite: A surface complexation model based on ab initio molecular geometries and EXAFS spectroscopy. Geochimica Et Cosmochimica Acta, 68, 2623-2637.

PEACOCK, C. L. & SHERMAN, D. M. 2005. Surface complexation model for multisite adsorption of copper(II) onto kaolinite. Geochimica Et Cosmochimica Acta, 69, 3733-3745.

PEACOCK, C. L. & SHERMAN, D. M. 2007. Sorption of Ni by birnessite: Equilibrium controls on Ni in seawater. Chemical Geology, 238, 94-106.

POWER, G., GRAFE, M. & KLAUBER, C. 2011. Bauxite residue issues: I. Current management, disposal and storage practices. Hydrometallurgy, 108, 33-45.

REEVES, H. J., WEALTHALL, G. & YOUNGER, P. L. 2011. Advisory visit to the bauxite processings tailings dam near Ajka, Vesprem County, western Hungary. . Keyworth, UK: British Geological Survey.

REKASI, M., FEIGL, V., UZINGER, N., GRUIZ, K., MAKO, A. & ANTON, A. 2013. Effects of leaching from alkaline red mud on soil biota: modelling the conditions after the Hungarian red mud disaster. Chemistry and Ecology, 29, 709-723.

RENFORTH, P., MAYES, W. M., JARVIS, A. P., BURKE, I. T., MANNING, D. A. C. & GRUIZ, K. 2012. Contaminant mobility and carbon sequestration downstream of the Ajka (Hungary) red mud spill: The effects of gypsum dosing. The Science of the total environment, 421-422, 253-9.

RICHTER, R. O. & THEIS, T. L. 1980. Nickel Speciation in a Soil/Water System. In: NRIAGU, J. O. (ed.) Nickel in the Environment.

RUBINOS, D. A. & BARRAL, M. T. 2013. Fractionation and mobility of metals in bauxite red mud. Environmental science and pollution research international, 20, 7787-802.

SCHWAB, A. P., HICKEY, J., HUNTER, J. & BANKS, M. K. 2006. Characteristics of blast furnace slag leachate produced under reduced and oxidized conditions. J Environ Sci Health A Tox Hazard Subst Environ Eng, 41, 381-95.

SPARKS, D. L., SCHEIDEGGER, A. M., STRAWN, D. G. AND SCHECKEL, K.G. 1998. Kinetics and Mechanisms of Metal Sorption at the Mineral-Water Interface. In: SPARKS, D. L. A. G., T. J. (ed.) Mineral-Water Interfacial Reactions: Kinetics and Mechanisms. Washington: ACS

STEVENSON, F. J. 1994. Humus chemistry: genesis, composition, reactions, John Wiley and Sons Inc.

THOMAS, B. 2000. Solid phase extraction for the removal of organic-iron complexes in contaminated groundwater. MSc MSc The University of Leeds.

WEBER, F.-A., VOEGELIN, A. & KRETZSCHMAR, R. 2009. Multi-metal contaminant dymanics in temporarily flooded soil under sulfate limitation. Geochimica Et Cosmochimica Acta, 73, 5513-5527.

WILKIE, M. P. & WOOD, C. M. 1996. The adaptations of fish to extremely alkaline environments. Comparative Biochemistry and Physiology B-Biochemistry & Molecular Biology, 113, 665-673.

WU, J., WEST, L. J. & STEWART, D. I. 2001. Copper(II) humate mobility in kaolinite soil. Engineering Geology, 60, 275-284.

WU, J., WEST, L. J. & STEWART, D. I. 2002. Effect of humic substances on Cu(II) solubility in kaolin-sand soil. Journal of Hazardous Materials, 94, 223-238.

YIN, Y. J., IMPELLITTERI, C. A., YOU, S. J. & ALLEN, H. E. 2002. The importance of organic matter distribution and extract soil : solution ratio on the desorption of heavy metals from soils. Science of the Total Environment, 287, 107-119.

ZACHARA, J. M., FREDRICKSON, J. K., SMITH, S. C. & GASSMAN, P. L. 2001. Solubilization of Fe(III) oxide-bound trace metals by a dissimilatory Fe(III) reducing bacterium. Geochimica Et Cosmochimica Acta, 65, 75-93.

Chapter 8 Leaching of vanadium in soil-water systems contaminated by red mud from Ajka, Hungary

Abstract

Red mud is a highly alkaline (pH >12) waste product from bauxite ore processing, it contains elevated concentrations of vanadium, an oxyanion forming element that is mobilised at high pH. In 2010, a tailings dam failure at a red mud repository released 1 million m^3 of red mud into the surrounding area. It has been determined that V is a likely contaminant from red mud, due to a lack of immobilisation during neutralisation processes and elevated concentrations of V found at depositional hot spots. The mobilisation of V from red mud into affected soil-water systems was investigated in experiments analogous to soil conditions following the remediation efforts. Three different Hungarian soils with a red mud addition were incubated in aerobic and anaerobic batch microcosm experiment to assess the mechanisms of V mobilisation, together with XAS spectroscopy and solid phase extraction techniques. The results showed that V release in red mud affected soil-water systems was highly dependent upon the different properties of the three soils. XAS spectroscopy showed that V in two of the soils was reduced from V(V) to V(IV), in one soil this resulted in a reduction of aqueous V concentrations but in another soil with a high TOC content, increased concentrations due to complexation with DOC. These results also proved that the extensive remediation efforts by the Hungarian authorities were justified but that red mud should be used with caution as a soil amendment especially in soils with a high TOC content. These results also highlight the complex competing processes of V at high pH and how a more fundamental understanding of these processes is required.

8.1 Introduction

Red mud is the name given to the fine fraction residue that remains after alumina is extracted from bauxite ore during the Bayer process. The composition of red mud is highly dependent upon the type of bauxite ore used (Hind et al., 1999; Liu et al., 2007), but is typically comprised of; residual iron oxides, quartz, sodium aluminosilicates, titanium dioxide, calcium carbonate/aluminate and sodium hydroxide (Hind et al., 1999; Grafe et al., 2011; Gelencser et al., 2011). The use of NaOH during the Bayer process means that unless neutralisation steps are taken during the refining process then red mud often has pH in excess of 12, (Grafe et al., 2011; Power et al., 2011). Red mud also is known to contain elevated concentrations of toxic and potentially toxic metals and metalloids (such as Al, As, Cr, Cu, Mo, Ni and V) (Cornelis et al., 2008; Grafe et al., 2011). High pH red mud leachates (up to pH 13 (Burke et al., 2013)) also have high levels of dissolved salts (up to 160 mS cm^{-2}) (Mayes et al., 2011) and can mobilise high concentrations of oxyanion forming elements which are more soluble at high pH (Langmuir, 1997; Burke et al., 2013).

Since the catastrophic tailings dam failure at the Ajkai Timfoldgyar Zrt alumina plant in Ajka, western Hungary in October 2010 there have been several studies on the possible consequences from large quantities of caustic red mud reaching the wider environment. These studies have investigated the effects of red mud on human health (Gelencser et al., 2011); soil toxicity (Ruyters et al., 2011; Anton et al., 2012); freshwater and soil ecology (Klebercz et al., 2012; Rekasi et al., 2013); the mobility of red mud associated trace metals in the wider environment (Mayes et al., 2011; Burke et al., 2012a) and the effectiveness of the remediation efforts (Renforth et al., 2012; Burke et al., 2013).

Remediation efforts began almost immediately following the spill and consisted of the addition of gypsum and acids (acetic and sulfuric) to reduce the pH of affected rivers and streams and, removal of red mud from affected land. The removal of red mud from land sought to prevent any complications red mud dust inhalation and to lessen effects to soils (Adam et al., 2011a). The land remediation effort was split in to two categories, thick red mud deposits (>5cm) were removed from the soil whereas thin red mud deposits (<5cm) were ploughed into soils (Klebercz et al., 2012).

The oxyanion forming element vanadium has been highlighted as a persistently mobile contaminant since the red mud spill. Mayes et al. (2011) found that although V was mostly associated with residual phases, at some sample points down the affected Marcel and Rába river systems, V was associated with weak acid and oxalate extractable phase which could lead to further contamination of the river system in the future. Another study focusing on the effectiveness of the gypsum addition to affected rivers and streams also found that V was not substantially removed from solution by gypsum or indeed any of the other neutralisation methods commonly used in practice (Burke et al., 2013). Previous work detailed in this thesis has also highlighted the mobility of V from red mud into soil-water systems (see Chapters 5 and 7).

Vanadium has a very complex chemistry, it has a range of redox states (between -1 to +5) but exists in most natural waters in the V(V) oxidation state as the highly mobile phosphate-like oxyanion vanadate [H_2VO^{4-}, HVO_4^{2-}] (Peacock and Sherman, 2004b). In more reducing environments, the V(IV) oxidation state can exist as the vanadyl cation [VO^{2+}, $VO(OH)^{+}$]. Vanadate can form complexes with humic and fulvic acids between pH 7 to 9 (Lu et al., 1998) and can also be easily reduced to VO^{2+} by soil organic matter (Szalay and Szilagyi, 1967) thus increasing the stability and solubility of [VO^{2+}] across a wide range of pH and Eh boundaries (Goncalves and Mota, 1987; Breit

and Wanty, 1991). It is estimated that between 20-80% of V is complexed with DOC in natural waters depending upon DOC concentrations (Breit and Wanty, 1991).

The complexation of Cu to DOC (dissolved organic carbon) has been found to be very important in controlling the aqueous concentrations of Cu in red mud affected soil water systems. Soils with a high total organic carbon content released high concentrations of DOC complexed with Cu (and to a lesser extent Ni) due to soil alkalisation upon red mud addition (see Chapter 7). Both vanadate and vanadyl form complexes with organic matter therefore, increased aqueous concentrations of DOC may also affect aqueous V concentrations in red mud affected soil-water systems.

Due to the potential problems of vanadium contamination from red mud it is important to establish what controls the fate and transport of V from red mud into surrounding soil-water systems. The chemistry and control mechanisms of V are complex and a complete understanding of these processes at high pH and interactions with SOM are not yet fully understood. This chapter reports on a pilot study into the possible mechanisms controlling vanadium transport from red mud into soil-water systems analogous to post remediation conditions.

8.2 Materials and Methods

8.2.1 Field Sampling and Sample Handling.

As described in previous chapters (see Chapters 5, 6 and 7) sampling was undertaken in May 2011. Red mud (RM) was sampled from within Cell X of the Ajka impoundment (Location 47°05’18.48”N, 17°29’46.77”E). Uncontaminated soils were sampled from locations in the Torna and upper Marcal river catchments unaffected by

the release of red mud in 2010 (see Figure 3.2 for locations, PCA analysis see Figure 5.1). Two were agricultural top soils (one was organic-rich (Soil OR), the other a sandy soil (Soil SS)) and the third was collected from 50cm (under the rootlet layer) from below the surface of a wetland (Soil WL).

8.2.2 Reduction Microcosm Experiments

Triplicate aerobic and anaerobic microcosms for each soil type were prepared with differing loadings of red mud by mixing soils with red mud to achieve a 9% and a 33% addition of red mud on a dry weight basis with deionised water was added in a 5:1 ratio to the soil addition (as previously described in Chapters 6 and 7). The 9% addition was chosen as an analogue for where red mud had been ploughed into fields (based on ~5cm ploughed to a typical depth of 40-50cm, an approximate 5:50 mixing ratio). The 33% addition was used as a worst case scenario and for any unremediated wetland areas.

8.2.3 Geochemical Methods.

ORP (as an indicator for Eh) and pH were measured using a Thermo Scientific Orion Dualstar pH/ISE benchtop meter (pH was calibrated at pH 4, 7 and 10 daily). Aqueous V concentrations were determined using a Perkin Elmer Elan DRCII inductively coupled plasma-mass spectrometer. DOC in aliquots of end point solutions was determined by a multi N/C® 2100 using thermocatalytic oxidation, MC-NDIR detection analysis. Standards were used to check the accuracy and precision of the

methods and calibration regression had $R^2 \geq 0.999$. Reference materials were used where appropriate.

8.2.4 Solid Phase Extraction (SPE)

The solutions sampled at the end of the incubation period were passed through Isolute™ C18 1 g / 6 mL non polar SPE filters to retain organic substances (and therefore any organically bound vanadium). These filters were conditioned according to the manufacturer's instructions, and the solutions acidified to pH 5.5 prior to filtration using HNO_3 (the optimum pH for maximum organic matter retention by Isolute C18 filters (Thomas, 2000). The filtrates were further diluted with 2% HNO_3 for ICP-MS analysis to determine the inorganic/free aqueous metal concentrations. The concentration of organically bound metals was deemed to be the difference in aqueous metals concentrations measured before (total [V]) and after SPE (inorganic/free [V]).

8.2.5 X-ray Absorption Near Edge Structure Spectroscopy (XANES)

V K-edge (5465 eV) spectra were collected at Diamond Light Source, UK, in May 2012. Approximately 100 mg of moist paste RM and soils recovered from sediment recovered at the end points of the anaerobic microcosms were prepared for XANES analysis by mounting under argon atmosphere into Perspex holders with Kapton™ windows. Samples were frozen (-20°C) and transported to the synchrotron on dry ice and kept frozen until analysed.

Standard materials were prepared as pressed pellets using cellulose as a diluent to reduce chemical thickness (to achieve an edge step between 0.5 and 1.5 in transmission mode, see below) and held in Kapton™ tape. A sodium vanadate solution was prepared in 0.1 M NaOH, also at 1000 mg L^{-1}, and held in a polythene bags as above. Vanadate adsorbed to $Al(OH)_3$ was prepared by suspension of 1 g $Al(OH)_3$ in 1 L DIW and adding 1 ml of 1000 mg L^{-1} $NaVO_4$ (made up in 0.01 M NaOH at pH 12). The mixed suspension was stirred for 48 hours and the final pH was 7.0. The V-$Al(OH)_3$ solid was recovered by centrifugation (600 *g*) and prepared for analysis as a moist paste as above.

XANES spectra were collected at the V K-edge (5465 eV) on beamline I18 at the Diamond Light Source operating at 3 GeV with a typical current of 200 mA, using a nitrogen cooled Si(111) double crystal monochromator and focussing optics. A pair of plane mirrors was used to reduce the harmonic content of the beam and Kirkpatrick-Baez mirrors were used to produce a relatively unfocused beam (approximately 0.5 mm diameter at the sample). For standards prepared as pressed pellets, K-edge spectra were collected in transmission mode at room temperature (~295 °K). For samples and solutions, data were collected in fluorescence mode using a 9 element solid state Ge detector at room temperature. Multiple scans were then averaged to improve the signal to noise ratio using Athena version 0.8.061 (Ravel and Newville, 2005a; Ravel and Newville, 2005b). XANES spectra absorption was normalised in Athena over the full data range and plotted from approximately -15 eV to +30 eV relative to the edge position with no correction required for drift in E_0. V data was calibrated using E_0 measured from thin metal foil, The V pre-edge peak energy was determined by calculation of the area normalised centroid energy position following the method of Chaurand et al. (2007b).

8.3 Results

8.3.1 Sample Characterization

The full sample characterisation of the red mud and the 3 different soil samples has been described previously in Chapter 5, and is presented in Table 5.1 and full XRF analysis is presented in Table 5.2. Briefly, red mud was dominated by hematite (Fe_2O_3), calcite ($CaCO_3$), magnetite (Fe_3O_4), cancrinite ($Na_6CaAl_6Si_6(CO_3)O_{24}{\cdot}2H_2O$) and hydrogarnet ($Ca_3AlFe(SiO_4)(OH_8)$ with residual boehmite (γ-AlOOH) and gibbsite ($Al(OH_3)$) phases, very similar to other red mud analysed from the breach area (Gelencser et al., 2011; Burke et al., 2012a). All three soils had similar mineralogy, with quartz as the dominant mineral and feldspars and clays were also present. The principal differences between them were in the organic carbon content, and the proportion of the 0.5 N HCl extractable iron in the Fe(II) oxidation state (Table 5.1). The concentration of V in red mud was 1132 mg kg^{-1}. Soil OR had a highest concentration of V (72 mg kg^{-1}) followed by Soil WL and Soil SS (51 mg kg^{-1} and 30 mg kg^{-1} respectively). The percentage TOC followed the same order, Soil OR 4.15%, Soil WL 1.14% and Soil SS 0.74. The red mud had a %TOC of 0.23%.

8.3.2 Evolution of V from red mud affected soil-waters systems

Trends for evolution of aqueous V concentrations are shown in Figure 8.1). Here, the highest concentrations of V were seen in the Soil SS 33% RM amended experiment, under aerobic conditions where 900 μg L^{-1} was mobilised in the first 7 days of incubation. This rapid release of V was followed by a period of rapid removal. The Soil SS, 9% RM amended experiment followed a similar trend under aerobic conditions

but peak concentrations reach ~300 μg L^{-1}. Both Soils WL and OR followed a similar trend for both the 33 and 9% RM amended experiments under aerobic incubation but concentrations were much lower, especially for Soil OR.

Under anaerobic conditions, the trends are also very different. The Soil OR 33% RM amended experiment had the highest concentration of V (~650 μg L^{-1}). This is rapidly released over the first 30 days and then gradually continued to rise. The 9% RM amended system followed the same trend but with lower concentrations (<100 μg L^{-1}). Both Soil WL and Soil SS with 33% RM amendment had rapid mobilisation of V concentrations to 300 and 650 μg L^{-1} respectively, in the first 14 days followed by gradual removal. The concentration of V in the 9% RM amended systems for the WL and SS soils, however, remained constant (100 and 200 μg L^{-1} respectively) after an initial release in the first 15 to 30 days.

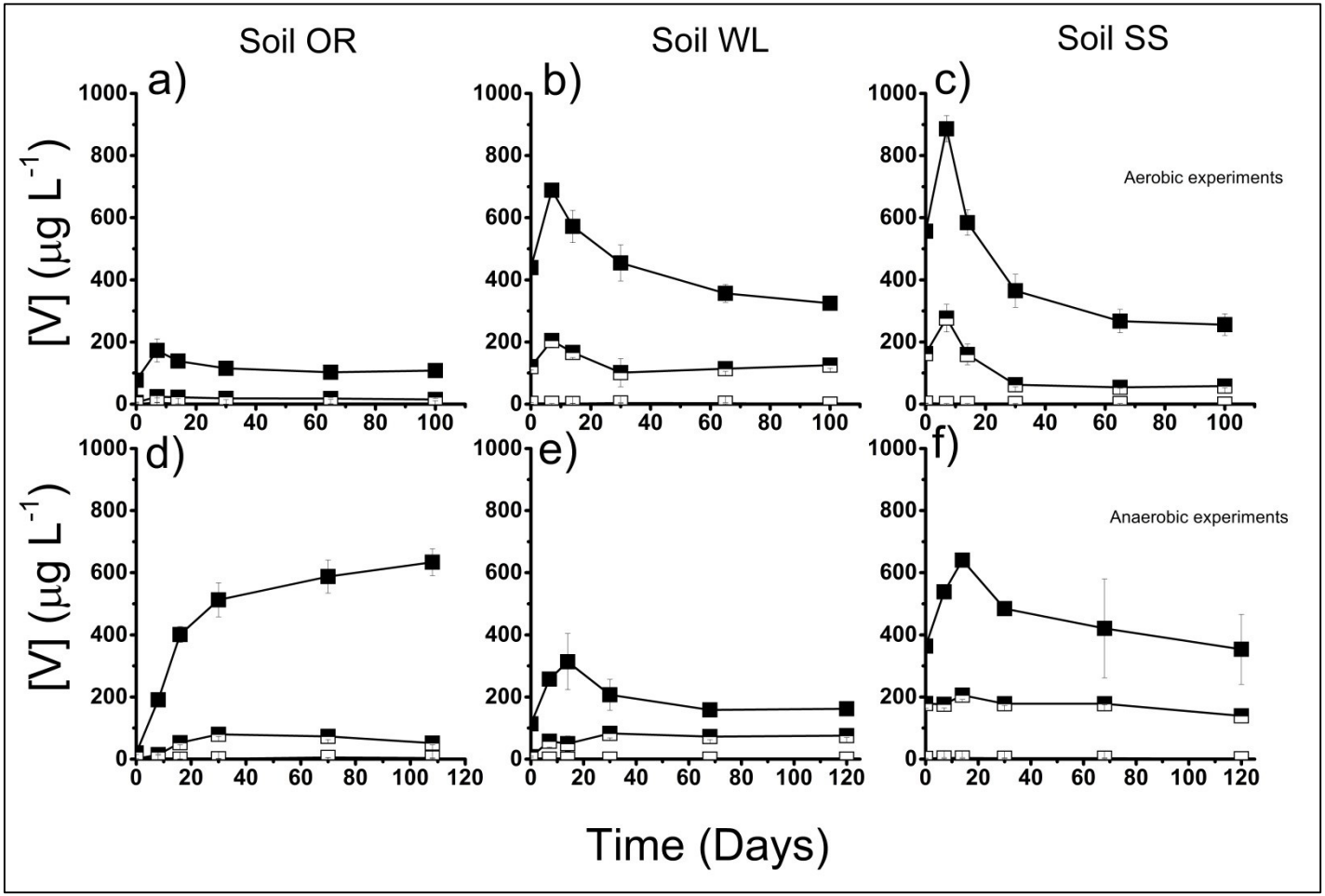

Figure 8.1 - Evolution of vanadium over time from aerobic (top) and anaerobic (bottom) experiments. Full squares = 33% RM addition, Half Squares = 9% RM addition, Empty squares = no red mud addition. Error bars are 1 σ of triplicate results (where not shown, error are within symbol size).

8.3.5 % Organically bound vanadium

Table 8.1 shows the percentages of V from the incubation end point solutions of the batch experiments that were organically complexed. In the experiments analysed there is no detectable organically bound V in any of the unamended control experiments or the anaerobically incubated experiments for Soil SS with a red mud addition. However aerobic experiments for Soil SS with a red mud addition showed some organically bound V (>20%). There was more organically bound V in Soil OR compared to Soil WL but there was little difference in the amounts of organically bound V between the aerobic and anaerobic experiments in the two soil systems. Increased red mud loading did not increase the amount of organically bound V in either the aerobic or anaerobic experiments but there was a large difference compared to unamended experiments (with the exception of the anaerobically bound Soil OR experiment).

Table 8.1 - % Organically bound aqueous V from aerobic and anaerobic end point solutions

Experimental Conditions	**Aerobic**			**Anaerobic**		
	Soil OR	Soil WL	Soil SS	Soil OR	Soil WL	Soil SS
Unamended Controls	nd	nd	nd	39 (±1)	nd	NR
9% RM addition	55 (±30)	36 (±2)	21 (±9)	45 (±6)	25 (±13)	0*
33% RM addition	55 (±9)	18 (±4)	29 (±9)	51 (±14)	28 (±7)	0*

nd – not detected

NR – not analysed,

0* - inorganic/free [V] was ≥ total [V] therefore organically bound [V] was deemed to be zero

8.3.6 XAS Spectroscopy

The V K-edge XANES spectra has been interpreted using the system proposed by Chaurand et al. (2007). This system is based upon the detailed observation of pre-edge peak intensity and energy position. V K-edge XANES spectra (Figure 8.2) collected from the red mud and red mud addition experiments under anaerobic incubation all have prominent pre-edge peaks between 5469.5 and 5470.1 eV. The main absorption edges ($E_{1/2}$ = point where absorption reaches 50% of the normalised absorption) are between 5480.5 and 5481.0 eV. A summary of the spectral information extracted from all samples and standards is shown in Table 8.2. A plot of normalised pre-edge peak intensity vs Pre-edge peak energy (eV) for samples and standards is shown in Figure 8.3.

Table 8.2 – Pre-Edge Peak Position, Normalised Pre-Edge Peak Intensity and Main Edge Position Determined from V K-edge XANES spectra shown in Figure 8.2. Energy values are quoted ±0.2 eV; normalised intensity values are quoted ±0.1.

sample/standard	valence	Pre-edge peak (eV)	Normalised intensity	Main edge $E_{1/2}$ (eV)
V_2O_3	3+	5468.0	0.1	5478.0
$VOSO_4.xH_2O$	4+	5470.0	0.3	5480.0
Soil OR + RM	4+	5469.5	0.45	5480.5
Soil WL + RM	4+	5470.0	0.41	5481.0
Soil SS + RM	5+	5470.0	0.7	5481.5
red mud (RM)	5+	5470.1	0.68	5481.0
vanadate sorbed to $Al(OH)_3$	5+	5470.0	0.7	5481.0
vanadate (aq)	5+	5470.0	1.07	5482.0
Calcium meta-vanadate	5+	5470.2	1.06	5482.2

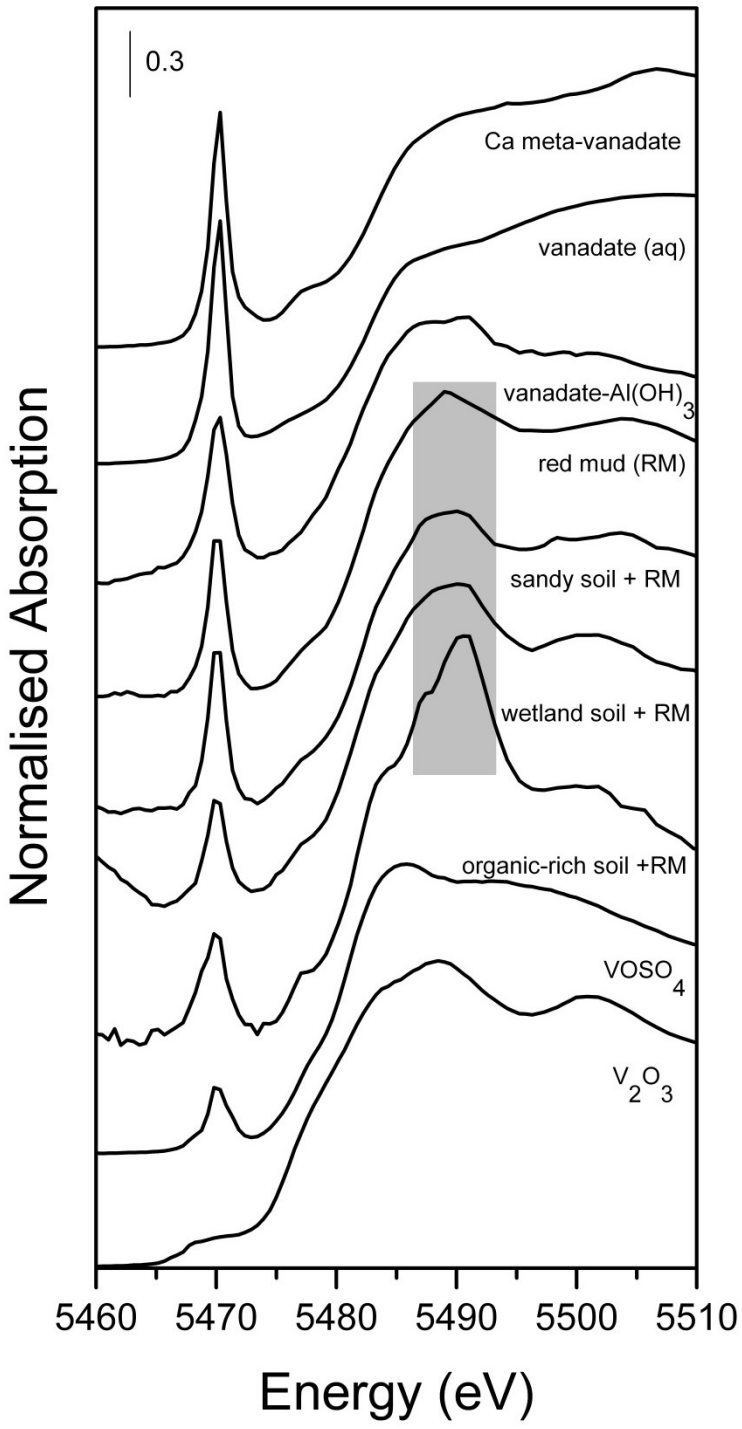

Figure 8.2 – Normalised V K-edge XANES spectra collected from original RM samples, moist pastes recovered from end points of 33% RM amended anaerobic experiments and standards containing V^{3+}, V^{4+} and V^{5+}. The vanadate standard is from a 1000 mg L^{-1} aqueous solution in 0.1 M NaOH. The grey box denotes where the white line peak if the La L_3-edge is visible in spectra from experimental samples.

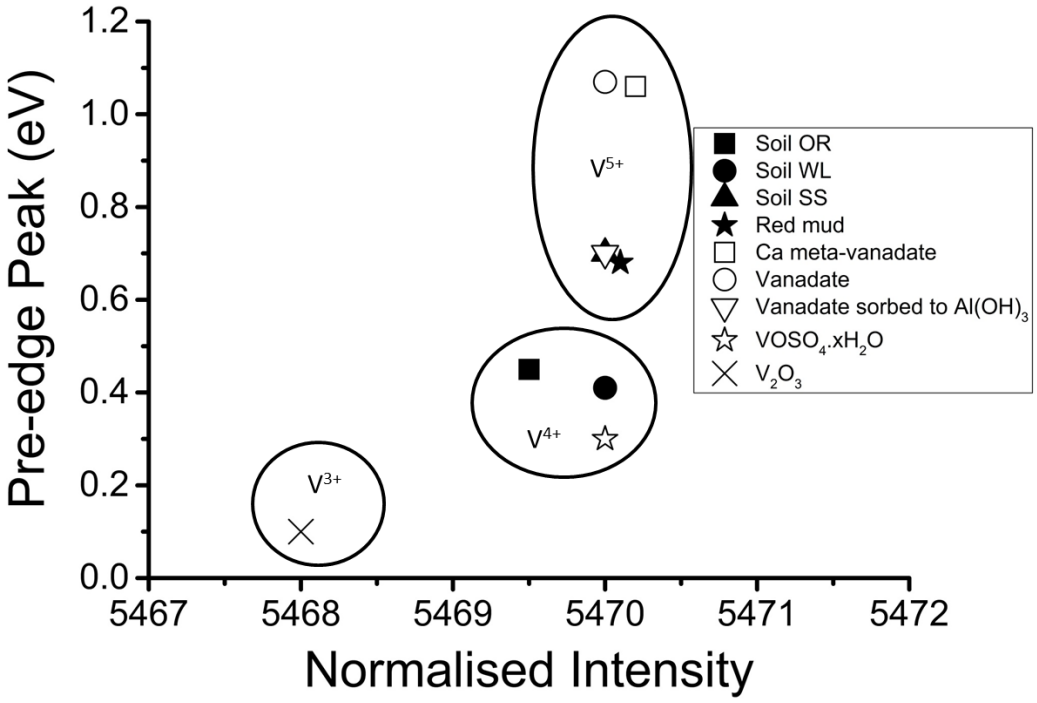

Figure 8.3 – Plot of pre-edge intensity vs. pre-edge peak energy derived from V K-edge XANES spectra. Empty symbols = Standards from this study (and Burke et al, 2013). Full symbols = samples from this study

8.4 Discussion

Vanadium solubility in soils is often controlled by variations in pH and Eh. High concentrations of V(V) are to be expected under oxic conditions at high pH as V(V) sorbs weakly above pH 10.5 (Peacock and Sherman, 2004b). Under more reducing conditions V(IV) is more prevalent and can be readily formed from V(V) in the presence of most reducing agents (Wehrli and Stumm, 1989). Vanadium(IV) is most commonly present as the vanadyl cation [as VO^{2+}] which is known to adsorb more strongly to solid phases than V(V) oxyanions (especially at high pH) and will

preferentially adsorb to metal (oxyhydr)oxides except under high ligand concentrations (Wehrli and Stumm, 1989). High V concentrations have been previously reported in areas with a high dissolved organic carbon content (Alberic et al., 2000; Pourret et al., 2012).

Under aerobic conditions the amount of aqueous V mobilised was very high at the start of the incubation period which gradually reduced over time. The same trend is seen with pH over time in the aerobic experiments (see figure 6.4) where the ingress of atmospheric CO_2 gradually reduces pH due to carbonation reactions. This would suggest that the V is being removed from solution and taken up by carbonates precipitates or becoming resorbed to mineral surfaces. There is a strong positive correlation with increased V concentrations and high pH under aerobic conditions (Table 8.3, r = 0.80, p value = <0.001).

Although the amounts of aqueous V associated with DOC is similar under both aerobic and anaerobic conditions (Table 8.1) there is much less DOC present in the aerobic experiments when compared to anaerobic experiments for all soils (see Table 7.1). The correlation of aqueous V concentrations and DOC in the aerobic experiments is not as strong when compared to that of aqueous V and pH, indicating that pH is the main control on V release in aerobic experiments compared to DOC.

There is a strong positive correlation of increased aqueous V concentrations and increased DOC in the anaerobic experiments (Table 8.3, r = 0.99, p-value = <0.001), which suggests that DOC is important for controlling V concentrations, especially where there is high concentrations of DOC (Table 7.1). However, the trend of aqueous V evolution is very different in the Soil OR system compared to Soils WL and SS under anaerobic conditions where a gradual removal of V is seen. Also, SPE extraction data

indicates that very little V is complexed with DOC in the Soil SS experiments (the concentration of inorganic/free V was greater than or equal to the concentration of total V determined so the concentration of organically bound V was deemed to be zero).

Table 8.3 – Pearson's regression correlation values for aqueous V concentrations vs pH or DOC for red mud amended experiments after 100-120 days incubation

Determinand	**Experimental Conditions**	
	Anaerobic (r; p-value)	Aerobic (r; p-value)
[V] vs		
DOC	0.99; <0.001	0.59; 0.01
pH	0.16; 0.5	0.80; <0.001

V K-edge XANES (Table 8.1) confirms that solid phase V in anaerobic experiments amended with 33% red mud were largely found as V^{4+} in the Soil OR and Soil WL experiments but as V^{5+} in Soil SS experiments. When the XANES spectra are interpreted using the system of Chaurand et al. (2007b) (based on detailed observation of pre-edge peak intensity and energy position), the Soil OR and Soil WL plot in a region near to the V^{4+} standard but the Soil SS plots very closely to the data from vanadate-$Al(OH)_3$ standard and close to the position of the original red mud sampled (also V^{5+}), suggesting that there has been little change in the solid phase V in the Soil SS experiments. These differences in oxidation state correspond with modelled oxidation states from Eh/pH diagrams (Figure 8.4), calculated for these experiments. Under these experimental conditions V would exist as V^{4+} in both the Soil OR and Soil WL, where V^{5+} found in the red mud (Table 8.2) has been reduced to V^{4+} but remains as V^{5+} in the Soil SS experiments.

It is clear from the differences in the solid phase oxidation states, trends of aqueous V evolution and SPE data that there is a different mechanism controlling the mobilisation of V from red mud amended experiments in each soil under anaerobic conditions. The suggested control mechanism (looking at the 33% red mud amended experiments) for each soil is listed below:

- Soil OR: The pH of the red mud amended system is sufficiently low enough for stable OM-V complexes at the experiment pH and Eh (~ pH 9.5, -300 mV Figure 6.5) (Breit and Wanty, 1991; Lu et al., 1998) therefore high concentrations of DOC can outcompete mineral surface hydroxyl groups for vanadyl cations to form stable complexes increasing aqueous V concentrations.

- Soil WL: The pH of the red mud amended system is between pH 10.5 – 11 (see Figure 6.5) hence V-OM complexes will be less stable but, there is still sufficient DOC for V-OM complexes to form. Redox conditions are such that some vanadate is reduced to vanadyl, which will preferentially sorb to mineral surfaces as redox potential drops but some V remains in the aqueous phase due elevated pH or as OM-bound complexes.

- Soil SS: The mechanisms controlling the mobilisation of V from these red mud amended systems are less clear. The pH of the experiments is too high for stable V-OM complexes to form and although some removal of V is seen it does not appear to be related to a decrease in redox conditions. V K-edge XANES indicates that V is relatively unchanged in the solid phases from the original red mud. The initial peak of V ~ day

14, closely matches a sharp rise in pH, which may account for increased vanadium at this point (see Figure 6.5). The gradual removal of aqueous V could relate to sorption although this is known to be limited for vanadate at this pH (Peacock and Sherman, 2004b).

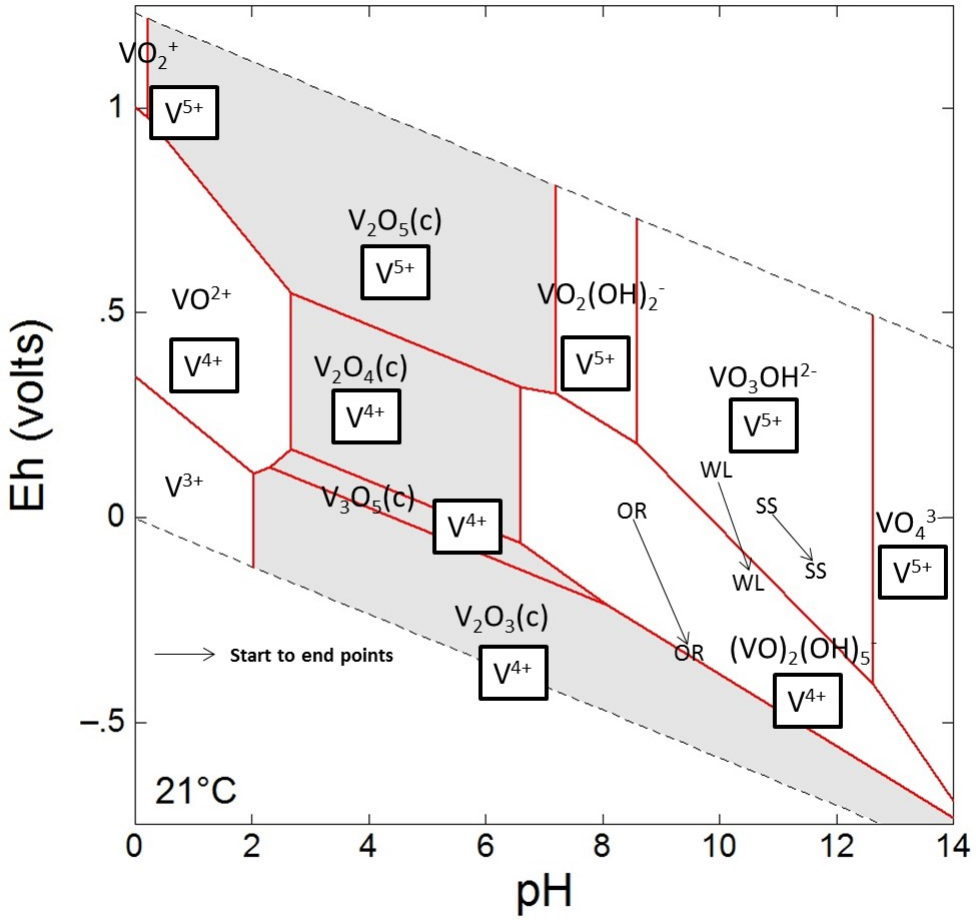

Figure 8.4 – Eh/pH conditions calculated for 33% RM amended anaerobic experiments superimposed on an Eh/pH V species predominance and relative mineral stability diagram calculated using Geochemists Workbench® for t = 21°C / P = 1 at, for the system V-O-H with log ∑V/m = -.0.9194 and a[$H_2O_{(aq)}$] = 1. Points plotted show geochemical conditions at day zero and experimental endpoints.

8.5 Conclusions

Vanadium remains an element of concern in red mud affected soils under both aerobic and anaerobic conditions. It is especially problematic where high concentrations of DOC are released upon soil alkalisation or in soil that has a low buffering capacity (see Chapter 5). Where DOC is low, V is quickly mobilised upon the addition of red mud and then gradually removed due to sorption processes but concentrations can still reach $\geq$0.2 mg L^{-1} even with low red mud loadings due to increased pH.

High pH red mud should be used with caution as a soil ameliorant for contaminated soils, especially those which are high in OM. This is due to the alkalisation of the soils which promotes DOC release and thus the mobilisation of any complexed metals such Cu and V. Further to previous studies following the Kolontár disaster, this study also verifies that costly large scale red mud removal from soils by Hungarian authorities was vindicated.

This chapter also highlights the complex chemistry of vanadium at high pH where competing processes such as SOM and sorption to mineral surfaces is not yet fully understood. The increased use of V over the past decade in steel and titanium alloys (Horn, 2010) could lead to increased vanadium contamination from alkaline wastes in the future. It is therefore important to understand the mechanisms controlling V transport at a much more fundamental level.

8.6 References

ADAM, J., BANVOLGYI, G., DURA, G., GRENERCZY, G., GUBECK, N., GUPTER, I., SIMON, G., SZEGFALVI, Z., SZEKACS, A., SZEPVOLGYI, J. & UJLAKY, E. 2011. The Kolontar report: Causes and Lessons from the Red Mud Disaster. In: B, J. (ed.). Budapest: Sustainable Development Committee of the Hungarian Parliament.

ALBERIC, P., VIOLLIER, E., JEZEQUEL, D., GROSBOIS, C. & MICHARD, G. 2000. Interactions between trace elements and dissolved organic matter in the stagnant anoxic deep layer of a meromictic lake. Limnology and Oceanography, 45, 1088-1096.

ANTON, A., REKASI, M., UZINGER, N., SZEPLABI, G. & MAKO, A. 2012. Modelling the Potential Effects of the Hungarian Red Mud Disaster on Soil Properties. Water Air and Soil Pollution, 223, 5175-5188.

BREIT, G. N. & WANTY, R. B. 1991. VANADIUM ACCUMULATION IN CARBONACEOUS ROCKS - A REVIEW OF GEOCHEMICAL CONTROLS DURING DEPOSITION AND DIAGENESIS. Chemical Geology, 91, 83-97.

BURKE, I. T., MAYES, W. M., PEACOCK, C. L., BROWN, A. P., JARVIS, A. P. & GRUIZ, K. 2012. Speciation of arsenic, chromium, and vanadium in red mud samples from the ajka spill site, hungary. Environmental Science & Technology, 46, 3085-92.

BURKE, I. T., PEACOCK, C. L., LOCKWOOD, C. L., STEWART, D. I., MORTIMER, R. J. G., WARD, M. B., RENFORTH, P., GRUIZ, K. & MAYES, W. M. 2013. Behavior of Aluminum, Arsenic, and Vanadium during the Neutralization of Red Mud Leachate by HCl, Gypsum, or Seawater. Environmental Science & Technology, 47, 6527-6535.

CHAURAND, P., ROSE, J., BRIOIS, V., SALOME, M., PROUX, O., NASSIF, V., OLIVI, L., SUSINI, J., HAZEMANN, J.-L. & BOTTERO, J.-Y. 2007. New methodological approach for the vanadium K-edge X-ray absorption near-edge structure interpretation: Application to the speciation of vanadium in oxide phases from steel slag. Journal of Physical Chemistry B, 111, 5101-5110.

CORNELIS, G., JOHNSON, C. A., VAN GERVEN, T. & VANDECASTEELE, C. 2008. Leaching mechanisms of oxyanionic metalloid and metal species in alkaline solid wastes: A review. Applied Geochemistry, 23, 955-976.

GELENCSER, A., KOVATS, N., TUROCZI, B., ROSTASI, A., HOFFER, A., IMRE, K., NYIRO-KOSA, I., CSAKBERENYI-MALASICS, D., TOTH, A., CZITROVSZKY, A., NAGY, A., NAGY, S., ACS, A., KOVACS, A., FERINCZ, A., HARTYANI, Z. & POSFAI, M. 2011. The Red Mud Accident in Ajka (Hungary): Characterization and Potential Health Effects of Fugitive Dust. Environmental Science & Technology, 45, 1608-1615.

GONCALVES, M. L. S. & MOTA, A. M. 1987. Complexes of vanadyl and uranyl ions with chealting groups of humic matter. Talanta, 34, 839-847.

GRAFE, M., POWER, G. & KLAUBER, C. 2011. Bauxite residue issues: III. Alkalinity and associated chemistry. Hydrometallurgy, 108, 60-79.

HIND, A. R., BHARGAVA, S. K. & GROCOTT, S. C. 1999. The surface chemistry of Bayer process solids: a review. Colloids and Surfaces a-Physicochemical and Engineering Aspects, 146, 359-374.

HORN, D. 2010. Vanadium: Going Green. Mining Journal, 19/02/2010, p.2.

KLEBERCZ, O., MAYES, W. M., ANTON, A. D., FEIGL, V., JARVIS, A. P. & GRUIZ, K. 2012. Ecotoxicity of fluvial sediments downstream of the Ajka red mud spill, Hungary. Journal of environmental monitoring : JEM, 14, 2063-71.

LANGMUIR, D. 1997. Aqueous environmental geochemistry, Upper Saddle River, N. J., Prentice Hall.

LIU, Y., LIN, C. & WU, Y. 2007. Characterization of red mud derived from a combined Bayer Process and bauxite calcination method. Journal of Hazardous Materials, 146, 255-261.

LU, X., JOHNSON, W. D. & HOOK, J. 1998. Reaction of Vanadate with Aquatic Humic Substances: An ESR and 51V NMR Study. Environmental Science & Technology, 32, 2257-2263.

MAYES, W. M., JARVIS, A. P., BURKE, I. T., WALTON, M., FEIGL, V., KLEBERCZ, O. & GRUIZ, K. 2011. Dispersal and Attenuation of Trace Contaminants Downstream of the Ajka Bauxite Residue (Red Mud) Depository Failure, Hungary. Environmental Science & Technology, 45, 5147-5155.

PEACOCK, C. L. & SHERMAN, D. M. 2004. Vanadium(V) adsorption onto goethite (alpha-FeOOH) at pH 1.5 to 12: A surface complexation model based on ab initio molecular geometries and EXAFS spectroscopy. Geochimica Et Cosmochimica Acta, 68, 1723-1733.

POURRET, O., DIA, A., GRUAU, G., DAVRANCHE, M. & BOUHNIK-LE COZ, M. 2012. Assessment of vanadium distribution in shallow groundwaters. Chemical Geology, 294-295, 89-102.

POWER, G., GRAFE, M. & KLAUBER, C. 2011. Bauxite residue issues: I. Current management, disposal and storage practices. Hydrometallurgy, 108, 33-45.

RAVEL, B. & NEWVILLE, M. 2005a. ATHENA and ARTEMIS: Interactive graphical data analysis using IFEFFIT. Physica Scripta, T115, 1007-1010.

RAVEL, B. & NEWVILLE, M. 2005b. ATHENA, ARTEMIS, HEPHAESTUS: data analysis for X-ray absorption spectroscopy using IFEFFIT. Journal of Synchrotron Radiation, 12, 537-541.

REKASI, M., FEIGL, V., UZINGER, N., GRUIZ, K., MAKO, A. & ANTON, A. 2013. Effects of leaching from alkaline red mud on soil biota: modelling the conditions after the Hungarian red mud disaster. Chemistry and Ecology, 29, 709-723.

RENFORTH, P., MAYES, W. M., JARVIS, A. P., BURKE, I. T., MANNING, D. A. C. & GRUIZ, K. 2012. Contaminant mobility and carbon sequestration downstream of the Ajka (Hungary) red mud spill: The effects of gypsum dosing. The Science of the total environment, 421-422, 253-9.

RUYTERS, S., MERTENS, J., VASSILIEVA, E., DEHANDSCHUTTER, B., POFFIJN, A. & SMOLDERS, E. 2011. The Red Mud Accident in Ajka (Hungary): Plant Toxicity and Trace Metal Bioavailability in Red Mud Contaminated Soil. Environmental Science & Technology, 45, 1616-1622.

SZALAY, A. & SZILAGYI, M. 1967. ASSOCIATION OF VANADIUM WITH HUMIC ACIDS. Geochimica Et Cosmochimica Acta, 31, 1-&.

THOMAS, B. 2000. Solid phase extraction for the removal of organic-iron complexes in contaminated groundwater. MSc MSc The University of Leeds.

WEHRLI, B. & STUMM, W. 1989. VANADYL IN NATURAL-WATERS - ADSORPTION AND HYDROLYSIS PROMOTE OXYGENATION. Geochimica Et Cosmochimica Acta, 53, 69-77.

Chapter 9 Summary and future considerations

9.1 Summary

This thesis sought to identify the main biogeochemical processes controlling the mobility of trace elements from alkaline wastes in soil-water systems. The main focus of the thesis was an investigation into the mobilisation of trace elements from red mud into soil-water systems analogous to conditions following the 2010 red mud spill in Hungary. The secondary focus was a pilot study into the mobility of vanadium in soil-water systems affected by leachate from iron and steel slag at a legacy steel slag site in the north of England. These two work packages both sought to improve our understanding of trace element transport and fate in alkaline waste affected soils, with a particular emphasis on several oxyanion forming elements that are mobilised at high pH. The effects of high pH on biogeochemical processes in soils that can either enhance or inhibit the release of these trace elements was also considered.

In this concluding chapter, the 11 preliminary research hypotheses (see Section 1.2) are revisited and are linked together with major findings from the thesis. Finally, the wider implications of the research and future considerations will be discussed.

9.2 Preliminary hypotheses revisited and major findings

9.2.1 V from iron and steel slag - Hownsgill Valley, nr Consett, U. K

There were two research hypotheses associated with the samples taken from the Hownsgill Valley study site.

i. Soils affected by steel slag leachates will contain an indigenous population of microorganisms that are adapted to survive and grow at high pH; microbial bioreduction processes will therefore, be supported in this environment.

ii. The observed decrease in aqueous vanadium concentrations in the alkaline leachate with distance away from the source is (at least in part) due to *in situ* microbially mediated reduction of V(V) to produce less soluble V(VI) species.

Chapter 4, reports a pilot study into the processes controlling vanadium in the Hownsgill Valley, near Consett. Although the hypotheses predicted that biological processes would play a role in the transport of V at the site, the results indicated that the main processes attenuating V at the site were abiotic. However, the existence of an alkaliphilic community at the site was confirmed. Vanadate (added as a spike to the experiments) was removed from solution when incubated with anoxic high pH soils. V in the soils was found as V(IV) therefore reductive removal was presumed, although the exact mechanism remains unclear (neither Fe(III)- or sulfate-reduction was observed in the experiments). Although the results were inconclusive regarding the exact mechanism of V reduction, the results highlighted several areas for future work which are discussed below (see section 9.4).

9.2.2 Addition of red mud to soils (Chapters 5 -8)

There were 5 preliminary hypotheses that predicted that effect of red mud addition to soils. The work undertaken to address these hypotheses is covered across the whole thesis.

i. Addition of caustic red mud to soils will cause an increase in soil pH and as a consequence concentrations of several toxic oxyanion forming elements (e.g. As, Al, V, Mo) will increase in associated waters due to their lower sorption to minerals at high pH.

ii. Soils containing higher concentrations of organic matter (or larger quantities of clay minerals) content will have a higher intrinsic buffering capacity with respect to addition of alkalinity (from red mud), producing lower soil pH, and lower concentrations of oxyanion forming elements.

iii. Addition of red mud in soils will cause the solubilisation of soil organic matter (due to higher pH), resulting in increased dissolved organic carbon (DOC) concentrations, and, higher concentrations of elements know to complex strongly with DOC (e.g. Cu and Ni)

iv. Addition of gypsum (as a source of Ca^{2+}) to red mud affected soils will promote OH^- consuming carbonate precipitation reactions, reducing soil pH, and producing lower oxyanion concentrations due to enhanced sorption at circumneutral pH.

v. Increasing the concentration of anionic species in solution (e.g. phosphate, carbonate) that are known to compete for available sorption sites on minerals, will result in enhanced solubility of toxic oxyanion forming species (such as As) regardless of soil pH.

The addition of Ajka red mud to soils does cause an increase in pH, total dissolved solids, dissolved organic carbon and concentrations of oxyanion forming trace elements, which is proportional to red mud loading (Chapter 5). The effect of red mud addition to

soils was found to be very different depending upon various soil properties; e.g. total organic carbon and clay content of the soils.

As predicted, the soils with lower organic matter and clay mineral content had a greater increases in pH after red mud addition (Chapter 5). Soils with increased TOC, however, experienced a different detrimental effect. In high TOC soils-red mud mixture very high concentrations of DOC were released under anaerobic conditions (up to850 mg L^{-1}). The increased DOC was found to complex to Cu, Ni and V increased aqueous concentrations of these elements considerably with respect to soils with lower overall TOC (Chapter 7 and 8).

The effect of gypsum addition to red mud affected soils was also examined in Chapter 5 with a view to emergency soil remediation after red mud spills. Gypsum addition to soils was found to lower pH values. This inhibited the release of Al, As, and V due and enhanced anion sorption at pH values <8.5. Lower DOC solubility was also found due to the lower soil pH. However, Mo solubility was found to be largely unaffected by gypsum addition as Mo (as molybdate) is not strongly sorbed to solids as circumneutral pH. Gypsum treated soils also exhibited high dissolved sulphate content (due to gypsum dissolution).

The effect of competitive ions on As mobilisation from red mud was investigated in Chapter 6. It was observed that ~15% of As in red mud is present as phosphate exchangeable surface bound complexes. Therefore As solubility from red mud is enhanced at high pH and in the presence of competing ions. This hypotheses could be further explored by looking at the effect of PO_4 and CO_3^{2-} on V mobility in red mud; like As, V is also a phosphate analogue (Wehrli and Stumm, 1989) and therefore mobility might be enhanced under high PO_4 concentrations.

9.2.3 Red mud addition to aerobic soil-water systems (Chapters 6 -8)

Results from aerobic microcosms were discussed in Chapters 6, 7 and 8. There was one hypothesis that related to the effect of aerobic conditions on red mud affected soil water systems.

vi. In aerobic soil-water systems containing red mud, equilibration with atmospheric CO_2 will result in lower soil pH and lower oxyanion concentrations.

The ingress of atmospheric CO_2 in these experiments and the subsequent carbonation reactions (Equations 2.1 to 2.7) had a dramatic effect reducing experimental pH. The reduced pH in these experiments, in comparison to those under anaerobic conditions where pH remained high, minimised the effect of pH related desorption of As and DOM. The minimised desorption of DOM (as DOC) into the aqueous phase under aerobic conditions meant that any OM complexed Cu, Ni and V were also retained in the solid phase. However, experimental pH was sufficiently high enough (> pH 8.5) for some As and V to be released into the aqueous phase from red mud affected soils despite the lower overall pH cf. anaerobic experiments.

9.2.4 Red mud addition to anaerobic soil-water systems (Chapters 6 - 8)

The final three hypotheses relate red mud soil-water systems under anaerobic condition. Chapters 6, 7 and 8 examine the mobilisation of trace metals from anaerobic experiments together with the effects of red mud addition on soil biogeochemical processes during anaerobic incubation.

vii. In anaerobic soil-water systems containing red mud, microbial bioreduction processes will produce reducing conditions with time, promoting the reduction of As(V) to generally more soluble As(III) species and, an increased risk of enhanced As mobility.

viii. Conversely, bioreduction processes will promote the transformation of V(V) to V(IV) species, which strongly adsorb to minerals at alkaline pH, resulting in lower aqueous V concentrations.

ix. Soil affected by red mud addition will not contain microbial communities that are adjusted to alkaline conditions, therefore bioreduction processes will be inhibited at high pH.

It was found that microcosm experiments with a pH < ~9.5 were able to support 'normal' microbially mediated soil Fe(III)-reduction. However, above this pH, Fe(III) reduction was inhibited. Likewise microbial sulfate- reduction was observed in some experiments with pH < ~10, but the efficiency of the process appeared to be a soil specific response to red mud addition rather than a simple relationship with pH.

Soil only control microcosms without red mud addition showed increased aqueous As concentrations with increased incubation time. This was most likely as a result of microbial As reduction; however contrary to the predicted outcome, this observation was inhibited upon red mud addition. XAS spectroscopy analysis showed that the reduction of solid phase V(V) to V(IV) only occurred in experiments where active sulphate-reduction was also observed (Chapter 8). In these tests, vanadate reduction was probably achieved by reaction with microbially generated sulphide. Despite evidence for solid phase reduction in some systems, aqueous V remained high in these experiments, this might be due to V complexation with DOC either inhibiting abiotic

reduction or maintaining V(IV) in solution. The exact controls on V solubility in anoxic red mud amended soils therefore remain poorly defined and could be a topic for further investigation (see section 9.4).

Anaerobic incubation had several other effects on contaminant mobility; 1) the lack of CO_2 ingression and subsequent carbonation reactions kept experimental pH high in anaerobic experiments, this lead to increased leaching of DOC with increased pH 2) Increased concentrations of DOC lead to increased concentration of organic matter complexing metals such as Cu, Ni and V 3) the reductive dissolution of Fe (oxyhydr)oxides during Fe(III)-reduction increased aqueous As concentrations by reducing the availability of sorption surfaces. .

9.3 Implications

Following the red mud spill the Hungarian authorities began an extensive clean up operation of removing red mud from affected land and ploughing red mud into soils (Klebercz et al., 2012). The main risks associated with the addition of red mud to soils have already been identified as increased Na^+ and alkalinity (Ruyters et al., 2011; Gruiz et al., 2012; Anton et al., 2012). Although some studies since the spill have considered the mobilisation of trace elements from red mud to soil-water systems (Anton et al., 2012; Milacic et al., 2012; Rekasi et al., 2013), few have examined the release of trace metals under both aerobic and anaerobic conditions and with respect to biogeochemical processes. This study together with other studies since the spill justify these expensive remediation efforts as red mud addition to soils will cause an increase Al, As, Cu, Mo and V (and to a lesser extent Ni) to soil-water systems.

Wetland areas affected by the 2010 spill were not been remediated, presumably due to logistical reasons (certainly this was the case in May 2011) but it is likely that some these areas received a high dosing of red mud. Results from experiments with a 33% red mud addition (an experimental analogue for these areas) showed problematic concentrations of As, Cu and V especially under anaerobic conditions. It is therefore possible that there is a serious contamination issue in these untreated wetland areas, especially those with high TOC content.

The red mud from the breached dam at Ajka represents the very worst case scenario, the pH of the red mud exceeded 12 and had a very high water content making the dam breach exceed provisions in disaster management planning (Adam, et al., 2011). Very few red mud repositories store red mud at such a high pH and water content as refineries have some sort of system for removing excess water and waste neutralisation (Power et al., 2011). In this respect, Ajka red mud may not be very representative of other red mud, however the possibility of red mud from other sites affecting land and homes is very real (there have been recent much smaller scale incidents in both China and India (Boily, 2012)). Therefore the results in this thesis can go some way to aid others in decision making processes regarding worst case scenarios when it comes to risk management.

Red mud has been considered as a potential soil ameliorant for certain contaminants, including As and Cu (Lombi et al., 2002; Garau et al., 2011) with encouraging results (the red mud used in these studies usually has a pH <12). However, the results from this thesis show the importance of soil properties with regards to red mud addition and that a thorough understanding of these soil properties must be held before red mud addition is considered for use as an amendment to reduce the effects of an additional red mud associated metal/loids.

9.4 Future considerations

As discussed earlier, the pilot study into mobilisation of V from iron and steel slags was unable to elucidate the exact mechanisms for V(V) reduction. This study could be extended in a number of ways. An alkaliphilic microbial community was found at the site, by producing microcosm experiments that span a pH range of the upper limits of microbial activity, it may be possible to find the optimum pH for this community. These experiments coupled with a detailed investigation into the soil profile to investigate the existence of any micro-niches where microbial Fe(III) reduction might occur would explain the reducing environment and Fe(II) observed in the deep soil sampled. A more detailed investigation of the site, examining the interactions of the leachate plume with the natural soils of the site could confirm the oxidation state of V during the leaching process (via XAS spectroscopy).

Chapters 4 and 8 examine the mobilisation of vanadium from both iron and steel slags and red mud. Both studies poorly constrained the exact processes resulting in removal of aqueous V(V). It is clear that more fundamental experiments investigating the interaction of V with NOM and mineral phases over an alkaline pH range is needed. This could be achieved using well characterised soil/NOM and minerals. The experiments should be carried out with and without the presence of Fe(III)-reducing bacteria to determine the main controls for V(V) removal from solution at high pH.

As mentioned previously, it is possible that wetland areas affected by the red mud spill could have serious contamination issues with regards to trace metal release from red mud. ICP-MS and OES analysis on the solutions extracted from the end point of the anaerobic experiments indicated that Al, Mo, Se and Ti are other potentially problematic elements. A logical progression from this project would be to investigate

any wetland areas affected by the spill. A number of years have now passed since the spill but the signal of the red mud may still be apparent: Nagy et al. (2013) were able to detect the signal of the red mud spill in the Torna and Marcel river system up to two years after the spill with increased As and Ni concentrations.

The anaerobic experiments highlighted the different effects that red mud addition had to the soil biogeochemical processes and indigenous microbial communities; this was largely due to experimental pH and the capacity of the soil to buffer the effects from red mud addition. A novel approach therefore would be to examine the effects of increased red mud addition on the different soils with respect to the microbial communities present and observe any changes in the dominant species of the microbial communities.

9.6 References

ADAM, J., BANVOLGYI, G., DURA, G., GRENERCZY, G., GUBECK, N., GUPTER, I., SIMON, G., SZEGFALVI, Z., SZEKACS, A., SZEPVOLGYI, J. & UJLAKY, E. 2011. The Kolontar report: Causes and Lessons from the Red Mud Disaster. In: B, J. (ed.). Budapest: Sustainable Development Committee of the Hungarian Parliament.

ANTON, A., REKASI, M., UZINGER, N., SZEPLABI, G. & MAKO, A. 2012. Modelling the Potential Effects of the Hungarian Red Mud Disaster on Soil Properties. Water Air and Soil Pollution, 223, 5175-5188.

BOILY, R. 2012. Twenty Cases of Red Hazard: An Inventory of Ecological Problems Caused by Bauxite Residue from Alumina Production. Inforex Inc. Laval, Quebec, Canada.

GARAU, G., SILVETTI, M., DEIANA, S., DEIANA, P. & CASTALDI, P. 2011. Long-term influence of red mud on As mobility and soil physico-chemical and microbial parameters in a polluted sub-acidic soil. Journal of Hazardous Materials, 185, 1241-1248.

GRUIZ, K., FEIGL, V., KLEBERCZ, O., ANTON, A. & VASZITA, E. Environmental Risk Assessment of Red Mud Contaminated Land in Hungary. In: HRYCIW, R. D., ATHANASOPOULOS-ZEKKOS, A. & YESILLER, N., eds. GeoCongress 2012: State of the Art and Practice in Geotechnical Engineering, 2012. American Society of Civil Engineers, 4156-4165.

KLEBERCZ, O., MAYES, W. M., ANTON, A. D., FEIGL, V., JARVIS, A. P. & GRUIZ, K. 2012. Ecotoxicity of fluvial sediments downstream of the Ajka red mud spill, Hungary. Journal of environmental monitoring : JEM, 14, 2063-71.

LOMBI, E., ZHAO, F. J., ZHANG, G. Y., SUN, B., FITZ, W., ZHANG, H. & MCGRATH, S. P. 2002. In situ fixation of metals in soils using bauxite residue: chemical assessment. Environmental Pollution, 118, 435-443.

MILACIC, R., ZULIANI, T. & SCANCAR, J. 2012. Environmental impact of toxic elements in red mud studied by fractionation and speciation procedures. Science of the Total Environment, 426, 359-365.

NAGY, A. S., SZABO, J. & VASS, I. 2013. Trace metal and metalloid levels in surface water of the Marcal River before and after the Ajka red mud spill, Hungary. Environmental Science and Pollution Research, 20, 7603-7614.

POWER, G., GRAFE, M. & KLAUBER, C. 2011. Bauxite residue issues: I. Current management, disposal and storage practices. Hydrometallurgy, 108, 33-45.

REKASI, M., FEIGL, V., UZINGER, N., GRUIZ, K., MAKO, A. & ANTON, A. 2013. Effects of leaching from alkaline red mud on soil biota: modelling the conditions after the Hungarian red mud disaster. Chemistry and Ecology, 29, 709-723.

RUYTERS, S., MERTENS, J., VASSILIEVA, E., DEHANDSCHUTTER, B., POFFIJN, A. & SMOLDERS, E. 2011. The Red Mud Accident in Ajka (Hungary): Plant Toxicity and Trace Metal Bioavailability in Red Mud Contaminated Soil. Environmental Science & Technology, 45, 1616-1622.

Appendix A Additional Results

A1 Clone Library

Table A1 – Full RDP Classification with 95% confidence threshold and OTU assignment for sequences obtained from Consett deep soil sample.

Clone ID	Accession Number	Sequence Number	OTU	Classification using the RDP classifier (95% confidence threshold)
CL-R0-4-T7	HE584557	522	A1	Proteobacteria, Gammaproteobacteria, Xanthomenadales, Xanthomonadaceae
CL-R0-5-T7	HE584558	532	A12	
CL-R0-6-T7	HE584559	503	A6	Deinococcus-Thermus, Deinococci
CL-R0-7-T7	HE584560	593	A7	Firmicutes, Clostridia, Natranaerobiales, Natranaerobiaceae, Dethiobacter
CL-R0-8-T7	HE584561	507	A9	-
CL-R0-9-T7	HE584562	531	A12	-
CL-R0-10-T7	HE584563	494	A4	-
CL-R0-11-T7	HE584564	595	A10	-
CL-R0-12-T7	HE584565	527	A2	Proteobacteria, Betaproteobacteria
CL-R0-13-T7	HE584566	594	A10	-
CL-R0-14-T7	HE584567	526	A5	Bacteroidetes
CL-R0-15-T7	HE584568	503	A6	Deinococcus-Thermus, Deinococci, Deinococcales, Trueperaceae, Truepera
CL-R0-16-T7	HE584569	527	A5	Bacteroidetes
CL-R0-17-T7	HE584570	503	A6	Deinococcus-Thermus, Deinococci, Deinococcales, Trueperaceae, Truepera
CL-R0-18-T7	HE584571	595	A10	-
CL-R0-19-T7	HE584572	527	A2	Proteobacteria, Betaproteobacteria
CL-R0-21-T7	HE584573	594	A7	Firmicutes, Clostridia, Natranaerobiales, Natranaerobiaceae, Dethiobacter
CL-R0-22-T7	HE584574	494	A4	-
CL-R0-23-T7	HE584575	514	A11	Firmicutes, Clostridia
CL-R0-24-T7	HE584576	503	A6	Deinococcus-Thermus, Deinococci
CL-R0-25-T7	HE584577	503	A6	Deinococcus-Thermus, Deinococci, Deinococcales, Trueperaceae, Truepera
CL-R0-26-T7	HE584578	527	A2	Proteobacteria, Betaproteobacteria
CL-R0-27-T7	HE584579	503	A6	Deinococcus-Thermus, Deinococci, Deinococcales, Trueperaceae, Truepera
CL-R0-28-T7	HE584580	523	A1	Proteobacteria, Gammaproteobacteria, Xanthomenadales, Xanthomonadaceae
CL-R0-29-T7	HE584581	531	A12	-
CL-R0-30-T7	HE584582	527	A2	Proteobacteria, Betaproteobacteria, Burkholderiales
CL-R0-31-T7	HE584583	526	A2	Proteobacteria, Betaproteobacteria, Burkholderiales, Comamonadaceae
CL-R0-32-T7	HE584584	594	A7	Firmicutes, Clostridia, Natranaerobiales, Natranaerobiaceae, Dethiobacter
CL-R0-33-T7	HE584585	494	A4	-
CL-R0-34-T7	HE584586	594	A7	Firmicutes, Clostridia, Natranaerobiales, Natranaerobiaceae, Dethiobacter
CL-R0-35-T7	HE584587	503	A6	Deinococcus-Thermus, Deinococci
CL-R0-36-T7	HE584588	527	A2	Proteobacteria, Betaproteobacteria
CL-R0-37-T7	HE584589	527	A2	Proteobacteria, Betaproteobacteria
CL-R0-38-T7	HE584590	503	A6	Deinococcus-Thermus, Deinococci, Deinococcales, Trueperaceae, Truepera
CL-R0-39-T7	HE584591	527	A2	Proteobacteria, Betaproteobacteria
CL-R0-40-T7	HE584592	527	A5	Bacteroidetes
CL-R0-41-T7	HE584593	523	A1	Proteobacteria, Gammaproteobacteria, Xanthomenadales, Xanthomonadaceae
CL-R0-42-T7	HE584594	517	A3	Proteobacteria, Betaproteobacteria, Burkholderiales, Comamonadaceae
CL-R0-43-T7	HE584595	594	A7	Firmicutes, Clostridia, Natranaerobiales, Natranaerobiaceae, Dethiobacter
CL-R0-44-T7	HE584596	503	A6	Deinococcus-Thermus, Deinococci, Deinococcales, Trueperaceae, Truepera
CL-R0-45-T7	HE584597	503	A6	Deinococcus-Thermus, Deinococci
CL-R0-46-T7	HE584598	527	A2	Proteobacteria, Betaproteobacteria
CL-R0-47-T7	HE584599	594	A7	Firmicutes, Clostridia, Natranaerobiales, Natranaerobiaceae, Dethiobacter
CL-R0-48-T7	HE584600	527	A2	Proteobacteria, Betaproteobacteria
CL-R0-49-T7	HE584601	590	A8	Firmicutes, Clostridia, Natranaerobiales, Natranaerobiaceae, Dethiobacter
CL-R0-50-T7	HE584602	527	A2	Proteobacteria, Betaproteobacteria
CL-R0-51-T7	HE584603	531	A12	-
CL-R0-52-T7	HE584604	503	A6	Deinococcus-Thermus, Deinococci
CL-R0-53-T7	HE584605	527	A5	Bacteroidetes
CL-R0-54-T7	HE584606	503	A6	Deinococcus-Thermus, Deinococci, Deinococcales, Trueperaceae, Truepera
CL-R0-55-T7	HE584607	503	A6	Deinococcus-Thermus, Deinococci, Deinococcales, Trueperaceae, Truepera
CL-R0-57-T7	HE584608	530	A12	-
CL-R0-58-T7	HE584609	527	A2	Proteobacteria, Betaproteobacteria, Burkholderiales
CL-R0-60-T7	HE584610	527	A2	Proteobacteria, Betaproteobacteria

A2 XRD Patterns

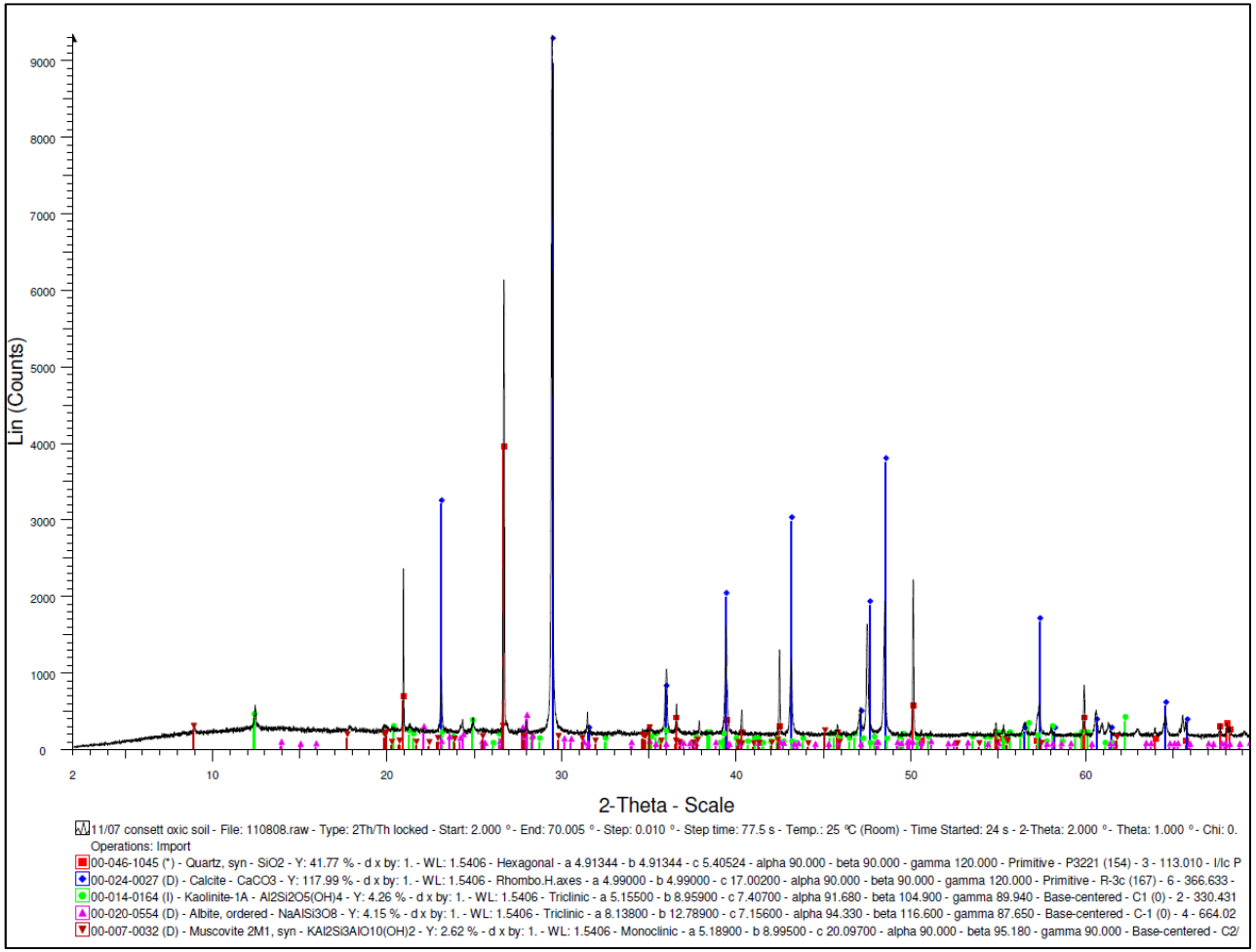

Figure A1 – Consett surface soil XRD pattern

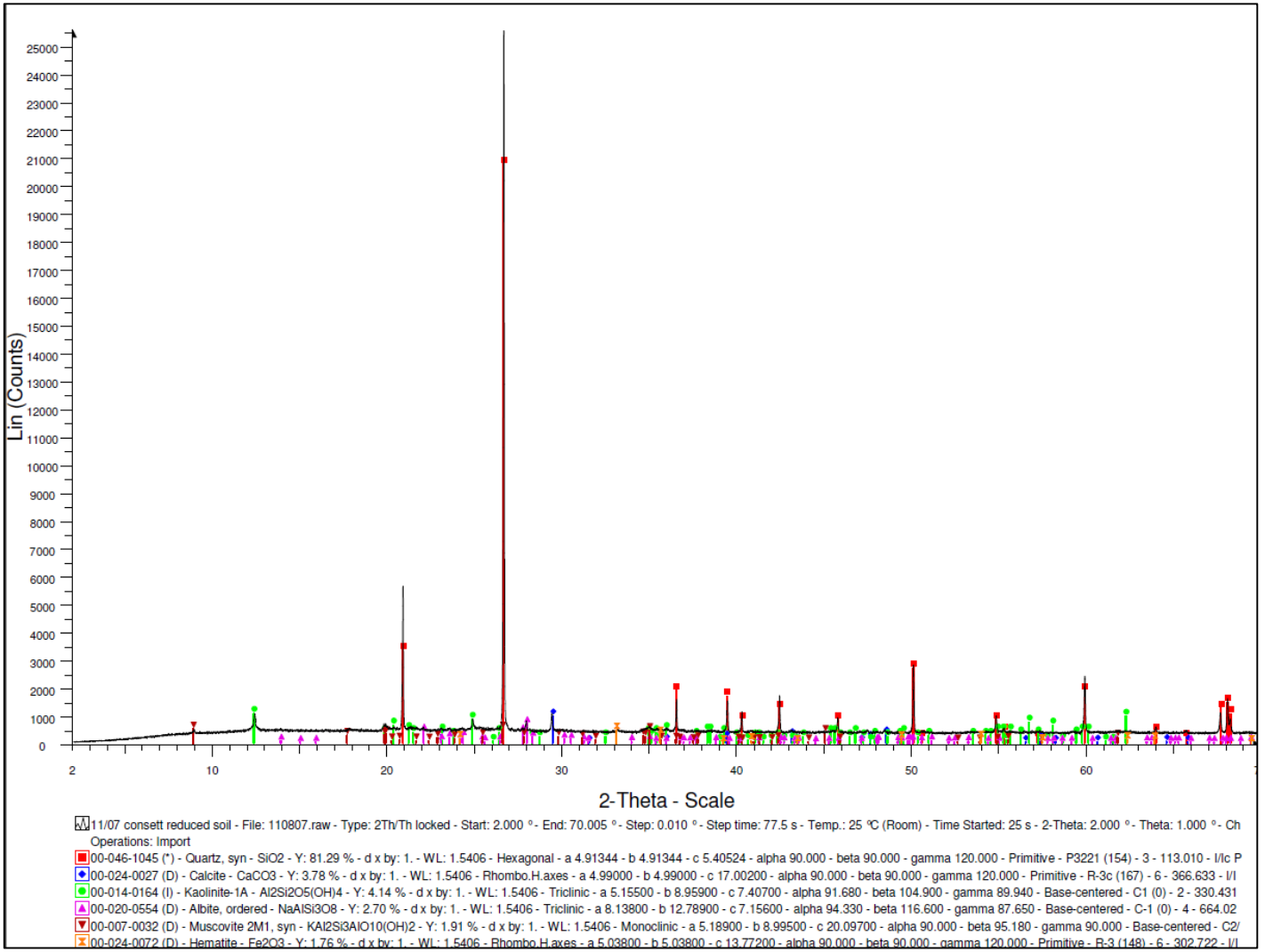

Figure A2 – Consett deep soil XRD pattern

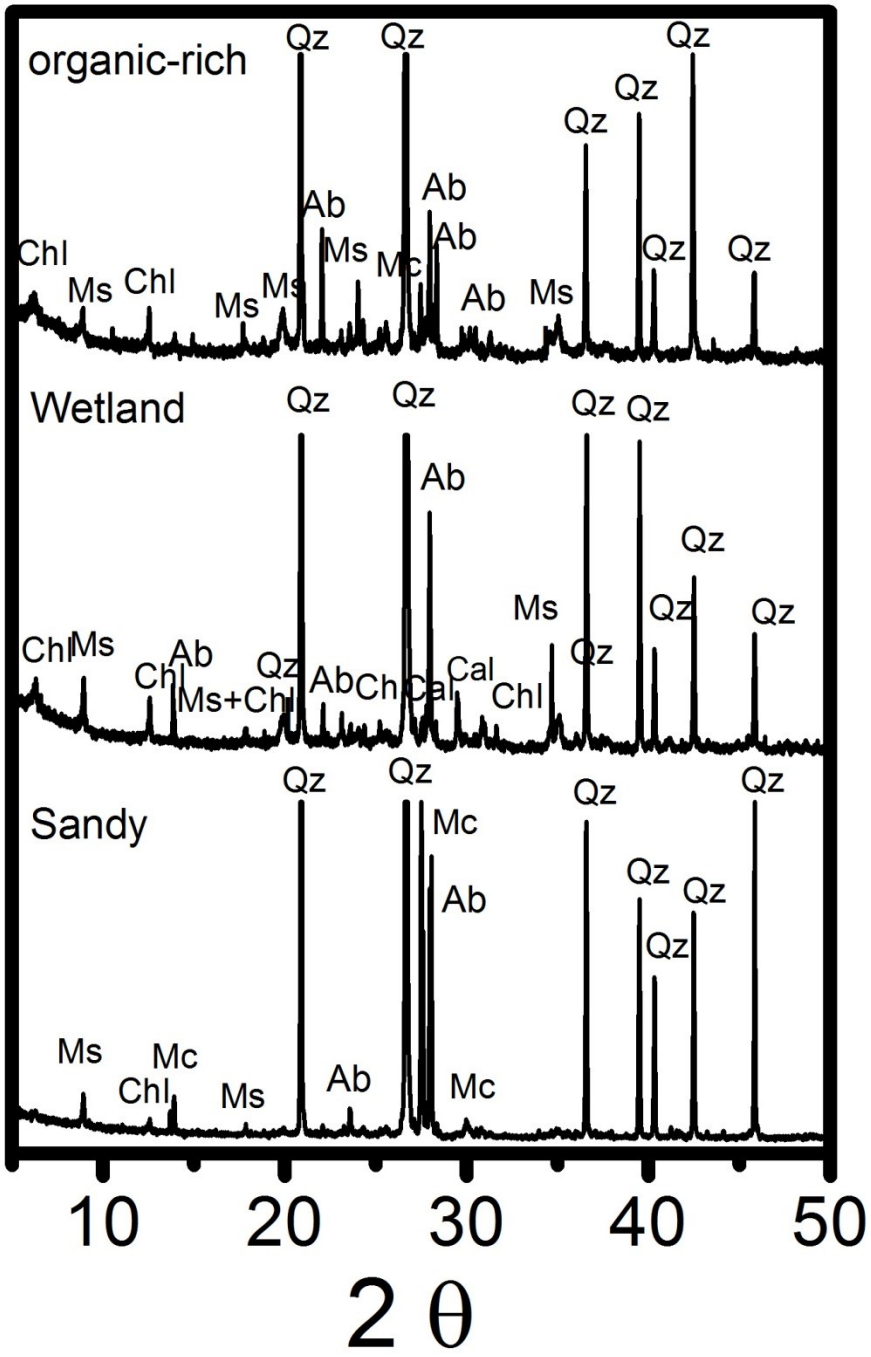

Figure A3 – XRD patterns of soils sampled from Torna-Marcel-Raba river system. Ab = albite, Cal = calcite, Chl = chlorite, Qz = quartz, Mc = microcline, Ms = muscovite

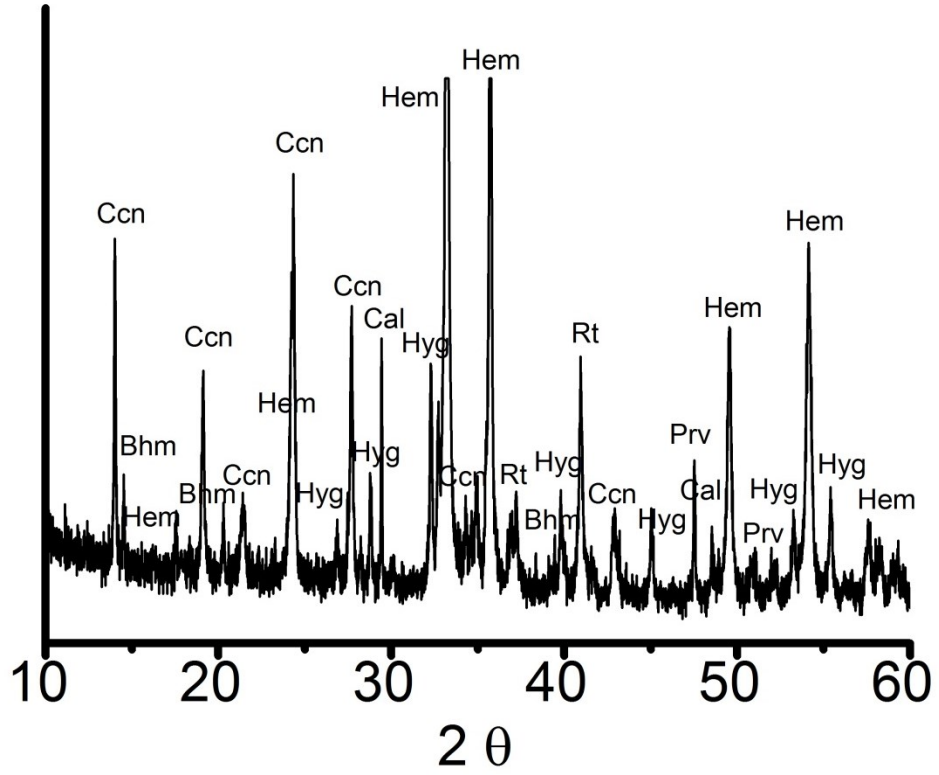

Figure A4 - XRD pattern for red mud sampled from inside the breached tailings dam at Ajka. Bhm = boehmite, Cal = Calcite, Ccn = cancrinite, Hem = hematite, Hyg = hydrogarnet, Prv = perovskite, Rt = rutile

Table A2 – Data from duplicate batch experiments performed using soils SS, OR, and WL

	pH	TDS (mg L^{-1})	DOC (mg L^{-1})	As (µg L^{-1})	V (µg L^{-1})	Mo (µg L^{-1})	Al (µg L^{-1})
9% red mud addition							
Soil SS	9.0, 9.6	998, 991	157, 99	62.7, 62.6	161, 157	48.8, 48.2	1,161, 930
	9.3 ±0.3	**994 ±4**	**128 ±29**	**62.7 ±0.1**	**159 ±2.0**	**48.5 ±0.3**	**1,045 ± 116**
Soil OR	7.9, 8.1	1253, 1252	143, 131	6.7, 6.6	31, 33	78.6, 78.0	<200 <200
	8.0 ±0.1	**1252 ±1**	**137 ±6**	**6.6 ±0.1**	**32 ±1.1**	**78.3 ±0.3**	-
Soil WL	9.2, 9.5	952, 960	105, 84	88.0, 87.0	189, 206	95, 100	328, 489
	9.4 ±0.15	**956 ±4**	**95 ±10**	**87.5 ±0.1**	**198 ±8.4**	**97.7 ±2.4**	**408 ±81**
9% red mud + 4 % gypsum addition							
Soil SS	7.6, 7.9	2703, 2647	39, 40	7.3, 7.3	19.2, 18.6	56.6, 59.8	<200 <200
	7.8 ±0.15	**2675 ±28**	**40 ±1**	**7.3 ±0**	**18.9 ±0.3**	**57.9 ±1.9**	-
Soil OR	7.7, 7.5	2945, 2933	75, 73	<0.5 <0.5	7.4, 7.6,	27.1. 29.6	<200 <200
	7.6 ±0.1	**2939 ±6**	**74 ±1**	-	**7.5 ±0.1**	**28.3 ±1.3**	-
Soil WL	8.1, 8.3	2826, 2585	11, 12	5.5, 5.5	13.2, 14.4	57.9, 61.1	<200 <200
	8.2 ±0.1	**2706 ±121**	**12 ±1**	**5.5 ± 0**	**13.8 ±0.6**	**59.5 ±1.6**	-

The mean value and the range of duplicates are quoted in italics

<, less than given limit of detection

Appendix B Associated Publications

Included with this section are publications associated with the work presented in this thesis. In addition, publications and conference proceedings, related to this work, that has included contributions from the author, Miss C. L. Lockwood, are also detailed.

B1 Relevant Publications

Lehoux, A. P., **Lockwood C. L.**, Mayes,W. M., Stewart D. I., Mortimer, R. J. G., Gruiz, K., and Burke, I. T. (2013) Gypsum addition to soils contaminated by red mud: Implications for aluminium, arsenic, molybdenum and vanadium solubility. *Environmental Geochemistry and Health, 35(5), 643-656.*

B2 Other Publications

Burke, I. T., Peacock, C. L., **Lockwood, C. L.,** Stewart, D. I., Mortimer, R. J. G., Ward, M. B., Renforth, P., Gruiz, K. and Mayes, W. M. (2013) Behaviour of Aluminium, Arsenic and Vanadium during Neutralization of Red Mud Leachate by HCl, Gypsum or Seawater. *Environmental Science and Technology, 47 (12), 6527-6535.*

B3 Conference proceedings

Stewart, D. I., Fuller, S., Burke, I. T., Whittleston, R. A., **Lockwood, C. L**., Baker, A. The Role of Molecular Biology in Geotechnical Engineering. 18th International *Conference on Soil Mechanics and Geotechnical Engineering, Paris, France, 2-6 September 2013, 3077-3080 (Poster)*

Lockwood, C.L., Mortimer, R. J. G., Stewart, D.,I., Mayes, W. I., Burke, I. T., Arsenic release from red mud affected soil-water systems. *Goldschmidt, Florence, Italy, 25-30 August 2013, Mineralogical Magazine, Vol. 77, pp 1535-1660 (Oral Presentation, CLL)*

Lockwood, C. L., Mortimer, R. J. G., Stewart, D. I., Mayes, W. M., Burke, I. T., The role of biogeochemistry during the release of oxyanions in soil-water systems affected by bauxite residue (red mud) from the Ajka repository failure, Western Hungary. *Geomicrobiology and its significance for biosphere processes, Manchester, UK, 19-20 April 2012 (Oral presentation, CLL)*